Volume 11, Number 3
May–June 2003

ISSN: 0869-5938

STRATIGRAPHY AND GEOLOGICAL CORRELATION

English Translation of *Stratigrafiya. Geologicheskaya Korrelyatsiya*

Editor-in-Chief
Boris S. Sokolov

http://www.maik.ru

Journal of the Fundamental and Applied Aspects of Stratigraphy and the Correlation of Geologic Events and Processes in Time and Space

МАИК "НАУКА/INTERPERIODICA" PUBLISHING

Stratigraphy and Geological Correlation

(Stratigrafiya. Geologicheskaya Korrelyatsiya)

ISSN: 0869-5938

Editor-in-Chief
Boris S. Sokolov
Member of the Russian Academy of Sciences,
Counsellor of the Presidium of the Russian Academy of Sciences (RAS)
Address for correspondence:
Staromonetnyi per. 22, Moscow, 109180 Russia
Phones: 7 (095) 951-2164; Fax: 7 (095) 953-5590.

Deputy Editor-in-Chief
Mikhail A. Semikhatov
Member of the Russian Academy of Sciences
Head of Laboratory, Geological Institute, RAS
E-mail: semikhatov@ginran.msk.su

Assistant Editor
Aleksei B. Herman
Senior Scientist,
Geological Institute, RAS
E-mail: herman@ginran.msk.su

EDITORIAL BOARD

Mikhail A. Akhmet'ev
Dr. Sci. (Geol.–Min.),
Head of Laboratory, Geological Institute, RAS
akhmetev@ginran.msk.su

Aleksandr S. Alekseev
Professor, Dr.Sci. (Geol.–Min.),
Department of Paleontology,
Moscow State University
aaleks@geol.msu.ru

Mikhail N. Alekseev
Dr. Sci. (Geol.–Min.),
Chief Scientist, Geological Institute, RAS
alekseev@ginran.msk.su

Ivan A. Basov
Dr. Sci. (Geol.–Min.), Laboratory Chief,
Institute of the Lithosphere, RAS
basov@ilsan.msk.ru

Michael G. Basset
Professor, National Museum of Wales,
Cardiff, UK

William A. Berggren
Professor, Department of Geology and Geophysics,
Woods Hole Oceanographic Institute, USA

Elena V. Bibikova
Dr. Sci. (Geol.–Min.), Chief Scientist,
Vernadsky Institute of Geochemistry
and Analytical Chemistry, RAS
sergei@bibikov.genebee.msu.su

Nikita A. Bogdanov
Corresponding Member of
RAS, Director, Institute of the Lithosphere, RAS
bogdanov@ilsan.msk.ru

Kiyotaka Chinzei
Professor, Institute of Geology,
University of Tokyo,
Tokyo, Japan

Nikolai M. Chumakov
Dr. Sci. (Geol.–Min.),
Chief Scientist, Geological Institute, RAS
chumakov@ginran.msk.su

Yurii B. Gladenkov
Dr. Sci. (Geol.–Min.),
Head of Laboratory, Geological Institute, RAS
gladenkov@ginran.msk.su

Mikhail A. Fedonkin
Corresponding Member of RAS, Laboratory Chief,
Paleontological Institute, RAS
mfedon@paleo.ru

Dmitrii L. Kaljo
Professor, Institute of Geology, Tallinn, Estonia

Kirilla I. Kuznetsova
Dr. Sci. (Geol.–Min.), Chief Scientist,
Geological Institute, RAS
kuznetsova@ginran.msk.ru

Victor E. Khain
Member of RAS, Chief Scientist,
Institute of the Lithosphere, RAS

Lidiya A. Nevesskaya
Dr. Sci. (Biol.), Laboratory Chief,
Institute of Paleontology, RAS
lenin33@paleo.ru

Aleksandr G. Ponomarenko
Dr. Sci. (Biol.), Chief Scientist,
Institute of Paleontology, RAS
vtopor@paleo.ru

Jurgen Remane
Professor, Institute de Géologie,
Université de Neuchâtel, Switzerland

Aleksei Yu. Rozanov
Corresponding Member of RAS,
Director, Institute of Paleontology, RAS
aroza@paleo.ru

Boris A. Sokolov
Corresponding Member of RAS, Professor, Dean,
Faculty of Geology, Moscow State University
mfedon@paleo.ru

Otto Walliser
Professor, Göttingen University, Göttingen,
Germany

Sun Weigo
Professor, Nanjing Institute of Geology
and Paleontology, Academia Sinica, China

Victor A. Zakharov
Dr. Sci. (Geol.–Min.), Head of Laboratory, Institute
of Geology, Geophysics, and Mineralogy, Siberian
Division, RAS, Novosibirsk

Aleksandr I. Zhamoida
Corresponding Member of RAS,
Russian Geological Institute, St. Petersburg

Staff Editor Tamara V. Trishkina

Editor of the English Translation Anatolii Ya. Sharas'kin, Dr. Sci. (Geol.–Min.)

SCOPE

Stratigraphy and Geological Correlation (*Stratigrafiya. Geologicheskaya Korrelyatsiya*) is the only journal in the world designed to provide comprehensive coverage of the fundamental and applied aspects of stratigraphy and the correlation of geological events and processes in time and space. Articles are based on the results of multidisciplinary research and are directed toward researchers, university professors, students, and geologists interested in understanding stratigraphy and the chronological features of the world's geological record.

Stratigraphy and Geological Correlation is abstracted and/or indexed in *Petroleum Abstracts*, *Research Alert*, *SciSearch*, *Current Contents* (*Physical*, *Chemical*, and *Earth Sciences*) and *World Translations Index*.

SUBSCRIPTION OFFICE
INTERPERIODICA
P.O. BOX 1831, BIRMINGHAM, AL 35201-1831 USA
PHONE: (800) 633-4931; (205) 995-1567 (outside US and Canada)
FAX: (205) 995-1588

PUBLISHER
INTERNATIONAL ACADEMIC PUBLISHING
COMPANY "NAUKA/INTERPERIODICA"
PROFSOYUZNAYA UL. 90, MOSCOW, 117997 RUSSIA
PHONE: 7 (095) 336-1600; FAX: 7 (095) 336-0666
E-mail: compmg@maik.ru
Web Site: http://www.maik.ru

SUBSCRIPTION PRICES (2003, Volume 11, 6 issues)
US $1270.00 (North America), $1455.00 (elsewhere). Subscriptions may be entered at any time. Orders may be placed at agencies or directly. Cancellations not allowed except for duplicate payment. Prepayment required. Advance payment required in US$/US bank. MasterCard/Visa accepted. Make checks payable to *Stratigraphy and Geological Correlation* or Interperiodica.

Stratigraphy and Geological Correlation (ISSN: 0869-5938) is published bimonthly for US $1270.00 (North America), outside North America for $1455.00 per year by MAIK "Nauka/Interperiodica", 5724 Hwy. 280 East, Birmingham, Alabama 35242-5724 USA. Periodical postage paid at Birmingham, Alabama, and additional mailing offices. POSTMASTER: Send address changes to *Stratigraphy and Geological Correlation*, P.O. Box 1831, Birmingham, Alabama 35201 USA.

The journal was founded in 1993.

Original Russian Edition Copyright © 2003 by the Russian Academy of Sciences.
English Translation Copyright © 2003 by MAIK "Nauka/Interperiodica" (Russia).

Printed in the USA by Pleiades Publishing, Inc.

Contents

Vol. 11, No. 3, 2003

Simultaneous English language translation of the journal is available from MAIK "Nauka/Interperiodica" (Russia).
Stratigraphy and Geological Correlation ISSN 0869-5938.

Sr Isotope Composition in Paleoproterozoic Carbonates Extremely Enriched in ^{13}C: Kaniapiskau Supergroup, the Labrador Trough of the Canadian Shield
A. B. Kuznetsov, V. A. Melezhik, I. M. Gorokhov, N. N. Mel'nikov, and A. E. Fallick 209

Diversity Dynamics of Fusulinid Genera and Main Stages of Their Evolution
E. Ya. Leven 220

New Data on Fauna and Biostratigraphy of Norian Deposits in the Kotel'nyi Island (New Siberian Islands)
A. G. Konstantinov, E. S. Sobolev, and T. V. Klets 231

Comprehensive Substantiation of Jurassic Phytostratigraphy and Correlations in the Kansk Coal Basin, Siberia
A. I. Kirichkova, E. I. Kostina, and N. A. Timoshina 244

Structure and Age of Mesozoic Sedimentary-Volcanogenic Deposits of the Palana Section (Western Kamchatka)
T. N. Palechek, A. V. Solov'ev, and M. N. Shapiro 261

Stratigraphy of the Talitsa Horizon (Paleocene) in the Central Trans-Urals
E. O. Amon, O. N. Vasil'eva, and V. I. Zhelezko† 278

Pliocene–Lower Quaternary Planktonic Foraminiferal Biostratigraphy and Paleoceanology, ODP Hole 677A
N. V. Bubenshchikova 293

To the Problem of Milankovitch Paleoclimatic Cycles
A. A. Kosov 305

Stratigraphy and Geological Correlation, Vol. 11, No. 3, 2003, pp. 209–219. Translated from Stratigrafiya. Geologicheskaya Korrelyatsiya. Vol. 11. No. 3, 2003, pp. 3–14.
Original Russian Text Copyright © 2003 by Kuznetsov, Melezhik, Gorokhov, Mel'nikov, Fallick.
English Translation Copyright © 2003 by MAIK "Nauka/Interperiodica" (Russia).

Sr Isotope Composition in Paleoproterozoic Carbonates Extremely Enriched in ^{13}C: Kaniapiskau Supergroup, the Labrador Trough of the Canadian Shield

A. B. Kuznetsov*, V. A. Melezhik, I. M. Gorokhov*, N. N. Mel'nikov*, and A. E. Fallick*****

**Institute of Precambrian Geology and Geochronology, Russian Academy of Sciences, nab. Makarova 2, St. Petersburg, 199034 Russia*

***Norway Geological Survey, Trondheim, N-7491 Norway*

****Environment Research Center, Scotland University, Glasgow, G75 0QF Great Britain*

Received February 5, 2001; in final form, November 21, 2001

Abstract—Paleoproterozoic dolostones of the Dunphy, Portage, Alder, and Uve formations representing lower horizons of the Kaniapiskau Supergroup in the Labrador trough of the Canadian Shield are remarkable, as is known, owing to their extremely high $\delta^{13}C$ values ranging from +5.3 to +15.4‰ PDB. Petrographic characteristics of dolostones suggest limy composition of original sediments, which were dolomitized immediately after formation of the early diagenetic calcite cement in nonconsolidated deposits. Dolostones with Mg/Ca > 0.62 and with low Mn/Sr and Fe/Sr ratios are products of the early diagenesis, which display minimal signs of secondary alteration. Another group of rocks (Mg/Ca < 0.62) is represented by dolostones with relics of mosaic drusy calcite, which could be formed after sediments containing aragonite at the time of the early dolomitization. Prior to investigation of R-Sr systematics, carbonate samples were leached in 1N solution of ammonium acetate in order to remove late diagenetic carbonate phases for a more reliable assessment of $^{87}Sr/^{86}Sr$ ratio in sedimentation medium. The Rb–Sr systems of dolostones from lower formations of the Kaniapiskau Supergroup have been reset in response to their partial dedolomitisation that took place likely at the time of Hudsonian regional metamorphism 1.8 Ga ago. The least altered sample from the Alder Formation (Mn/Sr = 2.7, Fe/Sr = 11.8) with $^{87}Sr/^{86}Sr = 0.70479$ characterizes the admissible maximum of this ratio in seawater 2.15 Ga ago. The obtained low value of $^{87}Sr/^{86}Sr$ ratio excludes a possibility that a high rate of continental erosion could be responsible for intensified burial of organic matter and for concurrent precipitation of carbonates enriched in ^{13}C.

Key words: strontium isotopes, carbonate rocks, epigenesis, Paleoproterozoic, Canadian Shield.

INTRODUCTION

Investigation of Sr isotope composition in Paleoproterozoic carbonates is an important approach elucidating variations of $^{87}Sr/^{86}Sr$ ratios in seawater of that time and environments of carbonate accumulation. The available reconstructions of secular Sr isotope variations in Paleoproterozoic seawater (Veizer and Compston, 1976; Veizer *et al.*, 1992; Mirota and Veizer, 1994; Whittaker *et al.*, 1998; Gorokhov *et al.*, 1998) are unfortunately lacking the desirable substantiation by reliable experimental data, being based on limited results obtained for carbonate samples, which have been collected from sedimentary successions not always well calibrated in terms of chronostratigraphy. Moreover, not all the $^{87}Sr/^{86}Sr$ initial ratios used in the reconstructions seem to characterize marine sediments, and some of analyzed samples may represent carbonates accumulated in paleobasins, which were isolated from ocean. As a result, the available data (Veizer and Compston, 1976; Mirota and Veizer, 1994) are insufficient for understanding of interconnections between secular $^{87}Sr/^{86}Sr$ variations in Paleoproterozoic ocean and well-known geological events of that time.

One of the most important events of that time was mass accumulation of carbonates 2.3–2.0 Ga ago, which reveal high $\delta^{13}C$ values, up to +16‰ PDB inclusive (Galimov *et al.*, 1975; Shidlowski *et al.*, 1976; Baker and Fallick, 1989; Yudovich *et al.*, 1990; Karhu, 1993; Melezhik and Fallick, 1996; Akhmedov *et al.*, 1996; Melezhik *et al.*, 1997a, 1997b, 1999). Among factors assumed to be responsible for accumulation of carbonates enriched in ^{13}C, there were mentioned the following ones: an elevated burial rate of organic carbon as a consequence of intensified erosion and greater continental runoff (Des Marais *et al.*, 1992, 1994; Derry *et al.*, 1992); "intense processes of mount building" by no means based on geological data (Galimov, 1999); and accumulation of carbonates in isolated evaporite paleobasins (e.g., Reitsema, 1980; McKenzie, 1981; Stiller *et al.*, 1985). At the same time, some

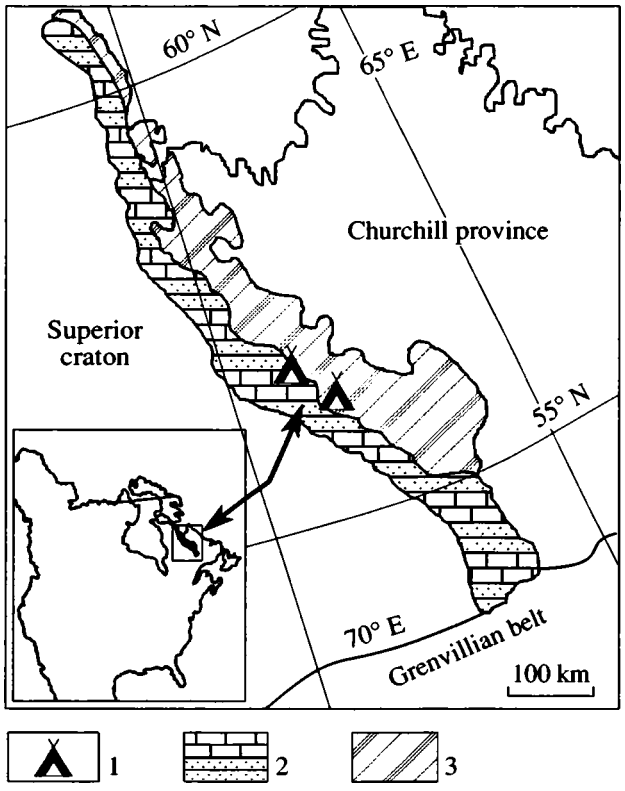

Fig. 1. Schematic geological map of the Labrador trough, Canadian Shield, and localities of studied sections of the Kaniapiskau Supergroup (1) in the western (2) and eastern (3) zones of the trough.

researchers who paid attention to coincidence between the positive $\delta^{13}C$ anomaly under consideration, on the one hand, and to concurrently recorded maximum of lateral dispersal and diversity of stromatolites, on the other, suggested that global biogeochemical cycle of carbon could be influenced by intense expansion of benthic cyanobacterial (stromatolitic) ecosystems (Melezhik *et al.*, 1997c; Semikhatov *et al.*, 1999). In terms of two first concepts suggesting an increase of continental runoff and/or "intense processes of mountain building," data on Sr isotope variations in Paleoproterozoic seawater are able to insert real limitations into models aimed to explain accumulation of carbonates with extremely high $\delta^{13}C$ values.

In this work, methods of isotopic geochemistry are used to evaluate $^{87}Sr/^{86}Sr$ initial ratios in Paleoproterozoic sedimentary basins in order to assess independently the accumulation environments of carbonates displaying extremely high $\delta^{13}C$ values. The analyzed carbonate samples characterize the lower part of the Kaniapiskau Supergroup exposed in the Labrador trough of the Canadian Shield. In distinction from similar rocks of North America, Europe, Africa, and Australia, chronostratigraphic position of samples, which have been studied, is substantiated quite well.

STRATIGRAPHY

The Labrador trough represents a submeridional antiform situated in the southeastern part of the Canadian Shield (Dimroth, 1970). Rocks of the trough are in contact with the Archean Superior craton in the west, with the Paleoproterozoic Churchill province affected by Hudsonian orogeny in the east, and the Grenvillian foldbelt that was formed in the terminal Middle-initial Late Riphean bounds the trough on the south (Fig. 1). Inside the trough, there are two lithofacies zones: the western one of terrigenous-carbonate sediments and the eastern zone, where volcanic rocks and dike swarms have been distinguished in addition.

Carbonate, terrigenous, and volcanogenic deposits of the Labrador paleobasin, which are 2.17 to 1.87 Ga old (Fryer, 1972; Machado *et al.*, 1989; Rohon *et al.*, 1993), discordantly overlie the Archean basement and represent the Kaniapiskau Supergroup of the Paleoproterozoic. The supergroup is divided in two groups: the Knob Lake Group of volcanogenic-sedimentary rocks, which is distinguishable in both lithofacies zones of the trough, and the Doublet Group of volcanogenic rocks terminating the rock succession in the eastern zone (Dimroth, 1970). The Knob Lake Group includes two transgressive-regressive megacycles: one composed of deposits of the Seward, Pistolet, Swampy Bay, and Attikamagen subgroups and the other one including deposits of the Wishart, Sokoman, and Menihek formations (Dimroth, 1970, 1978). Carbonate rocks are present in the Seward, Pistolet, and Attikamagen formations of the first megacycles, but extremely high $\delta^{13}C$ values have been established in carbonates of two lower subgroups only (Melezhik *et al.*, 1997a).

The Knob Lake Group of the Labrador trough is of a complex lithofacies structure, and we describe here only stratigraphy of its lower horizons, which are of interest to our investigation (Fig. 2). The Seward Subgroup begins with conglomerates and red arkoses of the Chakonipau Formation (860–1390 m). In the eastern zone, these rocks are overlain by dolostones of the Dunphy Formation (365–610 m), which grade laterally into fine-grained sandstones with dolomite interlayers of the Portage Formation (150–250 m) distinguished in the western zone. Both formations underlie shales of the Lace Lake Formation (310 m) representing the basal subdivision of the Pistolet Subgroup. The overlying Alder Formation (up to 510 m) is known in the western zone only, where it is composed of alternating quartzitic sandstone and stromatolitic dolostone beds. Next in the subgroup section of that zone are massive dolostones of the Uve Formation (up to 210 m), which are overlain by conglomerate, graywacke, and black shale beds of the Swampy Bay Subgroup (250–1500 m). In the eastern zone of the Labrador trough, that part of the Pistolet Subgroup, which is above shales of the Lace Lake Formation, and siliciclastic rocks of the Swampy Bay Subgroup are replaced by volcanogenic-sedimentary facies of the Bacchus Formation (250–750 m, see

Fig. 2). The overlying Mistamisk Formation of basaltic and rhyolitic lavas is correlated with shales and siltstones representing a lower portion of the Attikamagen Subgroup in the west of the trough.

Geochronology of lower horizons in the Kaniapiskau Supergroup is based on concordant U-Pb dates obtained for zircons from volcanic rocks. The date of 2169 ± 4 Ma has been obtained for zircons from a sill intruding carbonates of the Seward Subgroup in the central part of the trough (Rohon *et al.*, 1993). Another U-Pb date of 2142 ± 4 Ma characterizes zircons from rhyolites of the Mistamisk Formation (unpublished result of T.E. Krogh and B. Dresser cited by Machado *et al.* without supplementary analytical data). These dates imply that deposits of the Seward, Pistolet, and Swampy Bay subgroups accumulated within a rather short interval (2.17–2.14 Ga) of geological time.

Sedimentary rocks of the Kaniapiskau Supergroup experienced metamorphism of the greenschist to amphibolite grade 1.8 Ga ago during the Hudsonian orogeny (Machado *et al.*, 1989). In the western zone of the Labrador trough, metamorphic transformations were however weaker than in the eastern zone adjacent to the Churchill province, where the Hudsonian folding is intensively manifested (Cheve *et al.*, 1985).

Carbonate rock samples have been collected for analysis in the central segment of the Labrador trough from the Portage, Alder, and Uve formations of the western zone and from the Dunphy Formation of the eastern zone (Figs. 1, 2).

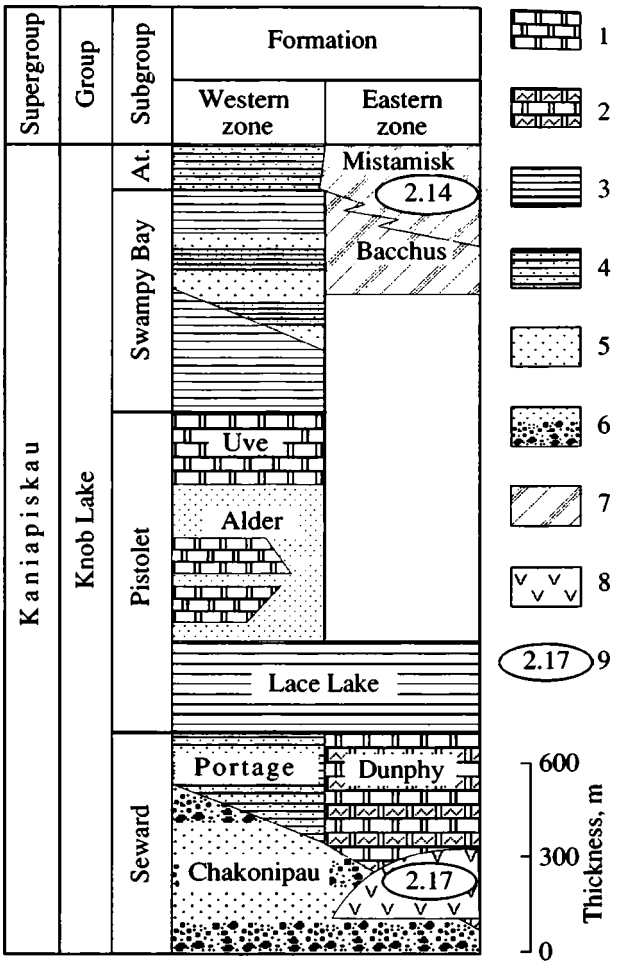

Fig. 2. Lithostratigraphy of lower formations of the Kaniapiskau Supergroup, Labrador trough, and U-Pb dates for zircons from volcanic rocks: (1) dolostone; (2) cryptalgal dolostone; (3) shale; (4) siltstone; (5) sandstone; (6) gravely sandstone; (7) basic volcanic rocks; (8) U-Pb date (abbreviation At. denotes the Attikamagen Formation).

PETROGRAPHY OF CARBONATE ROCKS

Pinkish to yellowish pink dolostones with microbial lamination are predominant rocks of the Dunphy Formation. Their pinkish tint is caused by finely dispersed hematite (Cheve *et al.*, 1985). Many samples reveal a mosaic texture and alternation of medium- and fine-grained dolomite laminae crossed by infrequent stylolite seams. Dolomite matrix sometimes encloses irregular patches of sparry calcite and relics of the early diagenetic bird's-eye texture. The content of non-carbonate fraction, predominantly of quartz, that is commonly low in middle and upper beds of the Dunphy Formation (Table 1) can be as high as 60% in dolostones of the Portage Formation.

Light gray flaggy stromatolitic dolostones of the Older Formation display the cross-lamination and presence of flakestone lenses. Stromatolites are represented by columnar and layered buildups. Dolarenite and dolorudite fragments distinguishable in the rocks are composed of unsorted intraclasts cemented by dolosparite (Melezhik *et al.*, 1997a). The fine-crystalline matrix encloses rare patches composed of non-crystalline micritic dolomite. Quartz representing main mineral of non-carbonate fraction is associated with mica, when the fraction content grows up to 20%.

The Uve Formation of predominant light gray massive dolostones also encloses subordinate dark gray aphanitic dolostones with locally distinguishable fine cross-lamination. The massive rock varieties are composed of medium- to coarse-grained crystalline dolomite. In dolosparite matrix of some samples, there were distinguished relics of fine lamination, intraclasts, and minute druses of mosaic sparry calcite. Siliciclastic admixture consisting of quartz usually ranges in abundance from 2.1 to 8.2%, but near the formation top its content can be as high as 39% (Table 1).

Relationships between lithofacies of the lower Knob Lake Group reflect a gradual deepening of the Labrador paleobasin during the accumulation time of the Seward and Pistolet subgroups (Dimroth, 1970). Continental red beds of alluvial-deltaic origin, which represent the Chakonipau Formation, are overlain by shallow-water basinal facies of the carbonate Dunphy and terrigenous-

Table 1. Trace element concentrations in the bulk carbonate material of dolostones from the lower part of the Kaniapiskau Supergroup and corresponding oxygen and carbon isotopic parameters

Sample no.	Siliciclastic fraction, %	Mg/Ca	Mn, ppm	Fe, ppm	Mn/Sr[(1)]	Fe/Sr[(1)]	$\delta^{18}O^{(2)}$ ‰ PDB	$\delta^{13}C^{(2)}$ ‰ PDB
Uve Formation								
TC-80-264	39	0.530	1940	7360	12.8	48.4	−10.1	8.1
TC-82-15-1	5.4	0.591	2210	11700	29.9	158.5	−9.6	7.9
TC-82-19	4.2	0.607	1680	8230	24.1	118.9	−10.4	7.6
TC-82-89	3.1	0.592	1960	15050	30.6	235.2	−13.2	5.3
TC-82-97	2.1	0.629	1430	6940	19.7	95.6	−13.2	5.9
TC-82-101	5.4	0.633	1055	4430	16.2	68.9	−9.3	10.4
TC-82-106A	3.6	0.580	1865	11500	14.9	95.0	−11.3	8.6
TC-82-109	8.2	0.642	680	3790	5.5	30.8	−7.3	10.1
Alder Formation								
TC-82-8	10.3	0.632	770	1985	9.3	23.8	−7.7	9.9
TC-82-87	19.8	0.629	900	2040	9.4	21.3	−9.2	8.7
TC-82-88	3.1	0.641	310	1340	2.7	11.8	−6.7	10.2
Portage Formation								
TC-80-275	60	0.552	1760	785	13.5	6.0	−14.2	6.1
Dunphy Formation								
TC-83-221	11.8	0.659	200	795	3.8	15.0	−6.3	15.0
TC-83-2532	0.6	0.637	935	4830	13.9	71.7	−8.1	14.5
TC-146-82	2.9	–	310	1545	5.4	27.2	−6.0	15.4
TC-149-82	2.5	–	460	3895	5.5	46.4	−7.9	14.2

Note: [(1)]Ratio is calculated based on Sr concentrations in residues after leaching (Table 2) assumed to be close to those in the bulk carbonate material; [(2)]data after Melezhik *et al.*, 1997a.

carbonate Portage formations. Higher in the succession, there are clayey sediments of the Lace Lake Formation and terrigenous-carbonate sediments of the Alder Formation, which have been deposited in distal and coastal zones of a shallow-water basin. Carbonates of the Uve Formation were deposited in relatively deep-water settings below the storm-wave base (Dimroth, 1978).

INVESTIGATION PROCEDURE

With due regard for the extent of secondary alterations in dolostones, we selected 16 of 21 samples available in our collection as appropriate for subsequent geochemical and isotopic analyses: four from Dunphy Formation, one from Portage Formation, three from Older Formation, and eight from Uve Formation. Aliquots of samples dissolved in 1N HCl were used to determine Ca and Mg contents by gravimetric chemical analysis and to measure Mn and Fe concentrations by atomic absorption technique in the chemical laboratory of Geological Institute, Moscow. After preliminary treatment in 1N solution of ammonium acetate (NH_4OAc), powdered samples were subjected to dissolution in 10% acetic acid in order to extract their carbonate components for investigation of Rb-Sr systematics. The isotope dilution technique was used to determine Rb and Sr concentrations in carbonates. Sr isotope composition was determined in static mode on the multi-collector mass spectrometer Finnigan MAT-261. The normalized to $^{86}Sr/^{88}Sr = 0.1194$ averages of $^{87}Sr/^{86}Sr$ ratio for standard samples SRM 987 and EN-1 were 0.71025 ± 0.00002 ($n = 6$) and 0.70918 ± 0.00002 ($n = 1$), respectively, during the period of data gathering. The age value of 2150 Ma was assumed to calculate $^{87}Sr/^{86}Sr$ initial ratios for analyzed dolostone samples.

The step-wise dissolution that partially removes secondary carbonate phases enriched in Rb and radiogenic ^{87}Sr is the obligatory procedure when one is going to study the isotopic systematics of Precambrian carbonates (Gorokhov *et al.*, 1995; Kuznetsov *et al.*, 1997). Its efficiency is demonstrated in works dedicated to Rb-Sr systematics of Riphean carbonates from Siberia (Gorokhov *et al.*, 1995; Semikhatov *et al.*, 2002), the results of which imply that concentrations of Rb and Sr in the carbonate fraction removed after the first step of leaching are 30 and 3 times higher, respectively, than in the carbonate material entering the solution at the

Table 2. Rb–Sr concentrations in and isotopic parameter of carbonate residues after preliminary leaching in 1N solution of ammonium acetate, dolostone samples from the Kaniapiskau Supergroup

Sample no.	Rb, ppm	Sr, ppm	$^{87}Rb/^{86}Sr$	$^{87}Sr/^{86}Sr$ measured	$^{87}Sr/^{86}Sr$ initial
Uve Formation					
TC-80-264	0.79	152	0.0151	0.70747	0.70700
TC-82-15-1	0.11	73.8	0.0045	0.70985	0.70971
TC-82-19	0.18	69.2	0.0076	0.70998	0.70975
TC-82-89	0.23	64.0	0.0105	0.71052	0.71019
TC-82-97	0.39	72.6	0.0157	0.71188	0.71140
TC-82-101	0.13	64.9	0.0058	0.71209	0.71192
TC-82-106A	0.45	125	0.0104	0.71187	0.71154
TC-82-109	0.39	123	0.0091	0.70822	0.70794
Alder Formation					
TC-82-8	0.10	83.4	0.0036	0.70544	0.70533
TC-82-87	0.04	95.6	0.0012	0.70654	0.70651
TC-82-88	0.14	114	0.0037	0.70490	0.70479
Portage Formation					
TC-80-275	0.63	130	0.0141	0.70620	0.70578
Dunphy Formation					
TC-83-221	0.23	52.9	0.0125	0.70704	0.70665
TC-83-2532	0.35	67.4	0.0149	0.71328	0.71282
TC-146-82	0.03	56.7	0.0014	0.71192	0.71188
TC-149-82	0.25	84.0	0.0085	0.71516	0.71490

second step. Difference between $^{87}Sr/^{86}Sr$ ratios measured in these carbonate phases was 0.0024 in average.

The negative interdependence of the carbonate material amount extracted by 1N NH_4OAc solution and Mg/Ca ratio measured in dolostones, along with positive correlation between Mn/Sr and Fe/Sr ratios, on the one hand, and $^{87}Sr/^{86}Sr$ ratios, on the other, clearly indicated that rocks bear secondary calcite formed at the late stages of their late diagenetic recrystallization (Gorokhov *et al.*, 1995; Ovchinnikova *et al.*, 1998, 2000; Vasil'eva *et al.*, 1998, 2000; Semikhatov *et al.*, 2002). Consequently, $^{87}Sr/^{86}Sr$ initial ratios in the carbonate residues after preliminary leaching are closer to the Sr isotope composition of primary carbonates than the corresponding ratios measured in the bulk carbonate material. In this work, we did not consider the Rb-Sr systematics of the leached carbonate phase, and Mn/Sr and Fe/Sr ratios (Table 1) were calculated based on the assumption that Sr concentrations in residues after leaching in 1N solution of ammonium acetate (Table 2) characterize as well the bulk carbonate material. This assumption is admissible because of a slight difference (4% in average) between the Sr concentrations in that material and main carbonate phase of a given sample (Gorokhov *et al.*, 1995; Semikhatov *et al.*, 2002).

ISOTOPIC AND GEOCHEMICAL CHARACTERISTICS OF DOLOSTONES

All the samples studied are composed of dolomite, and the average ratio Mg/Ca = 0.62 calculated for their carbonate fractions is close to that parameter of stoichiometric dolomite (Chilingare *et al.*, 1967). Nevertheless, the total range of these ratios is rather wide (0.53–0.64), and samples with Mg/Ca > 0.62 and with Mg/Ca < 0.62 are conventionally attributed to groups 1 and 2, respectively. Rocks of the latter are localized predominantly in the Uve and Portage formations (Table 1). The lowest Mg/Ca ratios are established in samples TC-80-264 and TC-80-275, which enclose microscopic lenses of sparry calcite and show considerable contents of siliciclastic material (39 and 60%, respectively).

The average Mn and Fe concentrations in dolostones are equal to 1150 and 5390 ppm, respectively, and grow up to 2210 and 15050 ppm in most dolostones of group 2 representing rocks of the Uve Formation (Fig. 3). Similarly high Mn and Fe concentrations are

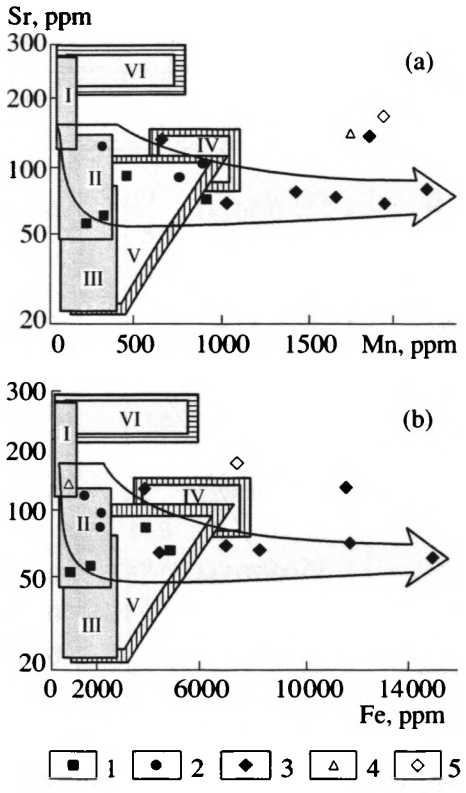

Fig. 3. Sr versus Mn (a) and Sr versus Fe (b) diagrams for studied carbonate samples from the Kaniapiskau Supergroup; rocks lacking (1–3) or bearing (4–5) drusy calcite are from (1) Dunphy, (2) Alder, (3) Uve; (4) Portage, and (5) Uve formations. Numbered fields are for data points of Cenozoic (I), Paleozoic (II), and Paleoproterozoic to Riphean dolostones (III), which retain $^{87}Sr/^{86}Sr$ initial ratios characterizing seawater of corresponding period in distinction from recrystallized Riphean limestones (IV) and Paleozoic (V) or Riphean (VI) dolostones. Arrow denotes trend of late diagenetic recrystallization of carbonate rocks.

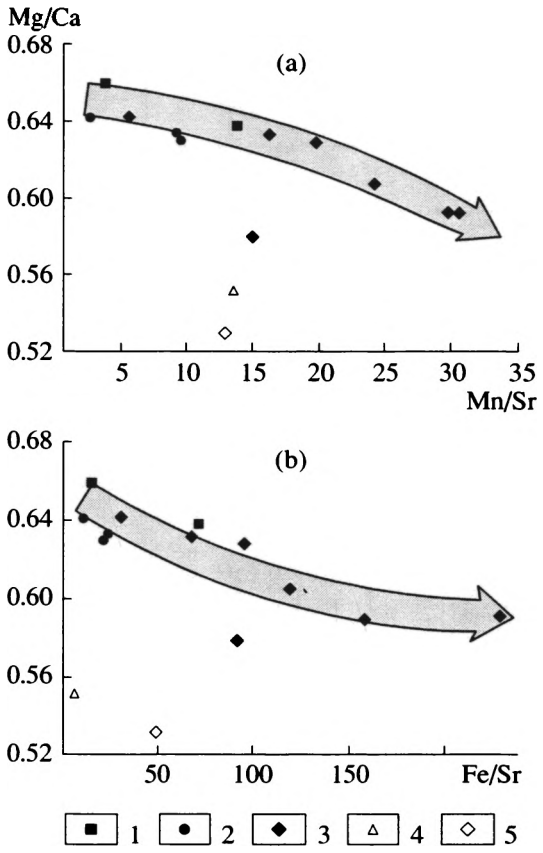

Fig. 4. Mg/Ca versus Mn/Sr (a) and Mg/Ca versus Fe/Sr (b) diagrams for studied carbonate samples from the Kaniapiskau Supergroup (arrow denotes trend of late diagenetic recrystallization of carbonate rocks; symbols as in Fig. 3).

characteristic of Paleoproterozoic dolostones from Australia, Africa, and North America (Veizer *et al.*, 1992). The lower Mn (<1000 ppm) and Fe (<5000 ppm) concentrations are typical of dolostones from group 1 exemplifying rocks of the Dunphy and Alder formations, but they are however higher than in dolostones of some Paleoproterozoic sections of the Baltic Shield, where these rocks are obviously depleted in both elements. For instance, the average Mn and Fe concentrations in Jatulian dolostones of the Tulomozero Formation correspond to 275 and 60 ppm, respectively (Gorokhov *et al.*, 1998).

The Sr concentration in dolostones from lower formations of the Kaniapiskau Supergroup is rather high (52.9–152 ppm, Table 2). Values greater than 100 ppm are established in five samples (Fig. 4) representing dolostones of group 1 (TC-82-88 from the Alder Formation and TC-82-109 from the Uve Formation) and of group 2 (TC-82-106A and TC-80-264 from the Uve Formation and TC-80-275 from the Portage Formation). An elevated level of Sr concentrations in two last samples is obviously connected with presence of relict drusy calcite in these rocks. Microscopic calcite inclusions may be also present in sample TC-82-106A, but we failed to detect them in the available thin section. The Rb concentration in carbonate residues after preliminary leaching is usually not greater than 0.45 ppm, being higher in two samples only, which contain more than 20% of siliciclastic material. The established ranges of $^{87}Sr/^{86}Sr$ initial ratios in studied samples are as follows: 0.70665-0.71490 for the Dunphy Formation, 0.70578 for the Portage Formation, 0.70479–0.70561 for the Alder Formation, and 0.70700–0.71192 for the Uve Formation. These values are independent of abundance of siliciclastic admixture in the rocks, as it is practically free of mica or feldspar grains, which could represent a source of radiogenic ^{87}Sr addition. In each of the formations, the lowest $^{87}Sr/^{86}Sr$ ratios are typical of dolostones lacking calcite inclusions and simultaneously showing low Mn/Sr and Fe/Sr ratios (Fig. 5) but high $\delta^{18}O$ values (Fig. 6a). Despite the relict drusy calcite present in samples TC-80-275 and TC-80-264,

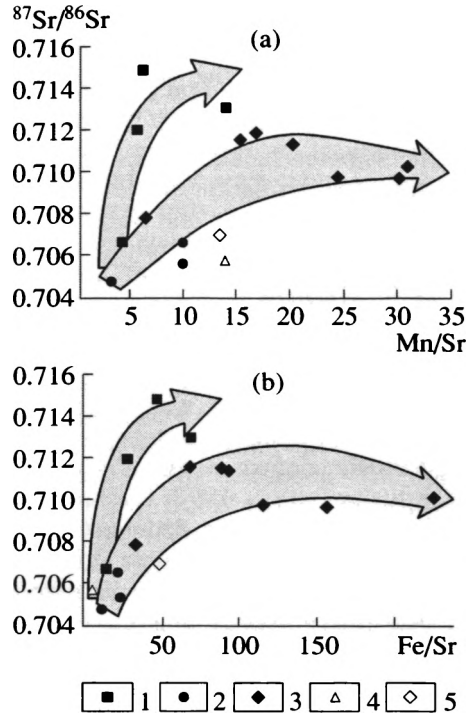

Fig. 5. $^{87}Sr/^{86}Sr$ versus Mn/Sr (a) and $^{87}Sr/^{86}Sr$ versus Fe/Sr (b) diagrams for studied carbonate samples from the Kaniapiskau Supergroup (arrows denote trends of late diagenetic recrystallization of carbonate rocks; symbols as in Fig. 3).

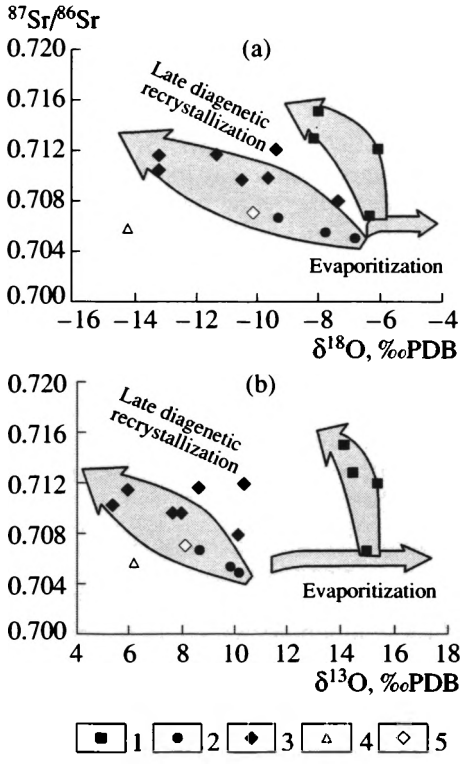

Fig. 6. $^{87}Sr/^{86}Sr$ versus $\delta^{18}O$ (a) and $^{87}Sr/^{86}Sr$ versus $\delta^{13}C$ (b) diagrams for studied carbonate samples from the Kaniapiskau Supergroup (symbols as in Fig. 3).

they are also characterized by rather low $^{87}Sr/^{86}Sr$ ratios (Table 2).

In dolostones of the Dunphy, Alder, and Uve formations, $\delta^{18}O$ values range from –0.6 to –13.2‰ PDB (Table 1), displaying negative correlation with Mn (r = –0.81) and Fe (r = –0.81) concentrations in the rocks. The lowest $\delta^{18}O$ value of –14.2‰ PDB is established for sandy dolostone (TC-80-275) from the Portage Formation. In distinction from many Recent, Phanerozoic, and Riphean carbonates, dolostones of the lower Kaniapiskau Supergroup are characterized by high $\delta^{13}C$ values ranging from +5.3 to +15.4‰ PDB, with their maximum values of +14.2 to +15.4‰ PDB recorded in dolostones of the Dunphy Formation (Melezhik *et al.*, 1997a).

Wide ranges of Mn, Fe, and Sr concentrations, as well as a high variability of $\delta^{18}O$ and $^{87}Sr/^{86}Sr$ values and the established correlations between these parameters suggest that the Knob Lake carbonates experienced significant late diagenetic (metamorphic) alterations.

LATE DIAGENETIC TRANSFORMATIONS IN DOLOSTONES

Early and late diagenetic alterations of carbonate sediments usually result in the partial Sr removal from the rocks, which become simultaneously enriched in Mn and Fe and characterized by decline of $\delta^{18}O$ values (Brand and Veizer, 1980, 1981; Gorokhov, 1996; Wenzel, 2000). Consequently, it is possible, using the geochemical approach, to define carbonate samples with the least-disturbed Rb-Sr isotopic systems. The Sr concentration in a given carbonate rock is grossly dependent on the mineral composition of primary sediment. The early diagenetic calcite formed after recrystallization of high-Mg calcite should have a lower Sr concentration than calcite formed after aragonite (Yudovich *et al.*, 1980; Brand and Veizer, 1980), because the latter, other things being equal, is originally much more rich in Sr. Dolomitized calcites are also partially depleted in Sr, because the crystal lattice of calcite has two times as many points suitable for isomorphic substitution by Sr, as compared to that of dolomite. In general, the Sr loss can take place at any subsequent stage of late diagenetic recrystallization. For instance, Cenozoic dolomites, which replaced the high-Mg calcites of marine origin contain 110–280 ppm Sr in contrast to 40–140 ppm Sr established in late dolomite generations from Paleozoic marine carbonates (Vahrenkamp and Swart, 1990; Barnaby and Read, 1992; Montanez and Read, 1992). Nevertheless, some Proterozoic dolostones containing only 20–95 ppm Sr retain $^{87}Sr/^{86}Sr$ ratios approaching those in ancient oceans (Gorokhov *et al.*, 1995, 1998). In such a case, it is necessary to admit two points: first, the direct con-

nection between composition of seawater and fluids responsible for dolomitization of primary carbonate sediments; second, the absence of subsequent late diagenetic alterations in dolostones.

The Mn/Sr, Fe/Sr, and $^{87}Sr/^{86}Sr$ ratios in meteoric and ground waters, which may interact with carbonates, are higher than the same parameters of seawater (McNutt *et al.*, 1984, 1990; Chaudhuri *et al.*, 1987; Banner *et al.*, 1989; Kharaka and Thordsen, 1992; Stueber *et al.*, 1993; Chaudhuri and Clauer, 1993; Hartman *et al.*, 2000). Accordingly, the increased Mn/Sr and Fe/Sr ratios in carbonates indicate recrystallization of the latter under influence of fluids likely differing from seawater in their Sr isotope compositions. These ratios and $\delta^{18}O$ values are therefore the effective indicators enabling selection of carbonate samples with the least-disturbed Rb–Sr systems.

Dolomitic rocks of the Dunphy, Portage, Alder, and Uve formations contain relics of synsedimentary rim cementation, early diagenetic cavities filled with dolomite, and biosedimentary products of microbial metabolic activity, suggesting altogether that primary sediments consisted of calcareous material (James and Choquette, 1983; Moore, 1989; Knoll and Sweet, 1990). These sediments experienced pervasive dolomitization immediately after development of the earliest calcite cementation in the non-consolidated deposits (Cheve *et al.*, 1985). If this is correct, the early diagenetic dolomite could incorporate strontium that was in isotopic equilibrium with buried sedimentary waters thus retaining the $^{87}Sr/^{86}Sr$ ratio characteristic of primary sediment. The isotopic and geochemical systems of early diagenetic carbonates have likely been reset, when the latter experienced the late diagenetic recrystallization. This is inferable from comparison of average Mn and Fe concentrations, which are greater in dolosparites (0.23 and 0.58%, respectively) than in dolomicrites (0.05 and 0.35%, respectively) of the Dunphy Formation (Cheve *et al.*, 1985).

A high level of Sr concentrations (114–152 ppm) established for five samples from the Portage, Alder, and Uve formations seems to be either a consequence of specific mineral composition of primary sediments, or the result of insignificant recrystallization of early diagenetic dolomites. At the same time, $^{87}Sr/^{86}Sr$ ratios in four of these samples (0.70479–0.70794) are lower than in rocks relatively depleted in Sr, and we regard this fact as an argument in favor of the last assumption. According to Mn/Sr, Fe/Sr, and $\delta^{18}O$ values characterizing the samples under consideration, only one of them from group 1 (TC-82-88) can be regarded as the least altered during the late diagenesis and retaining the $^{87}Sr/^{86}Sr$ ratio approaching that of the early diagenetic dolomite. A combination of low $^{87}Sr/^{86}Sr$ ratios and high Sr concentrations in two samples from group 2 (TC-80-275 and TC-80-264) indicates that either primary sediments contained aragonite, or the early diagenesis left intact a part of the original calcite. In any case, the high Mn and Fe concentrations in these two and one more sample (TC-82-106A) clearlysuggest their recrystallization at the late diagenetic stage (Fig. 3).

Dolostone samples lacking relics of drusy calcite reveal the negative correlation between Mg/Ca ratios, on the one hand, and Mn/Sr and Fe/Sr ratios, on the other (Fig. 4). Interdependences of this kind reflect an effect of dedolomitisation that affected rocks of the Dunphy, Alder, and Uve formations. A similar origin of coarse-crystalline low-Mg dolomite (Mg/Ca = 0.55–0.61) was distinguished in the Upper Riphean Min'yar Formation of southern Urals, where dedolomitisation took place in underground environments at the time of Paleozoic tectonic deformation of Upper Riphean deposits (Kuznetsov *et al.*, 1998; Ovchinnikova *et al.*, 2000). Fluids responsible for dedolomitisation could have low Mg/Ca ratios. Par example, Mg/Ca ratios in recent groundwaters circulating in Paleozoic sandy-carbonate deposits of North America (Banner *et al.*, 1989; Stueber *et al.*, 1993) are within the range of 0.15–0.59. It is also remarkable that $^{87}Sr/^{86}Sr$ ratios in these waters are rather high, ranging from 0.7082 to 0.7161.

The late diagenetic fluids, which affected dolostones of the Dunphy, Alder, and Uve formations, were likely rather uniform with respect to their Mg/Ca parameters (Fig. 4). In contrast, the $^{87}Sr/^{86}Sr$ ratios were greater than 0.715 in fluids, which penetrated into the first formation, and ranged from 0.710 to 0.712 in those, which reacted with rocks of the Uve Formation and with some dolostones of the Alder Formation (Fig. 5). The variability of last ratios could be connected with different source reservoirs of fluids, which were likely derived from the thick (about 1390 m) arkose succession of the Chakonipau Formation in the first case and from overlying carbonaceous shales (60–600 m) of the Swampy Bay Subgroup in the second one. The late diagenetic fluids, which originated in shales of the Lace Lake Formation (310 m), could be able to penetrate into the underlying Dunphy Formation of carbonate rocks and into the overlying Alder Formation of quartzite-carbonate composition (Fig. 2), thus producing the comparable $^{87}Sr/^{86}Sr$ ratios in secondary carbonates of both rock successions.

In general, the isotopic-geochemical systems of early diagenetic dolomites in the lower part of the Knob Lake Group were disturbed by metasomatic dedolomitization of rocks (samples of group 1) and by later dolomitization of rocks with drusy calcite relics (samples of group 2). It is possible also to assume that at least one of these events took place at the time of Hudsonian orogeny, terminal metamorphism of which affected volcanogenic-sedimentary deposits of the Kaniapiskau Supergroup 1.8 Ga ago.

ESTIMATED SR ISOTOPE COMPOSITION IN SEAWATER 2.15 GA AGO

Low Mn/Sr (2.7) and Fe/Sr (11.8) ratios and high $\delta^{18}O$ value (-6.7 PDB) in dolostone sample TC-82-88 from the Alder Formation (group 1) allow us to assume that it was affected to the least extent by late diagenetic alterations. Consequently, $^{87}Sr/^{86}Sr$ ratio characterizing this sample and equal to 0.70479 can be regarded as most closely corresponding to this parameter in Paleoproterozoic (2.15 Ga old) seawater (Fig. 7). Being slightly above the range of 0.70343–0.70419 established for the Jatulian (2.10–2.06 Ga) marine carbonates of southeastern Karelia enriched in ^{13}C (Gorokhov *et al.*, 1998; Kuznetsov *et al.*, 2000), this ratio simultaneously falls within the interval of $^{87}Sr/^{86}Sr$ values (0.70474–0.70508) characterizing Paleoproterozoic carbonates of the Duck Creek Formation (2.25–1.84 Ga), the Wyloo Group of western Australia, and of the Cowels Lake Formation (1.91 Ga), the Coronation Supergroup of northern Canada. At the same time, the value under consideration is noticeably lower than the range of 0.70515–0.70600 established in the Canadian Shield for slightly younger carbonates of the Taltheilei and Utsingi formations, the Phethei Group, and of the Albanel Formation (1.85 ± 0.15 Ga), the Misstassini Group (Veizer *et al.*, 1992; Mirota and Veizer, 1994; Whittaker *et al.*, 1998).

Despite a considerable extent of secondary alterations in dolostones of the Dunphy Formation, $\delta^{18}O$ and $\delta^{13}C$ mean values measured in these rocks are somewhat higher than in dolostones of the Alder Formation (Fig. 6). We assume therefore that carbonates of the Dunphy Formation accumulated in a partially isolated evaporite basin, where Mn and Fe concentrations could be differing from those in paleoocean. Accordingly, the value $^{87}Sr/^{86}Sr = 0.70665$ calculated for the dolostone sample of the Dunphy Formation, in which Mn/Sr (3.8) and Fe/Sr (15.0) ratios are lower than in others, can be regarded as indicative of the Sr isotope composition in that evaporite basin. This value is well within the range of 0.70607–0.70668 measured for dolostones of members A and B of the Tulomozero Formation, southeastern Karelia, which have been similarly deposited in isolated shallow-water ponds (Gorokhov *et al.*, 1998; Kuznetsov *et al.*, 2000). It is remarkable that carbonates of the Dunphy Formation and lower dolostone members of the Tulomozero Formation overlie the alluvial-deltaic red beds and represent transitional lagoonal-sabkha facies deposited at the beginning of transgressive cycle. In addition, the elevated Mg/Ca ratios represent a peculiar characteristic of lowermost carbonate beds of both aforementioned formations (Table 1), and this feature is indirect evidence in favor of carbonate accumulation in isolated paleobasins (Gorokhov *et al.*, 1998).

In general, the Sr isotope parameters in carbonates from lower formations of the Kaniapiskau Supergroup of the Canadian Shield and from the Upper Jatulian

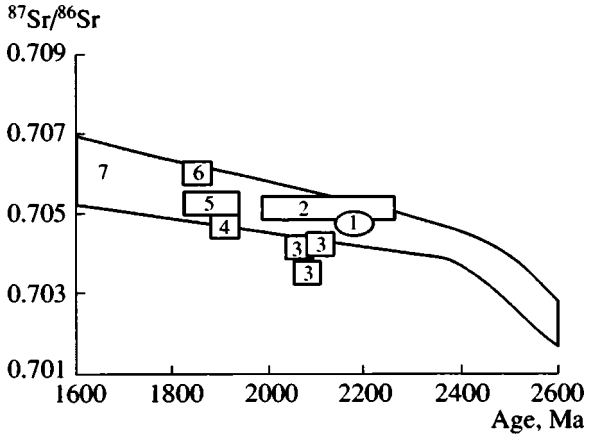

Fig. 7. Secular variations of $^{87}Sr/^{86}Sr$ ratio in Paleoproterozoic seawater: (1) Alder Formation, Kaniapiskau Supergroup (this work); (2) Wyloo Group (Veizer *et al.*, 1992); (3) Tulomozero Formation, Upper Jatulian (Gorokhov *et al.*, 1998): (4) Coronation Supergroup (Veizer *et al.*, 1992); (5) Phethei Group (Whittaker *et al.*, 1998); (6) Misstassini Group (Mirota and Veizer, 1994); (7) generalized trend (Veizer and Compston, 1976).

succession of the Baltic Shield (Karelia) suggest that the $^{87}Sr/^{86}Sr$ ratio in the Paleoproterozoic ocean decreased in the time span of 2.17–2.06 Ga from 0.7048 to 0.7034. The low $^{87}Sr/^{86}Sr$ ratio in seawater about 2.0 Ga ago may reflect a decrease of this parameter in the continental runoff in response to a greater proportion of eroded juvenile material and low erosion rate of concurrent collisional and accretionary orogens that was characteristic, for instance, of the post-Grenvillian Earth's history 1.05–0.8 Ga ago (Semikhatov *et al.*, 2002). However, significant orogenic events, "tectonic activations," or emergences of collisional structures were untypical of the early Paleoproterozoic time under consideration (2.3–2.0 Ga ago). In contrast, it was a time of a vast marine transgression that flooded considerable areas of stable post-Archean cratons and resulted in appearance of numerous shallow basins favorable for accumulation of carbonate sediments and evaporites (Dimroth, 1970; Hoffman, 1989; Semikhatov and Raaben, 1994, 1996; Akhmedov *et al.*, 1996; Melezhik *et al.*, 1997a, 1997b, 1999; Semikhatov *et al.*, 1999). These data inconsistent with the continental runoff increase at that time discredit the assumption that accumulation of Paleoproterozoic carbonates with extremely high $\delta^{13}C$ values can be indicative of the intense continental erosion and high burial rate of organic carbon.

Data on carbon isotope composition in carbonates of the Kaniapiskau Supergroup, Upper Jatulian succession of Karelia, and some other Paleoproterozoic formations show that $\delta^{13}C$ values in marine carbonates accumulated 2.3–2.0 Ga ago are usually not greater than +6‰ PDB, whereas in contemporaneous carbonate rocks with cyanobacterial buildups, which have been deposited in isolated basins, these values could be

as high as +15.4 to +16.7‰ PDB (Melezhik *et al.*, 1997a, 1999). Thus, the specific environments and enlarged distribution areas of cyanobacterial communities can be regarded as local factors responsible for accumulation of carbonates with extremely high $\delta^{13}C_{carb}$ values 2.3–2.0 Ga ago (Melezhik *et al.*, 1997b, 1999; Semikhatov *et al.*, 1999). The worldwide distribution of Paleoproterozoic carbonates with $\delta^{13}C$ values of about +6‰ PDB needs however in the other explanation.

CONCLUSION

Lower carbonate horizons of the Kaniapiskau Supergroup were partially dedolomitized probably at the time of intense tectono-thermal activation that terminated 1.8 Ga ago and caused metamorphism of volcanogenic-sedimentary deposits of the Labrador trough. The isotopic-geochemical approach and stepwise dissolution of carbonates were used to select carbonate samples of that supergroup with the least-altered Rb-Sr systems. The $^{87}Sr/^{86}Sr$ initial ratios in these samples can be regarded as reflecting the Sr isotope composition in sedimentation medium.

The low $^{87}Sr/^{86}Sr$ ratios in early Paleoproterozoic marine carbonates (0.70479, Alder Formation 2.15 Ga old, and 0.70343–0.70419, Tulomozero Formation 2.10–2.06 Ga old) suggest either an insignificant continental runoff into oceans of that time, or a considerable proportion of eroded juvenile material in the runoff. The analyzed general paleogeographic environments of the geological time span under consideration are in favor of the first assumption. Consequently, it is necessary to exclude a high erosion rate from possible factors responsible for the intense burial of organic carbon at the beginning of the Paleoproterozoic.

ACKNOWLEDGMENTS

We are grateful to M.A. Semikhatov and V.A. Ponomarchuk for their constructive comments used to improve our original manuscript, and to I.V. Kislova who donated data on concentrations of trace elements in the studied samples. We also thank G.V. Konstantinova, T.L. Turchenko, and E.P. Kutyavina for their assistance in analytical work. Our work was supported by the Russian Foundation for Basic Research, project nos. 00-05-64915 and 00-05-72011, by the INTAS project 99-9024, and by the Youth Commission of Russian Academy of Sciences, project no. 301.

Reviewers V.A. Ponomarchuk and M.A. Semikhatov

REFERENCES

Akhmedov, A.M., Travin, L.V., and Tikhomirova, M., Glaciation and Evaporite-Accumulation Epochs of the Paleoproterozoic and Interregional Correlation, *Reg. Korrelyatsiya Metallogeniya*, 1996, no. 5, pp. 84–97.

Baker, A.J. and Fallick, A.E., Evidence from Lewisian Limestone for Isotopically Heavy Carbon in Two-Thousand-Million-Year-Old Sea Water, *Nature* (London), 1989, vol. 337, pp. 352–354.

Banner, J.L., Wasserburg, G.J., Dobson, P.F., *et al.*, Isotopic and Trace Element Constraints on the Origin and Evolution of Saline Groundwaters from Central Missouri, *Geochim. Cosmochim. Acta*, 1989, vol. 53, no. 3, pp. 383–398.

Barnaby, R.J. and Read, J.F., Dolomitization of a Carbonate Platform during Late Burial: Lower to Middle Cambrian Shady Dolomite, Virginia Appalachians, *J. Sediment. Petrol.*, 1992, vol. 62, no. 6, pp. 1023–1043.

Brand, U. and Veizer, J., Chemical Diagenesis of a Multicomponent Carbonate System: 1. Trace Elements, *J. Sediment. Petrol.*, 1980, vol. 50, no. 4, pp. 1219–1236.

Brand, U. and Veizer, J., Chemical Diagenesis of a Multicomponent Carbonate System: 2. Stable Isotopes, *J. Sediment. Petrol.*, 1981, vol. 51, no. 3, pp. 987–997.

Chaudhuri, S. and Clauer, N., Strontium Isotopic Compositions and Potassium and Rubidium Contents of Formation Waters in Sedimentary Basins: Clues to the Origin of the Solutes, *Geochim. Cosmochim. Acta*, 1993, vol. 57, no. 2, pp. 429–437.

Chaudhuri, S., Broedel, V., and Clauer, N., Strontium Isotopic Evolution of Oil-Field Waters from Carbonate Reservoir Rocks in Bindley Field, Central Kansas, USA, *Geochim. Cosmochim. Acta*, 1987, vol. 51, no. 1, pp. 45–53.

Cheve, S.R., Schrijver, K., and Tasse, N., Cryptalgalaminate Dolomite of the Dunphy Formation, Labrador Trough: Diagenetic and Tectono-Metamorphic Evolution Related to Copper Mineralization, *Can. J. Earth, Sci.*, 1985, vol. 22, no. 12, pp. 1835–1857.

Chilingare, G.V., Bissell, J., and Fairbridge, R.W., Carbonate rocks, I. Origin, Occurrence and Classification. II. Physical and Chemical Aspects, *Developments in Sedimentology*, London: Wiley, 1967, vols. 9A, 9B.

Derry, L.A., Kaufman, A.J., and Jacobsen, S.B., Sedimentary Cycling and Environmental Change in the Late Proterozoic: Evidence from Stable and Radiogenic Isotopes, *Geochim. Cosmochim. Acta*, 1992, vol. 56, no. 3, pp. 1317–1329.

Des Marais, D.J., Tectonic Control of the Crustal Organic Carbon Reservoir during the Precambrian, *Chem. Geol.*, 1994, vol. 114, no. 3/4, pp. 303–314.

Des Marais, D.J., Strauss, H., Summons, R.E., and Hayes, J.M., Carbon Isotope Evidence for the Stepwise Oxidation of the Proterozoic Environment, *Nature* (London), 1992, vol. 359, pp. 605–609.

Dimroth, E., Evolution of the Labrador Geosyncline, *Geol. Soc. Amer. Bull.*, 1970, vol. 81, no. 9, pp. 2717–2742.

Dimroth, E., *Region de la Fosse du Labrador (54°30′ and 56°30′)*, Ministere des Ressources naturelles du Quebec, RG 193, 1978.

Fryer, B.J., Age Determinations in the Circum-Ungava Geosyncline and the Evolution of Precambrian Banded Iron-Formations, *Canad. J. Earth Science*, 1972, vol. 9, no. 6, pp. 652–663.

Galimov, E.M., Factors Controlling Global Variations of Carbon Isotope Composition in Biosphere, *Geokhimiya*, 1999, no. 8, pp. 787–803.

Galimov, E.M., Migdisov, A.A., and Ronov, A.B., Variations of Carbonate Carbon Isotope Composition in Sedimentary

Rocks in the Earth's History, *Geokhimiya*, 1975, no. 3, pp. 323–342.

Gorokhov, I.M., Diagenesis of Carbonate Sediments: Behavior of Trace Elements and Sr Isotopes, *Litologiya i paleogeografiya. Vyp. 4* (Lithology and Paleogeography), Verba, Yu.L., Ed., St. Petersburg: SPb. Gos. Univ., 1996, pp. 141–164.

Gorokhov, I.M., Kuznetsov, A.B., Melezhik, V.A., *et al.*, Sr Isotope Composition in the Upper Jatulian Dolostones of the Tulomozero Formation, Southeastern Karelia, *Dokl. Ross. Akad. Nauk*, 1998, vol. 360, no. 4, pp. 533–536.

Gorokhov, I.M., Semikhatov, M.A., Baskakov, A.V., *et al.*, Sr Isotopic Composition in Riphean, Vendian, and Lower Cambrian Carbonates from Siberia, *Stratigr. Geol. Korrelyatsiya*, 1995, vol. 3, no. 1, pp. 3–33.

Hartmann, B.H., Ramseyer, K., and Matter, A., Diagenesis and Pore-water Evolution in Permian Sandstones, Gharif Formation, Sultanate of Oman, *J. Sediment. Research*, 2000, vol. 70, no. 3, pp. 533–544.

Hoffman, F., Precambrian Geology and Tectonic History of North America, The Geology of North America, *Geol. Soc. America*,1989, vol. A, pp. 447–512.

James, N.P. and Choquette, P.W., Diagenesis 6. Limestones—The Sea Floor Diagenetic Environment, *Geosci. Canad.*, 1983, vol. 10, no. 4, pp. 162–179.

Karhu, J.A., Palaeoproterozoic Evolution of the Carbon Isotope Ratios of Sedimentary Carbonates in the Fennoscandian Shield, *Geol. Surv. Finland Bull.*, 1993, vol. 371, no. 1, pp. 1–87.

Kharaka, Y.K. and Thordsen, J.J., Stable Isotope Geochemistry and Origin of Waters in Sedimentary Basins, Isotopic Signatures and Sedimentary Records, *Lect. Notes Earth Sci.*, 1992, vol. 43, pp. 411–466.

Knoll, A.H. and Sweet, K., Carbonate Deposition during the Late Proterozoic Era: An Example from Spitsbergen, *Amer. J. Sci.*, 1990, vol. 290-A, pp. 104–132.

Kuznetsov, A.B., Gorokhov, I.M., Melezhik, V.A., *et al.*, Geochemical and Isotopic Study of Paleoproterozoic Carbonate Rocks from the Canadian and Baltic Shields: variations of $^{87}Sr/^{86}Sr$ Ratio in the Jatulian Seawater, *Obshchie voprosy raschleneniya dokembriya* (General Problems Concerning Subdivision of the Precambrian), Apatity: MUP Poligraf, 2000, pp. 132–133.

Kuznetsov, A.B., Gorokhov, I.M., Semikhatov, M.A., *et al.*, Dolomitization of Upper Riphean Carbonates, the Min'yar Formation of the Karatau Group, Southern Urals, *Osadochnye formatsii dokembriya i ikh rudonosnost', Tez. dokl.*, (Abstracts of Conference: Precambrian Sedimentary Formations and their Mineral Reserves), St. Petersburg, 1998, p. 31.

Kuznetsov, A.B., Semikhatov, M.A., Gorokhov, I.M., and Mel'nikov, N.N., Sr Isotopic Composition in Limestones of the Inzer Formation, the Upper Riphean Stratotype, Southern Urals, *Dokl. Ross. Akad. Nauk*, 1997, vol. 353, no. 2, pp. 249–254.

Ovchinnikova, G.V., Vasil'eva, I.M., Semikhatov, M.A., *et al.*, U-Pb Systematics on Proterozoic Carbonate Rocks: The Inzer Formation of the Upper Riphean Stereotype (Southern Urals), *Stratigr. Geol. Korrelyatsiya*, 1998, vol. 6, no. 4, pp. 20–31.

Ovchinnikova, G.V., Vasil'eva, I.M., Semikhatov, M.A., *et al.*, The Pb-Pb Trail Dating of Carbonates with Open U-Pb Systems: The Min'yar Formation of the Upper Riphean Stratotype, Southern Urals, *Stratigr. Geol. Korrelyatsiya*, 2000, vol. 8, no. 6, pp. 3–19.

Semikhatov, M.A. and Raaben, M.E., Dynamics of the Global Diversity of Proterozoic Stromatolites. Article 1: Northern Eurasia, China, and India, *Stratigr. Geol. Korrelyatsiya*, 1994, vol. 2, no. 6, pp. 10–32.

Semikhatov, M.A. and Raaben, M.E., Dynamics of the Global Diversity of Proterozoic Stromatolites. Article 2: Africa, Australia, North America, and General Synthesis, *Stratigr. Geol. Korrelyatsiya*, 1996, vol. 4, no. 1, pp. 26–54.

Semikhatov, M.A., Raaben, M.E., Sergeev, V.N., *et al.*, Biotic Events and Positive δC_{carb} Anomaly at 2.3–2.06 Ga, *Stratigr. Geol. Korrelyatsiya*, 1999, vol. 7, no. 5, pp. 3–27.

Semikhatov, M.A., Kuznetsov, A.B., Gorokhov, I.M., *et al.*, Low $^{87}Sr/^{86}Sr$ Ratios in Seawater of the Grenville and Post-Grenville Time: Determining Factors, *Stratigr. Geol. Korrelyatsiya*, vol. 10, no. 1, pp. 3–46.

Vasil'eva, I.M., Ovchinnikova, G.V., Kuznetsov, A.B., *et al.*, Evolution of Pb-Pb Systems in Upper Jatulian Carbonates of the Tulomozero Formation, Southeastern Karelia, *Tez. dokl., 15-i Simpozium po geokhimii izotopov* (Abstracts, 15th Symposium on Isotopic Geochemistry), Moscow, 1998, pp. 42–43.

Vasil'eva, I.M., Ovchinnikova, G.V., Melezhik, V.A., *et al.*, Pb–Pb Age of Carbonate Rocks from the Tulomozero Formation, Northern Onega Lake Region, *Obshchie voprosy raschleneniya dokembriya* (General Problems Concerning Subdivision of the Precambrian), Apatity: MUP Poligraf, 2000, pp. 53–54.

Yudovich, Ya.E., Maidl', T.V., and Ivanova, T.I., *Geokhimiya strontsiya v karbonatnykh otlozheniyakh* (Strontium Geochemistry of Carbonate Deposits), Leningrad: Nauka, 1980.

Yudovich, Ya.E., Makarikhin, V.V., Medvedev, P.V., and Sukhanov, N.V., Carbon Isotopic Anomalies in Carbonates of the Karelian Complex, *Geokhimiya*, 1990, no. 7, pp. 972–978.

Stratigraphy and Geological Correlation, Vol. 11, No. 3, 2003, pp. 220–230. Translated from Stratigrafiya. Geologicheskaya Korrelyatsiya, Vol. 11, No. 3, 2003, pp. 15–26.
Original Russian Text Copyright © 2003 by Leven.
English Translation Copyright © 2003 by MAIK "Nauka/Interperiodica" (Russia).

Diversity Dynamics of Fusulinid Genera and Main Stages of Their Evolution

E. Ya. Leven

Geological Institute, Russian Academy of Sciences, Pyzhevskii per. 7, Moscow, 119017 Russia

Received March 9, 2001

Abstract—Curves depicting the diversity dynamics of fusulinid genera in general and in some individual biogeographic provinces are plotted. Some of them illustrate dynamics of appearance and extinction of fusulinid genera and orders. As is evident from the curves, there were three major stages in the fusulinid evolution, each beginning with the diversity increase (the Moscovian, Asselian and Midian peaks) and ending with the diversity minimum (the early Gzhelian, late Kungurian, and late Dorashamian minima). In addition to three major stages, several second-order stages can be distinguished. The diversity peaks were likely associated with extensive transgressions, which might enlarge the habitat areas of fusulinids, thus favoring appearance of new taxa adapted to different environments, and represented the main controlling factor. These peaks were followed by extinctions, the greatest of which took place in the late Moscovian, post-Sakmarian, late Kungurian, late Midian, and late Dorashamian epochs. The latter two were of catastrophic character: nearly 80% of fusulinid genera became extinct in the late Midian and all others in the late Dorashamian time. The extinctions mostly affected the highly specialized taxa far advanced in their evolution. The origin of new elements in the assemblages that replaced the disappearing ones was confined to crises in the fusulinid evolution.

Key words: fusulinids, evolutionary stages, diversity, diversification, extinction.

INTRODUCTION

Much attention has been recently given to dynamics of taxonomic diversity of different fossil groups throughout the Phanerozoic and to possible factors responsible for secular variations of taxa abundance. Fusulinids, which were most diverse and widespread organisms of the Carboniferous and Permian periods, have not been subjected to analysis, however. Some calculations were made only in connection with the late Early Permian ecosystem changes and with the Late Permian extinction events (Leven *et al.*, 1996; Leven and Korchagin, 2001). This article is aimed to fill the gap. The calculations presented are mainly based on the reference book on taxonomy of Paleozoic foraminifers (Rauser-Chernousova 1996) with my amendments. In total, 220 genera and subgenera were involved into analysis. To check the results, additional calculations were made using data from works "Foraminiferal Genera and Their Classification" by Loeblich and Tappan (1987) and "Composition, Systematics, and Phylogeny of the Order Fusulinida" by Rozovskaya (1975). The taxonomic diversity was estimated separately for the every age endings (Figs. 1, 2, 6) and for the first and second halves of the ages (Figs. 3–5). It is to be noted that the exact appearance and extinction times of many taxa have not been defined so far. The plotted curves, informative as they are, have to be verified in the future. Because the ages are of unequal duration, the results obtained cannot be used to estimate the real (absolute) rate of evolution of the faunal group under consideration. In addition, radiometric dates determine durations of different ages with such a large uncertainty (e.g., 10 to 16 myr for the Moscovian, 3 to 10 myr for the Asselian, 2 to 10 myr for the Kungurian and Kubergandian, and so on) that the usage of astronomical time scale seems impossible at present.

DIVERSITY DYNAMICS OF FUSULINID GENERA

The secular diversity dynamics of genera estimated based on the guidebook of Rauser-Chernousova *et al.* (1996) is shown in Fig. 1 (curve *1*). Fusulinids appeared first in the Visean, when they were represented by few genera. Their diversification began in the Bashkirian to reach the maximum in the Moscovian. The number of genera was rapidly and noticeably reduced in the Kasimovian, increased again in the Gzhelian through Asselian, and decreased afterward until the Kungurian time. A steady growth of generic diversity in the Kubergandian through Midian was followed by a sharp reduction of genera number across the Midian–Dzhulfian boundary time and by a steady and insignificant decrease during the Dzhulfian and Dorashamian. Fusulinids became extinct at the end of the Dorashamian.

Thus, the diversity curve shows three peaks of the Moscovian, Asselian and Midian epochs separated with two, the Kasimovian and Kungurian minima. Calculations based on the American guidebook (Loeblich and

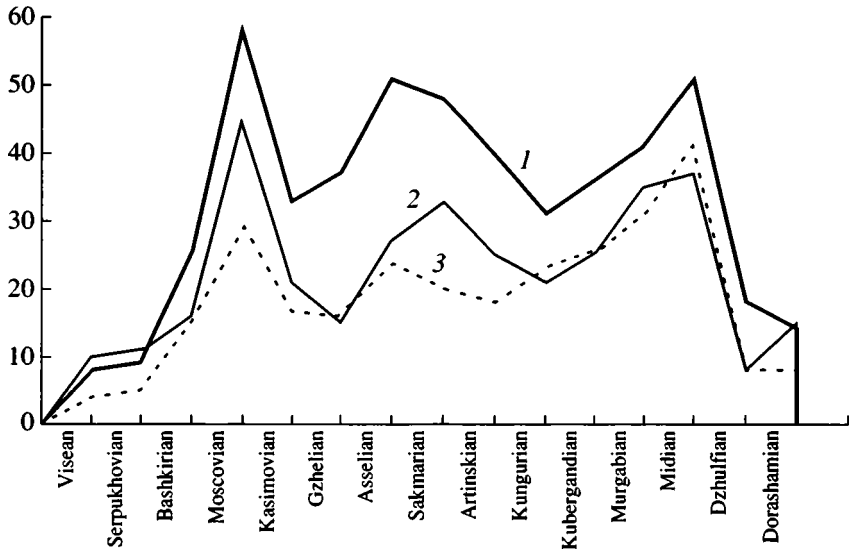

Fig. 1. Quantitative secular variations of fusulinid genera (total per ages) according to data by Rauser-Chernousova *et al.*, 1996 (*1*), Loeblich and Tappan, 1987 (*2*), and Rozovskaya, 1975 (*3*).

Tappan, 1987) yielded an analogous picture (Fig. 1, curve *2*) with the differences that the second peak is shifted from the Asselian to the Sakmarian and the total quantity of genera is less than that calculated based on data by Rauser-Chernousova her colleagues. Curve *3* in Fig. 1 depicts the calculation results based on the fusulinid systematics by Rozovskaya (1975). Like in the curve *1*, one can see the Moscovian, Asselian and Midian peaks, but the former two are much lower than their counterparts in other curves. In addition, the diversity minimum after the Asselian peak corresponds in this case to the Artinskian Age with the subsequent growth of genera number. The more complicated patterns have been obtained after calculations for the substage intervals (Fig. 2). The Late Carboniferous minimum of diversity is now displaced from the Kasimovian to the terminal early Gzhelian. The Asselian-Sakmarian maximum is divided into the late Asselian and late Sakmarian peaks with a minor diversity decrease against boundary between these ages. The Kungurian minimum widens to the Kubergandian, and the curve goes upward beginning from the Murgabian.

Being based on different systematics of fusulinids, all the curves in Fig. 1 show large peaks, which are approximately concurrent and can be considered as objectively reflecting the general evolutionary trends of the fossil group under consideration. At the same time, the results of calculations appear to be strongly dependent on the fusulinid systematics taken for the base. The curve based on the earliest, and thus less elaborated, system of Rozovskaya (1975) is the least fluctuating and lowest one. The most distinct peaks are characteristic of the upper curve that is based on reference book of 1996 whose authors established many new taxa, including those of the generic rank. The calculation results evidently depend on subjective factors and need to be treated with caution: the curves depict more or less confidently the greatest and most significant changes in the generic diversity, while other results may be misleading.

The curves under consideration characterize in general all the data on fusulinids. It is reasonable to ask, however, whether the mentioned peculiarities of the curves depict the general trends of the global fusulinid evolution, or they represent a superposition (summarization) of trends characteristic of different biogeographic areas and provinces, in which the diversity variation could be very different. To answer the question, the general curve (Fig. 3, curve *1*) was compared with the others plotted in Fig. 3 for the main habitat provinces of fusulinid, i.e., for the Tethys (Fig. 3, curve *2*), Eastern Europe (Fig. 3, curve *3*), North America (Fig. 3, curve *4*), and southern Peri-Gondwanan part of the Tethys (Fig. 3, curve *5*). The general curve (*1*) almost completely coincides with the Tethyan one (*2*), thus indicating that the presumable global trend of fusulinid genera diversity is greatly dependent on their evolution history in the Tethys, predominantly in the equatorial part of that ocean. The Visean-Sakmarian interval of the East European curve (*3*) is similar to that of the Tethyan curve (*2*). This can be easily explained by the fact the pre-Sakmarian East European basin was closely connected with the Tethys, representing virtually its northern periphery. Since the latest Sakmarian, the East European basin became isolated from the Tethys, and this affected development of fusulinids. Because of progressing salinization of that basin, their diversity rapidly decreased, and they become completely extinct in the Kungurian time.

Curve *4* evidences in favor of essentially lower diversity of fusulinid genera in the North American

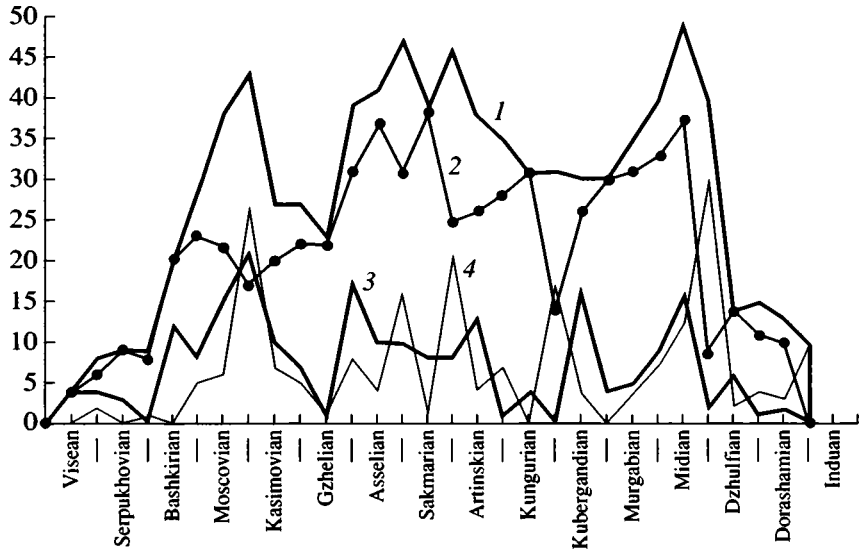

Fig. 2. Quantitative secular variations of fusulinid genera (total per subages): (*1*) all, (*2*) transitional, (*3*) newly appeared, and (*4*) extinct genera.

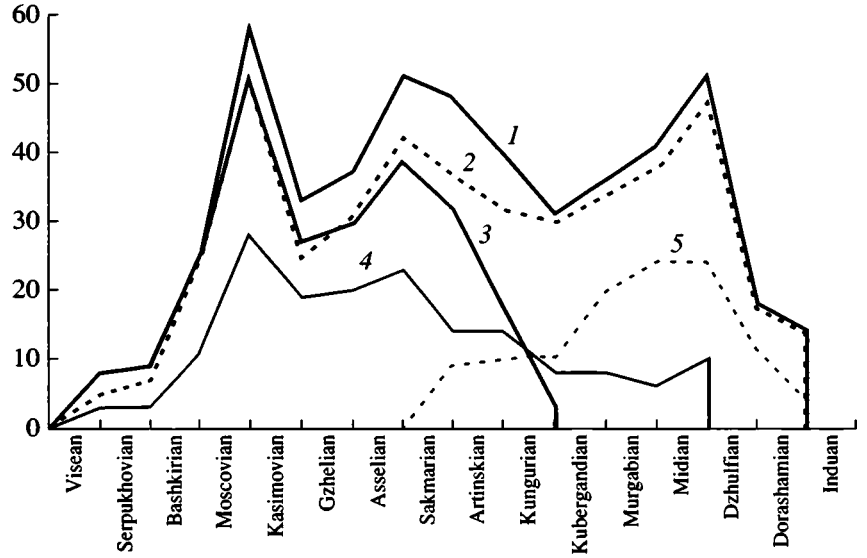

Fig. 3. Quantitative secular variations of fusulinid genera (total per ages): (*1*) over the globe, (*2*) in the Tethys, southern Peri-Tethys included, (*3*) in the East European basin, (*4*) in Texas, western United States, (*5*) in the southern Peri-Tethys.

basin, which had a limited or no connection with the Tethyan and East European basins during the greater part of the Carboniferous–Permian time interval. This basin was connected with the Tethys from time to time in the Early-Middle Carboniferous. Therefore the Visean-Moscovian segments of corresponding curves are identical more or less. Beginning from the Late Carboniferous, the North American fusulinids evolved autonomously, and their low diversity tended to be decreased further. In the latest Midian, the diversity slightly increased owing to the penetration of some Tethyan genera into the North American basin during the short-term transgression. Immediately after the transgression, the basin underwent a rapid salinization that caused the complete extinction of fusulinids.

As can be seen, the development of fusulinid communities, the diversity dynamics of their genera in particular, essentially varied in different basins corresponding to biogeographic regions. The variation trends were also not identical in the large basins, which occupied not a single, but two or three climatic belts. First of all, this concerns the East European and Tethyan basins with their zones adjacent to the cold Boreal and Notal provinces. A good example is the diversity dynamics of fusulinid genera in the Peri-

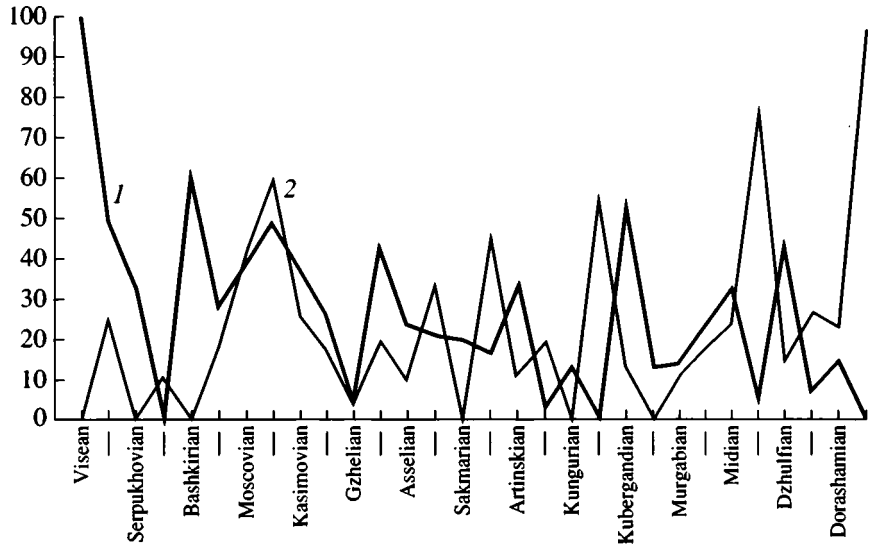

Fig. 4. Percentages of newly appeared (*1*) and extinct (*2*) fusulinid genera relative to their total amount.

Gondwanan parts of the Tethys, i.e., in the southern Afghanistan, southern Pamirs, eastern Hindu Kush, Karakorum, southern Tibet, Himalayas, and the Salt Range (Fig. 2, curve *5*). Fusulinids did not inhabit these regions until the Sakmarian because of the relatively cold climatic conditions induced by the Gondwana glaciation in the Late Carboniferous–Early Permian. The deglaciation and milder climate favored the local appearance of fusulinids in the late Sakmarian time (Dickins, 1985; Leven, 1993c). Their initially uniform assemblages show diversification beginning from the Kubergandian and have reached the generic diversity peak in the Midian, like the tropical assemblages of the Tethys. Then the generic diversity sharply decreased during the Dzhulfian and Dorashamian until the complete extinction of fusulinids by the beginning of the Triassic. Thus, the data on Peri-Gondwanan part of the Tethys show that the almost complete coincidence of the general and Tethyan trends in development of fusulinid genera is correct with respect to the tropical and subtropical parts of the Tethyan province only.

It was the geographic isolation of particular basins that resulted in different evolutionary trends of their fusulinid communities. I do not exclude the effect of other factors (historical, evolutionary, ecological), but they were likely of subordinate importance, derivative from the paleogeographic changes.

The general analysis of plotted curves leads to the following conclusions.

1. The global diversity dynamics of fusulinid genera is defined by their evolution in equatorial and tropical parts of the Tethyan province.

2. The most distinct are three diversity peaks of the Moscovian, Asselian–Sakmarian and Midian epochs, which are separated the late Kasimovian–early Gzhelian and the late Kungurian–early Kubergandian minima. According to calculations for the periods twice shorter than ages, the Asselian–Sakmarian peak likely consists of two, the late Asselian and late Sakmarian maximums separated by the early Sakmarian minimum.

3. The general curve of generic diversity variation is an integral result of data on extinction and appearance of taxa, which represents only a rough and partly distorted approximation to real events. For instance, that curve (Fig. 2, curve *1*) is lacking noticeable fluctuations in the Kungurian–Kubergandian interval. However, the Kungurian–Kubergandian boundary marks one of the most significant turning points in the fusulinid evolution: the great extinction of the latest Kungurian time was succeeded by the mass appearance of genera and higher rank taxa in the earliest Kubergandian epoch, when the fusulinid community was entirely renewed. Both events are not reflected in the general curve because the extinct Kungurian genera were compensated by appearance of the earliest Kungurian genera so that the total amount of taxa remained unchanged.

4. The fusulinid evolution is illustrated more emphatically by the variation curves depicting abundance (absolute and relative) of either the newly appeared and extinct genera (Fig. 2, curves *3*, *4*; Figs. 4, 5), or the genera, which crossed boundaries between the time intervals used by calculation (Fig. 2, curve *2*). Informative as well is the thick curve in Fig. 5 that shows the extent of taxonomic renewal across the boundaries between stages and substages that is defined as quantitative difference between genera, which appeared in the given period, and those, which became extinct in the previous one. One can judge from these curves about principal turning points in the fusulinid development, which are manifested in the extinction,

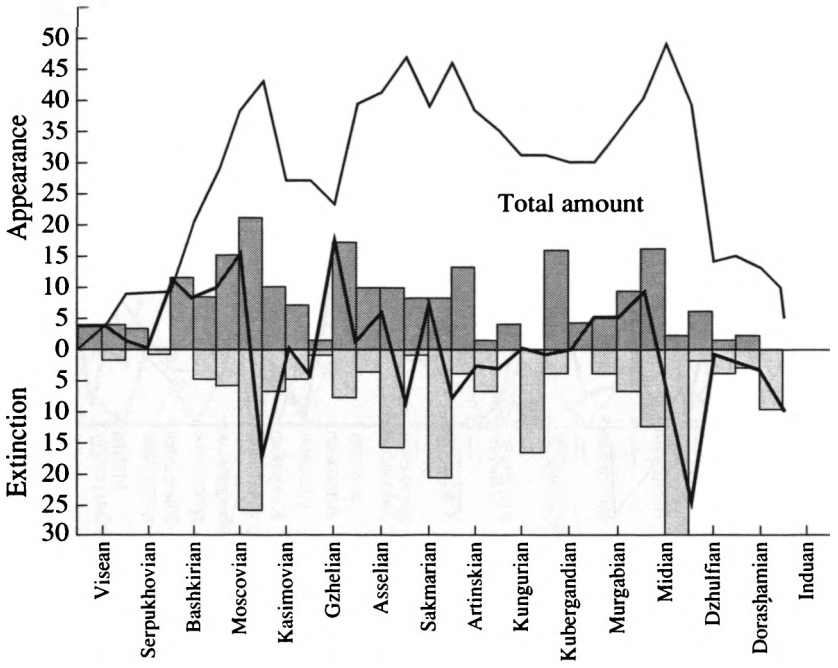

Fig. 5. Histogram illustrating proportions between newly appeared and extinct fusulinid genera against their quantitative secular variations.

diversification, and restoration peaks of their generic groups.

5. Besides the complete disappearance at the Permian–Triassic boundary time, the most significant extinctions of fusulinids occurred in the latest Moscovian, when 26 genera or 60% of their total amount in the age disappeared, and in the latest Midian, when 30 genera or 77% of the generic group became extinct (Fig. 2, curve *4*; Fig. 4, curve *2*). According to these assessments, both events of a comparable range can be regarded as catastrophes. However, this is not quite correct. The total amount of Moscovian genera is overestimated because of practice, frequently unjustified, to identify forms transitional between allied taxa as independent genera. The diversity variation curve based on data by Rozovskaya (Fig. 1), which do not account for genera distinguished later, implies amount of Moscovian genera that is two times lesser than that estimated based on recent publication taking into account all the genera established afterward. Such "transitional genera," which disappeared, as a rule, immediately after their appearance, enlarge the total magnitude of the genera extinction in the Moscovian time. The late Midian extinction was more significant than the latter, because two dominant orders of fusulinids completely disappeared in this age in addition to a greater number of genera (Fig. 6). All the facts mentioned above suggest that the late Midian event only can be considered as a catastrophe, after which the fusulinid biota was under stress until its complete extinction at the Permian–Triassic boundary time. The late Moscovian crisis was not so destructive and gave place shortly after to a rapid diversification of fusulinids.

Significant extinctions took place at the Sakmarian–Artinskian (21 genera, or 46%) and the Kungurian–Kubergandian (17 genera, or 55%) boundary epochs. Extinctions of lesser significance are recorded across the Asselian-Sakmarian boundary (16 genera, or 34%) and in terminal strata of the Gzhelian, Artinskian and Dzhulfian sequences (approximately 20–25% of total amount of genera). Ten genera survived till the Late Permian to disappear almost simultaneously near the Triassic boundary (Leven and Korchagin, 2001).

6. Figures 2, 4, and 5 show that events of renewal and extinction in fusulinid communities were irregular. Not always, the appearance of new genera immediately followed the extinction. For instance, the highest diversification and extinction peaks characterizing the second half of the Moscovian Age essentially compensated each other, because many short-lived genera became extinct soon after origin. The nature of these genera is briefly commented above. After the Moscovian–Kasimovian boundary crisis, the generic diversity was reducing until the first half of the Gzhelian because of extinction of persistent taxa. Some genera, such as *Obsoletes* and *Montiparus*, the taxa transitional between Fusulinida representatives with four-layer walls to Schwagerinida forms with walls having keriotheca, appeared and became extinct in the Kasimovian. The mass appearance of new genera began in the mid-Gzhelian to reach a peak in the latest Gzhelian–mid-Asselian. At the Asselian–Sakmarian boundary time there was an insignificant diversity decrease compen-

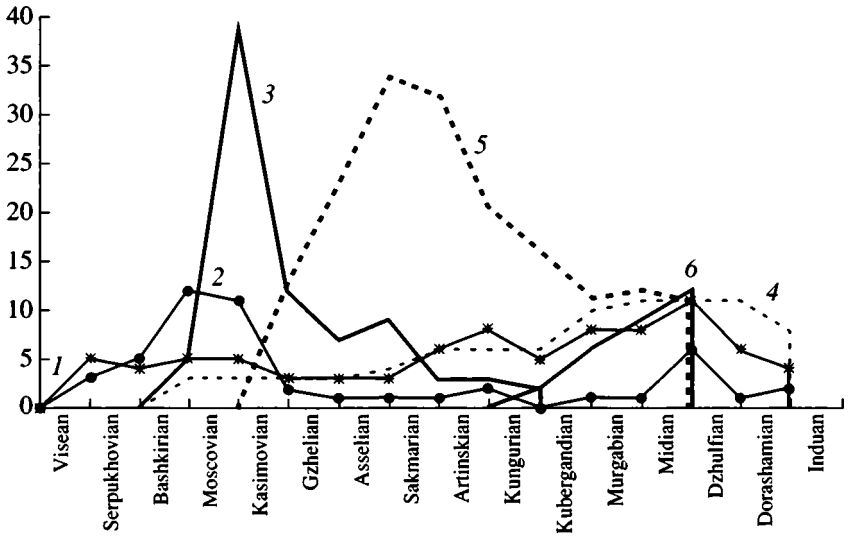

Fig. 6. Quantitative secular variations of fusulinid genera representing orders Staffellida (*1*), Ozawainellida (*2*), Fusulinida (*3*), Schubertellida (*4*), Schwagerinida (*5*), and Neoschwagerinida (*6*).

sated rapidly. The significant post-Sakmarian extinction was balanced a little by appearance of some new genera in the early Artinskian. The generation minimum (as well as the extinction maximum) occurred in the latest Kungurian to be followed by the new diversification outburst that gave birth to 16 genera, which represented 53% of the Kubergandian fusulinids. The generation rate became slower in the latest Kungurian, but afterward it rapidly increased to reach a maximum by the mid-Midian time. The catastrophic late Midian extinction was succeeded by the minor diversification peak in the early Dzhulfian–Dorashamian epoch before the complete extinction of fusulinids at the Permian–Triassic boundary.

MAIN STAGES IN FUSULINID EVOLUTION

Different views on stages and periodicity of fusulinid development have been discussed in works by Rauser-Chernousova (1961, 1963, 1965, 1968), Rauser-Chernousova and Reitlinger (1957), Reitlinger (1963, 1969), Solov'eva (1966), Ross and Ross (1987), and some others. Conclusions formulated by Rauser-Chernousova (1961, 1963), especially those on the Carboniferous history of fusulinids, fit the data of this article best of all. She interpreted their Permian history not quite correct, because data on the Middle and Late Permian fusulinids and their stratigraphic distribution were incomplete at that time.

The general curve of generic diversity variations clearly shows that the fusulinid history, beginning from their origination in the Visean and until the complete extinction at the Permian–Triassic boundary time, is divisible into three large stages. These are the Visean–Kasimovian, Gzhelian–Kungurian and Kubergandian–Dorashamian stages. Each stage began with the generic diversity increase that diminished after reaching a certain maximum. Being not uniform, they all consisted of several second-order stages, the largest of which were Visean–Serpukhovian (Stage 1 after Rauser-Chernousova, 1965, 1968), Bashkirian-Kasimovian (Stage 2 after Rauser-Chernousova), Gzhelian–Asselian (Stage 3 after Rauser-Chernousova), Sakmarian and Artinskian–Kungurian (Stage 4 after Rauser-Chernousova), Kubergandian, Murgabian–Midian, and Dzhulfian–Dorashamian (all three representing Stage 5 after Rauser-Chernousova).

The indicated stages of fusulinid development are considered below.

Visean–Serpukhovian Stage. The earliest subspherical and lentiform, laterally compressed fusulinid morphotypes appeared in the **Visean.** Being of a similar morphology, they differed in the wall structure, however, and gave rise to the orders Ozawainellida and Staffellida. There are known three families and seven genera of the late Visean time. In the **Serpukhovian** epoch, all the Visean genera, except for *Eoparastaffella*, still existed, being associated with two new Ozawainellida genera represented by evolute forms similar to *Millerella* that appeared earlier.

The Visean and Serpukhovian ages of development of primitive fusulinids genera, in terms of their abundance and degree of morphological diversity, can be considered in general as the origin stage of fusulinid community as a whole.

The Bashkirian–Kasimovian Stage marks the appearance the early *Bashkirian* fusulinids with elongated shells, which gave rise to the new orders Schubertellida and Fusulinida. The former included a single family and three genera, whereas the latter consisted of five families and eight genera owing to the rapid diver-

sification. The diversity maximum of Ozawainellida representatives corresponds to one family and 12 genera. The generic diversity of Staffellida was like that in the previous stage.

The **Moscovian** Age can be regarded in general as a time of maximum diversification of Fusulinida forms, which started in the Bashkirian. One more family appeared in addition to five families, which existed before. The order included 36 of 55 Moscovian genera in total. Orders Ozawainellida, Staffellida, and Schubertellida were at the previous level of taxonomic diversity. Across the Bashkirian–Moscovian boundary, there is recorded a minor extinction event that affected few Ozawainellida and Staffellida genera of a narrow distribution range.

The boundary time between the Moscovian and **Kasimovian** ages corresponds to a rapid and significant reduction of taxonomic diversity, primarily of Fusulinida taxa. The boundary was crossed by 3 of 6 families and 11 of 36 genera of the order, the majority of which disappeared in the early Kasimovian. Only 3 or 4 genera continued their evolution. One of them (*Quasifusulina*) appeared in the early Kasimovian and existed until the end of the Early Permian. The mentioned boundary is also marked by appearance of the earliest Schwagerinida forms representing two families (Triticitidae and Schwagerinidae) and 12 genera. The order Ozawainellida also went into crisis: 11 of 12 its genera became extinct, including the genus *Neostaffella* widespread in the late Moscovian time. Remaining at the low abundance level, two other orders Staffellida and Schubertellida remained without significant taxonomic changes. In general, the Kasimovian can be considered a period transitional between the predominance time of Fusulinida beginning from the Bashkirian and the prosperity period of Schwagerinida whose representatives first appeared in the Kasimovian and then became abundant in the Gzhelian, Asselian (abundance peak), and the Sakmarian.

Gzhelian–Asselian Stage. A rapid increase of general taxonomic diversity, especially intense diversification of Schwagerinida, which got two new families (Rugosofusulinidae and Pseudofusulinidae) represented by 13 genera, discriminate the **Gzhelian** from the Kasimovian. The order included 23 genera in total. Four other orders inherited from the Kasimovian consisted of 12 genera, 6 of which belonged to Fusulinida. The **Asselian** was characterized by further increasing general taxonomic diversity. Schwagerinida (34 genera), especially their families Schwagerinidae (8 genera) and Pseudofusulinidae (13 genera), were at their diversification peaks. There were no changes in taxonomic compositions of Fusulinida, Ozawainellida, Staffellida and Schubertellida, except for the appearance of a new family Boultoniidae (Schubertellida) represented by a single genus. At the Asselian–Sakmarian boundary time, 11 Schwagerinida and 4 Fusulinida genera, most of which appeared in the Late Carboniferous, became extinct.

Sakmarian Stage. During the **Sakmarian** time, the generic diversity of fusulinids was rapidly restored and quickly reached the Asselian level. It was the appearance time of a new Schubertellidae genus, three Staffellidae genera, and of the mentioned Schwagerinida families. At the Sakmarian–Artinskian boundary time, almost a half of the Sakmarian genera (21) became extinct, among them 18 of the families Pseudofusulinidae and Schwagerinidae, order Schwagerinida.

Artinskian–Kungurian Stage. Among 13 new genera, which appeared in the **Artinskian**, six were of the order Schwagerinida. *Parafusulina*, the first genus of the family Polydiexodinidae, was widespread in the Middle Permian. The majority of newly appeared genera represented the order Staffellida, and some of them (*Staffella, Nankinella*) became widespread in the Middle–Late Permian. Of special importance was the appearance of *Pamirina*, which is conventionally referred to the family Eostaffellidae of the order Ozawainellida. This genus is the ancestor of higher fusulinids of the order Neoschwagerinida whose forms dominated in the Middle Permian. The inconsiderable Artinskian peak of diversification was replaced by the **Kungurian** stagnation and then by extinction of more than a half of genera (16 of 28) at the end of the latter. In general, the Kungurian fusulinid community did not differ essentially from the Artinskian one. Only two new genera appeared in the former, one of which (*Nagatoella*) became extinct in the early Kubergandian, but the other one (*Misellina*), which originated from the Artinskian *Pamirina*, was the first representative of multiapertural higher fusulinids of the order Neoschwagerinida.

Kubergandian Stage. The Kungurian–Kubergandian boundary marks a rather remarkable moment in development of fusulinids, i.e., the extinction of majority of the formerly existing genera and subsequent rapid diversification of the families, which became dominant in the Middle Permian. These were mostly Neoschwagerinida representatives, which included, along with Misellinidae of the Kungurian origin, new families Neoschwagerinidae (*Cancellina*), Verbeekinidae (*Paramisellina*), and Pseudodoliolinidae (*Pseudodoliolina*). Dominants also changed in the order Schwagerinida. *Pseudofusulina* and allied genera, which dominated in the Early Permian, especially in the Artinskian–Kungurian time span, were replaced, beginning from the Kubergandian, by *Chusenella, Skinnerella*, and *Parafusulina*. Probably in the late Kubergandian, the last genus gave rise to *Eopolydiexodina* very characteristic of the Middle Permian. In the order Schubertellida there appeared the family Yangchienidae, representatives of which are typical of the Middle Permian. The order Staffellida also experienced a certain renewal. The Kubergandian can be regarded in general

as a formation time of the Middle Permian fusulinid community that mostly consisted of the Neoschwagerinida representatives. In total, there were 30 Kubergandian genera of fusulinids.

Murgabian–Midian Stage. In terms of fusulinid development, the **Murgabian** was a continuation of the Kubergandian. All the previous genera passed into the Murgabian. Further branching of the Neoschwagerinida phylogenetic tree resulted in appearance of the family Sumatrinidae and genera *Verbeekina* and *Neoschwagerina*, which represented corresponding families. Representatives of Schwagerinida, genera *Parafusulina, Skinnerella, Chusenella*, and multiapertural *Eopolydiexodina* of the Kubergandian origin included, were still most widespread and significant components of the fusulinid community. Multiapertural forms of Schwagerinida (*Skinerrina*) originated at the stage under consideration in the North American basin. In total, there were 36 Murgabian genera of fusulinids.

The **Midian** was a time of the maximal fusulinid diversity in their history. Formally, the quantity of Midian genera is comparable with that of the Moscovian ones, but this can be an overestimation, because many short-lived genera are defined based on unjustified detailing. Among 51 Midian genera, 12 correspond to highly specialized taxa of Neoschwagerinida, and orders Schwagerinida, Staffellida, and Schubertellida included 11 genera each, i.e., all these orders were slightly more diverse than the Murgabian ones. The diversity increase was also characteristic of Ozawainellida (6 genera). It is remarkable that among Ozawainellida and Schubertellida there appeared the so-called "aberrant" taxa with uncoiled last whorl of the spiral (*Reichelina, Codonofusiella, Lantschichites*, and *Paradoxiella*).

Dzhulfian–Dorashamian Stage. The boundary between the Midian and **Dzhulfian** ages marks the most significant and rapid extinction of fusulinids in their history, and this event can be reasonably considered as catastrophic. Thirty genera, or 77% of their overall quantity (39), disappeared at that time or slightly earlier. Two of five orders (Schwagerinida and Neoschwagerinida) disappeared completely. The crisis also affected other orders. Two of four Schubertellida families (Schubertellidae and Yangchienidae) did not crossed the boundary. *Reichelina* was the only survived genus of Ozawainellida. Staffellida suffered least of all, but they lost the families Cheniidae and Kahlerinidae. The generic diversity of Schubertellida did not change, because amounts of the extinct and newly appeared genera were equal. Orders Staffellida and Ozawainellida had two and six times less genera than before. In total, there were 18 Dzhulfian genera.

Twelve genera typical of the early **Dorashamian** survived till the end of the age, and only two new genera appeared. The dominating components of the Dorashamian community were representatives of Palaeofusulinidae (Schubertellida), the majority of which originated in the Dzhulfian. At the end of the Dorashamian, fusulinids became completely extinct.

Thus, the Murgabian and, especially, the Midian are ages of peak development of fusulinids, which became highly specialized and diverse, whereas the Dzhulfian and Dorashamian can be regarded, despite certain diversification of Schubertellida, as epochs of few taxa, which survived the Midian–Dzhulfian crisis.

Stages in development of fusulinids, which are discussed above in terms of their generic diversity dynamics, let me to formulate the following conclusions.

1. It is apparent that periods of the highest generic diversity correspond to three first-order stages in the fusulinid development and primarily reflect the evolutionary cycles of the orders Fusulinida, Schwagerinida, and Neoschwagerinida (Fig. 6).

2. Earliest representatives of orders and families, which dominate in either of three cycles, originated at the time of preceding crises, each marked by the fusulinid diversity minimum. For instance, Schwagerinids originated by means of transformation of four-layer shell walls typical of Fusulinida forms, which dominated in the Moscovian fusulinid community, into the forms having two-layer shells with keriotheca. These progressive changes were characteristic of the family Fusulinellidae only. Other families of the order died out, and the only genus *Quasifusulina* (Fusulinidae) survived till the end of the Early Permian. Thus, there was a close the dominant orders of the first and second stages of the fusulinid development had direct genetic links. To the contrary, *Pamirina*, the ancestral genus of the order Neoschwagerinida that dominated in the third stage, appeared suddenly in the earliest Artinskian. It was probably related in origin with the genus *Eostaffella*, which can be attributed to the so-called "lazarus-taxa," because its last occurrence is established in the Moscovian. The order Schwagerinida that dominated during the preceding stage continued its evolution in the third stage, though having a considerably reduced number of constituent genera, as compared with their diversity maximum in the Asselian and Sakmarian.

3. Many rapidly progressing phylogenetic lines, e.g., *Profusulinella–Aljutovella–Beedeina* of Fusulinida or *Misellina–Cancellina–Neoschwagerina–Yabeina* and *Misellina–Cancellina–Presumatrina–Afghanella–Sumatrina* of Neoschwagerinida, produced taxa of the most complex morphology at the time of maximal diversity of both orders, and these were the first to become extinct during the subsequent crises. Schwagerinida evolved in a different manner. Their diversity maximum confined to the Asselian and Sakmarian was a result of evolution of genera with spherical and subspherical tests (representatives of the obviously heterogeneous family Schwagerinidae) rather than the consequence of a rapid progress in individual phyla. Such forms with evolute tests appeared in the early Kasimovian (subgenus *Tumefactus* of the genus *Schwagerini-*

formis and genera *Kushanella* and somewhat younger *Darvasoschwagerina*) and gained the widest distribution range in the Asselian (*Occidentoschwagerina, Likharevites, Sphaeroschwagerina, Paraschwagerina, Pseudoschwagerina, Alpinoschwagerina, Eozellia, Zellia, Robustoschwagerina*, and *Acervoschwagerina*). These genera originated at different times, maybe repeatedly from *Schwageriniformis, Montiparus, Triticites, Daixina, Rauserites*, and *Dutkevichites*. As a rule, the evolution was very rapid, without transitional forms, and all the branches from the ancestors were blind. Subspherical fusulinid genera appeared sporadically in the late Sakmarian and went out of "fashion" at the end of the Kungurian. Some relapses occurred in the late Murgabian–Midian, when *Pseudofusulina* and *Chusenella* gave rise to *Rugososchwagerina* and *Orientoschwagerina*.

4. As shown in Fig. 6, the diversity outbursts of dominated orders during the first and second stages of fusulinid development have not been accompanied by diversification of other orders, except for the coincidence of diversity peaks of Ozawainellida and Fusulinida. On the contrary, all the fusulinid orders, along with dominated Neoschwagerinida, increased in diversity during the third stage, when of Schubertellida and Staffellida attained the diversity maximums in their history.

POSSIBLE FACTORS RESPONSIBLE FOR DIVERSITY VARIATIONS IN THE HISTORY OF FUSULINIDS

Stages in the fusulinid development, which are manifested as alternating periods of diversification and crises, were under control of many factors, because scenarios of events at different stages have, as is shown, similar and distinctive features. Speaking of similarity, it is necessary to mention first that three main peaks of genera amount were mainly controlled by diversification of one of three dominant orders. Accordingly, the orders can be considered as integral systems, the appearance, diversification and decline of which can be explained in the context of the system analysis (Markov and Naimark, 1998). Another feature of similarity is the apparent close relationship between the diversity peaks and the of marine transgressions maximums, and also between the crises and regressions. Differences are reflected in peculiarities and various rates of evolutionary morphological changes, which determined the general development of the orders, in responses to environmental factors, etc. The short article is inappropriate for a comprehensive system analysis of development of the fusulinid orders. In addition, there is no uniform approach to systematics of this fossil group, and some taxa of high order, e.g., the family Schwagerinidae, one of the main in the order Schwagerinida, is obviously of a summative character (Chernykh, 1986) and cannot be considered as the natural object suitable for the system analysis. The latter is hardly possible, because we do not know exactly to what extent in the morphogenesis, in some phylogenetic lineages at least, is predetermined by genetic factors. Significance of the latter, for instance, the genetic inertia is evident from the parallel evolution of some allied phyla, e.g., of families Neoschwagerinidae and Sumatrinidae, which demonstrate a successive and uniform, though unequal-rate complication of shells' morphology (Leven, 1993a). This puts under doubts the idea that the progressive morphological complication of shells is always a result of progressing specialization of taxa tending to be less eurybiontic. The inverse relation is equally admissible: the lower tolerance may be a result of advanced morphological changes in evolution of a taxon. In general, it is often difficult to define functions of the morphological features and, consequently, their role in adaptation. At the present state of knowledge of the basin development, the system analysis is also constrained by difficulties in chronological correlations between the biotic crises and abiotic events, so much more that the same abiotic events frequently pròduce different impacts on different basins. Nevertheless, below is an attempt to evaluate environmental effects on the dynamics of development of the fossil group under consideration, which is reflected in the generic diversity diagrams. The most important environmental factors are climatic and paleogeographic changes. Climate controls the temperature and salinity of water masses, while paleogeographic changes, primarily marine transgressions and regressions, enlarge or reduce habitat areas of organisms, determine their migration paths, food resources, and so on.

Fusulinids, the habitants of shallow and warm basins, were very sensitive to temperature drop in their habitats. Consequently, it seems reasonable to expect that their abundance should decrease sharply during the Gondwana glaciation, the culmination of which was in the Asselian. The general curve of generic diversity indicates, however, the largest number of genera at that time. This contradiction can be readily explained by the virtual coincidence of the general curve with that plotted for the tropical part of the Tethys. In essence, the former reflects, to a great extent, the distribution parameters of fusulinid genera, which populated tropical belt, where the high-latitude climatic fluctuations had a little impact and insignificantly influenced the fusulinid community. It is admissible, however, that climatic fluctuations were able to influence the rate of phyla evolution. I arrived at this conclusion based on the mentioned differences in the evolution of three main orders Fusulinida, Schwagerinida and Neoschwagerinida during the major stages of fusulinid development. For instance, some phylogenetic lineages of Fusulinida and Neoschwagerinida, which were prosperous before and after the Gondwana glaciation, demonstrated a rapid successive evolution of taxa toward the complication and enlargement of shells with the increased number of whorls. In contrast, Schwagerinida, the diversity peak of which was in the Asselian, i.e., at the culmination

time of the Gondwana glaciation, the progressive changes were very slow and ended by the middle of the next third stage, when they gave birth to multiapertural genera *Eopolydiexodina* and *Polydiexodina*. In the Asselian however, there was also an outburst of generation of heterogeneous subspherical forms. It is possible that this is a mere coincidence, and origin of the latter had no connections with climatic conditions. Nevertheless, influence of the last factor on the rate of phylogenetic changes, accelerated in the hot and decelerated in the cool climate, is hypothetically possible. Available data on paleotemperatures are controversial and insufficient for a more definite conclusion. For instance, the mean temperature of surface water of the Moscow basin of the Kasimovian time ranged, as estimated, from 17–18°C (Davydov and Dorofeeva, 1991) to 23°C (Yasamanov and Astaf'eva-Urbaitis, 1987). According to data of Davydov and his colleagues (Davydov *et al.*, 1983; Davydov and Dorofeeva, 1991), the water temperature in the East European and Central Asian basins abruptly increased by 5–8°C in the first third of the Gzhelian. In the southern hemisphere, glacial sheets enlarged at that time.

Climatic conditions insignificantly influenced the generic diversity of fusulinids or, to be exact, their communities in equatorial and tropical parts of the Tethys. In contrast, impact of this factor was very significant in the basins of higher latitudes, for example, in the southern Peri-Tethys.

Transgressions and regressions were likely the main environmental factors, which controlled the general development of fusulinid and dynamics of their generic diversity (Ross and Ross, 1987; Leven, 1993b). Transgressions led to enlargement of fusulinid habitats and, consequently, to diversification and specialization of taxa. These effects were characteristic of the Moscovian, Asselian, and Kubergandian–Midian transgressions. Regressions, especially rapid ones, sharply changed paleogeography and diminished habitat areas suitable for fusulinids, thus causing first of all the extinction of most specialized stenobionts. The extent and destructive effect of the regression-related changes in ecosystems depend on the scale and rate of regressions and on the specialization degree of biocoenoses and constituent species subjected to the ruinous influence of environmental changes. The good examples are the post-Moscovian and, especially, the catastrophic post-Midian extinctions. Certainly, the abiotic factors of extinctions are not limited by regressions. For instance, being coincident with the regression, the biotic crisis of Permian–Triassic boundary time was most likely caused by some events of a greater scale, because it affected both the marine and continental biotas. It could be connected with the aerosol climatic catastrophe produced by the intense volcanic activity or with a giant cosmic body impact on the Earth (Budyko *et al.*, 1985; Kozur, 1994; Rene *et al.*, 1995; Alvarez *et al.*, 1982). Nevertheless, exactly the regressions gave initial impetuses to the biotic crises, as it is evident from the history of fusulinids discussed above. It is also interesting that appearance of the earliest elements in new assemblages, which replaced the destroyed ones, was confined to the crisis situations. Figures 3 and 6 clearly demonstrate that the most significant events in the fusulinid evolution, i.e., the origination of new progressive forms, the ancestors of the orders, occurred during the post-Tournaisian (appearance of the earliest Staffellida and Ozawainellida forms), post-Serpukhovian (appearance of Fusulinida and Schubertellida), post-Moscovian (appearance of Schwagerinida), and post-Sakmarian (appearance of earliest *Pamirina*, the ancestors of Neoschwagerinida) regressions. The same epochs are marked by generic diversity declines.

In conclusion, I would like to emphasize that the above consideration of the fusulinid development and dynamics of their generic diversity is not the ultimate one. It is aimed to outline general trends based on available data. Additional data may undoubtedly improve it without changing the essence. As for the factors of fusulinid development, there is still much to be understood about the inherent biological processes of evolution of this group and about the abiotic impacts. It is necessary to carry out special system study based on the detailed stratigraphy in order to clarify the problems. Regretfully, such investigations are scarce and likely cannot be conducted in the nearest future.

ACKNOWLEDGMENTS

The work was supported by the Russian Foundation for Basic Research, project no. 00-05-64298.

Reviewers A.V. Markov and K. I. Kuznetsova

REFERENCES

Alvarez, L.W. *et al.*, Current Status of the Impact Theory for the Terminal Cretaceous Extinction, *Spec. Pap. Geol. Soc. Am.*, 1982, no. 190, pp. 305–316.

Budyko, M.I., Ronov, A.B., and Yanshin, A.L., *Istoriya atmosfery* (History of the Atmosphere), Leningrad: Gidrometeoizdat, 1985.

Chernykh, V.V., *Problema tselostnosti vysshikh taksonov* (Problem of the Higher Taxa Completeness), Moscow: Nauka, 1986.

Davydov, V.I. and Dorofeeva, L.A., Paleotemperature Analysis of Ca/Mg Ratios in Upper Paleozoic Biogenic Carbonates from Moscow Area and Donbass, *Byul. Mosk. O-va Ispyt. Prir., Otd. Geol.*, 1991, vol. 66, no. 4, pp. 1001–1009.

Davydov, V.I., Dorofeeva, L.D., and Kashik, D.S., Paleotemperatures and Trends of Changes in Fusulinid Assemblages of the Darvaz Sea Basin across the Carboniferous-Permian Boundary, *Tr. XXV sessii VPO* (Proc. 15th Session of the All-Union Paleontol. Soc.), Leningrad: Vses. Geol. Inst., 1983, pp. 111–116.

Dickins, J.M., Late Palaeozoic Glaciation, *B.M.R. J. Austral. Geol., Geophys.*, 1985, no. 7, pp. 163–169.

Kozur, H.W., The Permian-Triassic Boundary and Possible Causes of Faunal Change Near the P/T Boundary, *Permophiles*, 1994, no. 24, pp. 51–54.

Leven, E.Ya., Phylogeny of Sumatrinids and Problem of Zonation of Murgabian and Midian Stages of the Permian Syatem, *Paleontol. Zh.*, 1993a, no. 3, pp. 23–29.

Leven, E.Ya., Main Events in Permian History of the Tethys and Fusulinids, *Stratigr. Geol. Korrelyatsiya*, 1993b, vol. 1, no. 1, pp. 59–75.

Leven, E.Ja., Early Permian Fusulinids from the Central Pamir, *Riv. Ital. Paleontol. Stratigr*, 1993c, vol. 99, no. 2, pp. 151–198.

Leven, E.Ya., Evolutionary Stages of Early Permian Fusulinid Communities as Related to Abiotic Events, *Byul. Mosk. O–va Ispyt. Prir., Otd. Geol.*, 1995, vol. 70, no. 5, pp. 66–71.

Leven, E.Ya. and Korchagin, O.A., Permian-Triassic Biotic Crisis and Foraminifers, *Stratigr. Geol. Korrelyatsiya*, 2001, vol. 9, no. 4, pp. 55–64.

Leven, E.Ya., Bogoslovskaya, M.F., Ganelin, V.G., *et al.*, Reorganization of Marine Biota during the Mid-Early Permian Epoch, *Stratigr. Geol. Korrelyatsiya*, 1996, vol. 4, no. 1, pp. 66–70.

Loeblich, A.R. and Tappan, H., *Foraminiferal Genera and Their Classification*, New York: Van Nostrand Reinhold, 1987, vols. 1 and 2.

Markov, A.V. and Naimark, E.B., *Kolichestvennye zakonomernosti makroevolyutsii. Opyt primeneniya sistemnogo podkhoda k analizu razvitiya nadvidovykh taksonov* (Quantitative Macroevolution: An Experience of Applying System Approach to Analysis of Supergeneric Taxa Evolution), Moscow: GEOS, 1998.

Rauzer-Chernousova, D.M., Evolution of Close Schwagerinid Genera and Problem of Carboniferous-Permian Boundary, *Vopr. Mikropaleontol.*, 1961, no. 4, pp. 3–32.

Rauzer-Chernousova, D.M., Evolution History of Fusulinids and Boundaries of Stratigraphic Subdivisions, *Vopr. Mikropaleontol.*, 1963, no. 7, pp. 3–12.

Rauzer-Chernousova, D.M., Stages and Cycles in the Evolution History of Fusulinids, *Dokl. Akad. Nauk SSSR*, 1965, vol. 160, no. 4, pp. 914–917.

Rauzer-Chernousova, D.M., Some Aspects of Foraminifera Evolution and Their Significance for Biostratigraphy, *Tr. XII sessii Vses. Paleontol. O–va. 1968* (Proc. 12th Session of the All-Union. Paleontol. Soc.), Moscow: Nauka, pp. 18–24.

Rauzer-Chernousova, D.M. and Reitlinger, E.A., Evolution of Foraminifers in Paleozoic Time and Their Stratigraphic Significance, *Izv. Akad. Nauk SSSR, Ser. Geol.*, 1957, no. 4, pp. 45–57.

Rauzer-Chernousova, D.M., Bensh, F.R., Vdovenko, M.V., *et al.*, *Spravochnik po sistematike foraminifer paleozoya (endotiroidy, fuzulinoidy)* (Reference Book on Taxonomy of Paleozoic Foraminifers: Endotiroids and Fusulinids), Moscow: Nauka, 1996.

Reitlinger, E.A., About One Paleontological Criterion Defining Boundaries of the Carboniferous System Based on Foraminifers, *Vopr. Mikropaleontol.*, 1963, no. 7, pp. 22–56.

Reitlinger, E.A., Stages of Foraminifera Evolution and Their Significance for Carboniferous Stratigraphy, *Vopr. Mikropaleontol.*,1969, no. 12, pp. 3–33.

Renne, P.R., Zhang, Z., Richards, M.A., *et al.*, Synchrony and Causal Relations Between Permian-Triassic Boundary Crises and Siberian Flood Volcanism, *Science*, 1995, vol. 269, pp. 1413–1416.

Ross Ch., A. and Ross, J.R.P., Biostratigraphic Zonation of Late Paleozoic Depositional Sequences, *Cushman Foundation for Foraminiferal Res., Spec. Publ.*, 1987, no. 24, pp. 151–168.

Rozovskaya, S.E., *Sostav, sistema i filogeniya otryada fuzulinida* (Composition, Systematics, and Phylogeny of the Order Fusulinida), Moscow: Nauka, 1975.

Solov'eva, M.N., Temps and Stages of Foraminifera Evolution as Correlated with the Earth's History, *Vopr. Mikropaleontol.*, 1966, no. 10, pp. 68–79.

Yasamanov, N.A. and Astaf'eva-Urbaitis, K.A., Peculiarities of Climatic Environments in Eurasia during the Carboniferous Period, *Dokl. Akad. Nauk SSSR*, 1987, vol. 295, no. 6, pp. 1432–1435.

Stratigraphy and Geological Correlation, Vol. 11, No. 3, 2003, pp. 231–243. Translated from Stratigrafiya. Geologicheskaya Korrelyatsiya, Vol. 11, No. 3, 2003, pp. 27–39.
Original Russian Text Copyright © 2003 by Konstantinov, Sobolev, Klets.
English Translation Copyright © 2003 by MAIK "Nauka/Interperiodica" (Russia).

New Data on Fauna and Biostratigraphy of Norian Deposits in the Kotel'nyi Island (New Siberian Islands)

A. G. Konstantinov*, E. S. Sobolev*, and T. V. Klets**

**Institute of Geology, United Institute of Geology, Geophysics, and Mineralogy, Siberian Division, Russian Academy of Sciences, pr. Akademika V.A. Koptyuga 3, Novosibirsk, 630090 Russia*

***Novosibirsk University, ul. Pirogova 2, Novosibirsk, 630090 Russia*

Received June 6, 2001

Abstract—A section of lower and middle Norian deposits in the Tikhaya River lower courses of (the central part of Kotel'nyi Island, New Siberian Islands) is described. After revision, the taxonomic composition of fauna from the sequence is verified, and formerly unknown taxa are identified. Stratigraphic range of ammonoids, nautiloids, coleoids, and conodonts in the section are analyzed, and the local biostratigraphic scheme, which includes zones, subzones, and beds with fauna, is suggested for the lower-middle Norian interval. Distinguished for the first time are beds with nautiloids, the *Striatosirenites kinasovi* Zone, and *Cyrtopleurites* ex gr. *altissimus* Beds with ammonoids. The local biostratigraphic scheme of Norian deposits is correlated with the ammonoid zonation in Canada and with the standard scale. Ammonoids of the genus *Cyrtopleurites*, which have been found for the first time in deposits of the Kotel'nyi Island and are characteristic of the *Cyrtopleurites bicrenatus* Zone, the lower one in the middle Norian of the standard scale, enabled the direct Boreal-Tethyan correlation of their host rocks and positioning of the lower-middle Norian boundary in Boreal regions. Geographic ranges of ammonoid, nautiloid, coleoid, and conodont taxa from Norian deposits of the Kotel'nyi Island are considered. Based on peculiar features of the studied fauna (coexistence of Boreal and Tethyan elements, a significant proportion of cosmopolitan taxa, and presence of species known from North America), the Kotel'nyi island region is defined as a separate subprovince in the Siberian Province of the Boreal Realm.

Key words: Triassic, cephalopods, conodonts, biostratigraphy, correlation, biogeography, Siberia.

INTRODUCTION

The taxonomic diversity of most invertebrate groups gradually increased during the Triassic and enhanced biogeographic distinctions between faunas of lower- and high-latitude areas (Dagys, 1974, 1976; Dagys *et al.*, 1979; Dagys and Shevyrev, 1981). In the Late Triassic, when geographic differentiation between marine invertebrates became obvious, the distinction of Tethyan fauna from those of the Boreal and Notal regions enhanced further.

Clear biogeographic distinctions between the Boreal and Tethyan faunas of the Late Triassic resulted in elaboration of autonomous Upper Triassic zonal schemes for these regions, on the one hand, and brought about a series of debatable problems concerning significant biostratigraphic boundaries and interregional correlation, on the other. Still debatable are the position of Middle-Upper Triassic boundary and ranges of Carnian and Norian stages in the Boreal Realm, and the problem of the Rhaetian calls for further investigations. The lower-upper Carnian and lower-middle Norian boundaries are also conventional to a considerable extent in distribution areas of Boreal deposits.

The direct correlation of Triassic deposits in the Boreal and Tethyan regions seems to be possible only for some intervals corresponding to episodes of eustatic sea-level rise, which resulted in a greater taxonomic similarity of faunas in different biochores. For instance, the lower boundary of the upper Norian is reliably traceable in all the regions at the appearance level of the cosmopolitan bivalve genus *Monotis* (Dagys and Tozer, 1989; *Obshchaya shkala...*, 1984). Ammonoids of the genus *Neoprotrachyceras* enable correlation between the lower Carnian *Neoprotrachyceras seimkanense* Zone of Siberia and the standard *Austrotrachyceras austriacum* Zone (Krystyn, 1978; *Obshchaya shkala...*, 1984). Some stratigraphic intervals of the Carnian and of the lower and middle Norian in Boreal regions are correlated with coeval deposits of the Tethys based on transitional sections of British Columbia and Arctic Canada. As is well known, the abundant and diverse ammonoid fauna of British Columbia includes taxa (genera *Stolleyites, Pterosirenites, Wangoceras, Norosirenites, Pleurodistichites, Neohimavatites)* widespread in Boreal sections and are associated here with numerous Tethyan ammonoids.

In addition to recognition and tracing of reference levels and to the analysis of ecotones, the comprehensive study of different fossil groups and geographic differentiation of faunas within the Boreal region are also of interest for the Boreal–Tethyan correlation of the

Upper Triassic. The complete marine sequences of the Upper Triassic well characterized by fauna are known in the Boreal Realm of northeastern Asia. The corresponding sea basin represented a system of shelf marginal seas bounded by the Siberian paleoland on the west and by the pre-Pacific ocean on the southeast (Bychkov, 1992). The geographic differentiation of Late Triassic ammonoid, nautiloid, bivalve, and brachiopod faunas was insignificant in the vast territory of northeastern Asia, although some distinctions between non-orthostratigraphic groups of faunas from Yakutia and Kolyma–Okhotsk region have been reported (Dagys *et al.*, 1996). In some regions, however, e.g., in upper courses of the Bol'shoi Anyui River and in the Anadyr River basin, representatives of Tethyan bivalves and ammonoids appeared in Boreal fauna assemblages during the late Norian (Kiparisova *et al.*, 1966; Afitskii, 1970; Dagys *et al.*, 1979; Bychkov, 1992). Some Tethyan ammonoid genera are also known from Norian deposits of the Kotel'nyi Island (Diener, 1916; 1924). Investigation of these mixed faunas from northeastern Asia, which include Tethyan and Boreal taxa, are of a great interest for paleobiogeography and detailed stratigraphy. Unfortunately, we should mention a different standard of knowledge on the Upper Triassic fauna and stratigraphy in separate regions of northeastern Asia.

The purpose of this work is to fill partially the gap by means of comprehensive biostratigraphic and biogeographic analyses of the Norian ammonoids, nautiloids, bivalves, and conodonts from the New Siberian Islands, the insufficiently studied and hard-to-reach region of northeastern Asia.

INVESTIGATION HISTORY OF UPPER TRIASSIC DEPOSITS IN THE KOTEL'NYI ISLAND

Triassic deposits of New Siberian Islands are poorly studied, as the region is rather remote and not easily accessible. Few publications are devoted to these deposits. Presence of Triassic deposits in the Kotel'nyi Island was established for the first time in 1801, when M.M. Hedenstrom found the *Hedenstroemia hedenstroemi* Keyserling ammonite species of the Early Triassic. His collection was comprehensively described by Keyserling (1845). Later geological expeditions to carried out on New Siberian Islands, with E.V. Toll and K.A. Vollosovich as participants, were organized by the Russian Academy of Sciences in 1886, 1893, and 1900, and afterward Diener (1916; 1924) described collection of the Upper Triassic fauna from the Kotel'nyi Island. In 1955–1956, geologists from the Research Institute of Arctic Geology (NIIGA) performed the geological survey at the scale of 1 : 1000000 in New Siberian Islands. D.A. Vol'nov, D.S. Sorokov, and S.V. Cherkesov studied the northern part of the Kotel'nyi Island. They established that the Triassic System of the Kotel'nyi Island includes three series with all stages except for the Induan and Rhaetian (Vol'nov *et al.*, 1970).

New data on the Triassic stratigraphy were obtained by geologists from NIIGA (D.A. Vol'nov, E.N. Preobrazhenskaya, M.K. Kos'ko, V.G. Trufanov, N.S. Bondarenko, B.P. Gavrilov, and V.F. Nepomiluev) in the course of thematic studies and geological survey in the Kotel'nyi Island in 1972–1974. Identification of numerous paleontological materials made it possible to verify the Triassic stratigraphy and to suggest a scheme of biostratigraphic subdivisions in Triassic deposits, which included stages and beds with fauna (Preobrazhenskaya *et al.*, 1975; Korchinskaya, 1977). The *Discophyllites taimyrensis*, *Sirenites hayesi*, and *Halobia* beds were distinguished within the Carnian. No ammonoids were found in overlying beds, although many *Halobia* species were found to occur in Norian deposits as well. In the Norian sequence (250 m thick), Korchinskaya distinguished the lower mudstone member with foraminifers, spores, and pollen of the Triassic habit, which have been attributed previously to the Carnian fossils. She divided the overlying deposits into the *Otapiria ussuriensis*, *Monotis scutiformis*, and *Monotis ochotica* beds were singled out. The mudstone sequence about 100 m thick that overlies the *Monotis ochotica* Beds was arbitrarily attributed to the Norian-Rhaetian based on foraminifers and palynological data.

In 1984, Triassic deposits in the central part of the Kotel'nyi Island and along its northwestern coast were studied by A.Yu. Egorov, Ya.A. Bogomolov, and Yu.M. Baranov, the researchers of the Cosmoaerogeological Expedition No. 3 (Moscow), and by A.G. Konstantinov from the Institute of Geology and Geophysics (Novosibirsk). Based on the results of field work and paleontological materials collected in abundance, they verified thickness, nomenclature, paleontological characteristics, and biozonation of some Lower and Middle Triassic subdivisions and significantly corrected the detailed stratigraphy of the Upper Triassic, especially of the Norian (Egorov *et al.*, 1987). In particular, they proved presence, using paleontological data, of the lower Norian *obručevi* Zone previously distinguished by convention (Dagys *et al.*, 1979). In addition, they subdivided the middle and upper Norian in detail and distinguished subzones of the *scutiformis* and *ochotica* zones. At the same time, in distinction from predecessors, bivalves *Otapiria dubia* (Ichikawa) and *O. korkodonensis* Polubotko were considered as characteristic of the *Eomonotis* Beds in the *daonellaeformis* Subzone of the *scutiformis* Zone.

The ammonoids and nautiloids collected in 1984 from lower and middle Norian deposits of the Balyktakh River basin, Kotel'nyi Island, were revised and identified anew in the course of works aimed to revise the Boreal Triassic fauna, to verify further the Triassic biostratigraphic schemes for northeastern Asia, and to perfect their paleontological substantiation. Recently, conodonts have been found for the first time at some levels in Upper Triassic deposits of the Kotel'nyi Island (Klets, 1996, 1998). The results of fauna revision allow us to refine substantially the paleontological character-

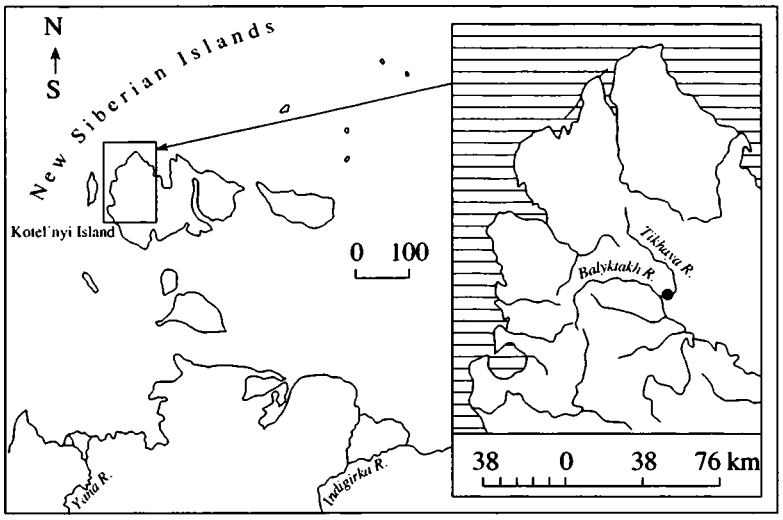

Fig. 1. The Tikhaya River locality of the studied Norian sequence (the Balyktakh River upper courses in central part of the Kotel'nyi Island).

istics and biostratigraphy of Norian deposits, and to distinguish for the first time some subdivisions, which were formerly missed from the local stratigraphic scheme of lower and middle Norian deposits of the Kotel'nyi Island. New data are also used to establish a more justified position of the lower-middle Norian boundary in the region. The refined taxonomy of the regional Norian fauna is undoubtedly of interest for the Boreal-Tethyan correlation of the Upper Triassic and for the comparative biogeographic analysis of the Late Triassic faunas of the Boreal realm.

The lower-middle Norian sequence studied in lower courses of the Tikhaya River, the most complete one among others known in the Kotel'nyi Island (Fig. 1), is description below. Ammonoids were identified by Konstantinov, nautiloids and coleoids by Sobolev, conodonts by Klets. Data by Egorov *et al.* (1987) are used to determine bivalves and to subdivide deposits based on this fossil group. In addition, Konstantinov and Sobolev identified *Halobia* forms in samples stored in the Central Siberian Geological Museum (CSGM), United Institute of Geology, Geophysics, and Mineralogy, Siberian Division, Russian Academy of Sciences (Novosibirsk).

The studied collection of ammonoids, nautiloids, and conodonts is stored in the CSGM under nos. 635, 759, and 792.

STRATIGRAPHY OF THE STUDIED SECTION

Lower and middle Norian deposits were studied in exposures along the right bank of Tikhaya River (a left tributary of Balyktakh River in its upper courses), 2–3 km upstream of the mouth. In this region, Norian deposits are faulted against the underlying clay sequence with lenses of bituminous limestone (Exp. 189).[1] The latter yield ammonoids *Neosirenites irregularis* (Kiparisova), *Yakutosirenites* aff. *pentastichus* (Vozin), *Proarcestes* sp.) of the upper Carnian *Yakutosirenites pentastichus* Zone (Fig. 2). Above the fault, the following succession of beds is observable:

Exposure 190

1. Dark gray, mudstone-like clay with rare interlayers of clayey limestone concretions (15 m).

Paleontological characteristics: (1–2 m)[2] bivalves *Halobia kawadai* Yehara, *Zittelihalobia fallax* (Mojsisovics), *Z.* aff. *obručevi* (Kiparisova) and conodonts *Norigondolella navicula* (Huckriede); (9 m) bivalves *Zittelihalobia fallax* (Mojs.).

2. Dark gray, mudstone-like clay with frequent lenticular horizons of siderite concretions (20 m).

Paleontological characteristics: (1 m) ammonoids *Striatosirenites* ex gr. *kinasovi* Bytschkov, *Arctophyllites popovi* (Archipov), *Cladiscites tolli* Diener; nautiloids *Germanonautilus* cf. *popowi* Sobolev; bivalves *Zittelihalobia indigirensis* (Popow), *Z.* aff. *obručevi* (Kiparisova); (5 m) ammonoids *Striatosirenites kinasovi* Bytschkov (Fig. 3a; Plate, no. 1), *Arcestes* sp. juv.; nautiloids *Proclydonautilus* cf. *spirolobus* (Dittmar) (Figs. 3b, 3c); phragmocone remains of coleoids; bivalves *Zittelihalobia fallax* (Mojs.); brachiopods *Sinuplicorhynchia wollosowitschi* (Diener); (9–13 m) ammonoids *Arctophyllites* cf. *popovi* (Arch.); bivalves *Zittelihalobia fallax* (Mojs.); (17–18 m) bivalves *Halobia* ex gr. *austriaca* Mojs., *Zittelihalobia indigirensis* (Popow), *Z. fallax* (Mojs.), *Z.* aff. *obručevi* (Kipar.).

[1] Numbers of exposures and brief lithological description of rocks are given after Egorov *et al.* (1987).

[2] By paleontological characterization, levels of fossils above the bed base are given in parentheses.

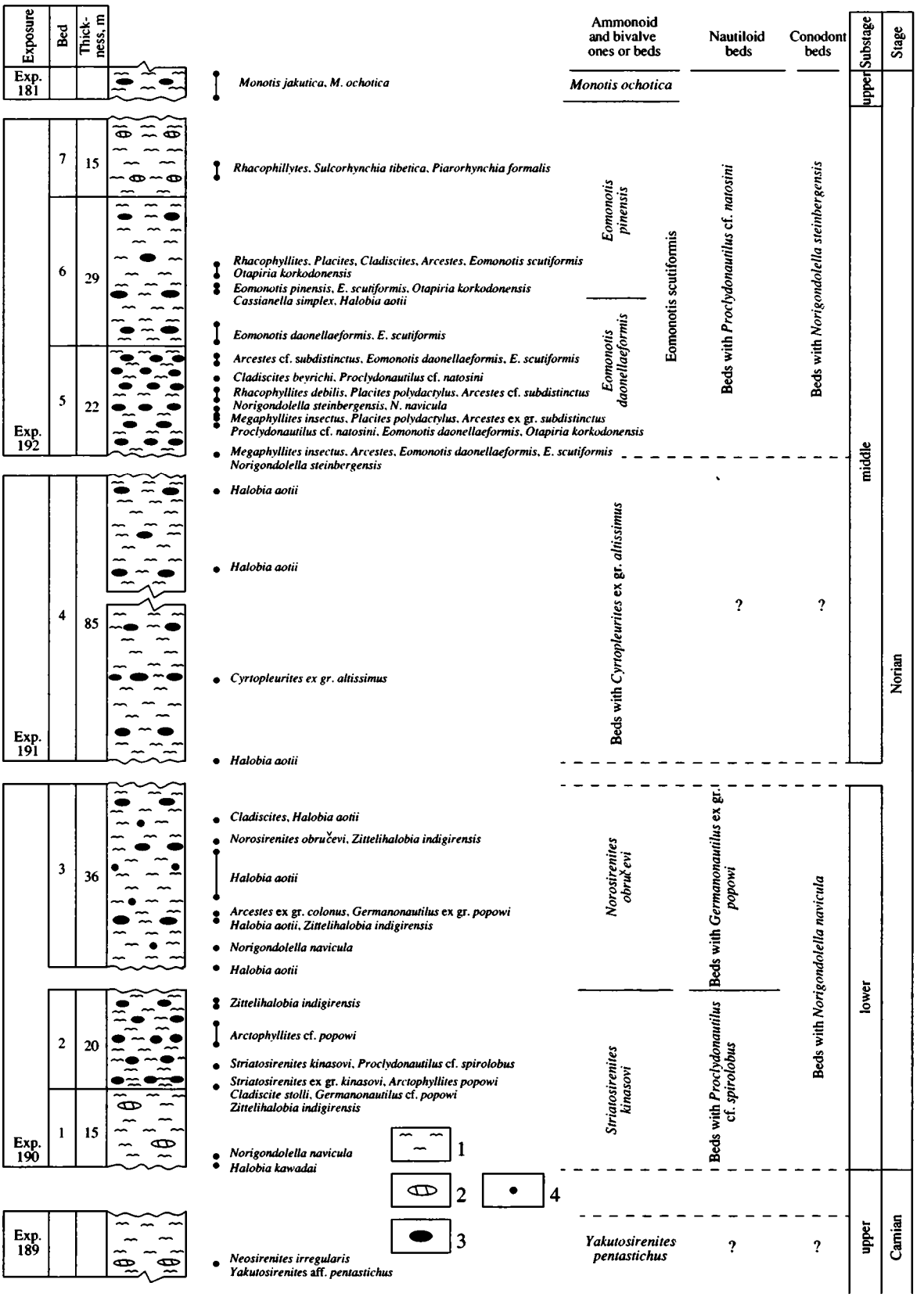

Fig. 2. Biostratigraphy of lower and middle Norian deposits, the Tikhaya River locality (the Balyktakh River upper courses in central part of the Kotel'nyi Island): (1) clay; (2–4) concretions: (2) clayey limestone, (3) siderite, and (4) phosphate.

Ammonoids *Anatomites* sp. indet., *Pinacoceras regiforme* Diener and *Cladiscites tolli* Diener, described long ago (Diener, 1916, 1924) from the Balyktakh River right bank, were probably derived from the stratigraphic interval corresponding to Bed 2. The boundary with overlying bed is faulted.

3. Black, mudstone-like clay with rare, large, scattered, bun-shaped siderite concretions. Small phosphate concretions are scattered throughout the bed (36 m).

Paleontological characteristics: (0–1 m) bivalves *Halobia aotii* Kobayashi et Ichikawa; (4 m) conodonts *Norigondolella navicula* (Huckriede) (Plate, no. 5); (10 m) ammonoids *Arcestes* sp. indet.; nautiloids *Germanonautilus* ex gr. *popowi* Sob.; bivalves *Halobia aotii* Kob. et Ichik., *Zittelihalobia indigirensis* (Popow), *Z. fallax* (Mojs.), *Z.* aff. *obručevi* (Kipar.); (11 m) ammonoids *Arcestes* ex gr. *colonus* Mojsisovics; nautiloids *Germanonautilus* ex gr. *popowi* Sob. (Plate, no. 3); brachiopods *Sulcorhynchia tibetica* (Bittner), *Costispiriferina* sp.; gastropods; (14–23 m) bivalves *Halobia aotii* Kob. et Ichik., *H.* ex gr. *hoernesi* Mojs.; brachiopods *Sulcorhynchia tibetica* (Bittn.); (25 m) ammonoids *Norosirenites obručevi* (Bajarunas) (Plate, no. 2); bivalves *Halobia aotii* Kob. et Ichik., *Zittelihalobia indigirensis* (Popow); brachiopods *Sulcorhynchia tibetica* (Bittn.); gastropods; (29 m) ammonoids *Cladiscites* sp. indet.; bivalves *Halobia aotii* Kob. et Ichik. The contact with the overlying bed is faulty.

Exposure 191

4. Black, mudstone-like clay with horizons of siderite concretions (85 m).

Paleontological characteristics: (16 m) ammonoids *Cyrtopleurites* ex gr. *altissimus* Mojsisovics (Plate, no. 6).

Rare bivalves *Halobia aotii* Kob. et Ichik., *H.* ex gr. *plicosa* Mojs., *Zittelihalobia fallax* (Mojs.), *Z.* aff. *obručevi* (Kipar.); brachiopods *Orbiculoidea* sp. are dispersed throughout the bed.

Further downstream of Tikhaya River, there is an unexposed interval in the section.

Exposure 192

5. Black, dense clay with lenticular horizons of siderite concretions (22 m).

Paleontological characteristics: (the base) ammonoids *Megaphyllites insectus* (Mojs.), *Arcestes* sp. indet.; conodonts *Norigondolella steinbergensis* (Mosher) (Plate, no. 7); (6 m) ammonoids *Arcestes* sp. indet.; nautiloids *Proclydonautilus* cf. *natosini* McLearn (Fig. 3d, e; Plate, no. 8); gastropods; (7–8.5 m) ammonoids *Megaphyllites insectus* (Mojs.), *Placites polydactylus* (Mojs.), *Arcestes* ex gr. *subdistinctus* Mojs, *A.* sp. indet.; fragments of coleoid phragmocones; (9 m) conodonts *Norigondolella steinbergensis* (Mosher), *N. navicula* (Huckriede); (11–13 m) ammonoids *Rhacophyllites debilis* (Hauser), *Placites*

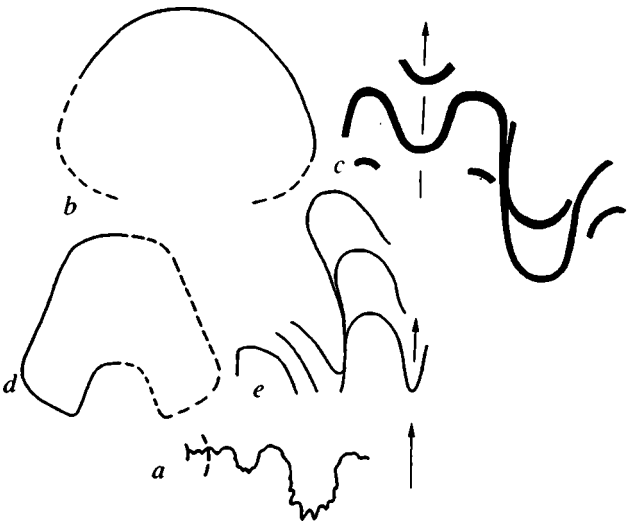

Fig. 3. Suture lines and cross sections of whorls characteristic of *Proclydonautilus* and *Striatosirenites* genera from Norian deposits of the Kotel'nyi Island (Tikhaya River locality, the Balyktakh River upper courses): (*a*) *Striatosirenites kinasovi* Bytschkov, Specimen 759/97a, CSGM, lobe line at H = 4.2 mm (×6), Exp. 190, Sample 190-2-5p, the lower Norian, the *Striatosirenites kinasovi* Zone; (*b*) whorl cross section and (*c*) suture line at H = 92 mm of *Proclydonautilus* cf. *P. spirolobus* (Dittmar), Specimen 759/97, (×0.33), CSGM, the same exposure, sample number, and age; (*d*) whorl cross section and (*e*) suture line at H = 90 mm of *Proclydonautilus* cf. *P. natosini* McLearn, Specimen 759/99, (×0.33), CSGM; Exp. 192, Sample 192-1-6p; the middle Norian, the *Eomonotis scutiformis* Zone, the *Eomonotis daonellaeformis* Subzone.

polydactylus (Mojs.), *Arcestes* cf. *subdistinctus* Mojs., *A.* sp. indet.; fragments of coleoid phragmocones; (15 m) ammonoids *Cladiscites beyrichi* Welter, *C.* sp. indet., *Placites polydactylus* (Mojs.), *Arcestes* sp. indet.; nautiloids *Proclydonautilus* cf. *natosini* McLearn; (18–20 m) ammonoids *Arcestes* cf. *subdistinctus* Mojs., *A.* sp. indet.; fragments of coleoid phragmocones.

In addition, bivalves *Eomonotis daonellaeformis* Kipar., *E. scutiformis* (Teller), *Otapiria korkodonensis* Polubotko, *O. dubia* (Ichik.) are numerous throughout the bed. It is likely that ammonoids *Dittmaritoides* sp. described earlier (Korchinskaya, 1977; Preobrazhenskaya and Korchinskaya, 1979) are derived from this part of the section.

6. Gray, mudstone-like, shaly clay with horizons of siderite concretions (29 m).

Paleontological characteristics: (0–5 m) bivalves *Eomonotis daonellaeformis* Kipar., *E. scutiformis* (Teller), *Halobia* sp.; (11–12 m) bivalves *Eomonotis pinensis* Westermann, *E. scutiformis* (Teller), *Otapiria korkodonensis* Polub., *Halobia aotii* Kob. et Ichik., *Cassianella simplex* Kipar.; (14–16 m) ammonoids *Placites polydactylus* (Mojs.), *Rhacophyllites* cf. *debilis* (Hauer), *Cladiscites* ex gr. *beyrichi* Welter, *Arcestes*

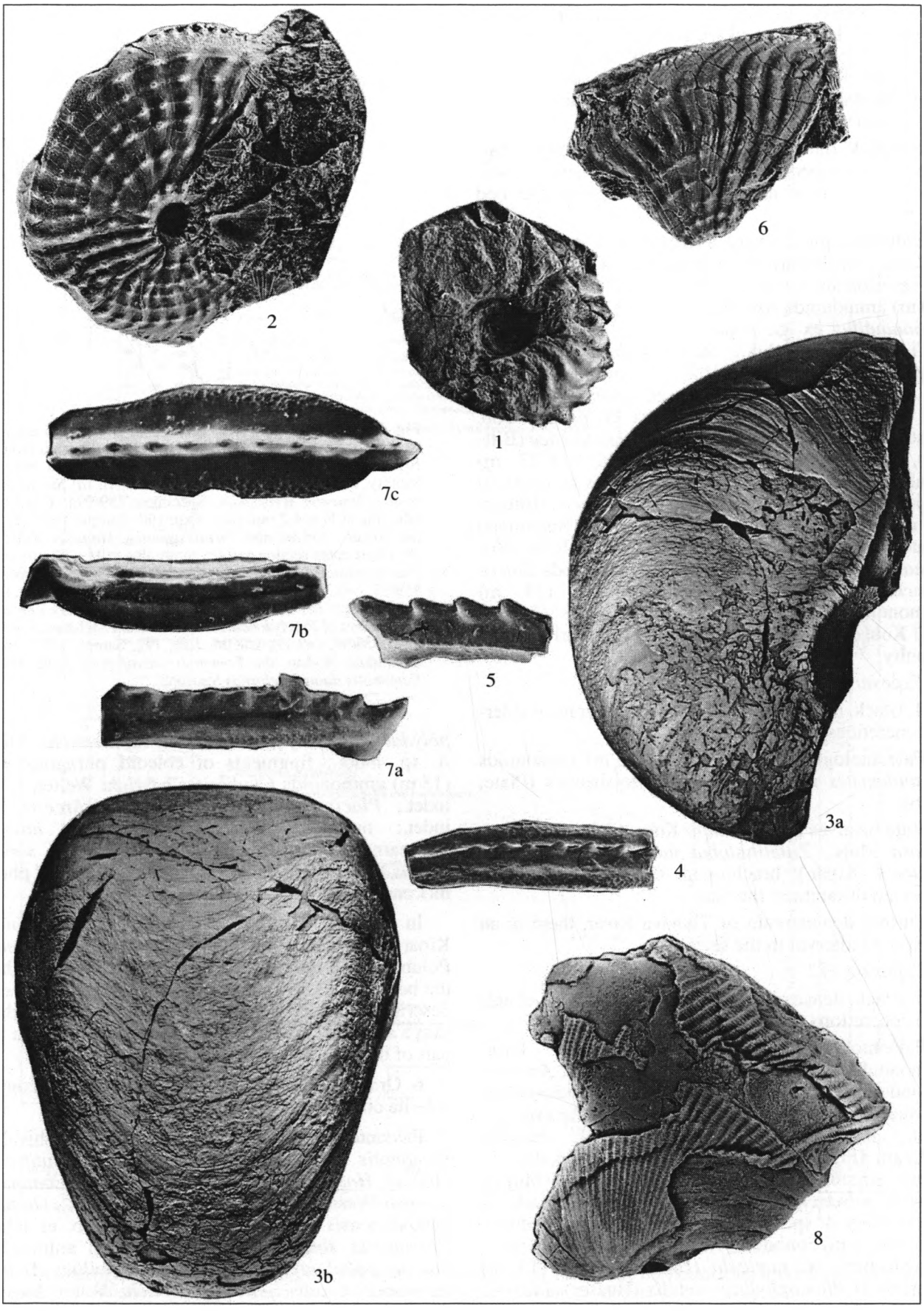
2
6
1
7c
7b
5
7a
3a
4
3b
8

ex gr. *subdistinctus* Mojs., *A.* sp., orthoceratids *Trematoceras* sp.; fragments of very large (up to 80 mm in diameter) coleoid phragmocones; bivalves *Eomonotis scutiformis* (Teller), *Otapiria korkodonensis* Polub.; brachiopods *Sulcorhynchia* cf. *tibetica* (Bittn.).

7. Dark gray clay with rare thin horizons of clayey limestone concretions (15 m).

Paleontological characteristics: (1 m) fragments of very large coleoid phragmocones; (4–7 m) ammonoids *Rhacophyllites* sp.; brachiopods *Sulcorhynchia tibetica* (Bittn.), *Piarorhynchia formalis* Dagys, *Orbiculoidea* sp.

Greenish gray clays with numerous late Norian bivalves *Monotis* are exposed at some distance downstream.

BIOSTRATIGRAPHIC SUBDIVISIONS AND CORRELATION

The analyzed stratigraphic ranges of ammonoids, nautiloids, and conodonts in the Tikhaya River section are used to distinguish the successive fauna assemblages and corresponding zones and beds with fauna of the lower–middle Norian sequence of the Kotel'nyi Island.

Bed 2 from Exposure 190 yields ammonoids *Cladiscites tolli* Diener and *Arctophyllites popovi* (Archipov). In addition, treating and revising the collection, we found two specimens of *Striatosirenites kinasovi* Bytschkov. This form found for the first time in the Kotel'nyi Island is the index species of the lowermost *kinasovi* Zone of the Norian, which had been recently distinguished in northeastern Russia (Konstantinov and Sobolev, 1999a, 1999b). The *Arctophyllites popovi* (Arch.) is also typical of that zone. The *Striatosirenites kinasovi* Zone was first established in the Omolon Massif, in the northern coast of the Sea of Okhotsk, and in the Adycha River basin. Age equivalents of the zone were formerly assumed for the Kotel'nyi Island. The assumption was based on the fact that *Pinacoceras regiforme* Diener, which has been described for the first time from Upper Triassic deposits of the Balyktakh River right bank in the Kotel'nyi Island (Diener, 1924), is known from the ammonoid assemblage of the *kinasovi* Zone distinguished in the Omolon Massif and in the northern coast of the Sea of Okhotsk (Konstantinov and Sobolev, 1999a, b). The refined taxonomic composition of ammonoids and found index species imply for the first time that the described section begins with the *Striatosirenites kinasovi* Zone that includes Bed 2 and arbitrarily Bed 1, in the lower part of which conodonts *Norigondolella navicula* (Huckriede) and early Norian *Halobia kawadai* Kob et Ichik. were found.

Based on the nautiloid assemblage of *Germanonautilus* cf. *popowi* Sobolev and *Proclydonautilus* cf. *spirolobus* (Dittmar), the section interval under discussion can be distinguished as *Proclydonautilus* cf. *spirolobus* Beds corresponding in range to the lower *Proclydonautilus spirolobus* Subzone of the nautiloid *Proclydonautilus seimkanensis* Zone (Konstantinov and Sobolev, 1999b).

In the overlying Bed 3, Exposure 190, ammonoids *Arcestes* ex gr. *colonus* Mojs were found in the lower part, whereas *Norosirenites obručevi* (Bajar.) is confined to the upper one. Both species are typical of the lower Norian *Pinacoceras verchojanicum* Zone (Dagys *et al.*, 1979) that was renamed at the last stratigraphic conference (Dagys, 1986), being known now as the *Pterosirenites* (= *Norosirenites*) *obručevi* Zone. Accordingly, the Bed 3 of Exp. 190 is referred to the *Norosirenites obručevi* Zone. Nautiloids *Germanonautilus* ex gr. *popowi* Sob. found in the same stratigraphic interval allow us term this interval as *Germanonautilus* ex gr. *popowi* Beds. As the species *Proclydonautilus spirolobus* (Dittmar) of clydonautilids has not been found in these beds, they are likely to correspond in range to the upper *Proclydonautilus seimkanensis* Subzone of the lower Norian nautiloid zone of the same name (Konstantinov and Sobolev, 1999b).

Conodonts found at two stratigraphic levels in Bed 1 and Bed 3 imply that the corresponding interval in Exposure 190 can be termed as the *Norigondolella navicula* Beds. The lower boundary of the beds is established based on the appearance of index species. The overlying 85-m-thick member of mudstone-like clay with horizons of siderite concretion (Exp. 190, Bed 4), which was arbitrarily referred before to the *Otapiria ussuriensis* Zone (Egorov *et al.*, 1987), yields individual fragments of ammonoids *Cyrtopleurites* ex gr.

PLATE

Cephalopods and conodonts from Norian deposits of the Kotel'nyi Island (Tikhaya River locality, the Balyktakh River upper courses).

(1) *Striatosirenites kinasovi* Bytschkov, Specimen 759/97a (×3), lateral view; Exp. 190, Sample 190-2-5p; the lower Norian, the *Striatosirenites kinasovi* Zone. (2) *Norosirenites obručevi* (Bajarunas), Specimen. 792/1 (natural size), lateral view; Exp. 190, Sample 190-3-25p; the lower Norian, the *Norosirenites obručevi* Zone. (3) *Germanonautilus* ex gr. *G. popowi* Sobolev, Specimen 759/157 (×0.66): (3a) lateral view, (3b) ventral view; Exp. 190, Sample 190-3-11p, the same age. (4) *Norigondolella navicula* (Huckriede), Specimen 635/2 (×100), top view; Exp. 190, Sample 190-3-4p, the same age. (5) *Norigondolella navicula* (Huckriede), Specimen 635/4 (×150), lateral view; the same locality and age. (6) *Cyrtopleurites* ex gr. *C. altissimus* Mojsisovics, Specimen 792/2 (natural size), lateral view; Exp. 191, Sample 190-1-16p; the middle Norian, *Cyrtopleurites* ex gr. *C. altissimus* Beds. (7) *Norigondolella steinbergensis* (Mosher), Specimen 635/9: (7a) lateral view (×200), (7b) bottom view (×200), (7c) top view (×232); Exp. 192, Sample 192-1-osn.; the middle Norian, the *Eomonotis scutiformis* Zone, the *Eomonotis daonellaeformis* Subzone. (8) *Proclydonautilus* cf. *P. natosini* McLearn, Specimen 759/99 (×0.66), lateral view; Exp. 192, Sample 192-1-6p; the same age.

altissimus Mojs. at the level of 16 m above the base. Halobians, the dominant *Halobia aotii* Kob. et Ichik. included, are dispersed throughout the member. This part of the sequence is distinguished as the *Cyrtopleurites* ex gr. *altissimus* Beds. Since ammonoids are rare in the beds, their lower and upper boundaries are conventional, assumed to be coincident with those of Bed 4.

Numerous bivalves, ammonoids, and more rare nautiloids, fragments of coleoid phragmocones, and brachiopods were found in overlying deposits represented by black and gray, pelitomorphic massive clays with lenticular horizons of siderite concretions and with thin interlayers of clayey limestone (Exp. 192, Beds 5, 6, and 7). This interval was previously subdivided into zones based on stratigraphic ranges of bivalves of the genus *Eomonotis* (Egorov *et al.*, 1987). Bed 5 coupled with the lower part of Bed 6 represent the *Eomonotis daonellaeformis* Subzone of the *Eomonotis scutiformis* Zone, whereas the rest of Bed 6 and Bed 7 correspond to the *Eomonotis pinensis* Subzone. Lower boundaries of both subzones are established based on the appearance of their index species. At some levels of the stratigraphic interval under discussion, there were found numerous well-preserved ammonoids representing cosmopolitan long-lived forms with smooth shells. These are *Megaphyllites insectus* (Mojs.), *Arcestes* ex gr. *subdistinctus* Mojs., *Placites polydactylus* (Mojs.), *Cladiscites beyrichi* Welter, and *Rhacophyllites debilis* (Hauer).

Nautiloids *Proclydonautilus* cf. *natosini* McLearn and conodonts *Norigondolella steinbergensis* (Mosher) were found at two stratigraphic levels in Bed 5 of Exposure 192. Nautiloids similar to *Proclydonautilus natosini* were also encountered in association with *Monotis jakutica* (Teller) and *M. zabaikalica* (Kiparisova) at the base of the upper Norian deposits of the described section. Consequently, the *Proclydonautilus* cf. *natosini* Beds of the Kotel'nyi Island correspond to the *Eomonotis scutiformis* Zone and probably to the lower part of the *Monotis ochotica* Zone. Large (up to 80 mm in diameter) coleoid phragmocones present in deposits of the *Eomonotis pinensis* Subzone are of interest. Coleoids of such a large size have not been known so far from Norian deposits in other regions of northeastern Russia. In addition to the middle Norian, the biozone of *Norigondolella steinbergensis* (Mosher) spans the upper Norian substage as well, and the *Norigondolella steinbergensis* Beds correspond therefore to the *Eomonotis scutiformis* and *Monotis ochotica* zones.

Hence, the biostratigraphic scheme for the lower and middle Norian that is established in this work based on distribution of ammonoids and bivalves includes five biostratigraphic units in the rank of zones and beds. From the base upward, these are the *Striatosirenites kinasovi* and *Norosirenites obručevi* zones of the lower Norian and the *Cyrtopleurites* ex gr. *altissimus* Beds and the *Eomonotis daonellaeformis* and *Eomonotis pinensis* subzones of the middle Norian. The lower Norian includes the *Proclydonautilus* cf. *spirolobus* and *Germanonautilus* ex gr. *popowi* beds with nautiloids, and also the *Norigondolella navicula* Beds with conodonts. In middle-upper Norian interval, there are distinguishable the *Proclydonautilus* cf. *natosini* Beds with nautiloids and the *Norigondolella steinbergensis* Beds with conodonts.

Let us consider now the correlation of local stratigraphic scheme proposed for the lower-middle Norian deposits of the Kotel'nyi island with the standard scale. Links necessary for the Boreal-Tethyan correlation of the Upper Triassic, in particular, of the Norian deposits can be found in sections of North America (Tozer, 1967; Silberling and Tozer, 1968; Tozer, 1994), the Pacific coast of which represented an ecotone of the Triassic time, where the ammonoid community consisted of mixed Tethyan and Boreal taxa.

The *Striatosirenites kinasovi* Zone was previously correlated with the lower subzone of the *Stikinoceras kerri* Zone of British Columbia (Konstantinov and Sobolev, 1999b) based on ammonoid species common for both zones, such as *Pterosirenites auritus* Tozer and *Pinacoceras regiforme* Diener (Table). At the same time, the *Stikinoceras kerri* Zone is correlated with the lower Norian *Guembelites jandianus* Zone of the standard ammonoid zonation, although Krystyn (1980) believes that only the upper subzone of the *jandianus* Zone has equivalents in the *kerri* Zone of North America. Nautiloids *Proclydonautilus spirolobus* (Dittmar) occurring in the *kinasovi* Zone and in the *jandianus* Zone of the Alps suggest their synchronism, at least partial. Conodonts *Norigondolella navicula* (Huckriede) and bivalves *Halobia kawadai* Yehara were encountered in the lower part of the *kinasovi* Zone on the Kotel'nyi Island. According to data reported by Krystyn (1980), *Norigondolella navicula* coexists in Austria (Hallstatt) with *Epigondolella abneptis* and *E. primitia* in the lower (*jandianus, paulckei*, and *magnus* zones) and middle (*bicrenatus* and *columbianus* zones) Norian deposits. In Canada (Orchard, 1991; Orchard and Tozer, 1997), *Norigondolella navicula* appears at the base of the *kerri* Zone and marks the base of Norian deposits and an upper part of the *Metapolygnathus primitius* Zone of the conodont scale. Suggesting the conodont standard for the Austrian-Alpine Province, Kozur (1980) who established the *navicula* Subzone of the lower Norian based on the appearance of its index species regarded it as the age analog of the *Stikinoceras kerri* and *Malayites paulckei* zones of the ammonoid scale. According to his data, that index species is frequent in the *Juvavites magnus* and *Cyrtopleurites bicrenatus* Zones and rare in the *Sirenites argonautae* and *Sagenites giebeli* Zones. As to halobians, species *Halobia kawadai* Yehara represented, according to I.V. Polubotko (*Obshchaya shkala..., 1984; Polubotko,* 1984), a vicarious form of the early Norian *Halobia styriaca* Mojsisovics. All the data confirm therefore a synchronism of the lower Norian boundary in the Boreal and Tethyan realms.

Correlation scheme for Norian deposits of the Kotel'nyi Island

Stage	Substage	the Kotel'nyi Island, Tikhaya River lower courses				British Columbia		Alps
		Conodont Beds	Nautiloid beds	Zones, subzones, and beds in ammonoid and bivalve successions		Ammonoid zonation		Ammonoid zonation
Norian	upper	Beds with *Norigondolella steinbergensis*		*Monotis ochotica*		*Gnomohalorites cordilleranus*	*Lissonites pecki*	*Rhabdoceras suessi*
							Paraquembelites ludingtoni	
	middle		Beds with *Proclydonautilus* cf. *P. natosini*	*Eomonotis scutiformis*	*Eomonotis pinensis*	*Mesohimavatites columbianus*	*Alloclionites welteri*	*Mesohimavatites columbianus*
							Neohimavatites canadensis	
					Eomonotis daonellae-formis		*Leiodistichites ursidens*	
							Parathisbites oineus	
		conodonts not found	nautiloids not found	Beds with *Cyrtopleurites* ex gr. *altissimus*		*Drepanites rutherfordi*		*Cyrtopleurites bicrenatus*
	lower			? presumable hiatus		*Juvavites magnus*	*Dimorphotoceras caurinum*	*Juvavites magnus*
							Indojuvavites brunneus	
						Malayites dawsoni	*Discomalayites carinatus*	*Malayites paulckei*
							Pseudocardioceras idunae	
							Wangoceras pax	
		Beds with *Norigondolella navicula*	Beds with *Germanonautilus* ex gr. *popowi*	*Norosirenites obručevi*		*Stikinoceras kerri*	*Gonionotites rarus*	*Guembelites jandianus*
			Beds with *Proclydonautilus* cf. *spirolobus*	*Striatosirenites kinasovi*			*Discostyrites ireneanus*	

Hence, the *Striatosirenites kinasovi* Zone of the Kotel'nyi Island is undoubtedly of the early Norian age and can be correlated, based on ammonoids, nautiloids, bivalves, and conodonts, with the *Stikinoceras kerri* Zone of British Columbia and with the standard *Guembelites jandianus* Zone.

An upper part of the *Norosirenites obručevi* Zone of Kotel'nyi Island, in which the index species was found, is correlative with the lower subzone of the *Malayites dawsoni* Zone of British Columbia. The arguments in favor are the presence of *Norosirenites* forms in both zones and similarity or even identity of the Canadian *Norosirenites krystyni* Tozer and Siberian *N. obručevi* (Bajarunas). The *Malayites dawsoni* Zone is an equivalent of the standard *Malayites paulckei* Zone (*Obshchaya shkala...*, 1984). The lower part of the *obručevi* Zone, which yields ammonoids *Arcestes* ex gr. *colonus* Mojs., is likely corresponding in stratigraphic range to the upper subzone of the *kerri* Zone and, accordingly, to the upper part of the *jandianus* Zone.

Ammonoids of the genus *Cyrtopleurites* found in overlying deposits of the Kotel'nyi Island have not been previously known in northeastern Asia and Boreal Realm. Up to the present, representatives of the genus have been reported to occur in the Eastern Alps, on the Sicily Island, in the Himalayas, on the Timor Island, in southeastern Asia, and in British Columbia. The *Cyrtopleurites* aff. *strabonis* described by Popov from the Cape Hansa, the Wilczek Land Island of Franz Josef Land (Popov, 1958, p. 18, Plate, no. 1) has sculpture different from that typical of the genus *Cyrtopleurites* and represents most likely a species of the *Norosirenites* genus, which is not described yet. Ammonoids of the genus *Cyrtopleurites* are confined everywhere to the lowermost middle Norian. They are characteristic components of the ammonoid fauna from the *Cyr-*

topleurites bicrenatus Zone of the lowermost middle Norian in the Eastern Alps and in correlative zones of other regions of the Tethyan realm.

Thus, the *Cyrtopleurites* ex gr. *altissimus* Beds of the Kotel'nyi Island can be directly correlated with the *Drepanites rutherfordi* Zone of British Columbia and with the *Cyrtopleurites bicrenatus* Zone of the eastern Alps, both bearing *Cyrtopleurites* forms. Units correlative with the *Juvavites magnus* Zone and with upper parts of the *Malayites dawsoni* and *Malayites paulckei* Zones cannot be established in the described section.

Ammonoids of the genus *Cyrtopleurites* found for the first time in Norian deposits of the Kotel'nyi Island specify the taxonomic composition of Late Triassic ammonoids of Boreal Realm and are important for recognition of reliable equivalents of the lower *Cyrtopleurites bicrenatus* Zone of the middle Norian and for determination of the lower-middle Norian boundary position in Boreal sections. The *Cyrtopleurites* ex gr. *altissimus* Beds of the Kotel'nyi Island span stratigraphic range (above the *Norosirenites obručevi* Zone and below the *Eomonotis scutiformis* Zone) that corresponds to the *Otapiria ussuriensis* Zone in the Norian zonal scale of northeastern Asia (Dagys, 1986). The lower boundary of the *Otapiria ussuriensis* Zone was arbitrarily placed at the base of the middle Norian Substage *Obshchaya shkala...*, 1984). Equivalents of the *bicrenatus* Zone, which are now established in the Kotel'nyi Island and occupy stratigraphic range of the *ussuriensis* Zone, indicate that the lower-middle Norian boundary should be placed in northeastern Asia somewhere inside the latter. This is evident from composition of ammonoids (*Norosirenites tenuistriatus* (Popow), *Malayites* ex gr. *parcus* McLearn, *Dittmaritoides guembeli* Vavilov et Archipov) found in the *ussuriensis* Zone and from interregional correlations (Dagys *et al.*, 1979; Bychkov, 1995; Konstantinov and Sobolev, 1999b; Konstantinov, 2000).

The *Eomonotis pinensis* Subzone of the *Eomonotis scutiformis* Zone is equivalent to the upper subzone of the *Mesohimavatites columbianus* Zone of British Columbia, where it yields *Eomonotis pinensis* (Westermann) (Tozer, 1994). Ammonoids *Neohimavatites canadiensis* McLearn found in the third (from the base) subzone of the *columbianus* Zone substantiate its correlation with the *Eomonotis daonellaeformis* Subzone, because *Neohimavatites* forms similar to Canadian species are typical of the latter (Bychkov and Polubotko, 1970). However, the *daonellaeformis* Subzone can be alternatively correlated with the second and lower (partially) subzones of the *columbianus* Zone, because Vavilov (1982) reported data on ammonoids *Dittmaritoides* (= *Pleurodistichites guembeli* Archipov et Vavilov) and *Eomonotis daonellaeformis* (Kiparisova) found associated in deposits of the Karadan Formation of the Kharaulakh Ridge and also known from the lower subzone of the *columbianus* Zone.

Such a correlation of the *daonellaeformis* Zone is consistent with data on distribution of nautiloids and conodonts in deposits of the Kotel'nyi Island. In particular, *Proclydonautilus natosini* McLearn was found in beds of British Columbia, which correspond to the second and third subzones of the *columbianus* Zone (McLearn, 1946, 1960; Tozer, 1994). Conodonts *Norigondolella steinbergensis* (Mosher) and *N. navicula* (Huckriede) found at two levels of the *daonellaeformis* Subzone (Exp. 192, Bed 5) are known to occur in association with *Epigondolella abneptis* (Huckriede) and *Mockina postera* (Mosher) in the middle Norian *bicrenatus* and *columbianus* zones of Austria (Krystyn, 1980). In British Columbia, the *Norigondolella steinbergensis* (Mosher) is a common component of the conodont assemblage from the *Epigondolella postera* Zone, a close age analog of the second (from the base) subzone of the *columbianus* Zone (Orchard, 1991; Orchard and Tozer, 1997).

BIOGEOGRAPHIC ANALYSIS OF FAUNA

The study region is a part the New Siberian structural-facies zone that was at the subplatform stage of evolution in the Triassic (Dagys *et al.*, 1979). The uniform carbonate-clayey composition of deposits with fossils, which mainly represent pelagic groups of fauna, indicate that sedimentation settings of an open and warm sea were situated rather far away from the coast (Egorov *et al.*, 1987). The Late Triassic, particularly Norian biota of the region was also peculiar. It was of a mixed type and consisted of Boreal and Tethyan taxa.

Norian ammonoids from the Kotel'nyi island represent 13 genera of 11 families: Megaphyllitidae (*Magaphyllites*), Gymnitidae (*Placites*), Pinacoceratidae (*Pinacoceras*), Cladiscitidae (*Cladiscites, Paracladiscites*), Arcestidae (*Arcestes*), Sirenitidae (*Striatosirenites, Norosirenites*), Cyrtopleuritidae (*Cyrtopleurites*), Distichitidae (*Dittmaritoides* = *Pleurodistichites*), Haloritidae (*Anatomites*), Ussuritidae (*Arctophyllites*), and Discophyllitidae (*Rhacophyllites*). Among genera, one (*Arctophyllites*) is characteristic of the Boreal Realm (Konstantinov, 1995). The other two, *Anatomites* described by Diener in 1924 and *Cyrtopleurites* established for the first time in the study region, are typical of the Tethyan Realm. All the others are cosmopolitan. Most of them represent long-lived ammonoids with smooth shells. Genera *Norosirenites* and *Dittmaritoides* are known from mixed ammonoid assemblages of British Columbia, where they are represented by forms similar, if not identical, to Siberian species. A characteristic feature of ammonoid fauna from the Kotel'nyi Island, other than presence of southern taxa, consists in abundance and taxonomic diversity of ammonoids at several levels, especially in the middle and upper Norian. This feature is untypical of synchronous fauna known in other regions of northeastern Asia. The fauna in question is most similar to that known

from upper reaches of the Bol'shoi Anyui River, where representatives of Tethyan haloritids (*Catenohalorites* and *Halorites*) and horistoceratids (*Rhabdoceras*) coexist with dominating cosmopolitan families and genera of ammonoids (Afitskii, 1970).

Norian coiled nautiloids are represented in the study region by two cosmopolitan genera *Germanonautilus* (Tainoceratidae) and *Proclydonautilus* (Clydonautilidae). The genus *Proclydonautilus* includes two species *P. spirolobus* (Dittmar) and *P. natosini* McLearn. The first one is of the almost global distribution, while the second is known from lower and middle Norian deposits of northeastern British Columbia and Yukon (Tozer, 1982). In the Late Triassic, the indicated regions were located in middle latitudes, being populated by the mixed Boreal-Tethyan invertebrate fauna. The genus *Germanonautilus* is represented by Siberian endemics *G. popowi* Sobolev.

Unusually large phragmocones of coleoids present in the Norian cephalopod fauna of the Kotel'nyi Island emphasize its peculiarity. Such forms formerly unknown in the Upper Triassic deposits of northeastern Asia are common in the Alpine region (Mojsisovics, 1871).

Conodonts have been found recently in Norian deposits of the Kotel'nyi Island and in other areas of Upper Triassic deposits of northeastern Asia (Klets, 1996, 1998). They are of a uniform morphology in distinction from conodonts of the Tethyan Realm. Southern conodont faunas (Burii, 1989; Klets, 1995; Igo and Koike, 1983; Koike *et al.*, 1991; Kozur, 1980; Krystyn, 1980; Zhao and Zhang, 1991; and others) considerably differ from those of northern latitudes. The genus *Epigondolella* possessing tuberculate platforms was most prosperous in the Tethys during the early and middle Norian. The genus *Mockina*, the ancestor of the late Norian-Rhaetian genus *Parvigondolella*, appeared in the terminal early Norian and became widespread in southern seas. The genus *Metapolygnatus* died out at the beginning of the Norian, and *Norigondolella* forms, presumable descendants of the genus *Paragondolella*, appeared in the same latitudes in the earliest Norian. Only representatives of the genus *Norigondolella*, which had a smooth upper surface of the platform, penetrated into northern Siberia during the Norian.

Kurushin (Egorov *et al.*, 1987; Kurushin, 1998) previously pointed out that Norian bivalve assemblages of the Kotel'nyi Island include the North American species *Monotis (Pacifimonotis) subcircularis* Gabb, *M. (Entomonotis) posteroplana* Westermann, the genus *Cassianella*. According to Bychkov (1992), the last genus is a typical Tethyan taxon.

Thus, typical Tethyan taxa indicative of warm (tropical) habitats coexist with Boreal elements nearly in all Norian fauna groups of the Kotel'nyi Island. Being not confined to a particular stratigraphic datum, they occur throughout the whole Norian sequence. This indicates the peculiarity of regional biota that likely characterizes an independent paleobiochore of the Boreal realm, i.e., the New Siberian subprovince of the Siberian province, rather than a short-term invasions of southern elements. Another characteristic feature of the regional Norian biota is a considerable proportion of cosmopolitan taxa in its composition and presence of forms identical or similar to North American fossils. This is likely indicative of free connections and fauna exchange between East Pacific paleobasins of the Norian time.

CONCLUSIONS

1. The lower-middle Norian sedimentary sequence exposed in lower reaches of the Tikhaya River (central part of the Kotel'nyi Island) has been studied and described. After revision, the taxonomic composition of Norian ammonoids, nautiloids, coleoids, and conodonts characteristic of the study region has been refined and elucidated further.

2. Based on the analysis of stratigraphic ranges of ammonoids, nautiloids, and conodonts, the regional stratigraphy has been refined and the local biostratigraphic scheme including zones, subzones, and beds with fauna is proposed for the lower-middle Norian sequence of the Kotel'nyi Island. Three biostratigraphic units of the ammonoid succession are distinguished: the *Striatosirenites kinasovi* (initially recognized) and *Norosirenites obručevi* zones in the lower Norian and the *Cyrtopleurites* ex gr. *altissimus* Beds (initially recognized) in the middle Norian. The lower-middle Norian biostratigraphic zonation of nautiloids is outlined the first time. It corresponds to the succession of *Proclydonautilus* cf. *P. spirolobus* and *Germanonautilus* ex gr. *G. popowi* beds of the lower Norian underlying the *Proclydonautilus* cf. *P. natosini* Beds of the middle and lower upper Norian. The *Norigondolella navicula* Beds of the lower Norian and the *Norigondolella steinbergensis* Beds of the middle-upper Norian are established in the conodont succession.

3. The local biostratigraphic scheme of the lower-middle Norian sequence of the Kotel'nyi Island is correlated with the Canadian and standard ammonoid scales. Ammonoids of the genus *Cyrtopleurites*, which are characteristic of the lower *Cyrtopleurites bicrenatus* Zone in the standard middle Norian zonation and of correlative zones, have been found for the first time in the Kotel'nyi Island. They enabled the direct Boreal-Tethyan correlation and substantiated positioning of the lower-middle Norian boundary in Boreal regions of northeastern Russia.

4. Biogeography of Norian ammonoids, nautiloids, coleoids, and conodonts from the Kotel'nyi Island is comprehensively analyzed. Characteristic features of the studied fauna are its mixed composition exemplifying coexistence of Boreal and Tethyan fossils, a substantial proportion of cosmopolitan taxa, and presence of forms identical or similar to North American taxa. This suggests that the peculiar Norian fauna of the

study region characterizes the independent New Siberian subprovince within the Siberian province of the Boreal Realm, on the one hand, and free connections between East Pacific paleobasins of the Norian time, on the other.

ACKNOWLEDGMENTS

The work was supported by the Russian Foundation for Basic Research, project nos. 99-05-64715 and 00-05-65193, and granted by the Program in the field of fundamental natural science and geology of the Ministry of Higher Education of Russian Federation, grant no. NE00-9.0-8, and by the Project "Universities of Russia," grant no. 015.09.24.

Reviewers V.G. Ganelin and V.A. Zakharov

REFERENCES

Afitskii, A.I., *Biostratigrafiya triasovykh i yurskikh otlozhenii basseina reki Bol'shoi Anyui* (Biostratigraphy of Triassic and Jurassic Deposits in the Bol'shoi Anyui River Basin), Moscow: Nauka, 1970.

Burii, G.I., *Konodonty i stratigrafiya triasa Sikhote-Alinya* (Conodonts and Triassic Stratigraphy of the Sikhote Alin), Vladivostok: Akad. Nauk SSSR, 1989.

Bychkov, Yu.M., Comparative Characterization of Late Triassic Faunas from Northeastern Asia, *Preprint of Severo-Vost. Kompl. Nauch.-Issled. Inst. Ross. Akad. Nauk*, Magadan, 1992.

Bychkov, Yu.M., Late Triassic Trachyceratids and Syrenitids from the Yana Okhotskaya Source Area, *Preprint of Severo-Vost. Nauchn. Tsentra*, Magadan, 1995.

Bychkov, Yu.M. and Polubotko, I.V., First *Himavatites* from Northeastern Asia, *Paleontol. Zh.*, 1970, no. 2, pp. 114–119.

Dagys, A.S., *Triasovye brakhiopody (morfologiya, sistema, filogeniya, stratigraficheskoe znachenie i biogeografiya)* (Triassic Brachiopods: Morphology, Taxonomy, Phylogeny, Stratigraphic Significance, and Biogeography), Novosibirsk: Nauka, 1974.

Dagys, A.S., Main Features of Biogeography of Triassic Seas, *Paleontologiya i morskaya geologiya. Mezhdunar. geol. kongress, 25-aya sessiya. Doklady sovetskikh geologov* (Paleontology and Marine Geology: Reports of Soviet Geologists to 25th Geol. Congress), Moscow: Nauka, 1976, pp. 109–119.

Dagys, A.S., Problems of Triassic Biostratigraphy in Siberia and Far East, *Biostratigrafiya mezozoya Sibiri i Dal'nego Vostoka* (Biostratigraphy of Siberia and Far East), Novosibirsk: Nauka, 1986, pp. 9–16.

Dagys, A.S., Arkhipov, Yu.V., and Bychkov, Yu.M., *Stratigrafiya triasovoi sistemy Severo-Vostoka Azii* (Stratigraphy of Triassic System in Northeastern Asia), Moscow: Nauka, 1979.

Dagys, A.S., Dagys, A.A., and Ermakova, S.P., *et al.*, *Triasovaya fauna Severo-Vostoka Asii* (Triassic Fauna of Northeastern Asia), Novosibirsk: Nauka, 1996.

Dagys, A.S. and Shevyrev, A.A., Zoogeography of Triassic Seas, *Paleontologiya, paleobiogeografiya i mobilism* (Paleontology, Paleobiogeography, and Mobilism), Magadan: Magadan. Kn. Izd., 1981, pp. 113–119.

Diener, C., Die obertriasische Ammonitenfauna der Neusibirischen Insel Kotelny, *Sitzungsber. Akad. Wiss. Wien. Math.-Naturwiss., Kl. Abt. I*, 1916, vol. 125, pp. 439–463.

Diener, C., Über triasische Cephalopoden, Gastropoden und Brachiopoden von der Insel Kotelny, *Zap. Ross. Akad. Nauk, Ser. 8*, 1924, vol. 21, no. 5, pp. 1–19.

Igo, H. and Koike, T., Conodont biostratigraphy of cherts in the Japanese Islands, *Develop. Sedimentol.*, 1983, vol. 36, pp. 65–77.

Keyserling, A., Beschreibung einiger von Dr. A. Th. v. Middendorff mitgebrachten Ceratiten des arktischen Sibiriens, *Bull. Acad. Imper. Sci. St. Petersburg*, 1845, vol. 5, pp. 161–174.

Kiparisova, L.D., Bychkov, Yu.M., and Polubotko, I.V., *Pozdnetriasovye dvustvorchatye mollyuski Severo-Vostoka SSSR* (Late Triassic Bivalves in the Northeastern USSR), Magadan: Magadan. Kn. Izd., 1966.

Klets, T.V., *Biostratigrafiya i konodonty triasa Srednego Sikhote-Alinya* (Triassic Conodonts and Biostratigraphy of Central Sikhote-Alin), Novosibirsk: Novosib. Univ., 1995.

Klets, T.V., First Discovery of Conodonts from Upper Triassic Deposits of Kotel'nyi Island, *Stratigr. Geol. Korrelyatsiya*, 1996, vol. 4, no. 6, pp. 96–98.

Klets, T.V., Conodonts of the Genus *Norigondonella* from the *Eomonotis scitiformis* Zone of Northeastern Asia (New Siberian Islands), *Aktual'nye voprosy geologii i geografii Sibiri* (Actual Problems of Geology and Geography in Siberia), Tomsk: Tomsk. Gos. Univ., 1998, pp. 231–233.

Konstantinov, A.G., *Arctophyllites*, the New Genus of Ammonoids from Carnian Deposits of Northeastern Asia, *Paleontol. Zh.*, 1995, no. 3, pp. 18–25.

Konstantinov, A.G., State of the Art and Problems of Boreal-Tethyan Correlation of the Carnian and Norian Stages, *Paleontologiya v Rossii: itogi i perspectivy. Tezisy dokladov XLVI sessii Paleontol. o-va pri RAN* (Paleontology in Russia: Results and Perspectives, Abstracts of XLVI Session of Paleontol. Soc. RAS), St. Petersburg: Vseross. Geol. Inst., 2000, pp. 43–44.

Konstantinov, A.G. and Sobolev, E.S., Biostratigraphic Scheme of Carnian and Norian in Northeastern Russia, Pt. 1: Description of Sections and Stratigraphic Ranges of Cephalopods, *Tikhookean. Geol.*, 1999a, vol. 18, no. 1, pp. 3–17.

Koike, T., Kodachi, Y., Matsuno, T., and Baba, H., Triassic Conodonts from Exotic Blocks of Limestone in North on Kuzuk, the Asio Mountains, *Sci. Repts. Yokohama Nat. Univ., Sec. 2*, 1991, no. 38, pp. 53–69.

Konstantinov, A.G. and Sobolev, E.S., Biostratigraphic Scheme of Carnian and Norian in Northeastern Russia, Pt. 2: New Zonal Scales and Correlation, *Tikhookean. Geol.*, 1999b, vol. 18, no. 4, pp. 48–60.

Korchinskaya, M.V., To Biostratigraphy of Triassic Deposits in the Kotel'nyi Island (New Siberian Islands), *Mezozoiskie otlozheniya Severo-Vostoka SSSR* (Mesozoic Deposits of the Northeastern USSR), Leningrad: Nauchno-Issled. Inst. Geol. Arctiki, 1977, pp. 43–49.

Kozur, H., Revision der Conodontenzonierung der Mittel- und Obertrias des tethyalen Faunenreichs, *Geol. Palaontol. Mitt. Innsbruck*, 1980, vol. 10, pp. 79–172.

Krystyn, L., Eine neue Zonengliederung im alpin-mediterranen Unterkarn, *Schriftenr. Erdwiss. Komm. Österr. Akad. Wiss.*, 1978, vol. 4, pp. 37–75.

Krystyn, L., Stratigraphy of the Hallstatt region, *Abhandl. Geol. Bundesanstalt Wien*, 1980, vol. 35, pp. 69–98.

Kurushin, N.I., Stratigraphy of Triassic Deposits in the Kotel'nyi Island, New Siberian Islands), *Boreal'nyi trias* (The Boreal Triassic), Moscow: Nauka, 1987, pp. 66–80.

Kurushin, N.I., Triassic Bivalves from Northeastern Asia (Morphology, Taxonomy, Biostratigraphy, Paleoecology, and Paleobiogeography), *Doctoral (Geol.–Min.) Dissertation*, Novosibirsk: United Inst. Geol., Geophys., Mineral., Ross. Acad. Sci., 1998.

McLearn, F.H., Upper Triassic Faunas in Halfway, Sikanni Chief and Prophet River Basins, Northeastern British Columbia, *Pap. Geol. Surv. Can.*, 1946, no. 46-25 (Appendix), pp. 1–5.

McLearn, F.H., Ammonoid Faunas of the Upper Triassic Pardonet Formation, Peace River Foothills, British Columbia, *Mem. Geol. Surv. Can.*, 1960, no. 311, pp. 1–118.

Mojsisovics, E., Über das Belemnitiden-Geschlesht *Aulacoceras* Fr. von Hauer, *Jahrb. K.-K. Geol. Reichsanstalt. Wien*, 1871, vol. 21, no. 4, pp. 41–58.

Orchard, M.J., Late Triassic Conodont Biochronology and Biostratigraphy of the Kunga Group, Queen Charlotte Islands, British Columbia, *Pap. Geol. Surv. Can.*, 1991, no. 90-10, pp. 173–193.

Orchard, M.J. and Tozer, E.T., Triassic Conodont Biochronology, Its Calibration with the Ammonoid Standard, and a Biostratigraphic Summary for the Western Canada Sedimentary Basin, *Bull. Can. Petrol. Geol.*, 1997, vol. 45, no. 4, pp. 675–692.

Polubotko, I.V., Late Triassic Halobiids: Zonation and Correlation Significance, *Sov. Geol.*, 1984, no. 6, pp. 40–50.

Popv, Yu.N., Late Triassic Ammonites and Pelecypods from the Franz Josef Land, *Sb. statei po paleontologii i biostratigrafii, Vyp. 12* (Collection of Works on Paleontology and Biostratigraphy), Leningrad: Nauchno-Issled. Inst. Geol. Arktiki, 1958, no. 12, pp. 16–22.

Preobrazhenskaya, E.N. and Korchinskaya, M.V., Basic Features of Stratigraphy and Most Important Triassic Sections in Northeastern Asia, Novosibirsk Structural-Facies Region, *Stratigrafiya triasovoi sistemy Severo-Vostoka Asii* (Triassic Stratigraphy of Northeastern Asia), Moscow: Nauka, 1979, pp. 107–112.

Preobrazhenskaya, E.N., Trufanov, G.V., Vol'nov, D.A., *et al.*, Mesozoic Deposits of the Kotel'nyi Island, *Geologiya i poleznye iskopaemye Novosibirskikh ostrovov i ostrova Vrangelya* (Geology and Mineral Deposits of New Siberian and Vrangel Islands), Leningrad: Nauchno-Issled. Inst. Geol. Arktiki, 1975, pp. 28–37.

Silberling, N.J. and Tozer, E.T., Biostratigraphic Classification of the Marine Triassic in North America, *Spec. Pap. Geol. Soc. Am.*, 1968, no. 110, pp. 1–63.

Tozer, E.T., A Standard for Triassic Time, *Bull. Geol. Surv. Can.*, 1967, no. 156, pp. 1–103.

Tozer, E.T., Marine Triassic Faunas of North America, Their Significance for Assessing Plate and Terrane Movements, *Geol. Rundschau*, 1982, vol. 71, no. 3, pp. 1077–1104.

Tozer, E.T., Canadian Triassic Ammonoid Faunas, *Bull. Geol. Surv. Can.*, 1994, no. 467, pp. 1–663.

Vavilov, M.N., Lithostratigraphy of Triassic Deposits in the Northern Verkhoyansk Region, *Bio- i litostratigrafiya triasa Sibiri* (Triassic Bio- and Lithostratigraphy in Siberia), Moscow: Nauka, 1982, pp. 37–47.

Vol'nov, D.A., Voitsekhovskii, V.N., Ivanov, O.A., *et al.*, Novosibirsk Islands, *Geologiya SSSR. Tom 26. Ostrova Sovetskoi Arktiki* (Geology of the USSR, vol. 26: Island of Soviet Arctic), Moscow: Nedra, 1970, pp. 324–374.

Zhao, X. and Zhang, K., Triassic Conodonts from the Ngari area, Xizang (Tibet), China, *Acta Micropaleontol. Sinica*, 1991, vol. 8, no. 4, pp. 433–440.

Stratigraphy and Geological Correlation, Vol. 11, No. 3, 2003, pp. 244–260. Translated from Stratigrafiya. Geologicheskaya Korrelyatsiya. Vol. 11, No. 3, 2003, pp. 40–56.
Original Russian Text Copyright © 2003 by Kirichkova, Kostina, Timoshina.
English Translation Copyright © 2003 by MAIK "Nauka/Interperiodica" (Russia).

Comprehensive Substantiation of Jurassic Phytostratigraphy and Correlations in the Kansk Coal Basin, Siberia

A. I. Kirichkova*, E. I. Kostina, and N. A. Timoshina***

**All-Russia Oil Research Geological Prospecting Institute (VNIGRI), St. Petersburg*

**Geological Institute, Russian Academy of Sciences, Moscow*

Received June 13, 2000; in final form, October 26, 2001

Abstract—Paleobotanical characteristics based on studied plant macrofossils and miospores from Jurassic sediments of the Kansk coal basin are discussed. The studied samples characterize the formation stratotypes and borehole sections. Plant macrofossils and palynologic samples have been collected from the same intervals of sections. The comparative analysis of distribution of miospores and plant macrofossils is used for the first time to distinguish independent phytostratigraphic units, i.e., the floral and palynologic beds, which are found to be of almost equal ranges. Remote correlations of spore-pollen assemblages with those from West Siberia and from marine sediments of northern Central Siberia enabled a more reliable dating of the distinguished phytostratigraphic units. Four spore-pollen assemblages are recognized: the Pereyaslovka assemblage of the Sinemurian–Pliensbachian age (from the lower part of eponymous formation), the Toarcian Ilan assemblage (characteristic of the uppermost Pereyaslovka and Ilan formations), the Aalenian Kamala and the Bajocian Borodino assemblages (from synonymous formations, respectively). Three assemblages of plant macrofossils termed as the Aban (Pereyaslovka and Ilan formations), Rybinskoe (Kamala Formation), and Quarry (Borodino Formation) floras have distribution ranges corresponding respectively to the Pliensbachian–Toarcian, Aalenian, and Bajocian interval.

Key words: Central Siberia, phytostratigraphy, Jurassic, palynology, plant macrofossils, floral beds.

INTRODUCTION

In recent years, plant macrofossils and microphytofossils from the continental Jurassic sediments of southern Central and West Siberia were thoroughly investigated. The obtained paleobotanical characteristics of continental Jurassic deposits in Siberia are complete, enabling the interregional correlation of coal-bearing sequences. This paper deals with the study of major Jurassic reference sections of the Kansk coal basin situated in the southeastern Krasnoyarsk region (Fig. 1). The deposits are represented completely by continental facies bearing a great variety of plant remains.

The Jurassic sequence of the Kansk coal basin unconformably overlies the Paleozoic sediments and is divided from the base upward into the Pereyaslovka, Ilan, Kamala, Borodino, and Tyazhin formations (*Resheniya 3-go...*, 1981). Lithologic composition of the formations and their distribution within the basin have been described previously (Lebedev, 1955; Aksarin, 1957; Grigor'ev, 1968; Markovich, 1970). Until recently, ages of the formations were estimated using palynologic records only (Sakhanova, 1957, 1960; Il'ina, 1970, 1976, 1980, 1981, 1985, 1988; Smokotina, 1997), because taxonomy of plant macrofossils was poorly known for a long period. The corresponding papers included commonly the summary lists of formally identified plant taxa (Aksarin, 1955, 1957; Lebedev, 1955, 1960; *Resheniya 3-go...*, 1981). Markovich (1970) published the most plausible data on fossil floras from Jurassic sediments in the Aban area of the Kansk coal basin. Unfortunately, she identified leaf remains of gymnosperms dominant in the Siberian Jurassic floras, without considering the epidermis structure, and did not defined concretely the taphofloras. However, the high-resolution taphonomy and correlation of coal seams and beds within the basin were worked out.

In 1990, Kirichkova and Travina first attempted to develop the Jurassic phytostratigraphy of the Kansk basin using plant macrofossils. In their work, they first applied the cuticle method to elaborate the taxonomy of plant remains. The studied materials were collected in a layer-by-layer mode from boreholes and outcrops of Jurassic rocks in the Kansk basin. Additionally the previous investigation results were critically analyzed. This resulted in a more concrete definition of taphofloras used to distinguish the Aban, Rybinskoe, and Quarry phytostratigraphic assemblages, which characterize the Pereyaslovka, Ilan, Kamala, and Borodino formations. The total range of the assemblages, namely, the terminal Early (Toarcian?)–mid-Middle Jurassic (Aalenian–Bajocian), was determined based on correlation with the Jurassic assemblages of the Kuznetsk basin, which are similar not so much in the taxonomic

composition as in the degree of general evolution of paleoflora.

Palynologic research in the Kansk basin was performed by N.S. Sakhanova in 1941–1957. In the coal-bearing Jurassic sediments of the Rybinskoe area, she distinguished two spore-pollen assemblages (SPA) characterizing the Pereyaslovka Formation of the Lower Jurassic and the Kamala and Borodino formations of the Middle Jurassic. The second pollen assemblage was subdivided in two subassemblages (SPS) confined to the Kamala and Borodino formations. Subsequently Verbitskaya (1970) distinguished three pollen assemblages from the same formations of the Aban area and four in the Rybinskoe area (Table 1). Working on materials for the Interdepartmental stratigraphic meeting in Central Siberia, Il'ina analyzed the Sakhanova's results and other regional palynologic data. She considered possible to distinguish eight pollen assemblages in Jurassic sequence of the Kansk basin by analogy with the sections from the northern Central Siberia (Il'ina, 1980, 1985). Her suggestion was included in resolutions of that meeting (*Resheniya 3-go...*, 1981).

Investigations in the Kansk basin that started in 1990 were continued in recent years. Plant remains and palynologic preparations sampled in a layer-by-layer mode from many boreholes of the Aban area and outcrops of the Borodino quarry and Rybnaya River were examined thoroughly. E.I. Kostina who studied plant macrofossils using the cuticle method even for the smallest fragments of leaf phytoleims considerably refined composition of plant assemblages distinguished earlier. She revealed a distinct stratigraphic confinement of certain taxa that enables nowadays a more reliable recognition of local phytostratigraphic units based on plant macrofossils. Concurrently N.A. Timoshina studied pollen spectra of samples collected in the intervals of sections with plant macrofossils. The Jurassic sediments of the Kansk basin, especially their lower beds, appeared to be significantly rich in microphytofossils. Based on changes in taxonomic composition and proportions of different palynologic groups throughout the section, the succession of four spore-pollen assemblages was recognized. This substantiated the distinction of palynologic units in the rank of palynoflora beds approximately corresponding in ranges to the floral beds. Thus, the Jurassic sequence of the Kansk coal basin and its lithologic units has got a complex paleobotanical characteristics based on pollen and macroflora assemblages occurring in the same intervals.

LOWER JURASSIC

The Lower Jurassic sediments of the Kansk basin are subdivided into the Pereyaslovka and Ilan formations. In full ranges, they are known in the Rybinskoe and Kansk-Taseevo structural facies zones (*Resheniya 3-go...*, 1981).

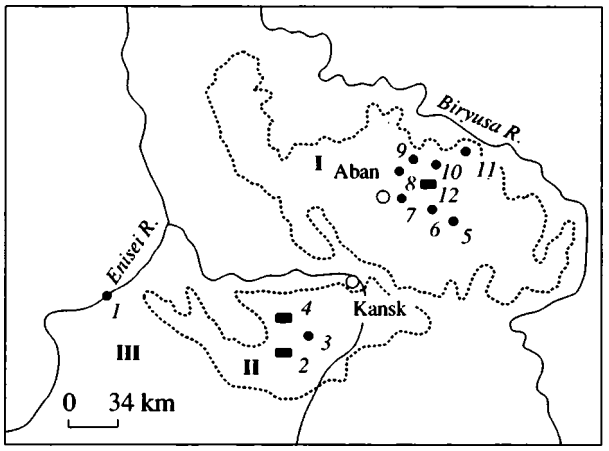

Fig. 1. Location of boreholes and outcrops in the Kansk coal-bearing basin:
(**I**) Aban area; (**II**) Rybinskoe area; (**III**) Sayan–Partizansk region; (1) outcrop on the Enisei River (nearby the Kubekovo Village); (2) Pereyaslovka coal field; (3) outcrop on the Rybnaya River; (4) Borodino coal field (Borodinskii quarry; (Wells 525, 576, 580); (5–10) boreholes in the Aban area (5) Well 8400; (6) Well 8500; (7) Well 219; (8) Well 312; (9) Well 1-C; (10) Well 16-C); (11) outcrop nearby the Voznesenka Village; (12) Aban coal field.

The Pereyaslovka Formation distinguished by Aksarin (1957) unconformably overlies the Permian and Carboniferous rocks. It is mainly represented by sandstones, siltstones, and, in part, by argillites, gravelstones, and coals. The thickness of the formation is up to 48 m in the Rybinskoe area and 27 to 100 m in the Aban area. In the stratigraphic schemes of the Kansk basin, the formation is subdivided into three subformations (*Resheniya 3-go...*, 1981). However, when studying the boreholes from the Aban area, where it is represented in full range, we had to agree with Semerikov (1970), who noted that the formation corresponds to a single megacyclothem and its subdivision into subformations, as adopted, is proved only by palynologic records. In the Aban area, the Pereyaslovka Formation was penetrated by numerous boreholes (Fig. 1). The most complete section is presented in Well 8500 (Fig. 2). Additionally, the formation is exposed in the outcrop nearby the Voznesenka Village (Dolgii Most depression), where the plant remains were collected and studied previously (Markovich, 1970).

The Ilan Formation distinguished by Sakhanova (1957, 1960 and) unconformably resting in places on the Pereyaslovka Formation is represented by regularly interbedding siltstones, argillites, sandstones, and greenish siderite beds. Its thickness is 10 to 70 m.

The formations are rather completely characterized by pollen and spores and by plant macrofossils. Sediments in the lower half of the Pereyaslovka Formation, which have been recovered from boreholes in the Aban area and are exposed in the road excavation near the Voznesenka Village (Fig. 2), yield the palynologic

Table 1. Different versions of palynostratigraphic subdivision of Jurassic sediments in the Kansk coal-bearing basin

Series	Stage	Sakhanova, 1957				Verbitskaya, 1970			Il'ina, Sakhanova, *Resheniya...*, 1981			Timoshina (this work)	
		Rybinskoe area				Aban area		Rybinskoe area					
Upper	Oxfordian					Tyazhin Formation	Third SPA		Tyazhin Formation		SPA-IX	Tyazhin Formation	
	Callovian												
Middle	Bathonian	Borodino Formation			Second SPS	Borodino Formation	Second SPA	Fourth SPA	Ust'-Yansk sequence		SPA-VIII		
								Third SPA					
	Bajocian	Kamala Formation	upper sub-formation	Second SPA	First SPS	Kamala Formation		Second SPA	Borodino Formation		SPA-VII	Borodino Formation	SPA-IV
	Aalenian		lower sub-formation				First SPA		Kamala Formation	upper sub-formation	SPA-VI	Kamala Formation	SPA-III
										lower sub-formation	SPS-2		
											SPS-1		
Lower	Toarcian	Pereyaslovka Formation		First SPA		Pereyaslovka Formation			Ilan Formation		SPA-V	Ilan Formation	SPA-II
	Pliensbachian								Pereyaslovka Formation	upper sub-formation	SPA-IV	Pereyaslovka Formation	SPA-I
										middle sub-formation	SPA-II-III		
	Hettangian-Sinemurian									lower sub-formation	SPA-I		

Note: abbreviations SPA and SPS are explained in the text.

assemblage of *Alisporites pergrandis, Cycadopites medius, Uvaesporites argentaeformis*, and *Stereisporites*. The assemblage is of a rather specific composition (Plate **I**, figs. 1–15). It includes large grains of *Alisporites pergrandis* (Bolch.) Iljina, *Piceaepollenites variabiliformis* (Mal.) M. Petr., *Paleoconiferus asaccatus* Bolch., *Dipterella oblatinoides* Mal., *Podocarpus permagna* Bolch., and *Podocarpidites* sp. sp. Rather abundant large monocolpate forms of the assemblage have infragranulate exine structure and have been previously considered as representing bennetites *Cycadopites percarinatus* (Bolch.) Iljina, *C. orbicularis* Sach. et Iljina, and *C. medius* (Bolch.) Iljina. All these taxa associate with abundant *Stereisporites* spores similar to those of bog mosses. These are *S. compactus* (Bolch.) Iljina, *S. bujargiensis* (Bolch.) Schulz, *S. seebergensis* Schulz, *S. congregatus* (Bolch.) Schulz, *S. psilatus* (Ross.), Pfl., and *S. antiquasporites* (Wilson et Webster) Dettm. Morphologically distinct spores *Uvaesporites argentaeformis* (Bolch.) Schulz and *Camptotriletes cerebriformis* Naum. et Jarosh. are common, whereas *Polycingulatisporites triangularis* (Bolch.) Playf. et Dettm., *Camptotriletes tenellus*

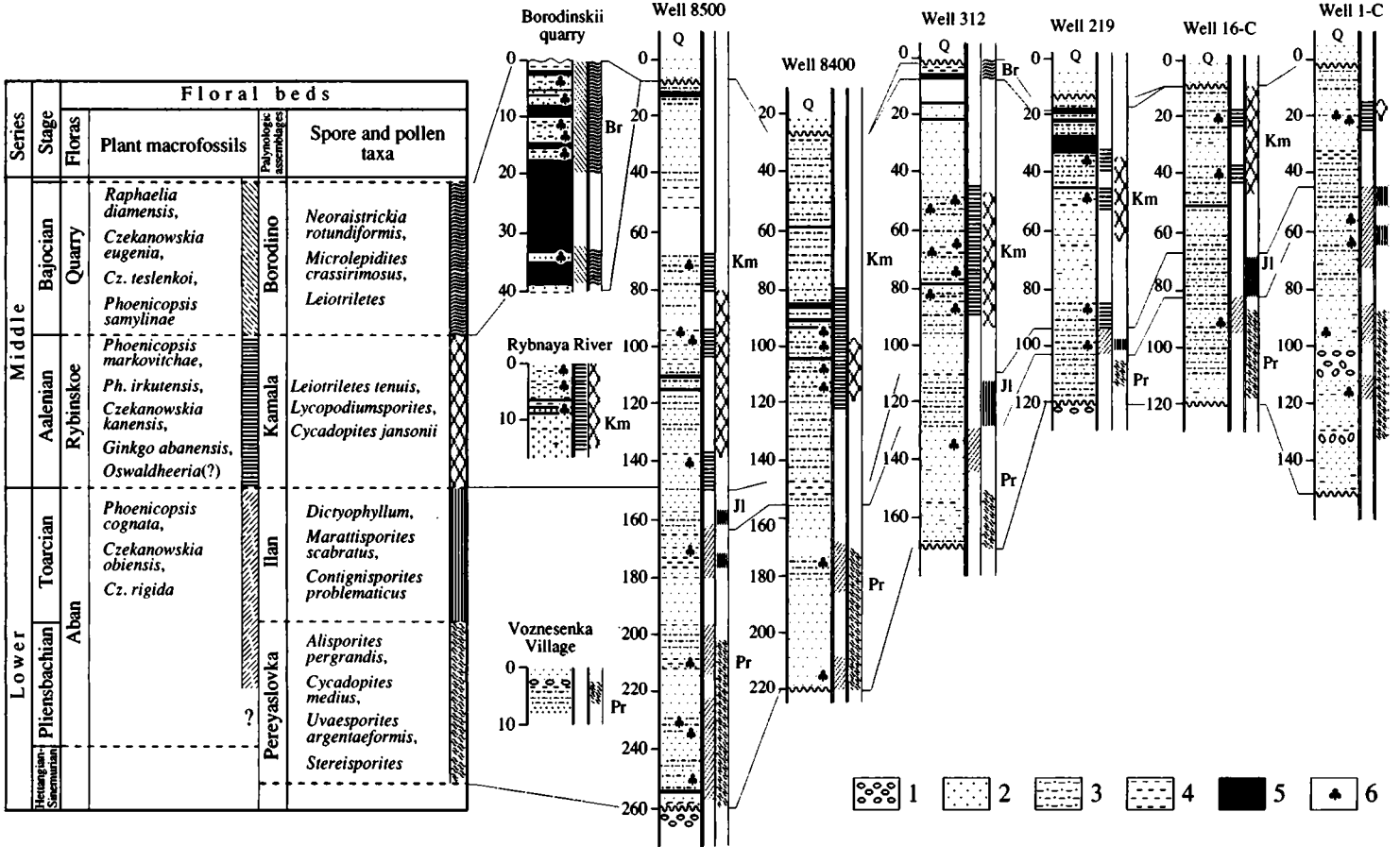

Fig. 2. Correlation of Jurassic reference sections (major boreholes and outcrops) in the Kansk basin: (1) conglomerates; (2) sandstones; (3) siltstones; (4) shales; (5) coal; (6) plant macrofossils; (Pr) Pereyaslovka, (Jl) Ilan, (Km) Kamala, and (Br) Borodino formations.

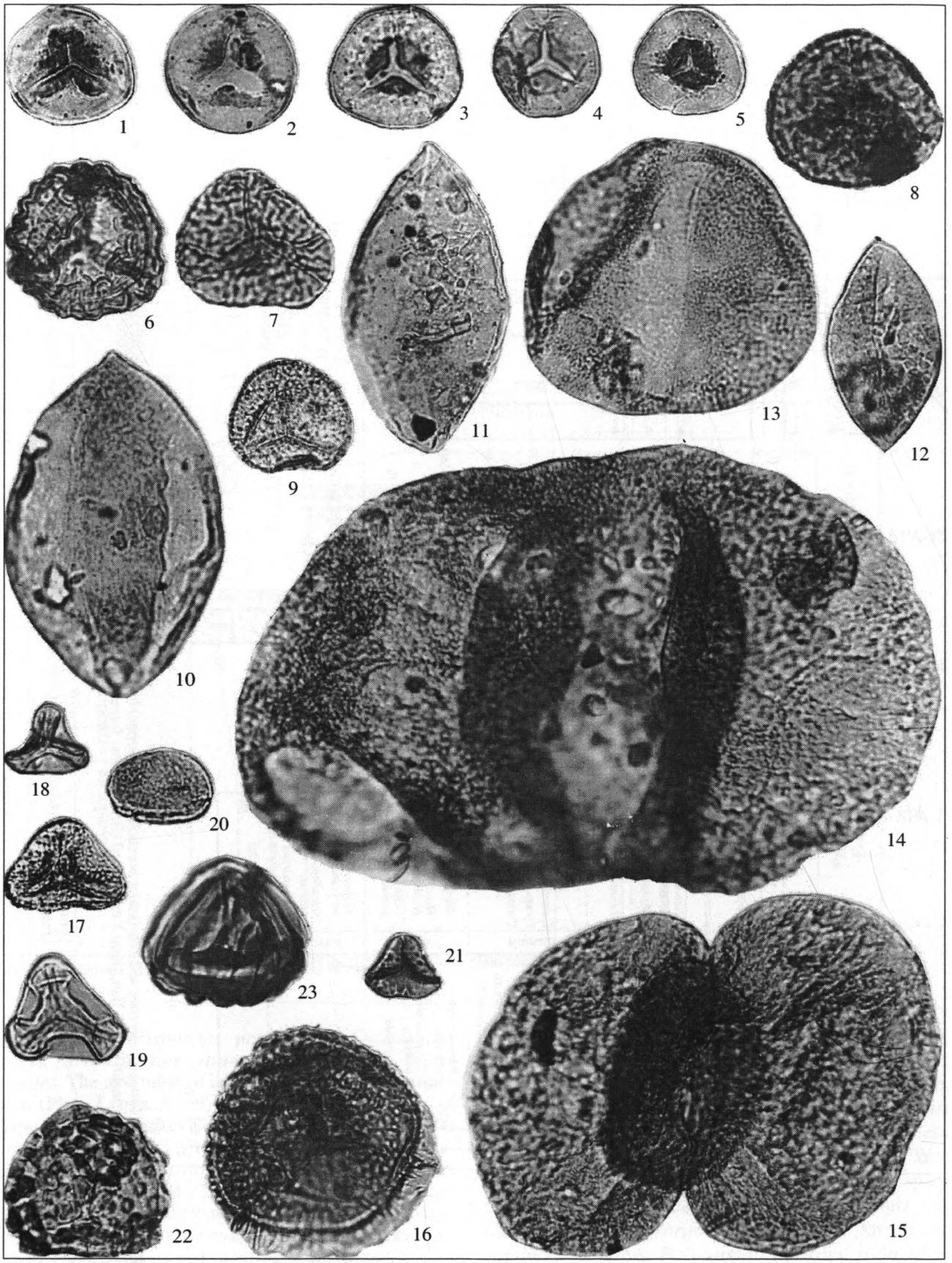
1
2
3
4
5
8
6
7
11
13
12
9
10
14
18
20
17
23
21
19
22
16
15

Naum. et Iljina, *Heliosporites altmarkensis* Schulz, and *Schizosporis limbatus* Iljina are scarcer.

The Pereyaslovka spore-pollen assemblage is easily traceable in almost all the Jurassic sections of the Kansk basin (Fig. 2), and sediments enclosing it can be distinguished as beds with *Alisporites pergrandis, Cycadopites medius, Uvaesporites argentaeformis*, and *Stereisporites*. The corresponding reference sections are established in Well 8500 (depth interval of 200–250) and in outcrops near the Voznesenka Village.

According to proportions of microfossil groups, the Pereyaslovka assemblage is correlative with the Sinemurian–Pliensbachian assemblages from the reference marine sections of northern Central Siberia (Il'ina, 1985) and combines characters of assemblages from palynozones 2, 3, 4, and 5a (Table 2). The Jurassic sediments in northern Central Siberia are subdivided into ammonoid zones (*Resheniya 3-go...*, 1981). Palynozones approximately corresponding in ranges to ammonite zones of the same sections yield palynological assemblages (Il'ina, 1985), which insignificantly differ from each other in taxonomic composition. Thus, it is practically impossible to distinguish such palynozones in continental sequences lacking beds with marine fauna. We encountered these difficulties when analyzing spore-pollen assemblages from Jurassic continental deposits recovered by the Tyumen superdeep borehole (Kirichkova *et al.*, 1999) and by other wells drilled in the Tomsk region (Kirichkova *et al.*, 1997; Timoshina *et al.*, 1999). Obviously, as Timoshina suggested, the palynologic units of a greater range and having more distinct diagnostic features, i.e., with palynologic assemblages clearly differing from underlying and overlying assemblages, should be distinguished in continental deposits.

In West Siberia, the palynologic assemblage similar to that of the Pereyaslovka Formation is characteristic of the Urman Formation (palynozones 2, 3, 4, and 5a) in the Nyurol'ka depression (Kasatkina, 1991; Kabanova and Kostesha, 1997; Kabanova *et al.*, 1989; Shurygin *et al.*, 1995).

The upper half of the Pereyaslovka and the Ilan formations yield a single Ilan palynologic assemblage with *Dictyophyllum, Marattisporites scabratus*, and *Contignisporites problematicus*, as it is termed by Timoshina. It is significantly different in taxonomic composition from the Pereyaslovka assemblage (Plate **I**, figs. 16–23; Plate **II**, figs. 1–6), being dominated by pollen of coniferous plants, though large forms are almost missing from this group, except for *Piceaepollenites variabiliformis* (Mal.) M. Petr., a common taxon in the Jurassic palynofloras. Large monocolpate grains of *Cycadopites*, such as *C. dilucidus* (Bolch.) Iljina and *C.* sp., are not numerous and diverse. Additionally the species diversity of *Stereisporites* is reduced. Spores typical of the Ilan assemblage are *Dictyophyllum* forms with echinate perispores (*D. simplex* Mensh. and *D.* sp.), *Clathropteris obovata* var. *magna* Tur.-Ket, *Auritulinasporites triclavus* Nilsson, *Marattisporites scabratus* Couper, *Klukisporites variegatus* Couper, *Contignisporites problematicus* (Couper) Dör., *Duplexisporites anogrammensis* (K.-M.) Shug., and *Tripartina variabilis* Mal. The last taxon is abundant in certain palynospectra. The index species *Cadargasporites robustus* Mensh. is scarce but lacking in both the older and all younger assemblages. Pollen of *Classopollis* spp. is rather abundant. Also present in the assemblage are *Quadraeculina limbata* Mal., common *Chasmatosporites elegans* Nilsson, and *C.* sp. The assemblage is widespread in the Kansk basin, and its distinctive features enable recognition of beds with *Dictyophyllum, Marattisporites scabratus*, and *Contignisporites problematicus*. The depth interval of 150–180 m in Well 8500 drilled in the Aban area is considered as the reference section of the beds.

According to its taxonomic composition, the Ilan assemblage is well correlative with Toarcian assemblages of palynozones 5b, 6, and 7 distinguished in marine sediments of northern Siberia (Il'ina, 1981, 1985; Kasatkina, 1998) and with palynologic assemblages 5b, 6, and 7 (Table 2), which are known from the Togur and Salat (lower half) formations penetrated by Borehole Ponomarevo 2 in the Nyurol'ka depression of the Tomsk region (Kontorovich *et al.*, 1995; Shurygin *et al.*, 1995). Similar assemblages are also characteristic of the following stratigraphic subdivisions: the upper Sherkalin Subformation (lower part) in the Krasnoleninsk arch (Well 3251, depth interval 2736–2741 m; Well 219, depth interval 2696–2705 m; Well 2012, depth interval 2723–2751 m), the lower Khudosei Subformation in the Tomsk region (Well Chertala 400,

Plate **I.** Lower Jurassic miospores (magnification ×600).

(1–15) Characteristic taxa of the Pereyaslovka palynologic assemblage: (1) *Stereisporites compactus* (Bolch.) Iljina, Well 312, depth int. 145.3–150.1 m; (2) *S. seebergensis* Schulz, ditto; (3) *S. bujargiensis* (Bolch.) Schulz, ditto; (4) *S. psilatus* (Ross.) Pfl., Well 8500, depth int. 240.5–243.5 m; (5) *S. antiquasporites* (Wilson et Webster) Dettm., Well 219, depth int. 108.9–113.1 m; (6) *Uvaesporites argentaeformis* (Bolch.) Schulz, ditto; (7) *Camptotriletes tenellus* Naum. et Iljina, ditto; (8) *C. cerebriformis* Naum. et Jarosh., ditto; (9) *Osmundacidites* sp., Well 8500; (int. 240.5–243.5 m; (10) *Cycadopites percarinatus* (Bolch.) Iljina, Well 8400; (int. 175.6–180.4 m; (11) *C. medius* (Bolch.) Iljina, ditto; (12) *C. dilucidus* (Bolch.) Iljina, Well 1-C, depth int. 125.5–133.7 m; (13) *Dipterella oblatinoides* Mal., Well 219, depth int. 108.9–113.1 m; (14) *Alisporites pergrandis* (Bolch.) Iljina, Well 8500, depth int. 254.7–260.7 m; (15) *Podocarpidites* sp., Well 219, depth int. 108.9–113.1 m. (16–23) Characteristic taxa of the Ilan palynologic assemblage: (16) *Cadargasporites robustus* Mensh., Well 312, depth int. 125.4–130.2 m; (17) *Dictyophyllum* sp., ditto; (18) *Clathropteris obovata* var. *magna* Tur.-Ket., Well 219, depth int. 98.7–103.5 m; (19) *Auritulinasporites triclavus* Nilsson, ditto; (20) *Marattisporites scabratus* Couper, Well 8500, depth int. 170.8–175.6 m; (21) *Tripartina variabilis* Mal., ditto; (22) *Klukisporites variegatus* Couper, Well 16-C, depth int. 77.3–81.2 m; (23) *Contignisporites problematicus* (Couper) Dör., ditto.

Table 2. Correlation of Jurassic palynostratigraphic subdivisions in the Kansk coal basin with those of West Siberia and palynozones of northern Siberia

Stage	Substage	Zonations of northern Siberia (Zakharov *et al.*, 1997)			West Siberia					Kansk coal basin	
					Nyurol'ka Depression, Ponomarevskaya 2 Borehole (Shurygin *et al.*, 1995)			Krasnoleninsk Arch (*Resheniya...*, 1991)			
		Ammonoid zones	Palynozones		formations	palynozones	depth, m	formations	Well 2012 (data of this work)	palynologic units*	formations
Bajocian	Upper	*Cranocephalites carlsbergensis*	9c	9	Tyumen			Tyumen: middle s	SPA-4 2623–2635 m	PU-4	Borodino
		Cranocephalites gracilis									
		Boreocephalites borealis									
	Lower	*Слои с Chondroceras* cf. *marshalli*									
		Arkeloceras tozeri	9b								
		Pseudolioceras (T.) fastigatus	9a					Tyumen: lower s			
Aalenian	U	*Pseudolioceras tugurensis*	8			8	2908				
	L	*H. Pseudolioceras maclintocki*			Salat				SPA-3 2706–2714 m	PU-3	Kamala
		Pseudolioceras beyrichi	7	7b				Sherkalin: upper s			
Toarcian	Upper	*Pseudolioceras falcodiscus*									
		Pseudolioceras wurttenbergeri				?	2955				
		Pseudolioceras compactile				7b	3018				Ilan
	Lower	*Нижний Porpoceras spinatum*		7a							
		Zugodactylites monestieri				7a				PU-2	
		Dactylioceras commune					3038				
		Harpoceras falciferum	6		Togur	6			SPA-2 2723–2751 m		
		Eleganticeras elegantulum					3067				
		Tiltoniceras propinquum	5	5b		5b	3070				
Pliensbachian	Upper	*Amaltheus viligensis*		5a	Urman	5a	3074				
		Amaltheus margaritatus	4			4				PU-1	Pereyaslovka
		Amaltheus stokesi					3086				
		?	3			2–3					
	L	*Polymorphites*	2					Sherkalin: lower subformation			
Sinemurian	U	*Angulaticeras colymicum*									
		Coroniceras siverti									
	L	*Arietites libratus*									
Hettangian	U	*Schlotheimia angulata*			?						
		Alsatites liasicus									
	L	*Psiloceras planorbis*	1								
		Primasiloceras primulum									

Note: (*) beds with palynoflora; (L) lower; (U) upper; (s) subformation.

depth interval 3221–3228 m), and the lowermost Kotukhtin Formation recovered by the superdeep Borehole TSG-6 (depth interval 5046–4997 m) in the Urengoi region (Kirichkova *et al.*, 1999).

The plant macrofossils occur throughout the Pereyaslovka Formation and are considerably scarcer in the Ilan Formation (Fig. 2). In taxonomic composition these taphofloras regarded here as the Aban assemblage are not very diverse. Kostina (Kostina and Doludenko, 1997; Kostina, 1999) markedly refined the assemblage composition. With due regard for data of Markovich (1970), it includes 24 species (Table 3). Among ferns, there are established rare *Cladophlebis, Raphaelia*, and scarcer *Coniopteris* forms. Gymnosperms, mainly Czekanowskiales, dominate in the assemblage. The genus *Czekanowskia* is the most diverse and includes six species. *Phoenicopsis* is less diversified. Fructifications (*Leptostrobus* and *Samaropsis*) are common components. This assemblage of persistent composition is well traceable in the study region. Based on the refined list of its characteristic forms, we distinguish sediments enclosing the assemblage as a particular phytostratigraphic unit—the *Czekanowskia obiensis–Cz. rigida–Phoenicopsis cognata* Beds (Fig. 2). The corresponding reference section is established in Well 8500, depth interval 150–260 m, the Aban area.

According to predominance of *Czekanowskia* forms (*Cz. rigida* Heer and *Cz. obiensis* Kiritch. et Samyl.) and *Phoenicopsis cognata*, the Aban assemblage is correlated with the Cheremkhovo assemblage from the lower productive member of the upper Cheremkhovo Subformation in the Irkutsk basin (Kirichkova and Travina, 2000) and with the Tomsk assemblage of the lower Osinniki Subformation in Kuzbass (Kirichkova *et al.*, 1992), which are attributed by convention to the terminal Lower Jurassic (Toarcian?). However, the Aban assemblage is most similar to flora of the Khudosei Formation (lower half and overlying member *I*) and to the flora of the Togur and Salat (lower half) formations distinguished by Il'ina in the Tomsk region (see in Shurygin *et al.*, 1995). These floras are dated back to the late Early Jurassic, supposedly to the Pliensbachian-Toarcian (Kirichkova and Travina, 1995). We consider it possible to determine the same age for the Aban assemblage, which is also allowed by the available palynologic data.

MIDDLE JURASSIC

The Middle Jurassic sediments of the Kansk basin are subdivided into the Kamala, Borodino, and Tyazhin formations (*Resheniya 3-go...*, 1981).

The Kamala Formation distinguished by Aksarin (1957) and Sakhanova (1957) is mainly represented by siltstones, argillites, and sandstones intercalated with rare gravelstone and coal beds. Its thickness ranges from 70–100 m in the Aban area to 140–172 m in the Rybinskoe area (Semerikov, 1970). The formation is rather well studied with respect to fossil spores and pollen. Palynologic samples were collected from boreholes of the Aban area and from outcrops of the Rybnaya River near the Rybnoe Village (Fig. 2). The palynospectra represent a single Kamala assemblage with characteristic *Leiotriletes tenuis, Lycopodiumsporites,* and *Cycadopites jansonii* (Plate **II,** figs. 7–20). The assemblage is markedly distinct from the Ilan assemblage by different proportions of dominating forms. It is characterized by predominance of *Leiotriletes* spores, among which there are forms with widely open, almost triangular aperture and smaller smooth trilete spores with thin exine and perispore, e.g., *Leiotriletes tenuis* (Leschik) Mensh. and *L. corrugatus* Mensh. Along with these species, we identified *Tripartina paradoxa* Mal., scarce *Cyathidites minor* Couper, and common or sometimes abundant spores of lycopods (*Lycopodiumsporites semimurus* Danze-Corsin et Lavaine, *L.* spp.) and *Osmundacidites* ferns (*O. jurassicus* (K.-M.) Kuz., *O.* spp.). The assemblage includes abundant and diverse small monocolpate pollen grains of *Cycadopites jansonii* Pocock, *C. angustus* M. Petr., etc. in association with bisaccate pollen of conifers *Piceaepollenites variabiliformis* (Bolch.) M. Petr., *Alisporites bisaccus* Rouse, and *Disaccites* spp.; *Araucariacites* sp. occur as well.

The Kamala palynologic assemblage is distinguished in all studied sections (Fig. 2) and sediments enclosing it are termed as *Leiotriletes tenuis–Lycopodiumsporites–Cycadopites jansonii* beds. Their reference section corresponds to the depth interval of 80–140 m in Well 8500. In its taxonomic composition the Kamala assemblage is correlative with that of palynozone 8 established by Il'ina in Aalenian marine deposits of north Siberia, which yields ammonoids *Pseudolioceras tugurites* and *P. maclintocki* (Il'ina, 1985), and distinguished (see in Kontorovich *et al.*, 1995) in the upper half of the Salat Formation penetrated by Borehole Ponomarevo 2 in the Nyurol'ka Depression, Tomsk region (Table 2). Timoshina distinguished a similar palynologic assemblage in of the superdeep borehole Tyumen TSG-6 (depth interval of 4734.5–4744.9 m; an upper part of the Kotukhtin Formation after Kirichkova *et al.* 1999), in the upper Khudosei Subformation of the latitudinal Ob' River region (Borehole Var-Egan 952, depth interval 3233–3270 m), and in the upper Sherkalin Subformation of the Krasnoleninsk arch (Well 129, depth interval 2582–2651 m; Well 2012, depth interval 2706–2714 m; Well 2007, depth interval 2520–2593 m).

Plant macrofossils characteristic of the entire Kamala Formation were collected from boreholes of the Aban area and in the Rybnaya River exposures. As indicated previously (Kirichkova and Travina, 1990), the Kamala taphofloras united here into the Rybinskoe assemblage considerably differ from the Aban flora by greater diversity of gymnosperms (Table 4). Kostina (1999) who revised taxonomic composition of the Kamala taphofloras clearly demonstrated that they are dominated by Czekanowskiales genera *Phoenicopsis*

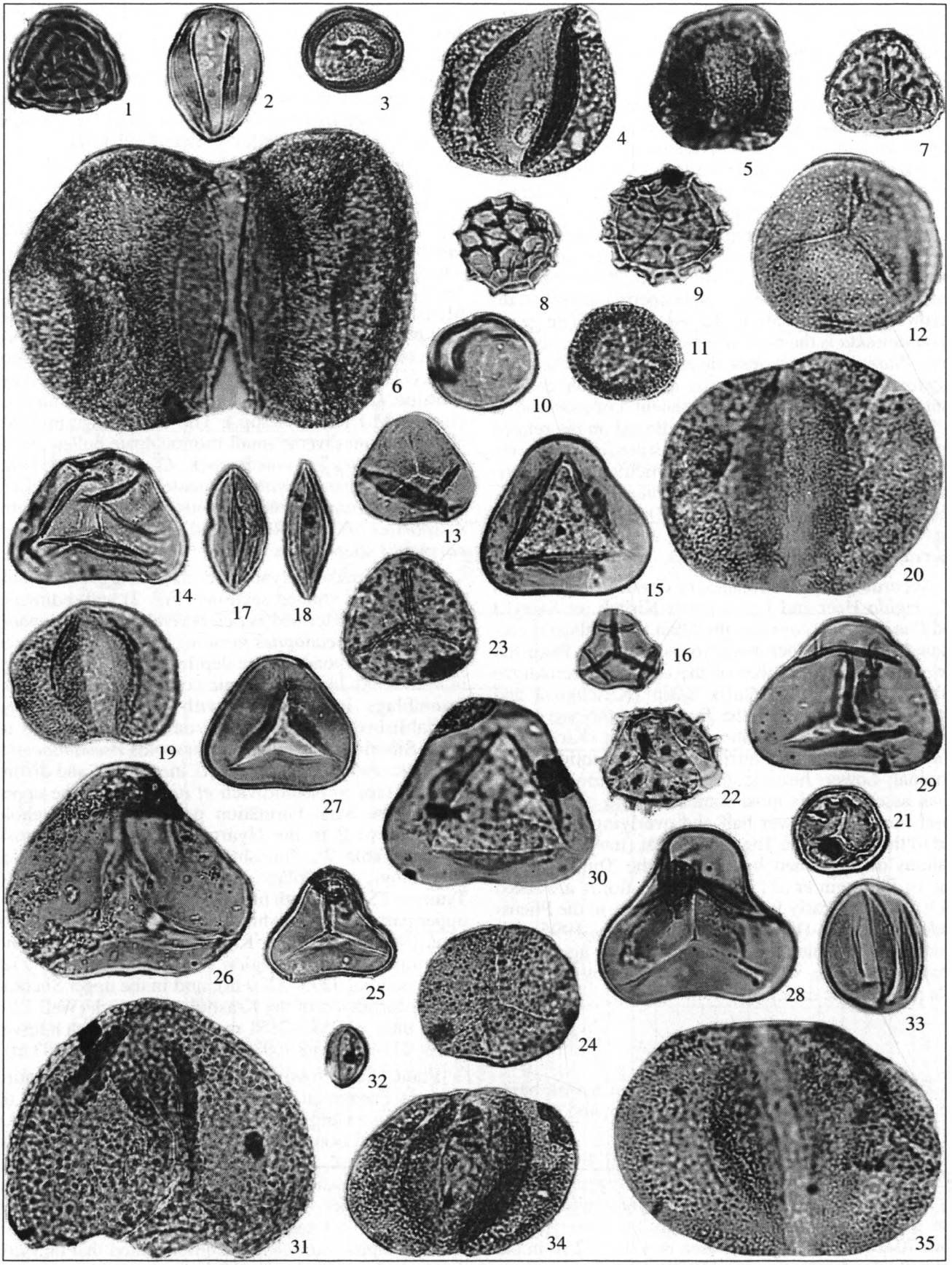
1
2
3
4
5
7
6
8
9
12
10
11
13
14
17
18
15
20
23
16
19
27
22
29
21
30
26
25
28
33
24
32
31
34
35

and *Czekanowskia*. These genera are of diverse species composition, and their leaf remains form in places the monotypic burials in the sequence. The first occurrence of *Phoenicopsis dentata* Pryn., *Ph. irkutensis* Dolud. et Rasskaz., *Ph. markovitchae* Kiritch. et M. Shishkina, *Czekanowskia ferganensis* Kiritch. et Samyl., and *Cz. kanensis* Kiritch. et Samyl. is recorded in the assemblage. Ginkgoales, among them *Ginkgo* and *Sphenobaiera*, are more diverse at this level. *Oswaldheeria (?)*, a presumable taxon of Scyadopitiales, becomes widespread among conifers. This assemblage composition is identical in all localities of the Kamala taphofloras, and host sediments are distinguished as beds with *Czekanowskia kanensis, Phoenicopsis irkutensis, Ph. markovitchae, Ginkgo abanensis*, and *Oswaldheeria (?)*. The Rybnaya River outcrop nearby the Rybnoe Village and depth interval of 43–100 m in Well 312, the Aban area (Tables 2, 3), are considered as reference sections of the beds.

Similar assemblages with dominating Czekanowskiales, which are represented mostly by the same species, are known from the upper sandy siltstone member of the upper Cheremkhovo Subformation of the Irkutsk basin (Kirichkova and Travina, 2000) and from the upper Khudosei Subformation (upper Salat Subformation after Il'ina; see in Kontorovich *et al.*, 1995) of the Tomsk region (Kirichkova and Travina, 1995), where we distinguished this subdivision in boreholes Talparovo-1 (depth interval 2800–3050 m), Zapadnyi Luginets 180 (depth interval 2570–2605 m), and others. Moreover, according to predominance and diversity of Czekanowskiales, the Rybinskoe assemblage may be compared with the Etap flora from the Upper Osinovo Subformation of Kuzbass (Kirichkova *et al.*, 1992), though the latter is of a more diverse taxonomic composition, especially with respect to *Coniopteris* ferns. By analogy with floras mentioned above, the Kamala flora is dated back to the early Middle Jurassic (Aalenian?).

The Borodino Formation that was distinguished by Aksarin (1957) above the slightly eroded surface of the Kamala Formation corresponds to siltstone–shale sequence with coal beds of industrial thickness. The formation is 180–240 m thick in the Rybinskoe area and 110–115 m thick in the Aban area (Semerikov, 1970). It is exposed in full range in the Borodinskii coal quarry of the Rybinskoe area. An upper part of the formation above the productive beds has been occasionally distinguished as the Bathonian Ust-Yana Formation (*Resheniya 3-go...*, 1981; Sakhanova, 1960). However, this idea was found to be useless in practice of geological prospecting. Our study in the Borodinskii quarry and adjacent borehole sections convinced us that the Borodino Formation below and above the Borodinskii coal bed is the integral lithologic unit indivisible in terms of paleobotanical characteristics.

We obtained palynologic data for the stratotype section in the Borodinskii quarry and for Well 312 in the Aban area (Fig. 2). In Well 312, the formation corresponds to the 7-m-thick shale sequence with a thin coal bed at the base. The formation is overlain by Quaternary deposits (Fig. 2). Palynospectra from both localities are analogous in taxonomic composition and represent the Borodino assemblage bearing *Neoraistrickia rotundiformis, Microlepidites crassirimosus*, and *Leiotriletes* (Plate **II**, figs. 21–35). It has much in common with the Kamala assemblage but differs in certain aspects. Large smooth trilete spores, among them *Leiotriletes karatauensis* Timosh. and those with strongly opened almost triangular aperture, are most abundant in this case. The assemblage also includes scarce spores *Microlepidites crassirimosus* Timosh. of distinctive morphology and common *Cyathidites minor* Couper. *Microreticulatisporites pseudoalveolatus* (Couper) Vin. and *Hemitelia parva* (Dör.) Timosh. occurring as single specimens are, however, the index taxa of the assemblage. The assemblage under consideration, like that of the Kamala Formation, is characterized by abundance of *Osmundacidites* spores associ-

Plate **II.** Lower and Middle Jurassic miospores.

(1–6) Characteristic taxa of the Ilan palynologic assemblage: (1) *Duplexisporites anogrammensis* Shug., Well 1-C, depth int. 56.2–61.4 m; (2) *Cycadopites* aff. *dilucidus* (Bolch.) Iljina, Well 8500, depth int. 170.8–175.6 m; (3) *Classopollis* aff. (K.-M.) *classoides* Pfl., Well 219, depth int. 98.7–103.5 m; (4) *Alisporites bisaccus* Rouse, ditto; (5) *Quadraeculina limbata* Mal., Well 16-C, depth int. 62.0–67.0 m; (6) *Podocarpidites* sp., Well 312, depth int. 125.4–130.2 m. (7–20) Characteristic taxa of the Kamala palynologic assemblage: (7) *Lycopodiumsporites semimuris* Danze-Corsin et Lavaine, Well 8400; (int. 115.0–119.0 m; (8, 9) *Lycopodiumsporites* sp. sp., ditto; (10) *Equisetites rotundiformis* (Mal.) Bolch., Well 8500, depth int. 137.0–142.0 m; (11) *Osmundacidites jurassicus* (K.-M.) Kuz., Well 312, depth int. 92.2–96.9 m; (12) *Osmundacidites* sp., ditto; (13) *Leiotriletes tenuis* (Leschik) Mensh., Well 219, depth int. 58.8–63.6 m; (14) *L. corrugatus* Mensh., ditto; (15) *Leiotriletes* sp., ditto; (16) *Tripartina paradoxa* Mal., Well 1G-C, depth int. 23.0–28.0 m; (17) *Cycadopites jansonii* Pocock, Well 219, depth int. 58.8–63.6 m; (18) *C. angustus* M. Petr., Well 312, depth int. 61.0–66.4 m; (19) *Alisporites bisaccus* Rouse, Well 1-C, depth int. 18.4–23.2 m; (20) *Disaccites* gen. sp., ditto. (21–35) Characteristic taxa of the Borodino palynologic assemblage: (21) *Stereisporites incertus* (Bolch.) Sem., Well 312, depth int. 1.7–7.5 m; (22) *Neoraistrickia rotundiformis* (K.-M.) Taras., ditto; (23) *Microreticulatisporites pseudoalveolatus* (Couper) Vin., outcrop on the left bank of the Enisei River near the Kubekovo Village (upper half of the Itat Formation); (24) *Osmundacidites* sp., ditto; (25) *Cyathidites minor* Couper, Borodinskii quarry, below the Borodinskii coal bed; (26) *Cyathidites australis* Couper, Well 312, depth int. 1.7–7.5 m; (27) *Microlepidites crassirimosus* Timosh., Borodinskii quarry, above the Borodinskii coal bed; (28) *Hemitelia parva* (Dör.) Timosh., ditto; (29) *Leiotriletes karatauensis* Timosh., Aban quarry (lowermost Borodino Formation); (30) *Leiotriletes* sp., Well 312, depth int. 1.7–7.5 m; (31) *Dicksonia densa* Bolch., Borodinskii quarry, below the Borodinskii coal bed; (32) *Cycadopites nitidus* (Balme) M. Petr., Borodinskii quarry, above the Borodinskii coal bed; (33) *Eucommiidites troedssonii* Erdtm., ditto; (34) *Alisporites bisaccus* Rouse, ditto; (35) *Disaccites* gen. sp., ditto.

Table 3. Distribution of plant taxa of the Aban flora in sections of the Kansk coal basin

Species \ Formations, depth localities	Pereyaslovka						Ilan		
	Well 8500, depth 160–260 m	Well 8400, depth 158–220 m	Well 312, depth 130–165 m	Well 16-C, depth 83–120 m	Well 1-C, depth 60–140 m	Voznesenka Village (Markovich, 1970)	Well 219, depth 97–105 m	Well 16-C, depth 62–82 m	Well 1-C, depth 45–60 m
Equisetites lateralis (Phill.) Phill.	+					sp.			
Gonatosorus sphenopteroides Brick						+			
Coniopteris hymenophylloides (Brong.) Sew.	sp.					+	sp.		
Cladophlebis argutula (Nath.) Font.						+			
C. bidentata Tur.-Ket.						+			
Raphaelia aff. *diamensis* Sew.	+								
Czekanowskia jenisseiensis Kiritch. et Samyl.	+	+							
Cz. cf. *irkutensis* Kiritch. et Samyl.		+					+		
Cz. obiensis Kiritch. et Samyl.	+	+		+	+		+	+	+
Cz. rigida Heer	+	+		+	+		+	+	+
Cz. cf. *suntarica* Kiritch. et Samyl.	+								
Cz. ex gr. *rigida* Heer	+		+						
Phoenicopsis angustifolia Heer	+								+
Ph. cognata Kiritch.	+						+		
Phoenicopsis sp.	+								
Leptostrobus sp.	+			+				+	
Ginkgo sp.		+	+						
Baiera sp.							+		
Pseudotorellia angustifolia Dolud.					+	sp.	sp.	sp.	
Pseudotorellia (?) sp.	+			+	+				
Ixostrobus heeri Pryn.	+	+				+			
Podozamites angustifolius (Echw.) Heer						+			
Elatocladus manchurica Yok.						+			
Samaropsis sp.		+							

ated with common *Lycopodiumsporites*, rather frequent *Camptotriletes cerebriformis* Naum. et Jarosh., and *Stereisporites* forms of low diversity, *S. incertus* (Bolch.) Sem. being an obligatory component among the latter. The occasional appearance of abundant *Neoraistrickia rotundiformis* (K.-M.) Taras. and single *Dicksonia densa* Bolch. is a peculiar feature of the assemblage. Basic components of the coniferous pollen that is still abundant are *Alisporites bisaccus* Rouse, *Piceaepollenites variabiliformis* (Mal.) M. Petr., and other bisaccate forms close to recent Pinaceae.

Based on the Borodino assemblage retaining its peculiar features in all localities, the host sediments are termed in our scheme as the *Neoraistrickia rotundiformis-Microlepidites crassirimosus-Leiotriletes* Beds with their reference section in the Borodinskii quarry. The beds are clearly correlative with the palynozone 9 distinguished by Il'ina (1985) in marine sediments of northern Central Siberia, which yield Bajocian ammonites (Table 2). Both subdivisions bearing *Cyathidites minor* Couper, *Neoraistrickia rotundiformis*, and *Leiotriletes* forms are likely of the same age.

According to several species in common, such as *Neoraistrickia rotundiformis*, *Lycopodiumsporites intortivallus*, *Dicksonia densa*, and *Pinus divulgata*, the Borodino assemblage is concurrent to assemblages from Beds 9 distinguished by Il'ina in the borehole Salat 1 (depth level of 2687 m) and in the Nyurol'ka Depression of West Siberia (Shurygin *et al.*, 1995).

Table 4. Distribution of plant taxa of the Rybinskoe flora in sections of the Kansk coal basin

Species \ Localities	Rybnaya River	Well 8500, depth 70–140 m	Well 8400, depth 80–125 m	Well 312, depth 43–90 m	Well 219, depth 35–93 m	Well 16-C, depth 20–43 m	Well 1-C, depth 15–40 m
Equisites lateralis (Pill.) Pill.	+	+			sp.		
Coniopteris hymenophylloides (Brongn.) Sew.					+		
C. spectabilis Brick	+						
Coniopteris sp.	+				+		
Cladophlebis kanskiensis Kostina	+						
Cladophlebis sp.	+						
Lobifolia sp.	+						
Phlebopteris aff. *polypodioides* Brong.					+		
Raphaelia cf. *diamensis* Sew.	+	+			+		
R. tapkensis (Heer) Pryn.	+						
Czekanowskia eugenia Kiritch. et Samyl.	cf.				+		
Cz. ferganensis Kiritch. et Samyl.			cf.	+		+	
Cz. jenissejensis Kiritch. et Samyl.		+	+	+			
Cz. irkutensis Kiritch. et Samyl.			+	+	cf.		
Cz. kanensis Kiritch. et Samyl.				+	+	+	
Cz. mchatica Kiritch. et Samyl.	+						
Cz. obiensis Kiritch. et Samyl.		+	+	+	+		
Cz. rigida Heer	cf.				+	+	+
Cz. tuvensis Kiritch. et Samyl.	+						
Czekanowskia exgr. *rigida* Heer	+	+	+	+	+		
Phoenicopsis angustifolia Heer				+			
Ph. dentata Pryn.	+		+	+			
Ph. irkutensis Dolud. et Rasskaz.	+		+	+			
Ph. markovitchiae Kiritch. et M. Shishkina	+						
Phoenicopsis sp.	+		+	+	+	+	
Ginkgo abanensis Kostina			+		+	+	
G. heeri Dolud. et Rasskaz.				+			
Ginkgo sp.		+		+	+		
Baiera sp.	+	+			+		
Sphenobaiera angarensis Travina		+	+				
Sphenobaiera aff. *czekanowskiana* (Heer) Flor.			+				
Erethmophyllum sp.		+					
Leptotoma prinadii Travina	+	aff.					
Leptotoma (?) sp.		+					
Pseudotorellia angustifolia Dolud.				+			
Pseudotorellia (?) sp.	+				+		
Oswaldheeria (?) sp.	+	+	+	+	+	+	
Pityophyllum nordenskioldii (Heer) Nath.		+			+		
Antholites sp.	+						
Ixostrobus sp.	+						
Leptostrobus sp.				+	+	+	
Stenorachis sp.	+			+			
Carpolites sp.	+		+		+		
Samaropsis sp.			+				

Table 5. Distribution plant taxa of the Quarry flora in sections of the Kansk coal basin

Species \ Localities	Borodinskii Quarry	Well 525, depth 10–28 m	Well 576, depth 12–50 m	Well 580, depth 12–48 m
Hepaticites sp.	+			+
Equisetites lateralis (Phill.) Phill.	+			+
Coniopteris hymenophylloides (Brongn.) Sew.			+	
Coniopteris sp.	+		+	
Cladophtebis haiburnensis (L. et H.) Brong.	+			
C. multinervis Golova	+			
Cladophlebis sp.	+			
Raphaelia diamensis Sew.	+		+	+
R. tapkensis (Heer) Pryn.	+		cf.	
Heilungia sp.	+			
Czekanowskia aksarinii Kostina	+			
Cz. eugenia Kiritch. et Samyl.	+	+	+	+
Cz. ferganensis Kiritch. et Samyl.		+	+	
Cz. jenissejensis Kiritch. et Samyl.		+		
Cz. irkutensis Kiritch. et Samyl.		+	+	
Cz. obiensis Kiritch. et Samyl.	+			
Cz. rigida Heer	+			
Cz. suntarica Kiritch. et Samyl.	+			
Cz. teslenkoi Kiritch. et Samyl.	+			cf.
Czekanowskia ex gr. rigida Heer	+	+	+	+
Phoenicopsis samylinae Kiritch. et Moskvin	+		+	
Ginkgo capillata Kostina et Kiritch.	+			
G. sibirica Heer	+			
G. tapkensis Dolud. et Rasskaz.		+		
Ginkgo sp.	+			
Leptotoma sp.		+		
Leptotoma (?) sp.	+		+	
Pseudotorellia (?) sp.	+			
Pagiophyllum sp.	+			
Pityophyltum nordenskioldii (Heer) Nath.	+		+	+
Elatides ovalis Heer	+			
Ixostrobus cf. *heeri* Pryn.	+	+	+	
Leptostrobus sp.	+	+		
Shizolepis sp.				+
Sorosaccus (?) sp.	+			
Stenorachis sp.	+			+

Timoshina established presence of analogous assemblages the upper part of the Itat Formation exposed nearby the Kubekovo Village on the Enisei River bank and in the lower and middle subformations of the Tyumen Formation recovered in the Tomsk region by boreholes Yuzhno-Tambaevo 76 (depth interval 2848–2855 m), Tolparovo 1 (depth interval 2703–2716 m), and Yuzhnyi Koltogor 1 (depth interval 2807–2803 m). She also reported on their occurrence in borehole Yakhlin 49 (depth interval 2406–2420 m) drilled in the Krasnoleninsk Arch, in wells 2012 (depth interval 2627–2635 m) and 2007 (depth interval 2508–2520 m)

Table 6. Stratigraphic distribution of characteristic plant groups in Jurassic sediments of the Kansk basin

Species \ Formations, age	Pereyaslovka	Ilan	Kamala	Borodino
	J_1^{3-4}		J_2^1	J_2^2
Phoenicopsis cognata Kiritch.				
Ph. angustifolia Dolud.				
Czekanowskia jenissejensis Kiritch. et Samyl.				
Cz. obiensis Kiritch. et Samyl.				
Cz. rigida Heer				
Pseudotorellia angustifolia Dolud.				
Coniopteris hymenophylloides (Brongn.) Sew.				
C. spectabilis Brick				
Cladophlebis kanskiensis Kostina				
Lobifolia sp.				
Phlebopteris polypodioides Brong.				
Raphaelia tapkensis (Heer) Pryn.				
Czekanowskia irkutensis Kiritch. et Samyl.	cf.	cf.		
Cz. kanensis Kiritch. et Samyl.				
Cz. mchatica Kiritch. et Samyl.				
Cz. tuvensis Kiritch. et Samyl.				
Cz. ferganensis Kiritch. et Samyl.				
Phoenicopsis dentata Pryn.				
Ph. irkutensis Dolud. et Rasskaz.				
Ph. markovitch Kiritch. et Shichkina				
Ginkgo abanensis Kostina				
G. heeri Dolud. et Rasskaz.				
Baiera sp.				
Sphenobaiera angarensis Travina				
Sph. czekanowskiana (Heer) Flor.			aff.	
Erethmophyllum sp.				
Leptotoma prinadii Travina				
Oswaldheeria (?) sp.				
Raphaelia diamensis Sew.	aff.		cf.	
Cladophlebis haiburnensis (L. et H.) Brong.				
Cl. multinervis Golova				
Czekanowskia eugenia Kiritch. et Samyl.			cf.	
Cz. aksarinii Kostina				
Cz. suntarica Kiritch. et Samyl.				
Cz. teslenkoi Kiritch. et Samyl.				
Phoenicopsis samylinae Kiritch. et Moskvin				
Ginkgo capillata Kostina et Kiritch.				
G. sibirica Heer				
G. tapkensis Dolud. et Rasskaz				
Leptotoma sp.				
Pagiophyllum sp.				

Note: plant remains were found in: —— single sections; ▬ two or three sections; ▬ almost all sections.

of the Talin coal field, in the Latitudinal Ob region (Well Var-Egan 952, depth interval 3020–3100 m), and in the Urengoi area (Tyumen superdeep borehole TSG-6, depth interval 4564.2–4415.5 m).

In the Kansk basin, plant macrofossils have been collected in the layer-by-layer mode from the Borodino Formation stratotype in the Borodinskii quarry and from boreholes, which penetrated an upper part of the formation in the Borodino coal field (Fig. 2). The Quarry assemblage of taphofloras from the formation includes about 40 species (Table 5). Species composition of dominant plant group differs it from the Rybinskoe flora. Czekanowskiales, Ginkgoales, and conifers are still the main groups of the Quarry flora. However, the genus *Czekanowskia* with nine species, the first appearing *Cz. teslenkoi* Kiritch. et Samyl. included, dominates among Czekanowskiales and the genus *Phoenicopsis* is represented only by *Ph. samylinae* Kiritch. et Mosk. Genera *Ginkgo* and *Leptotoma* are represented by different species (Table 5), and ferns are scarce. Sediments enclosing this plant assemblage of persistent taxonomic composition were distinguished previously (Kirichkova and Travina, 1990) as the *Raphaelia diamensis–Czekanowskia eugenia-Cz. teslenkoi–Phoenicopsis samylinae* Beds with their reference section in the Borodinskii quarry.

The Quarry flora is correlative with the Tapkino flora of the Sayan Formation in the Irkutsk coal basin (Kirichkova and Travina, 2000). Their similarity is grounded by equal proportions of characteristic plant groups mainly represented by the same *Czekanowskia* and *Ginkgo* species. According to the same criteria, the Quarry flora can be compared with that from the lower and middle subformations of the Tyumen Formation in West Siberia (Kirichkova and Travina, 1995), despite a somewhat different species composition of the latter. The Yachmenyukha flora from the Tersyuk Formation of Kuzbass (Kirichkova *et al.*, 1992) is comparable with the Quarry flora only in the general level and common tendency of vegetation evolution, because the former is of a higher taxonomic diversity of all plant groups.

The Jurassic section in the Kansk basin is crowned by the Tyazhin Formation 20–25 m thick. The formation of a limited distribution is recovered by a single borehole in the central Aban area near the Murma Village. The formation stratotype distinguished by I.V. Lebedev in 1955 is situated in the Kemerovo region near the Tyazhin railway station. The type section is represented by bluish gray to bluish green and gray siltstones and sandstones, and by green, red, and gray clays. Based on palynologic records, the formation is attributed to the Callovian–Oxfordian (*Stratigraficheskii slovar'...*, 1978). In the Aban area, it is represented by pelitic and silty grayish blue rocks. Rocks facies of the Tyazhin Formation are similar to those of the Borodino Formation (Markovich, 1970; Semerikov, 1970). Unfortunately, they lack plant macrofossils. According to palynologic data, the formation age was determined as the Late Jurassic (Verbitskaya, 1970). According to the collective decision (*Resheniya 3-go ...*, 1981), the unit it is referred to the Callovian–Oxfordian.

DISCUSSION

It was repeatedly noted that the age determination of continental stratigraphic units is a difficult task. There are two ways to solve the problem: first, to study peculiarities of paleoflora evolution in a certain region in order to reveal successive assemblages of both the plant macrofossils and miospores collected from the same localities; second, to correlate of taphofloras and certain assemblages of the study region with those from adjacent areas of the same phytochore.

The Jurassic flora of the Kansk basin is one of others typical of the Siberian paleoflora province. In the evolutionary level and composition it holds a certain position among floras of the Irkutsk basin, West Siberia, and even Kuzbass that was used to preliminary define ages of stratigraphic units in the Kansk basin (Kirichkova and Travina, 1995; Kirichkova *et al.*, 1997). However, the palynologic data obtained enable a complex approach to age determination of the distinguished phytostratigraphic units. The palynologic assemblages from Jurassic sediments of the Kansk basin appeared to be comparably stable in taxonomic composition and traceable not only in the Kansk basin, but also outside it, for instance, in Jurassic sections of West Siberia. Their correlation with assemblages from palynozones established in marine deposits of northern Central Siberia was used to date more reliably not only the corresponding stratigraphic units, but also the floral beds (Table 2, Fig. 2).

CONCLUSIONS

1. The comprehensive study of plant macrofossils, especially the cuticle method used to investigate gymnosperm leaves, significantly refined the taxonomic composition of Jurassic flora in the Kansk basin. Taphofloras characteristic of certain stratigraphic levels are defined more concretely, and taxonomic composition of floras from known formations of the Kansk basin is specified. The established correlative and index species are used to substantiate definition of floral beds recognized earlier (Table 6).

2. Palynologic assemblages from the same stratigraphic intervals enabled the sequence subdivision into palynoflora beds. Ranges of these beds are found to be almost equal to that of concurrent floral beds. Thus, we correlated for the first time the investigation results on plant macrofossils, spores, and pollen.

3. The analyzed changes in composition of taphofloras characterizing the studied sequence show that the vegetation evolution in the Kansk basin followed the common trend of paleoflora development in West Sibe-

ria. This primarily concerns the taxonomic changes in and the role of certain genera dominant in floral assemblages, especially of *Czekanowskia, Phoenicopsis, Sphenobaiera*, and *Ginkgo*. The results obtained represent a basis for correlation of Jurassic phytostratigraphic units of the Kansk basin with those known in other depressions of southern Central Siberia and recognized in borehole sections of West Siberia.

4. Palynoflora beds distinguishable in Jurassic sediments of the Kansk basin are traceable in West Siberia as well. This confirms once again the previous assumption that correlative beds with palynoflora can be distinguished and used for chronostratigraphic correlations in different Siberian regions.

5. We established a certain taxonomic similarity of palynologic assemblages from the Kansk basin with those characterizing palynozones of marine sediments in northern Siberia. This enabled for the first time the reliable age determination of stratigraphic units known in Jurassic continental sequence of the Kansk basin and of corresponding plant assemblages.

ACKNOWLEDGMENTS

The work was partly supported by the Russian Foundation for Basic Research, project no. 00-15-98490.

Reviewers A.S. Alekseev and M.P. Doludenko

REFERENCES

Aksarin, A.V., The Ust-Balei Assemblage, *Atlas rukovodyashchikh form iskopaemykh fauny i flory Zapadnoi Sibiri* (Atlas of Guide Fossil Fauna and Flora from West Siberia), Moscow: Gosgeoltekhizdat, 1955, vol. II, pp. 158–177.

Aksarin, A.V., Stratigraphic Scheme of Jurassic Coal-Bearing Deposits of the Kansk Basin, *Tr. Mezhvedomstvennogo soveshchaniya po stratigrafii Sibiri* (Proc. Interdepartmental Conference on Stratigraphy in Siberia), Leningrad: Gostoptekhizdat, 1957, pp. 32–34.

Grigor'ev, K.N., *Kansko-Achinskii ugol'nyi bassein (geologicheskoe stroenie, uglenosnost' i perspektivy razvitiya)* (Kansk-Achinsk Coal Field: Geological Structure, Coal Reserves, and Perspectives of Development), Moscow: Nedra, 1968.

Il'ina, V.I., Age of Jurassic Deposits in the Southeastern Margin of West Siberian Lowland, *Geol. Geofiz.*, 1970, no. 3, pp. 124–130.

Il'ina, V.I., A Comparative Analysis of Palynologic Assemblages from Marine and Continental Lower Jurassic Deposits of Siberia, *Palinologiya v SSSR* (Palynology in the USSR), Moscow: Nauka, 1976, pp. 76–79.

Il'ina, V.I., Palynologic Substantiation of Stratigraphy of Continental Jurassic Sequences in Central Siberia, *Paleopalinologiya Sibiri* (Paleopalynology of Siberia), Moscow: Nauka, 1980, pp. 29–38.

Il'ina, V.I., Subdivision and Correlation of Jurassic Deposits in Central and Eastern Siberia: Palynologic Data, *Geol. Geofiz.*, 1981, no. 5, pp. 9–19.

Il'ina, V.I., *Palinologiya yury Sibiri* (Palynology of Jurassic Deposits in Siberia), Moscow: Nauka, 1985.

Il'ina, V.I., Palynologic Characterization of Middle-Upper Jurassic Boundary Deposits in Southwestern Siberia, *Mikrofitofossilii i stratigrafiya mezozoya i kainozoya Sibiri* (Microphytofossils and Mesozoic to Cenozoic Stratigraphy in Siberia), Novosibirsk: Nauka, 1988, pp. 42–50.

Kabanova, V.M. and Kostesha, O.N., Early Jurassic Palynologic Assemblages from the Urman Formation (Tomsk Oblast), *Biostratigrafiya i mikroorganizmy fanerozoya Evrazii* (Phanerozoic Biostratigraphy and Microorganisms in Eurasia), Moscow: Geos, 1997, pp. 231–241.

Kabanova, V.M., Kostesha, O.N., Tkacheva, L.G., and Chesnokova, B.C., The Permian, Triassic, and Lower Jurassic of the Nyurol'ka Depression, *Geologicheskoe stroenie i neftegazonosnost' yugo-vostoka Zapadnoi Sibiri* (Geological Structure and Petroliferous Potential, the Southeastern Region of West Siberia), Novosibirsk: Nauka, 1989, pp. 58–66.

Kasatkina, G.V., Palynologic Characterization of the Lower-Middle Jurassic in the Zapadno-Pereval'naya and Ponomarevo Areas of West Siberia, *Geologya i neftegazonosnost' trias-sredneyurskikh otlozhenii Zapadnoi Sibiri* (Geology and Petroliferous Potential of Triassic to Middle Jurassic Deposits in West Siberia), Novosibirsk: Nauka, 1991, pp. 79–94.

Kasatkina, G.V., Spore-Pollen Assemblages from the Kiterbyut Horizon of West Siberia, *Aktual'nye voprosy geologii i geografii Sibiri* (Urgent Problems of Geology and Geography in Siberia), Tomsk: Tomsk Gos. Univ., 1998, vol. I, pp. 229–230.

Kirichkova, A.I. and Travina, T.A., Phytostratigraphy of Jurassic Deposits in the Kansk Coal Basin, *Bio- i litostratigrafiya mezozoya neftegazonosnykh raionov SSSR* (Bio- and Lithostratigraphy of Petroliferous Regions of the USSR), Leningrad: Vses. Nauch.-Issled. Geol.-Razved. Inst., 1990, pp. 69–93.

Kirichkova, A.I. and Travina, T.A., Phytostratigraphy and Correlation of the Jurassic Deposits of Western Siberia, *Stratigr. Geol. Korrelyatsiya*, 1995, vol. 3, no. 1, pp. 43–60.

Kirichkova, A.I. and Travina, T.A., Phytostratigraphy of Jurassic Coal-Bearing Formations of the Irkutsk Basin, *Stratigr. Geol. Korrelyatsiya*, 2000, vol. 8, no. 1, pp. 43–60.

Kirichkova, A.I., Batyaeva, S.K., and Bystritskaya, L.I., *Fitostratigrafiya yurskikh otlozhenii yuga Zapadnoi Sibiri* (Phytostratigraphy of Jurassic Deposits in Southwestern Siberia), Moscow: Nedra, 1992.

Kirichkova, A.I., Batyaeva, S.K., Bystritskaya, L.I., *et al.*, Jurassic Continental Deposits in Southwestern and Central Siberia: Stratigraphy and Correlation, *Voprosy sovershenstvovaniya stratigraficheskoi osnovy fanerozoiskikh otlozhenii neftegazonosnykh regionov Rossii* (Problems of Perfecting the Stratigraphic Basis for Phanerozoic Deposits in Petroliferous Regions of Russia), St. Petersburg: Vses. Nauch.-Issled. Geol.-Razved. Inst., 1997, pp. 72–81.

Kirichkova, A.I., Kulikova, N.K., Ovchinnikova, L.L., *et al.*, Biostratigraphic Subdivision of Mesozoic Deposits Penetrated by the Tyumen Superdeep Borehole, *Stratigr. Geol. Korrelyatsiya*, 1999, vol. 7, no. 1, pp. 71–85.

Kontorovich, A.E., Il'ina, V.I., Moskvin, V.I., *et al.*, A Reference Section and Petroliferous Potential of Lower Jurassic

Deposits in the Nyurol'ka Sedimentary Sub-Basin, *Geol. Geofiz.*, 1995, vol. 36, no. 6, pp. 110–126.

Kostina, E.I., Czekanowskiales from Jurassic Deposits of the Kansk Coal basin (Siberia), *Paleontol. Zh.*, 1999, no. 5, pp. 105–111.

Kostina, E.I. and Doludenko, M.P., Fossil Ferns from Middle Jurassic Deposits of the Kansk Coal Basin (Siberia), *Paleontol. Zh.*, 1997, no. 2, pp. 58–68.

Lebedev, I.V., Jurassic System (Stratigraphy), *Atlas rukovodyashchikh form iskopaemykh fauny i flory Zapadnoi Sibiri* (Atlas of Guide Fossil Fauna and Flora from West Siberia), Moscow: Gostoptekhizdat, 1955, vol. 2, pp. 154–157.

Lebedev, I.V., The Jurassic of the Chulym-Yenisei Depression, *Materialy po geologii Zapadno-Sibirskoi nizmennosti* (Data on Geology of West Siberian Lowland), Tomsk: Gosgeoltekhizdat, 1960, pp. 29–39.

Markovich, E.M., Correlation of Sections in the Nazarovo and Rybinskoe Areas Based on Paleobotanical Data, *Metodika korrelyatsii razrezov kontinental'nykh uglenosnykh tolshch* (Methods of Correlating Sections of Continental Coal-Bearing Sequences), Moscow: Nauka, 1970, pp. 28–52.

Resheniya 3-go Mezhvedomstvennogo regional'nogo stratigraficheskogo soveshchaniya po mezozoyu i kainozoyu Srednei Sibiri (Novosibirsk, 1978) (Resolutions of the 3rd Interdepartmental Regional Stratigraphic Conference on Mesozoic and Cenozoic of Central Siberia, Novosibirsk, 1978), Novosibirsk: Sovm. Nauch.-Issled. Inst. Geol. Geofiz. Mineral. Syr'ya, 1981.

Resheniya V Mezhvedomstvennogo regional'nogo stratigraficheskogo soveshchaniya po mezozoiskim otlozheniyam Zapadno-Sibirskoi ravniny (Tyumen', 1990) (Resolutions of the 5th Interdepartmental Regional Stratigraphic Conference on Mesozoic Deposits in the West Siberian Plain), Leningrad: Vses. Geol. Inst., 1991.

Sakhanova, N.S., Spore-Pollen Assemblages from Coal-bearing Deposits of the Kansk Basin, *Tr. Mezhvedomstvennogo soveshchaniya po stratigrafii Sibiri* (Proc. Interdepartmental Conference on Siberian Stratigraphy), Leningrad: Gostoptekhizdat, 1957, pp. 34–41.

Sakhanova, N.S., Stratigraphy of Coal-bearing Deposits in the Chulym-Yenisei Basin, *Materialy po geologii Krasnoyarskogo kraya* (Data on Geology of the Krasnoyarsk Krai), Moscow: Gosgeoltekhizdat, 1960, pp. 48–56.

Semerikov, N.A., Correlation of Sections Based on Lithologic Data, *Metodika korrelyatsii razrezov kontinental'nykh uglenosnykh tolshch* (Methods of Correlating Sections of Continental Coal-Bearing Sequences), Moscow: Nauka, 1970, pp. 71–87.

Shurygin, B.N., Nikitenko, B.L., Il'ina, V.I., *et al.*, Problems of Lower-Middle Jurassic Stratigraphy in the Southeastern Region of West Siberia, *Geol. Geofiz.*, 1995, vol. 36, no. 11, pp. 34–51.

Smokotina, I.V., Palynologic Characterization of Jurassic Deposits in the Yenisei Depression, Western Part of the Kansk-Achinsk Basin, *Biostratigrafiya i mikroorganizmy fanerozoya Evrazii* (Phanerozoic Biostratigraphy and Microorganisms of Eurasia), Moscow: Geos, 1997, pp. 259–262.

Stratigraficheskii slovar' mezozoiskikh i kainozoiskikh otlozhenii Zapadno-Sibirskoi vpadiny (Stratigraphic Glossary for Mesozoic and Cenozoic Deposits in the West Siberian Depression), Leningrad: Nedra, 1978.

Timoshina, N.A., Kulikova, N.K., and Fedorova, V.A., Reference Palynostratigraphic Units if the Continental Mesozoic, *Neftegazovaya geologiya na rubezhe vekov. Prognoz, poiski, razvedka i osvoenie mestorozhdenii. T. 2. Stratigrafiya, obshchaya geologiya, regional'nyi prognoz* (Petroleum-and-Gas Geology across the Boundary between Centuries, vol. 2: Stratigraphy, General Geology, and Regional Prognosis), St. Petersburg: Vses. Nauch.-Issled. Geol.-Razved. Inst., 1999, pp. 83–92.

Verbitskaya, Z.I., Correlation of Coal Seams and Their Host Deposits in the Rybinskoe and Aban Areas, *Metodika korrelyatsii razrezov kontinental'nykh uglenosnykh tolshch* (Methods of Correlating Sections of Continental Coal-Bearing Sequences), Moscow: Nauka, 1970, pp. 19–27.

Zakharov, V.A., Bogomolov, Yu.I., Il'ina, V.I., *et al.*, Standard Boreal Zonation and Biostratigraphy of the Mesozoic in Siberia, *Geol. Geofiz.*, 1997, vol. 38, no. 5, pp. 927–256.

Stratigraphy and Geological Correlation, Vol. 11, No. 3, 2003, pp. 261–277. Translated from Stratigrafiya. Geologicheskaya Korrelyatsiya, Vol. 11, No. 3, 2003, pp. 57–74.
Original Russian Text Copyright © 2003 by Palechek, Solov'ev, Shapiro.
English Translation Copyright © 2003 by MAIK "Nauka/Interperiodica" (Russia).

Structure and Age of Mesozoic Sedimentary-Volcanogenic Deposits of the Palana Section (Western Kamchatka)

T. N. Palechek,* A. V. Solov'ev,* and M. N. Shapiro**

**Institute of Lithosphere of Marginal Seas, Russian Academy of Sciences, Staromonetnyi per. 22, Moscow, 119180 Russia*
***Institute of Physics of the Earth, Russian Academy of Sciences, ul. Bol'shaya Gruzinskaya 10, Moscow, 103810 Russia*
Received May 28, 2001; in final form, October 17, 2001

Abstract—It is difficult to reconstruct the pre-Cenozoic history of western Kamchatka, because Mesozoic deposits are fragmentarily exposed here. The Palana section, the most complete one among Mesozoic sections of the region, is described and subdivided into volcanogenic and olistostrome sequences. Based on radiolarians, the volcanogenic sequence is attributed to the Campanian–Maastrichtian. The siliceous olistoliths have been formed in the Late Jurassic to Late Cretaceous time. Data on radiolarians indicate the late Campanian–Maastrichtian age of the olistostrome matrix, but volcanogenic olistoliths suggest that the tectonic imbrication and related olistostrome formation took place after the early Maastrichtian. According to published data, the general deformation of the Palana section, which brought about a sharp unconformity at the base of the Anadyrka Formation, has been finished by the mid-Danian.

Key words: Campanian–Maastrichtian, radiolarians, Upper Maastrichtian olistostrome, Palana section, western Kamchatka.

INTRODUCTION

Western Kamchatka is an area of distribution of predominantly Cenozoic deposits with few uplifted blocks composed of pre-Cenozoic deposits, mostly of Upper Cretaceous ones (*Ob'yasnitel'naya...*, 2000). Mesozoic sections, most of which are poorly exposed and incomplete, are unsuitable for understanding of pre-Cenozoic history of the peninsula and the adjacent areas of the Sea of Okhotsk. The Upper Cretaceous rocks exposed in sea cliffs are of particular significance in this situation. The northernmost exposure is located to the north of the Palana River mouth (figure).

Geology of this area was first studied by Dvali (1957), who described the Palana Horizon and tuff-shale sequence of the Cape Palanskii. Later on, in the course of geological mapping, scale 1 : 200000 (Demidov and Sulima, 1982), the Kingiveem, Irunei, Tal'nichnaya and Ust-Palana formations were distinguished. In the geological map, scale 1 : 1000000 (*Geologicheskaya...*, 1989), Cretaceous deposits of the Palana area are divided into the Lower Cretaceous Kingiveem (basalts, dolerites, and siliceous rocks), Campanian Irunei (dolerites, basalts, tuffs, and jaspers), and Maastrichtian Ust-Palana (tuffs, tuff breccias of basalt to trachybasalt composition, sandstones, and conglomerates) formations. In 1991, A.B. Tsukernik who studied the Palana section presented his results in special report of GNPP Aerogeologiya. He established that the northern larger part of seashore exposures southward of the Anadyrka River corresponds to volcanogenic-sedimentary rocks of the Campanian Irunei Formation and distinguished an olistostrome of the Ust-Palana Formation. Geological structure of Cenozoic deposits exposed in sea cliff to the north of the Palana River was described in detail by Gladenkov *et al.* (1977).

THE SECTION STRUCTURE

We divide the pre-Cenozoic Palana section in two, the volcanogenic and olistostrome sequences (figure). Characteristic volcanogenic clasts occurring in the olistostrome suggest that the latter initially overlapped the volcanogenic sequence.

Volcanogenic sequence. In the study area there are no sections where the base of volcanogenic rocks can be observed. These rocks exposed in northern seashore cliffs to the south of the Anadyrka River mouth are mostly represented by massive volcanic breccias (agglomerate) of basaltic and basaltic-andesite composition. Dark gray to black rock clasts in breccias are porphyritic, containing large (up to 3 or 4 mm) isometric phenocrysts of clinopyroxene. Some varieties of basaltic andesites reveal presence of needle-shaped hornblende phenocrysts. Angular basaltic clasts ranging in size from few centimeters to few meters are set, as a rule, in matrix of a similar composition. Some rocks with subangular clasts of different texture can be considered as tuff breccias. The deposits lack any bedding, even the coarse one, and it is impossible to define their attitude, although there are many long multidirectional cracks and fracture zones. Breccias and more massive basalts are intercalated with thin (10–30 m)

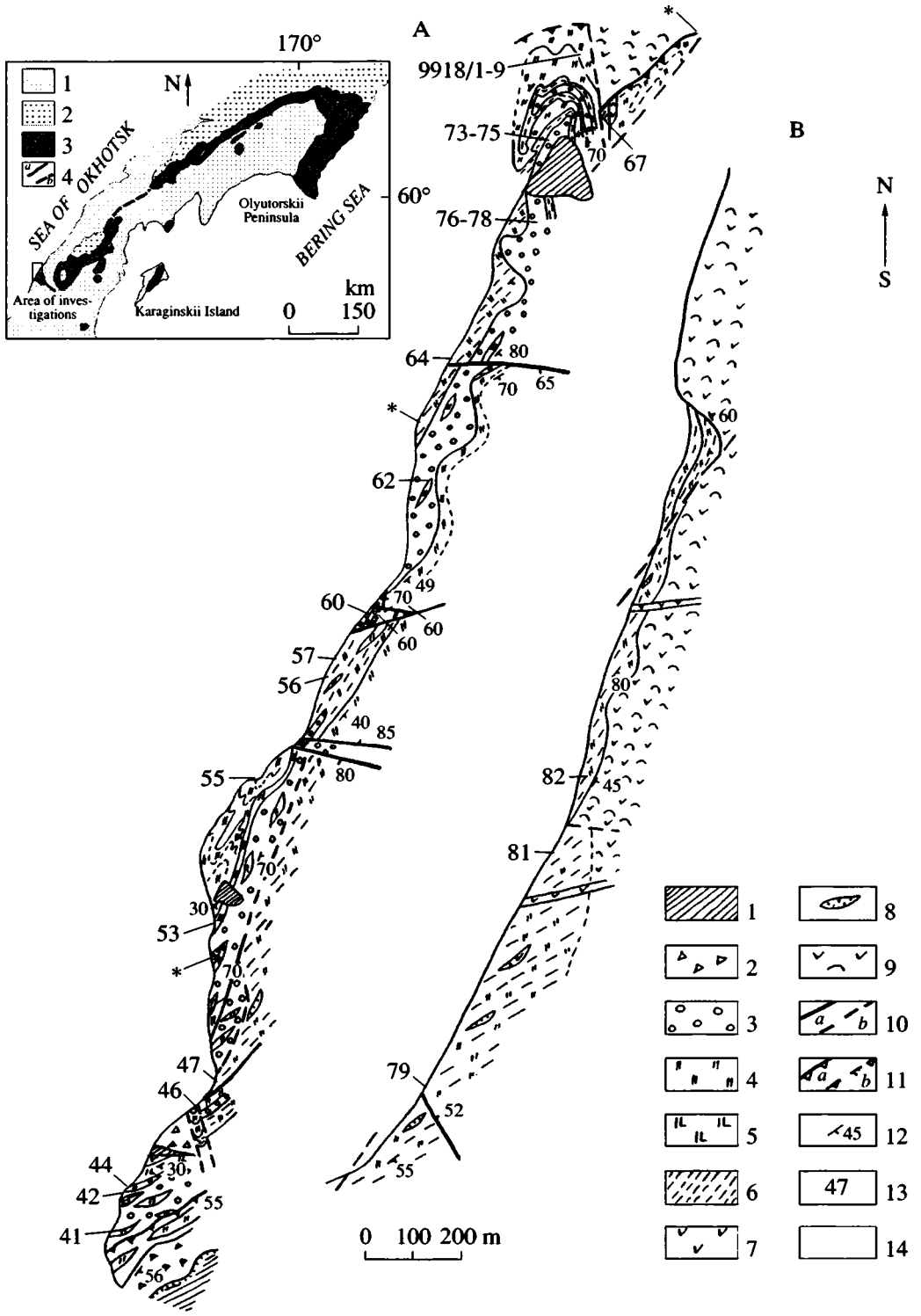

Geology of coastal exposures (A and continuation B) to the north of the Palana Settlement (plan view): (1) talus; (2) melange zone; (3) conglomerate, gravelstone, or sandstone; (4) chert; (5) cherts with fragments inoceramid shells; (6) siltstone, siliceous siltstone; (7) basalt; (8) sandstone lens; (9) basaltic breccia (agglomerate), basalt, and basaltic andesites; (10) established (*a*) and presumable (*b*) steep normal faults; (11) established (*a*) and presumable (*b*) thrust faults; (12) altitude; (13) number of sample with microfauna; (14) points of samples dated by Kurilov (2000).

The inset map shows distribution of Cretaceous deposits of the Olyutorskii zone and northern Kamchatka: (1) Cenozoic deposits; (2) Cretaceous-Paleogene deposits of the Ukelayat-Lesnaya depression; (3) Cretaceous siliceous-volcanogenic deposits; (4) Vatyna–Lesnaya thrust fault with established (*a*) and presumable (*b*) segments.

members of mudstones, tuffaceous siltstones and sandstones, siliceous siltstones, and with gray and black cherts having admixture tuffaceous material. Some tuffaceous sandstones and siltstones show indistinct graded bedding. The bedded members are usually in tectonic contacts with enclosing breccias and strongly deformed into tectonic breccias and broken small folds. As a rule, the deposits strike in submeridional direction and dip at steep angles to the east-southeast or west-northwest (in the northernmost outcrops). The strike is parallel to the seashore line and probably corresponds to the attitude of the entire sequence. The bedded members are of a uniform appearance, and some of them may be repeated in the sequence, although the lowest ones are almost entirely composed, in distinction from others, of mudstones with rare chert lenses and fragmented thin prismatic layers of inoceramid shells. It is difficult to precisely estimate the overall apparent thickness of volcanogenic rocks, which may be over one kilometer thick, if they form a monocline extending parallel to the seashore.

Age of volcanogenic rocks. The K/Ar dates of 72.5 ± 3.5 Ma (sample Sh88) and 72.0 ± 3.5 Ma (sample Sh89) have been obtained for amphiboles from two samples of basaltic andesites collected 3 km to the south of the Anadyrka River mouth (age determinations by M.M. Arakelyants).

Five samples of siliceous sediments intercalated with volcanogenic rocks yielded radiolarians, which are satisfactorily preserved (Table 1). The most representative radiolarian assemblages from samples 37 and 79/b indicate the late Campanian–Maastrichtian age of their host rocks. V. S. Vishnevskaya (personal communication) who previously studied a siliceous siltstone from the sequence (sample Ts17/1,2 from the Tsukernik's collection, GNPP Aerogeologiya) identified the Campanian radiolarians *Archaeospongoprunum nishiyamae* Nakaseko et Nishimura, *Orbiculiforma quadrata* Pessagno, *Pseudoaulophacus* sp., *Amphipyndax stocki* (Campbell et Clark), *Eucyrtis carnegiense* Campbell et Clark, and *Lithostrobus* sp.

Olistostrome. To the south of the volcanogenic sequence, in the northern Ust-Palana area, there are cliffs and tidal zone with exposures of olistostrome deposits (figure). The olistostrome is separated from the volcanogenic one by a steep normal fault of submeridional strike. It represents an accumulation, chaotic to poorly structured (oriented), of blocks and size-variable lenses (up to 80 m long) of bedded red, gray–green, and almost black cherts and siliceous mudstones set in the brecciated sandstone matrix. Some large olistoliths and smaller blocks enclose pyroxene basalts with agglomerate texture characteristic of the Palana volcanogenic sequence. Olistoliths of cherts and siliceous mudstones contain, as a rule, the inclusions of fragmented prismatic layers of thick-shell inoceramids. Occasionally these fragments are concentrated in coquina beds with relatively low content of cherty matrix.

The olistostrome matrix is composed of clastic rocks, such as fine-clastic breccia and breccia-conglomerate, gravelstones, and sandstones with rare thin lenticular interbeds of black siliceous mudstones and cherts. Clearly dominating clasts are those of different siliceous rocks, including their varieties with inclusions of fragmented inoceramid shells. The shell fragments frequently occur as separate grains in sandstones. Reworked radiolarians are also present in small clasts of their host rocks. Some sandstone varieties represent a two-component mixture of chert clasts and basaltoid fragments (plagioclases, pyroxenes, and microlitic matrix). In general mineral composition, the latter are analogous to pyroxene basalts of the volcanogenic sequence.

The chaotic complex is intensively dislocated and pierced by mylonitic zones, which frequently bound large blocks and olistoliths. Some blocks of siliceous sediments exhibit small folds, including those with steep hinge lines. The olistoliths are locally sharply bended. We do not consider this chaotic complex as a tectonic melange or megabreccia and identify it, following Tsukernik, as an olistostrome. This is based primarily on the type of matrix composed of peculiar but typical sedimentary deposits, i.e., of breccia–conglomerate, gravelstones, sandstones, and siltstones. Assuming the fragments of these rocks and cherts to be tectonically derived from an original integral sequence, we should admit that the latter represented an alternation of coarse-clastic terrigenous deposits, cherts devoid of terrigenous admixture, and basalts typical of island arcs that is hardly possible. Even if such a sequence existed, clastic material in its terrigenous sediments could not be identical in composition to intercalated siliceous beds, as it recorded in the olistostrome.

Despite the complex inner structure of the olistostrome, structural elements recognizable in the matrix and large olistoliths predominantly have submeridional strike and east-southeast dipping. If they characterize a monocline, the olistostrome thickness should be more than 500 m.

Age of olistostrome. Samples of cherts and siliceous mudstones have been collected from olistoliths and matrix to be dated based on radiolarians.

Dating the olistoliths. The siliceous samples studied yielded radiolarian assemblages of the Campanian–Maastrichtian age, more exactly, the late Campanian–Maastrichtian (samples 42, 55, 60, 9918/2), the Campanian–Maastrichtian (sample 44), the Campanian (samples 46 and 53), the middle Campanian–Maastrichtian (samples 62 and 9918/1), and the late Campanian–early Maastrichtian (sample 9918/7) ones (Tables 2, 5; Plate 3). In addition, Kurilov (2000) macerated some older (early Valanginian, Albian–Cenomanian, and Coniacian–Maastrichtian) radiolarian assemblages from olistoliths of the Palana olistostrome.

Dating the matrix. Ten sandstone and gravelstone samples from the olistostrome matrix yielded abundant

Table 1. Radiolarians from siliceous interbeds of the volcanogenic sequence (shaded boxes denote presence of species)

Species	Sample number				
	37	79b	81a	82a	87b
	1	2	3	4	5
Phaseliforma carinata Pessagno					
Phaseliforma subcarinata Pessagno					
Praestylosphaera pusilla (Campbell et Clark)					
Lithomespilus mendosa (Krasheninnikov)	cf				
Lithomespilus sp.					
Actinomma sp.					
Actinommidae Gen. et sp. indet					
Orbiculiforma renillaeformis (Campbell et Clark)					
Orbiculiforma quadrata Pessagno					
Orbiculiforma sp.					
Spongodiscus impressus Lipman					
Spongodiscus rhabdostylus (Ehrenberg)					
Porodiscus cretaceus Campbell et Clark					
Spongurus sp.					
Spongopyle ? sp.					
Amphibrachium sansalvadorensis Pessagno		aff			
Pseudoaulophacus lenticulatus (White)	cf				
Pseudoaulophacus sp.					
Neosciadiocapsa sp.					
Stichomitra livermorensis (Campbell et Clark)					
Stichomitra sp.					
Amphipyndax stocki (Campbell et Clark)					
Xitus asymbatos (Foreman)					
Lithostrobus rostovzevi Lipman					
Cornutella californica Campbell et Clark					
Theocampe vanderhoofi Campbell et Clark					
Dictyomitra densicostata Pessagno					
Dictyomitra sp.					
Clathrocyclas tintinnaeformis Campbell et Clark					
Sponge spicules					

radiolarians (Tables 3, 5; Plates 1, 2) of the Campanian age. The most representative assemblages have been macerated from samples 75v and 77v (lower–middle Campanian), 76b (Campanian), and 76d (middle–upper Campanian). It is apparent that the majority of the radiolarians of the matrix sandstones and gravelstones are reworked. Accordingly, the late Campanian–Maastrichtian age of radiolarian assemblages mentioned above corresponds to the former thickest part of siliceous deposits, which represented a source for the majority of olistoliths and cherty clasts set in the matrix. Siliceous interbeds of the olistostrome matrix (11 samples) also yielded radiolarians of late Campanian–Maastrichtian age, e.g., samples 76a, 76v, and 77b (Table 4; Plates 1, 2). Although the late Campanian–Maastrichtian age of the olistostrome matrix is evidenced by many radiolarian taxa, the occurrence of *Amphisphaera goruna* (Sanfilippo et Riedel), *Orbiculiforma renillaeformis* (Campbell et Clark), *Spongodiscus alveatus* (Sanfilippo et Riedel), *Spongotrochus polygonatus* (Campbell et Clark), and other forms (Table 5) suggests that the rock unit under consideration was still under formation in the early Paleocene.

Table 2. Radiolarians from siliceous olistoliths of the olistostrome (shaded boxes denote presence of species)

Species	Sample number													
	41	42	44	46	53	55	60	62	67	9918/1	9918/2	9918/6	9918/7	9918/9
	1	2	3	4	5	6	7	8	9	10	11	12	13	14
Phaseliforma carinata Pessagno		cf												
Phaseliforma sp.														
Praestylosphaera pusilla (Campbell et Clark)						cf								
Praestylosphaera hastata (Campbell et Clark)													cf	
Praestylosphaera sp.														
Haliomma schucherti Campbell et Clark														
Haliomma sp.														
Actinomma sp.														
Amphisphaera priva (Foreman)														
Actinommidae Gen.et sp. indet														
Lithomespilus mendosa (Krasheninnikov)						cf								
Cromyodruppa concentrica Lipman														
Orbiculiforma renillaeformis (Campbell et Clark)														
Orbiculiforma sp.														
Spongodiscus impressus Lipman														
Spongodiscus alveatus (Sanfilippo et Riedel)														
Spongodiscus rhabdostylus (Ehrenberg)														
Spongodiscus sp.														
Spongotripus morenoensis Campbell et Clark														
Spongotripus sp.														
Spongurus sp.														
Spongosaturnalis spiniferus Campbell et Clark								cf						
Spongosaturnalis sp.														
Archaeospongoprunum hueyi Pessagno														
Archaeospongoprunum sp.														
Pseudoaulophacus lenticulatus (White)		cf	cf											
Pseudoaulophacus sp.														
Histiastrum latum Lipman														
Histiastrum sp.														
Amphibrachium spongiosum Lipman			cf											
Prunobrachium sp.														
Patulibracchium petroleumensis Pessagno			cf											
Patulibracchium sp.														
Spummellaria Gen. et sp. indet														
Crucella sp.														
Praeconocaryomma sp.														
Gongylothorax verbeeki (Tan Sin Hok)		cf												
Kuppelella cayeuxi (Squinabol)				aff										

Table 2. (Contd.)

Species	Sample number													
	41	42	44	46	53	55	60	62	67	9918/1	9918/2	9918/6	9918/7	9918/9
	1	2	3	4	5	6	7	8	9	10	11	12	13	14
Neosciadiocapsa diabloensis Pessagno			cf											
Neosciadiocapsa sp.														
Tricolocapsa ? sp.														
Theocapsomma erdnussa (Empson-Morin)														
Theocapsomma amphora Campbell et Clark			aff											
Theocapsomma sp.														
Hemicryptocapsa conara Foreman														
Novodiacanthocapsa manifesta (Foreman)				cf										
Sciadiocapsa (?) *campbelli* Pessagno														
Holocryptocapsa sp.														
Myllocercion sp.														
Schadelfusslerus sp.														
Eucyrtidium carnegiense Campbell et Clark														
Stichopilium teslaense Campbell et Clark														
Stichomitra livermorensis (Campbell et Clark)					cf									
Stichomitra shirshovica Vishnevskaya														
Stichomitra campi (Campbell et Clark)														
Stichomitra sp.														
Amphipyndax stocki (Campbell et Clark)														
Amphipyndax streckta (Empson-Morin)														
Amphipyndax sp.														
Xitus asymbatos (Foreman)											cf			
Xitus sp.														
Lithostrobus rostovzevi Lipman														
Lithostrobus sp.														
Cornutella californica Campbell et Clark								cf						
Theocampe altamontensis (Campbell et Clark)														
Theocampe yaoi Taketani			cf											
Theocampe sp.														
Archaeodictyomitra regina (Campbell et Clark)														
Dictyomitra andersoni (Campbell et Clark)						cf								
Dictyomitra densicostata Pessagno					cf			cf						
Dictyomitra multicostata Zittel														
Dictyomitra sp.														
Clathrocyclas hyronia Foreman													cf	
Clathrocyclas tintinnaeformis Campbell et Clark														
Clathrocyclas sp.														
Sponge spicules														

Table 3. Radiolarians from cherty clasts in the olistostrome matrix (shaded boxes denote presence of species)

Species	Sample number									
	73	75b	75v	76b	76d	77a	77v	78a	78v	78d
	1	2	3	4	5	6	7	8	9	10
Phaseliforma carinata Pessagno					cf					cf
Phaseliforma sp.										
Praestylosphaera pusilla (Campbell et Clark)										
Praestylosphaera hastata (Campbell et Clark)										
Praestylosphaera sp.										
Actinomma sp.										
Cromyosphaera vivenkensis Lipman										
Lithomespilus mendosa (Krasheninnikov)		cf							cf	cf
Lithomespilus sp.										
? *Staurodictya fresnoensis* Foreman										
Orbiculiforma renillaeformis (Campbell et Clark)										
Orbiculiforma quadrata Pessagno				≤						
Orbiculiforma sp.										
Spongodiscus impressus Lipman										
Spongodiscus alveatus (Sanfilippo et Riedel)										
Spongodiscus sp.										
Porodiscus cretaceus Campbell et Clark										
Spongurus sp.										
Spongotripus morenoensis Campbell et Clark			cf							
Pseudoaulophacus lenticulatus (White)										cf
Patulibracchium sp.										
Spummellaria. Gen. et sp. indet										
Holocryptocapsa sp.										
Novodiacanthocapsa manifesta (Foreman)										
Theocapsomma sp.										
Stichomitra livermorensis (Campbell et Clark)								cf		
Stichomitra shirshovica Vishnevskaya										
Stichomitra campi (Campbell et Clark)							cf			
Stichomitra sp.										
Amphipyndax stocki (Campbell et Clark)										
Amphipyndax streckta (Empson-Morin)										
Amphipyndax tylotus Foreman										
Amphipyndax sp.										
Wildeus punctulatus (Pessagno)										
Lithostrobus rostovzevi Lipman				cf						
Theocampe vanderhoofi Campbell et Clark					cf		cf			cf
Theocampe sp.										
Archaeodictyomitra squinaboli Pessagno										
Archaeodictyomitra regina (Campbell et Clark)										
Dictyomitra andersoni (Campbell et Clark)										
Dictyomitra densicostata Pessagno						cf				cf
Dictyomitra multicostata Zittel										
Dictyomitra sp.										
Clathrocyclas hyronia Foreman										
Clathrocyclas sp.										
Sponge spicules										

Table 4. Radiolarians from siliceous interbeds in the olistostrome matrix (shaded boxes denote presence of species)

Species	Sample number										
	47	56	57	64	75a	76a	76v	76g	77b	78b	78g
	1	2	3	4	5	6	7	8	9	10	11
Phaseliforma carinata Pessagno											
Phaseliforma laxa Pessagno											
Phaseliforma sp.											
Praestylosphaera pusilla (Campbell et Clark)											
Praestylosphaera hastata (Campbell et Clark)											
Praestylosphaera sp.											
Haliomma minor Campbell et Clark		cf	cf				cf				
Haliomma sp.											
Actinomma sp.											
Acanthosphaera sp.											
Amphishaera goruna (Sanfilippo et Riedel)											
Lithomespilus mendosa (Krasheninnikov)											
Actinommidae Gen. et sp. indet											
Orbiculiforma renillaeformis (Campbell et Clark)			cf								
Orbiculiforma sp.											
Porodiscus cretaceus Campbell et Clark		cf									
Spongodiscus impressus Lipman											
Spongodiscus alveatus (Sanfilippo et Riedel)	cf										
Spongodiscus sp.											
Spongotrochus polygonatus (Campbell et Clark)											
Stylotrochus sp.											
Spongurus quadratus Campbell et Clark											
Spongurus sp.											
Spongosaturnalis spiniferus Campbell et Clark											
Protoxiphotractus perplexus Pessagno											
Patulibracchium sp.											
Pseudoaulophacus sp.											
Spummellaria. Gen. et sp. indet.											
Neosciadiocapsa sp.											
Eucyrtis sp.											
Eucyrtidium carnegiense Campbell et Clark											
Stichomitra livermorensis (Campbell et Clark)											
Stichomitra shirshovica Vishnevskaya											
Stichomitra sp.											
Novodiacanthocapsa manifesta (Foreman)											
Theocapsomma erdnussa (Empson-Morin)											
Theocapsomma sp.											
Amphipyndax stocki (Campbell et Clark)											
Amphipyndax stocki var. C Vishnevskaya											
Amphipyndax streckta (Empson-Morin)											
Amphipyndax tylotus Foreman											
Amphipyndax sp.											

Table 4. (Contd.)

Species	Sample number										
	47	56	57	64	75a	76a	76v	76g	77b	78b	78g
	1	2	3	4	5	6	7	8	9	10	11
Xitus asymbatos (Foreman)											
Lithostrobus rostovzevi Lipman											
Lithostrobus sp.											
Cornutella californica Campbell et Clark											
Theocampe altamontensis (Campbell et Clark)											
Theocampe vanderhoofi Campbell et Clark											
Theocampe sp.											
Archaeodictyomitra regina (Campbell et Clark)											
Archaeodictyomitra sp.											
Dictyomitra andersoni (Campbell et Clark)											
Dictyomitra densicostata Pessagno											
Dictyomitra multicostata Zittel											
Dictyomitra sp.											
Clathrocyclas hyronia Foreman			cf								
Clathrocyclas diceros Foreman											
Clathrocyclas tintinnaeformis Campbell et Clark											
Clathrocyclas sp.											
Sponge spicules											

RELATIONSHIPS BETWEEN THE CRETACEOUS AND PALEOGENE DEPOSITS

The coastal cliff located 1.5 km to the west-southwest of the Anadyrka River mouth shows a contact between the heavily deformed tuffaceous sediments of the volcanogenic sequence and rocks of the Anadyrka (Khulgun) Formation (conglomerates and sandstones). Gladenkov *et al.* (1997) referred this formation to the Paleocene. However, according to the latest biostratigraphic data, the Anadyrka Formation is of the younger, Eocene age (A.E. Shantser, personal communication). The formation is separated from the volcanogenic sequence by a normal fault oriented at the right angle to the shoreline. To the west of the section interval covered by coastal debris (about 2 m wide), there are exposed volcanic breccias and tuffaceous sediments of the volcanogenic sequence. As far as 200 m to the west, their beds dip to the west-southwest (290°–315°) at the angles of 45°–60° (15 measurements over the distance about 100 m along the shoreline). To the east of the contact between two formations, there are poorly exposed unlithified coarse-grained sandstones. Approximately 30 m to the east, the latter are overlain by conglomerates dipping to the northeast at the angle of about 40°. Farther on, coastal cliffs extending for a distance of 200 m exhibit a lenticular alternation of cross-bedded conglomerate, gravelstone, and sandstone beds with impressions of leaf flora, which gently dip northeastwards. These are the basal beds of the Anadyrka Formation described in detail by Gladenkov *et al.* (1997). According to their description, beds of the Anadyrka Formation have almost horizontal attitude in exposures

Plate 1. Radiolarians from the olistostrome

(1, 2) *Cromyosphaera vivenkensis* Lipman: (1) 1-76/b, ×100; (2) 75/v, ×100; (3) *Lithomespilus mendosa* (Krasheninnikov), 76/v, ×120; (4) *Acanthosphaera* sp., 76/v, ×100; (5) *Amphisphaera goruna* (Sanfilippo et Riedel), 76×, ×200; (6, 7) *Praestylosphaera pusilla* (Campbell et Clark): (6) 76/a, ×200, (7) 76/v, ×150; (8) *Protoxiphotractus perplexus* Pessagno, 76/a, ×200; (9) ? *Staurodictya fresnoensis* Foreman, 76/d, ×110; (10) *Spongosaturnalis siniferus* Campbell et Clark, 76/v, ×150; (11) *Phaseliforma carinata* Pessagno, 75/a, ×100; (12) *Phaseliforma subcarinata* Pessagno, 77/b, ×85; (13) *Phaseliforma laxa* Pessagno, 77/b, ×100; (14) *Spongurus quadratus* Campbell et Clark, 75/a, ×200; (15) *Spongurus* sp., 76/v, ×150; (16) *Orbiculiforma renillaeformis* Campbell et Clark, 76/a, ×85; (17, 18) *Porodiscus cretaceous* Campbell et Clark: (17) 76/b, ×100, (18) 77/v, ×100; (19) *Spongodiscus* cf. *alveatus* (Sanfilippo et Riedel), 47, ×80; (20) *Spongotrochus polygonatus* (Campbell et Clark), 76/a, ×150; (21) *Orbiculiforma quadrata* Pessagno, 77/v, ×100; (22) *Pseudoaulophacus lenticulatus* (White), 76/b, ×120; (23) *Patulibracchium* sp., 77/b, ×100; (24) *Spongotripus* cf. *morenoensis* Campbell et Clark, 75/v, ×120.

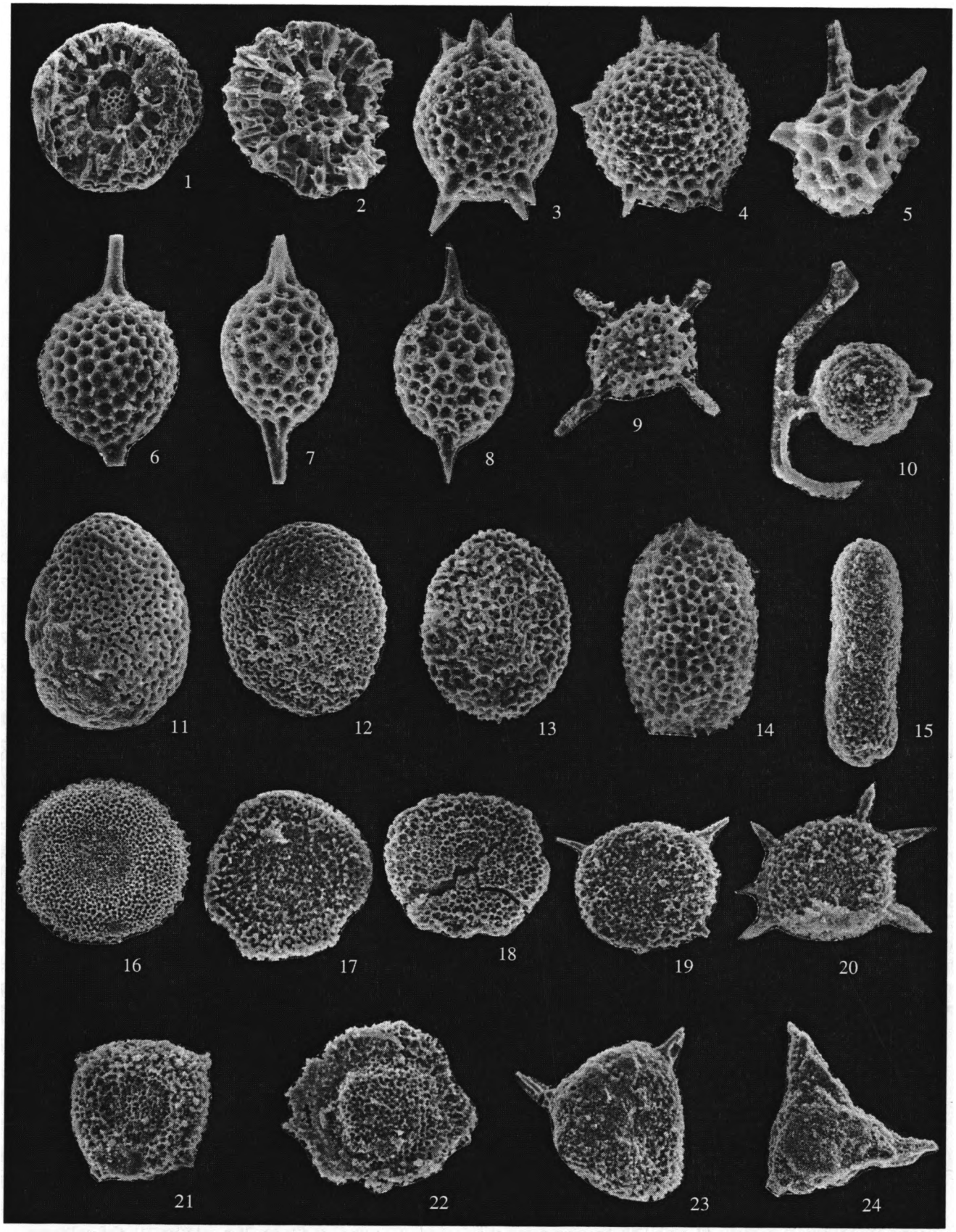
1
2
3
4
5
6
7
8
9
10
11
12
13
14
15
16
17
18
19
20
21
22
23
24

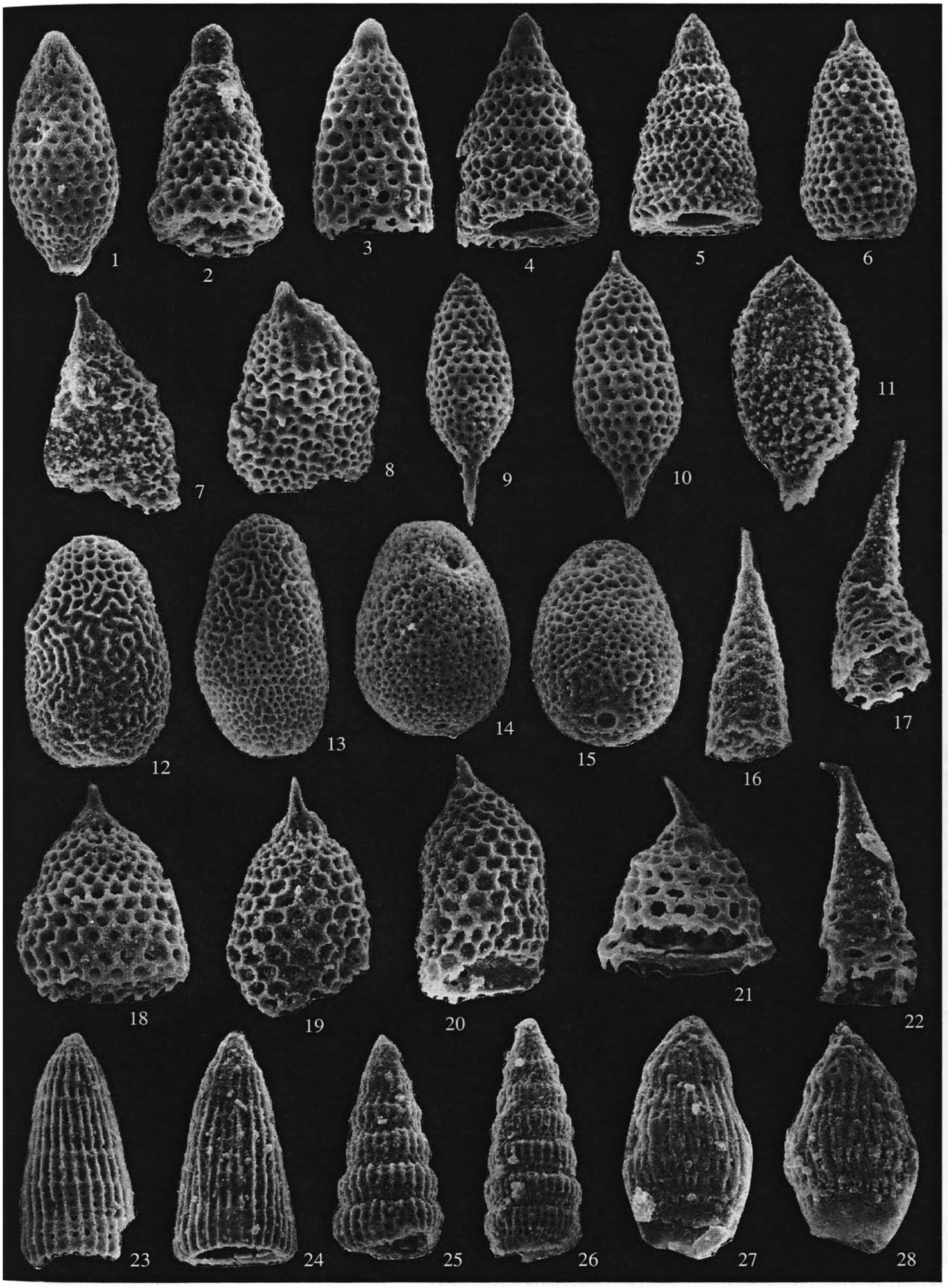
1
2
3
4
5
6
7
8
9
10
11
12
13
14
15
16
17
18
19
20
21
22
23
24
25
26
27
28

Plate 2. Radiolarians from the olistostrome.

(1) *Amphipyndax stocki* (Campbell et Clark), 76/a, ×150; (2) *Amphipyndax stocki* var. C Vishnevskaya, 76/a, ×150; (3) *Amphipyndax streckta* (Empson-Morin), 76/d, ×100; (4) *Amphipyndax tylotus* Foreman, 75/a, ×150; (5) *Wildeus punctulatus* (Pessagno), 75/v, ×120; (6) *Lithostrobus rostovzevi* Lipman, 76/v, ×120; (7) *Xitus* cf. *asymbatos* (Foreman), 76/v, ×100; (8) *Novodiacanthocapsa manifesta* (Foreman), 76/b, ×150; (9, 10) *Stichomitra livermorensis* (Campbell et Clark): (9) 77/b, ×150, (10) 76/a, ×200; (11) *Stichomitra* cf. *shirshovica* Vishnevskaya, 76/v, ×120; (12, 13) *Theocapsomma erdnussa* (Empson-Morin), 75/a, ×100; (14, 15) *Theocapsomma* ? sp., 75/a, ×100; (16, 17) *Cornutella californica* Campbell et Clark: (16) 76/v, ×150, (17) 76/v, ×180; (18) *Clathrocyclas hyronia* Foreman, 76/v, ×150; (19) *Clathrocyclas diceros* Foreman, 76/v, ×150; (20) *Clathrocyclas tintinnaeformis* Campbell et Clark, 77/b, ×110; (21) *Clathrocyclas* sp., 76/a, ×200; (22) *Cornutella californica* Campbell et Clark, 77/b, ×200; (23, 24) *Archaeodictyomitra squinaboli* Pessagno: (23) 76/b, ×100, (24) 76/d. ×190; (25, 26) *Dictyomitra densicostata* Pessagno: (25) 76/a, ×200, (26) 77/v, ×100; (27, 28) *Theocampe vanderhoofi* Campbell et Clark, 77/b, ×200.

extending for the distance over 2 km to the northeast of the river mouth. The basal conglomerate beds of the Anadyrka Formation are predominantly composed of basalts, the pyroxene and hornblende varieties typical of the Palana volcanogenic sequence included. Thus, lithological and structural data indicate a sharp unconformity between the Anadyrka Formation and underlying Cretaceous deposits.

DISCUSSION

Radiolarian assemblages. The radiolarian assemblages from the section studied are unique in terms of abundance and preservation state of species. Practically all of 60 samples collected for micropaleontological analysis contained radiolarians, most of which are well preserved.

Radiolarians were macerated from siliceous interbeds of the volcanogenic sequence and from olistoliths and matrix of the olistostrome. The most representative radiolarian assemblages of the Palana section include up to 31 species of 25 genera. Taxonomic analysis of radiolarian assemblages from the different deposits of the section (Tables 1–4) revealed a great similarity between those characterizing chert interbeds of the volcanogenic sequence, the olistostrome matrix, and some olistoliths. This suggests that all the deposits were formed in the immediate vicinity to each other. In the assemblages, the Campanian and Campanian–Maastrichtian forms are associated with many late Maastrichtian–Paleocene species, such as *Amphisphaera goruna* (Campbell et Clark), *Lithomespilus mendosa* (Krasheninnikov), *Orbiculiforma renillaeformis* (Campbell et Clark), *Spongodiscus alveatus* (Sanfilippo et Riedel), *S. rhabdostylus* (Ehrenberg), and *Spongotrochus polygonatus* (Campbell et Clark). Their presence in the olistostrome matrix (Table 5) suggests that it was still under formation in the early Paleocene.

The late Campanian–Maastrichtian radiolarian assemblages of the Palana section show a high taxonomic diversity. The order Spumellaria is represented by Phaseliformidae, Orbiculiformidae, *Praestylosphaera*, and *Lithomespilus* forms widespread all over the Olyutorskii zone and Kamchatka, by peculiar *Cromyosphaera* and *Actinomma* species, and by abundant representatives of Spongodiscidae (*Spongodiscus alveatus, S. impressus, Porodiscus cretaceus, Spongotrochus polygonatus*, and others) and Sponguridae. Some pseudoaulophacoid forms, such as *Pseudoaulophacus lenticulatus*, also occur. The order Nassellaria is represented by Amphipyndaxidae (*Amphipyndax stocki, A. streckta, A. tylotus, A. pseudoconulus*), Cyrtidae (forms abundant *Archaeodictyomitra, Dictyomitra, Stichomitra*), Theocampidae (*Theocampe altamontensis, T. vanderhoofi, T. yaoi*), and Clathrocyclidae (*Clathrocyclas hyronia, Cl. diceros, Cl. tintinnaeformis*). A distinctive feature of the Palana assemblages is abundance of triloculine Nassellaria species, such as *Theocapsomma amphora, T. erdnussa, Hemicryptocapsa conara, Novodiacanthocapsa manifesta, Sciadiocapsa campbelli*, and others.

The assemblages include forms with test walls of different types, i.e., porate (up to 70%), porous-spongy (24%), pseudoaulophacoid (2%) and xitoid (about 4%). This suggests the high-latitude habitat areas of the assemblages. The suggestion is confirmed by data on Campanian radiolarians from different areas of the globe (Empson-Morin, 1984). For instance, she considered the genus *Prunobrachium* whose representatives are present in our collection as a taxon indicative of the

Plate 3. Radiolarians from olistoliths of the olistostrome, (1–20, 25, 26) from Sample 9918/2 and (21–24) from Sample 44.

(1, 2) *Praestylosphaera pusilla* (Campbell et Clark): (1) ×120, (2) ×200; (3) *Amphisphaera priva* (Foreman), ×200; (4) *Lithomespilus mendosa* (Krasheninnikov), ×200; (5) *Spongodiscus rhabdostylus* (Ehrenberg), ×100; (6) *Cromyodruppa concentrica* Lipman, ×90; (7) *Phaseliforma carinata* Pessagno, ×100; (8) *Spongodiscus impressus* Lipman, ×100; (9) *Spongosaturnalis spiniferus* Campbell et Clark, ×100; (10) *Stichomitra livermorensis* Campbell et Clark), ×100; (11) *Stichomitra campi* (Campbell et Clark), ×120; (12) *Eucyrtidium carnegiense* Campbell et Clark, ×100; (13) *Stichopilium teslaense* Campbell et Clark, ×100; (14) *Xitus* cf. *asymbatos* (Foreman), ×110; (15) *Theocampe altamontensis* (Campbell et Clark), ×200; (16) *Clathrocyclas hyronia* Foreman, ×200; (17) *Clathrocyclas tintinnaeformis* Campbell et Clark, ×180; (18) *Clathrocyclas* sp., ×100; (19) *Stichomitra* ? sp., ×200; (20) *Cornutella californica* Campbell et Clark, ×200; (21) *Hemicryptocapsa* aff. *conara* Foreman, ×200; (22) *Patulibracchium* cf. *petroleumensis* Pessagno, ×100; (23) *Histiastrum* sp., ×100; (24) *Neosciadiocapsa* cf. *diabloensis* Pessagno, ×90; (25) *Dictyomitra multicostata* Zittel, ×180; (26) *Archaeodictyomitra regina* (Campbell et Clark), ×100.

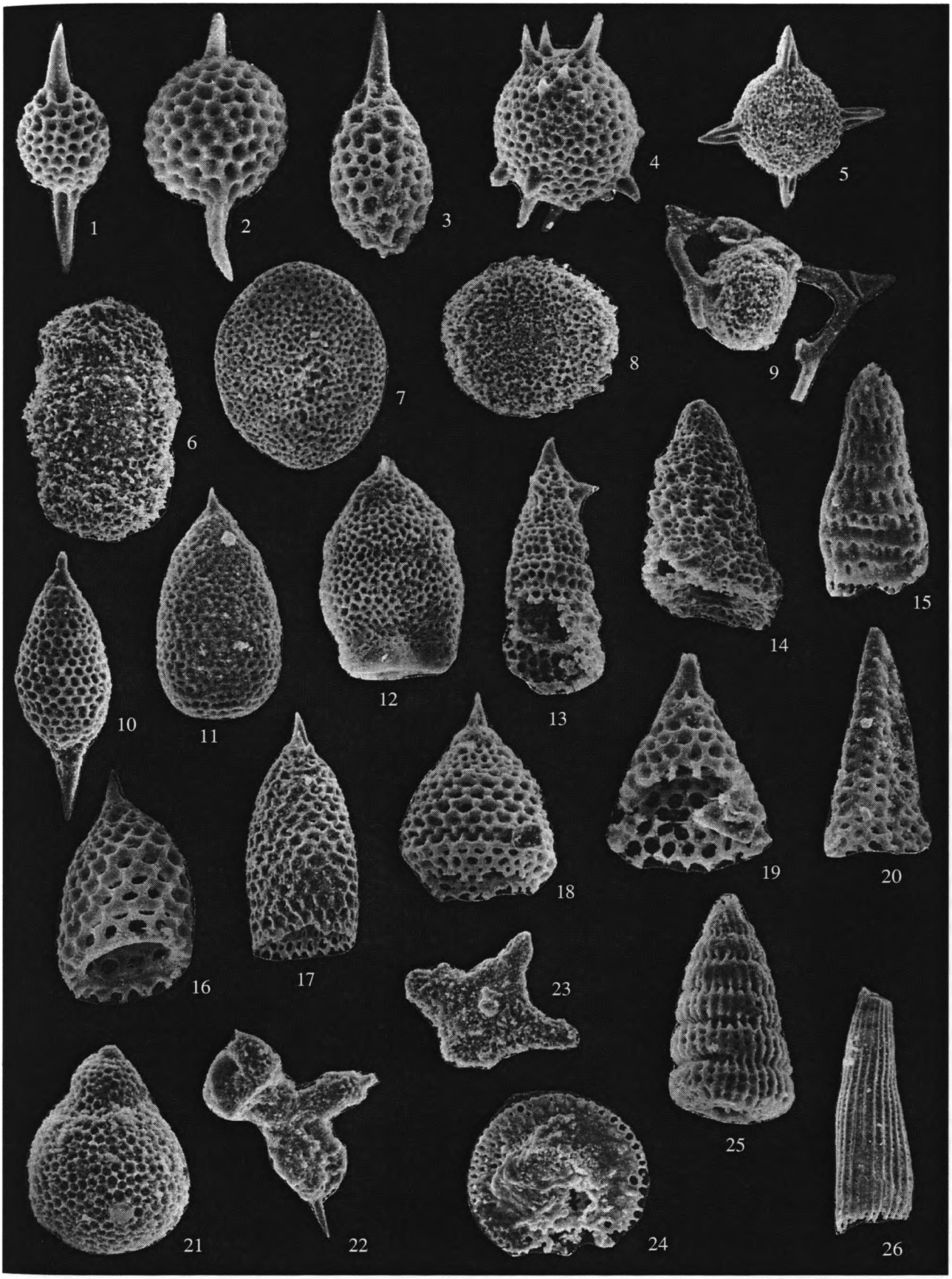
1
2
3
4
5
6
7
8
9
10
11
12
13
14
15
16
17
18
19
20
21
22
23
24
25
26

Table 5. Stratigraphic ranges of identified species according to published data

Species	st	cp			m		d
		cp1	cp2	cp3	m1	m2	
Archaeodictyomitra squinaboli Pessagno							
Dictyomitra densicostata Pessagno							
Orbiculiforma quadrata Pessagno							
Novodiacanthocapsa manifesta (Foreman)							
Theocapsomma erdnussa (Empson-Morin)							
Lithostrobus rostovzevi Lipman							
Kuppelella cayeuxi (Squinabol)							
Wildeus punctulatus (Pessagno)							
Cromyodruppa concentrica Lipman							
Pseudoaulophacus lenticulatus (White)							
Patulibracchium petroleumensis Pessagno							
Amphibrachium spongiosum Lipman							
Archaeospongoprunum hueyi Pessagno							
Histiastrum latum Lipman							
Haliomma minor Campbell et Clark							
Praestylosphaera hastata (Campbell et Clark)							
P. pusilla (Campbell et Clark)							
Prothoxiphotractus perplexus Pessagno							
Spongosaturnalis spiniferus Campbell et Clark							
Phaseliforma carinata Pessagno							
P. subcarinata Pessagno							
P. laxa Pessagno							
Spongurus quadratus Campbell et Clark							
Amphipyndax streckta (Empson-Morin)							
A. tylotus Foreman							
Clathrocyclas hyronia Foreman							
C. diceros Foreman							
C. tintinnaeformis Campbel et Clark							
Archaeodictyomitra regina (Campbell et Clark)							
Dictyomitra andersoni (Campbell et Clark)							
Stichomitra livermorensis (Campbell et Clark)							
S. shirshovica Vishnevskaya							
S. campi (Campbell et Clark)							
Cornutella californica Campbell et Clark							
Theocampe altamontensis (Campbell et Clark)							
T. yaoi Taketani							
T. vanderhoofi Campbell et Clark							
Gongylothorax verbeeki (Tan Sin Hok)							
Staurodictya fresnoensis Foreman							
Neosciadiocapsa diabloensis Pessagno							
Hemicryptocapsa conara Foreman							
Amphibrachium sansalvadorensis Pessagno							
Amphisphaera priva (Foreman)							
A. goruna (Campbell et Clark)							

Table 5. (Contd.)

Species	st	cp			m		d
		cp1	cp2	cp3	m1	m2	
Orbiculiforma renillaeformis (Campbell et Clark)							
Lithomespilus mendosa (Krasheninnikov)							
Spongodiscus alveatus (Sanfilippo et Riedel)							
S. rhabdostylus (Ehrenberg)							
Spongotrochus polygonatus (Campbel et Clark)							
Cromyosphaera vivenkensis Lipman							
Spongodiscus impressus Lipman							
Porodiscus cretaceus Campbell et Clark							
Spongotripus morenoensis Campbell et Clark							
Haliomma schucherti Campbell et Clark							
Theocapsomma amphora Campbell et Clark							
Sciadiocapsa campbelli Pessagno							
Stichopilidium teslaense Campbell et Clark							
Eucyrtidium carnegiense Campbell et Clark							
Xitus asymbatos Foreman							
Dictyomitra multicostata Zittel							
Amphipyndax stocki (Campbell et Clark)							
Amphipyndax stocki var. C Vishnevskaya							

high latitudes. The assemblages also include *Neosciadiocapsa* forms, which inhabited predominantly the high and temperate latitudes (Petrushevskaya, 1981).

Among 62 species radiolarians species from the Palana section, 23 are known from the upper Senonian deposits of California (Campbell and Clark, 1944), and 12 were described from the upper part of the upper Campanian Forbes Formation of northern California (Pessagno, 1976). The latter group includes *Phaseliforma carinata* Pessagno, the index-species of synonymous subzone of the lower part of the upper Campanian of northern California (Pessagno, 1976). Eight of our species are known from the upper Maastrichtian deposits of California (Foreman, 1968), and two, namely *Amphipyndax streckta* (Empson-Morin) and *Theocapsomma erdnussa* (Empson-Morin), are components of the Campanian radiolarian assemblage from DSDP Site 313, the central Pacific Ocean (Empson-Morin, 1984). Some species (for example, *Theocampe yaoi* Taketani) are characteristic of the Campanian deposits in northeastern Hokkaido (Iwata and Tajika, 1986). The majority of identified species are typical of the Campanian–Maastrichtian assemblages from the Olyutorskii zone of Koryakiya (Vishnevskaya, 1985; Palechek, 1997; Solov'ev *et al.*, 1998, 2000), and 13 species are listed in the Campanian–Maastrichtian assemblages of western Sakhalin (Kazintsova, 2000). The assemblages studied show some similarity with the Late Cretaceous–Paleocene radiolarians of New Zealand (Hollis, 1997). All the species mentioned above are characteristic of the circum-Pacific belt. In addition, seven species of the Palana section (*Lithostrobus rostovzevi, Histiastrum latum, Amphibrachium spongiosum*, and others) are known from Upper Cretaceous deposits of the West Siberian lowland (Lipman, 1962), and this may imply that Arctic and Pacific basins were interconnected at that time.

Geological events recorded in the Palana section. Rocks exposed in coastal cliffs between the Palana and Anadyrka rivers recorded a series of successive geological events. These were the accumulation of siliceous deposits now constituting olistoliths of the Ust-Palana Formation, the deposition of volcanogenic rocks and formation of the Ust-Palana olistostrome at the time of deformation of siliceous and volcanogenic sequences. Afterward, the final deformation of the entire Ust-Palana section resulted in elevation and erosion of its rocks followed by accumulation of the continental molasse (the Anadyrka Formation).

Siliceous deposits that represented source material for the most olistoliths and olistostrome matrix accumulated since the Late Jurassic probably to the end of the Cretaceous (Kurilov, 2000; Palechek *et al.*, 2000). Nevertheless, the olistoliths are predominantly of Campanian–Maastrichtian age, and this suggests a low sedimentation rate at the time of pre-Campanian chert deposition. Fragments of inoceramid shells in the Conia-

cian–lower Campanian olistoliths (Kurilov, 2000) indicate that beginning from the early Coniacian there appeared numerous inoceramid banks at the basin floor, and that the abundant shell detritus was transported by currents. In the Campanian–Maastrichtian time, siliceous deposits accumulated in a basin with a minor influx of tuffaceous and terrigenous material. According to the paleomagnetic data, it was at close to 40°–50° N, i.e., southward of the modern location of the olistostrome in the western Kamchatka (Chernov *et al.*, 2000). This assumption is supported by composition of cherts, which should be deposited far from the northeastern Asia margin supplying abundant terrigenous material into the adjacent basins.

In the second half of the Campanian, submarine basalt eruptions separated by short accumulation periods of bedded tuffaceous-sedimentary members gave rise to formation of the volcanogenic sequence. Composition of volcanic rocks is typical of island arcs and analogous to volcanics of the Kirganik Formation in southern areas of the Median Kamchatka Range (Flerov and Koloskov, 1976).

The age relationships between volcanogenic rocks and Campanian–Maastrichtian siliceous deposits, which produced olistoliths (Kurilov, 2000), cannot be clarified by means of similar results of radiolarian analysis. Because the cherts contain no significant tuffaceous admixture, their accumulation setting should be separated from the provenance of volcanic material either in space or with time. If rocks of both types are contemporaneous, the island arc must be located either nearer to or farther from the continent than the area of siliceous sedimentation. In the first case, it is difficult to explain why the olistostrome with cherty olistoliths is positioned at present closer to the continent than the Upper Cretaceous island-arc sequences of Kamchatka. In the second case, it is difficult to bring into accordance the paleomagnetic data on cherts and on the Median Range and the Karaginskii Island, because the latter structures were located at higher latitudes in the Campanian–Maastrichtian time (Kovalenko, 1990; Levashova and Shapiro, 1999). It seems most probable, therefore, that cherty and volcanic rocks have different ages within the Maastrichtian-Danian time span.

The olistostrome formation implies short-term movements and, probably, thrusting, which caused synchronous destruction of tectonic slices (blocks) of volcanogenic and siliceous deposits in submarine environments. Judging from the age of olistostrome matrix, these events took place in the late Campanian–Maastrichtian. However, the siliceous sedimentation and subsequent volcanic eruptions happened in the same time interval. Thus, the olistostrome was likely formed at the end of the interval. The volcanogenic sequence is dated back to the late Campanian–Maastrichtian based on radiolarians and to the early Maastrichtian based on K/Ar dates for amphiboles from basaltic andesites (72.5 ± 3.5 and 72.0 ± 3.5 Ma). Volcanogenic clasts, which are present in the olistostrome, suggest the post-early Maastrichtian age of the latter. Accordingly, the tectonic imbrication and related olistostrome formation occurred, most probably, after the early Maastrichtian. On the other hand, a sharp unconformity at the base of the Anadyrka Formation is a result of the general deformation of the Palana section. According to available date on the Anadyrka flora (Gladenkov *et al.*, 1997), this event occurred not later than in the mid-Danian time.

ACKNOWLEDGMENTS

We are grateful to PGO Kamchatgeologiya (the Lesnaya Geological Party headed by Yu.A. Burmanov) for their help in the field work organization, and to N.A. Bogdanov and V.S. Vishnevskaya for their attention to our investigations and fruitful consultations. The work was supported by the Russian Foundation for Basic Research, projects nos. 01-05-06205, 00-05-64301, and 98-05-64525.

Reviewers Yu.B. Gladenkov and A.E. Shantser

REFERENCES

Campbell, A. and Clark, B., Radiolaria from Upper Cretaceous of Middle California, *Spec. Pap. Geol. Soc. Am.*, 1944, no. 57, pp. 1–61.

Chernov, E.E., Kovalenko, D.V., and Kurilov, D.V., Paleomagnetism of Upper Cretaceous Island-Arc Complexes in the Area of the Palana River Mouth (Western Kamchatka), *Issledovaniya litosfery* (Investigation of the Lithosphere), Moscow: Ross. Akad. Nauk, 2000, pp. 39–40.

Demidov, N.T. and Sulima, G.S., *Gosudarstvennaya geologicheskaya karta SSSR. Masshtab 1 : 200000. Zapadno-Kamchatskaya seriya. List O-57-X, XI (Palana, Kinkil')* (State Geological Map of the USSR, Scale 1 : 200 000, West Kamchatka Series, Sheet O-57-X, XI, Palana, Kinkil), Leningrad: Vses. Geol. Inst., 1982.

Dvali, M.F., Geological Structure of the Palana Area (Western Coast of the Kamchatka Peninsula), *Tr. Vses. Nauch.-Issled. Geol.-Razved. Inst.*, 1957, issue 102.

Empson-Morin, K., Depth and Latitude Distribution of Radiolaria in Campanian (Late Cretaceous) Tropical and Subtropical Oceans, *Micropaleontol.*, 1984, vol. 30, no. 1, pp. 87–115.

Flerov, G.B. and Koloskov, A.V., *Shchelochnoi bazal'tovyi magmatizm Tsentral'noi Kamchatki* (Alkaline Basaltic Magmatism of Central Kamchatka), Moscow: Nauka, 1976.

Foreman, H., Upper Maastrichtian Radiolaria of California, *Spec. Pap. Paleontol. Assoc., London,* 1968, no. 3, pp. 1–82.

Geologicheskaya karta SSSR. Masshtab 1: 500000 (novaya seriya). List O-57, (58) - Palana. Ob"yasnitel'naya zapiska (Explanatory Notes to Geological Map of the USSR, Scale 1 : 500000, Sheet O-57, 58, Palana), Leningrad: Vses. Geol. Inst., 1989.

Gladenkov, Yu.B., Shantser, A.E., Chelebaeva, A.I., *et al.*, *Nizhnii paleogen Zapadnoi Kamchatki (stratigrafiya, paleogeografiya, geologicheskie sobytiya)* (Lower Paleogene of

Western Kamchatka: Stratigraphy, Paleogeography, Geological Events), Moscow: GEOS, 1997.

Hollis, C.J., *Cretaceous-Paleocene Radiolaria from Eastern Marlborough, New Zealand, Monograph 17*, Canberra: Inst. Geol. Nuclear Sci., 1997.

Iwata, K. and Tajika, J., Late Cretaceous Radiolarians of the Yubetsu Group, Tokoro Belt, Northeast Hokkaido, *J. Fac. Sci. Hokkaido Univ., Ser. IV*, 1986, vol. 21, no. 4, pp. 619–644.

Kazintsova, L.I., Albian-Maastrichtian Radiolarians from Western Sakhalin, XI seminar po radiolyariyam *"Radiolyariologiya na rubezhe tysyacheletii: itogi i perspektivy"* (11th Seminar on Radiolarians: Radiolariology at the Starting Point of New Millennium, Results and Perspectives), Petersburg: Vses. Geol. Inst., 2000, pp. 31–32.

Kovalenko, D.V., Paleomagnetic Study of Island-Arc Complexes in the Karaginskii Island and Malinovskii Ridge of the Olyutorskii Zone: Tectonic Interpretation, *Geotektonika*, 1990, no. 4, pp. 36–46.

Kurilov, D.V., New Findings of Jurassic-Cretaceous Radiolarians in Western Kamchatka, *Issledovaniya litosfery* (Investigation of the Lithosphere), Moscow: Ross. Akad. Nauk, pp. 40–42.

Levashova, N.M. and Shapiro, M.N., Paleomagnetism of Upper Cretaceous Island-Arc Complexes of the Median Kamchatka Ridge, *Tikhookean. Geol.*, 1999, vol. 18, no. 2, pp. 65–75.

Lipman, R.Kh., Late Cretaceous Radiolarians from the West Siberian Lowland and Turgai Depression, *Tr. Vses. Geol. Inst., Nov. ser.*, 1962, vol. 77, pp. 271–323.

Ob"yasnitel'naya zapiska k tektonicheskoi karte Okhotomorskogo regiona masshtaba 1 : 2 500 000 (Explanatory Notes to Tectonic Map of the Sea of Okhotsk, Scale 1 : 2500000), Bogdanov, N.A. and Khain, V.E., Eds., Moscow: Ross. Akad. Nauk, 2000.

Palechek, T.N., Structure and Accumulation Environments of Upper Cretaceous Volcanogenic-Cherty Deposits in the Olyutorskii Region: Data of Radiolarian Analysis, *Cand. Sci. (Geol.–Min.) Dissertation*, Moscow: Inst. of Lithosphere of Marginal and Inner Seas, 1997, p. 25.

Palechek, T.N., Solov'ev, A.V., and Shapiro, M.N., Age of Pre-Cenozoic Deposits in the Palana Area, *Issledovaniya litosfery* (Investigation of the Lithosphere), Moscow: Ross. Akad. Nauk, 2000, pp. 42-45.

Pessagno, E., Radiolarian Zonation and Stratigraphy of the Upper Cretaceous Portion of the Great Valley Sequence, California Coast Ranges, *Micropaleontol.*, 1976, no. 2, pp. 1–95.

Petrushevskaya, M.G., *Radiolyarii otryada Nassellaria Mirovogo okeana* (Radiolarians of the Order Nassellaria from the World Ocean), Leningrad: Nauka, 1981.

Solov'ev, A.V., Palechek, T.N., and Ledneva, G.V., Campanian–Maastrichtian Deposits in the Frontal Part of the Olyutor Zone (Southern Koryak Upland), *Stratigr. Geol. Korrelyatsiya*, 2000, vol. 8, no. 2, pp. 88–96.

Solov'ev, A.V., Palechek, T.N., and Palechek, R.M., Tectonostratigraphy of the Northern Olyutor Zone (Anastasiya Bay Area of Koryak Highland), *Stratigr. Geol. Korrelyatsiya*, 1998, vol. 6, no. 4, pp. 92–105.

Vishnevskaya, V.S., Radiolaria-Based Biostratigraphy of Upper Cretaceous Volcanogenic-Cherty Deposits in the Bering Sea Region of the USSR, *Tikhookean. Geol.*, 1985, no. 4, pp. 189–217.

Stratigraphy and Geological Correlation, Vol. 11, No. 3, 2003, pp. 278–292. Translated from Stratigrafiya. Geologicheskaya Korrelyatsiya, Vol. 11, No. 3, 2003, pp. 75–90.
Original Russian Text Copyright © 2003 by Amon, Vasil'eva, Zhelezko.
English Translation Copyright © 2003 by MAIK "Nauka/Interperiodica" (Russia).

Stratigraphy of the Talitsa Horizon (Paleocene) in the Central Trans-Urals

E. O. Amon, O. N. Vasil'eva, and V. I. Zhelezko[†]

Institute of Geology and Geochemistry, Uralian Division, Russian Academy of Sciences, Pochtovyi per. 7, Yekaterinburg, 620151 Russia

Received July 7, 2001; in final form, January 1, 2002

Abstract—Data on a series of boreholes drilled in the central trans-Urals are used to characterize the Paleocene marine deposits of the Talitsa Horizon, which are widespread all over the trans-Urals and in West Siberia. Presented paleogeographic considerations are based on distribution patterns of various fossils (foraminifers, radiolarians, dinocysts, and Selachii teeth) and on lithologic characteristics of their host deposits. Presented in addition are brief descriptions of underlying Maastrichtian (Gan'kino Formation) and overlying Thanetian (Serov Formation) deposits. The character and position of the Cretaceous–Paleogene boundary that is placed at the Talitsa Horizon base are described. Regional zonation of foraminifers and dinocysts is substantiated, and problems of regional and interregional correlations are briefly discussed.

Key words: trans-Urals, West Siberia, Talitsa Horizon, Paleocene, foraminifers, dinocysts, radiolarians, Selachii, biostratigraphic zones, Cretaceous–Paleogene boundary.

INTRODUCTION

All along the trans-Urals, running from north to south, and in adjacent areas of West Siberia, the Mesozoic–Cenozoic sedimentary cover includes Paleocene deposits of the regional Talitsa Horizon, the basal one in the marine terrigenous sequence of the Lower Paleogene. In central and southern segments of the trans-Urals and eastward, outside this structural-lithologic zone, the horizon is represented predominantly by clayey and clayey-sandy sediments of the Talitsa Formation. These rocks grade westward into massive sandstones with clayey-siliceous cement, which are characteristic of eastern flanks of the central and southern Urals. Northward, in the northern and near-polar Urals, rocks of the Talitsa Formation are replaced by sandy clays, siltstones, and clayey diatomites of the Marsyaty and Ivdel formations of the Talitsa Horizon. In the northern Turgai depression, the concurrent Paleocene sequence is composed of sand and clay beds (Fig. 1).

Stratigraphy of the trans-Uralian Talitsa Horizon was studied and described forty to fifty years ago by scientists from several institutions (VSEGEI, VNIGRI, GIN AN SSSR) and by Uralian geologists N.I. Arkhangel'skii, V.A. Lider, S.D. Rabinovich, A.P. Sigov, L.A. Umova, G.N. Papulov, and others. In the same period, R.Kh. Lipman, L.G. Dain, A.I. Eremeeva, N.A. Belousova, and F.V. Kipriyanova investigated foraminiferal biostratigraphy of the horizon, which was attributed to the Paleocene Stage. It was decided as well that the Cretaceous–Paleogene boundary should be placed at the Talitsa Horizon base, and its top was correlated with the Paleocene–Eocene boundary. Data on the trans-Uralian sections, especially on those studied in natural exposures, boreholes, and quarries of central and southern segments of the trans-Urals, were extrapolated far eastward to substantiate the Paleogene stratigraphy of the entire West Siberia.

Later on, there was a break in investigations of Paleogene stratigraphy in the trans-Urals, and only limited new data on that issue and regional Cretaceous stratigraphy were obtained and published during the last two decades. On the other hand, the general concept of Paleogene stratigraphy in the southern trans-Urals, Turgai, West Siberia, and adjacent regions was revised to a considerable extent. First of all, the Danian Stage was transferred from the Cretaceous to Paleogene System, other stages of which were reconsidered with respect to validity and their ranges. According to new geochronological scale, Danian Stage in the range of nannoplankton zones NP1-NP4 (lower part) corresponds to the lower Paleocene, and the upper Paleocene includes Selandian and Thanetian stages, the former in the range of zones NP4 (upper part) to NP6 (lower part) and the latter in the range of zones NP6 (upper part) to NP9. It has been also argued for that the Montian Stage is a valid subdivision appropriate for the General Stratigraphic Scale (Naidin and Beniamovskii, 1988). In addition, the specified biozonation of foraminifers enabled the more precise and reliable correlation. Other groups of microfossils used in stratigraphic practice, such as nannoplankton, dinocysts, and radiolarians, also enhanced possibilities of local and interregional

[†] Deceased.

correlations (Akhmet'ev *et al.*, 2001). All these innovations imply that the out-of-date schemes of Paleogene stratigraphy in the trans-Urals and West Siberia, which are still in use being based on data published in the 1950s to 1960s (e.g., Podobina, 1998), should be revised.

In this work, we present new data on stratigraphy of the Talitsa Horizon in a central segment of the trans-Urals in order to improve the situation described above. The data characterize sections penetrated by hydrogeological boreholes within the segment extending from the Shadrinsk field in the south (Kurgan oblast) to the town of Turinsk in the north (Sverdlovsk oblast). We also revised data on the Turinsk reference section in West Siberia (Papulov and Sitnikova, 1964). In total, we summarized materials obtained from more than thirty boreholes. Some of the data presented below were partially discussed not long ago (Amon, 1990; Akhmet'ev *et al.*, 2001; Vasil'eva *et al.*, 2001).

The Talitsa Horizon is situated immediately above the Cretaceous–Paleogene boundary, and this position dictates a necessity to consider briefly the underlying Cretaceous deposits of the Gan'kino Formation and overlying strata of the Serov Formation. The study region is conventionally divided in two, the southern and northern areas (Fig. 2). Cretaceous to Paleogene deposits of southern area recorded sedimentation environments and distribution patterns of microfossils, which are characteristic of the southern trans-Urals and resemble those of central West Siberia. They have been penetrated by boreholes of the Shadrinsk field and by Borehole IG-32 drilled near the village of Novopetropavlovskoe. In addition, we investigated them in the Pershinskoe Quarry near the synonymous village of the Kurgan oblast. The northern area includes borehole sections penetrated in the Kamyshlov, Irbit, Alapaevsk, and Turinsk districts of the Sverdlovsk oblast (Fig. 2).

LITHOSTRATIGRAPHY

In the southern study area (Figs. 2, 3), sedimentary sequence of the Talitsa Horizon is most representative in the Shadrinsk field of carbonate hydropathical waters (boreholes 3, 308, 304, 304-b, 306, 310, and 310-a). Clayey sediments of the Talitsa Formation rest here on basal beds of transgressive origin, which discordantly overlie the clayey-carbonate sequence of the Campanian–Maastrichtian Gan'kino Formation. Higher in the section, opoka beds of the Serov Formation conformably overlie the Talitsa strata without any sign of hiatus or erosion. Bases of the Talitsa and Serov formations are established respectively at the following depth levels: 132.5 and 99.5 m in Borehole 304 (Talitsa Formation is 33.0 m thick); 135.0 and 115.9 m in Borehole 306 (Talitsa Formation is 19.1 m thick); 129.7 and 92.4 m in Borehole 308 (Talitsa Formation is 37.3 m thick). In Borehole 310 incompletely characterized by core samples, the Talitsa Formation base is at the depth 187.7 m, and its thickness could be up to 27.9 m.

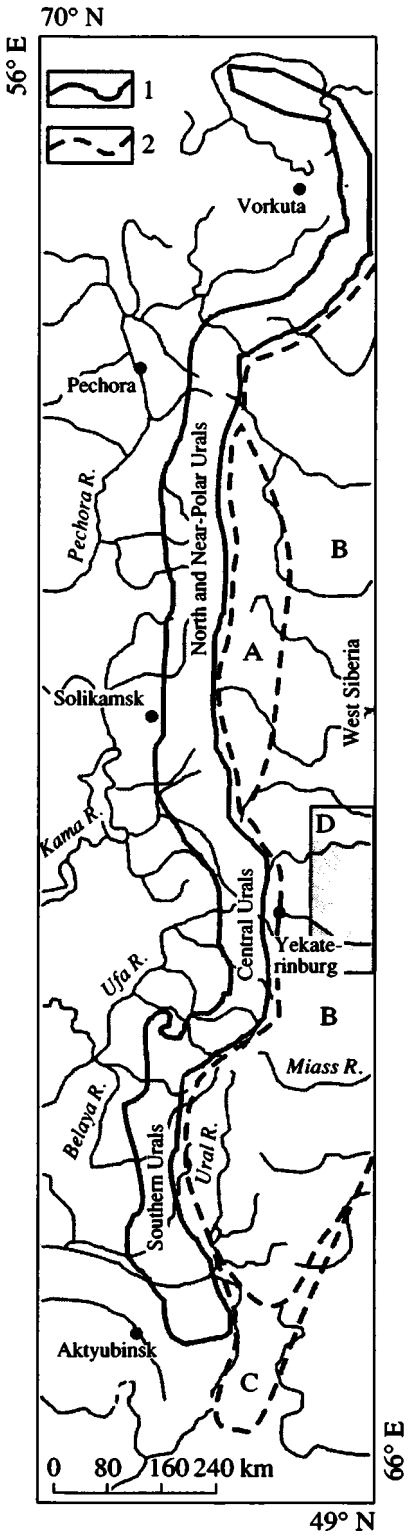

Fig. 1. Distribution areas of the Talitsa Horizon and its formations in the trans-Urals: (1) boundary of Uralian Mountains; (2) eastern distribution limit of the Talitsa Horizon; (A) distribution area of the Marsyaty and Ivdel formations in the northern and near-polar Urals; (B) distribution area of the Talitsa Formation; (C) distribution area of Paleocene deposits in the northern and central Turgai; (D) study region.

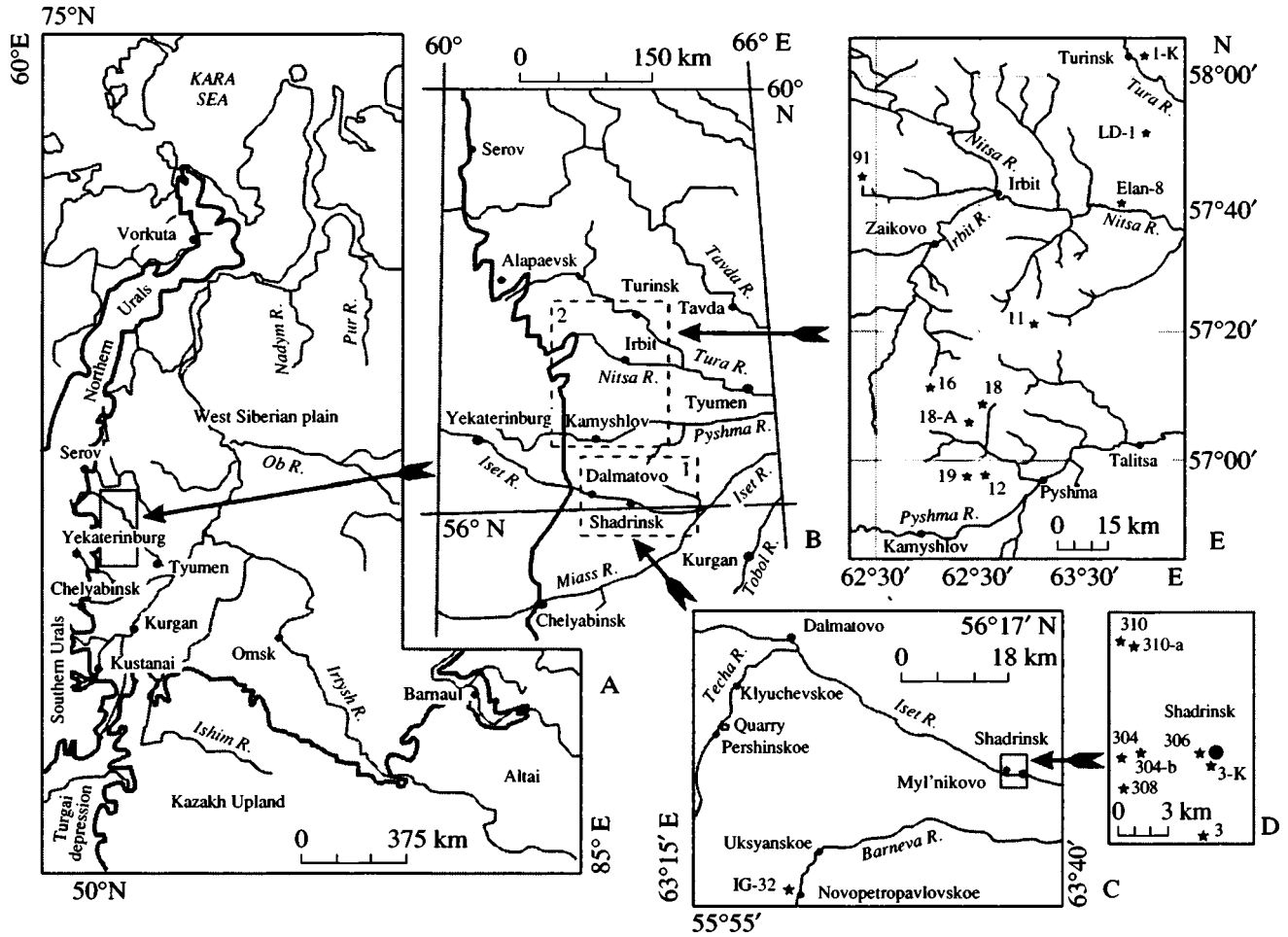

Fig. 2. Schematic maps illustrating geographic positions of the study region (A) subdivided into the southern and northern areas (dotted contours 1 and 2 in B); borehole localities in southern (C, D) and northern (E) areas are denoted by asterisks with corresponding letter symbols or numbers (thick solid lines show contours of Uralian mountains, Kazakh Upland, and Altai).

In different borehole sections of southern area, the base of Talitsa Formation is in contact with various strata of the underlying Gan'kino Formation. In boreholes 304, 306, and 308, the rock sequence of the Gan'kino Formation is of a three-member structure that is typical of this subdivision in the southern trans-Urals. Commonly it includes (a) the lower member of the late Campanian age that is composed of carbonate-free, often siliceous clays; (b) the middle member of the early Maastrichtian age that is composed of clayey (to variable extent) marls; and (c) the upper member of the late Maastrichtian age that is composed of calcareous clays. In the section of Borehole 310, the upper clayey member is missing, and Talitsa Formation overlies marly beds of the middle member. Sediments of the Gan'kino Formation yield abundant and diverse foraminifers, being less rich in radiolarian and dinocysts.

In boreholes 304 and 306, the upper Gan'kino member is composed of greenish gray, calcareous laminated clay with rare marl interlayers and disseminated pyrite crystals. Its basal 10-cm-thick layer of clay is of a pseudobrecciated structure and encloses subrounded pebbles of chert. Among organic remains, there are distinguishable fragments of bivalve shells, echinoid spines, abundant foraminifers, and rare radiolarians. The member was likely deposited under conditions of an insignificant regression, as one can judge from the character of sediments, their structural and textural peculiarities, predominance of benthic forms among foraminifers, and from a restricted distribution area.

Boreholes 304 and 306 also penetrated a thin member missing from other sections and defined as the Shadrinsk Beds in the rank of fauna-bearing strata (Amon, 1990, 1997). These beds situated between the upper Gan'kino member and Talitsa Formation base are 2.1 m thick in Borehole 304 (depth interval of 132.5–134.6 m) and 2.0 m thick in Borehole 306 (depth interval of 135.0–137.0 m).

The Shadrinsk beds are composed of greenish gray, fine-laminated "wash clay" with silty quartz admixture concentrated along the bedding planes. They reveal abundant pyrite inclusions (rod-like segregations ori-

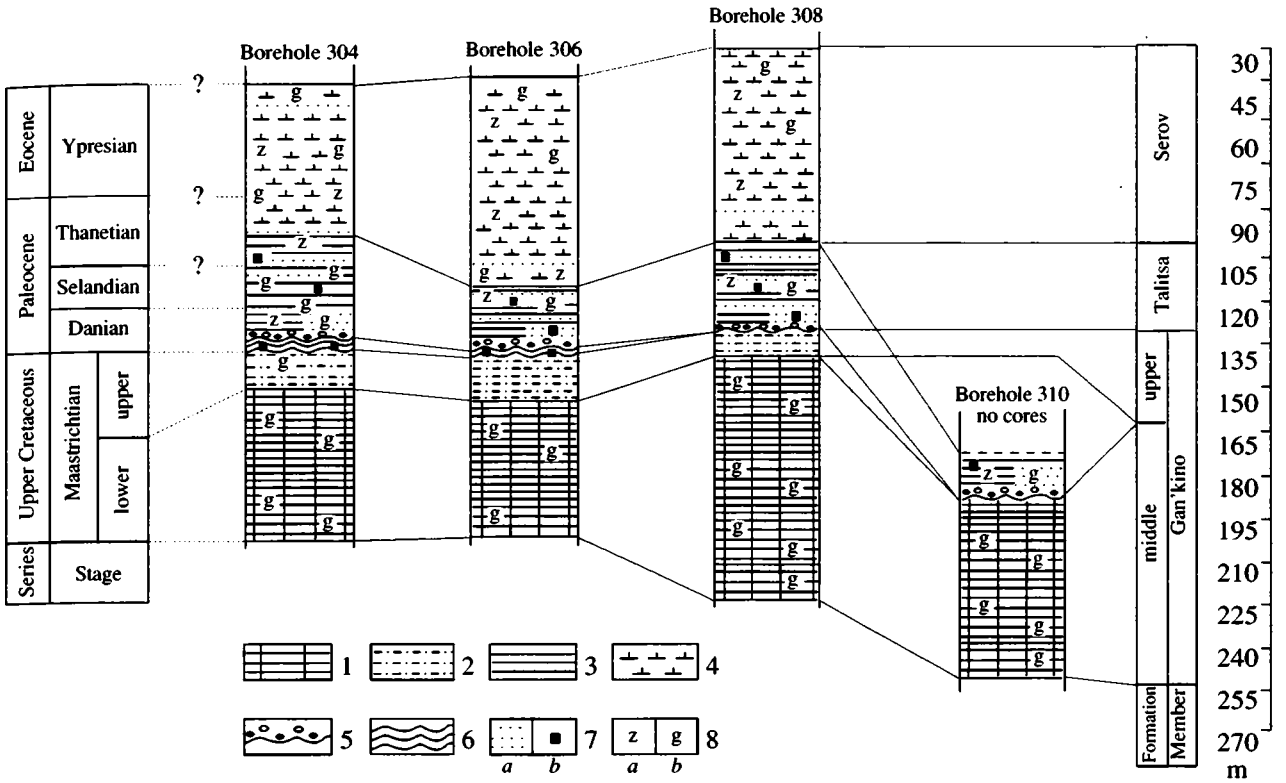

Fig. 3. Geological structure of the Cretaceous–Paleogene boundary deposits near the town of Shadrinsk (Gan'kino Formation is shown in the range of two upper members, other units in their complete ranges): (1) marly sediments of the middle Gan'kino member; (2) clayey-carbonate rocks of the upper Gan'kino member; (3) clayey-sandy deposits of the Talitsa Formation; (4) siliceous sediments of the Serov Formation; (5) basal horizon of sandy-gravely-pebbly sediments; (6) clayey carbonate-free Shadrinsk Beds; (7) sand (a), pyrite (b); (8) zeolite (a), and glauconite (b).

ented across to bedding) and white isometric to prismatic inclusions representing partially decomposed fragments of large bivalve shells, which are redeposited together with surrounding marly matrix from the underlying member of Gan'kino marls. The lower and upper boundaries of the beds are wavy and distinct. Foraminifers represent their characteristic organic remains.

Brownish to dark gray beidellite clays of the Talitsa Formation are irregularly enriched in sandy to silty material forming nests of irregular shape and interlayers of feldspar–quartz or glauconite–quartz composition. In places, there is visible flyschoid, almost rhythmical alternation of fine sandy clay and clayey sand laminae. Also characteristic are small pyrite segregations fresh and oxygenated, inclusions of glauconite and zeolites, and brown interlayers of hard cryptocrystalline siderite. The basal horizon 10 to 15 cm thick is of transgressive origin, rich in gravel, pebbles, and phosphorite concretions. The upper boundary is linear, distinct, and sharp. Among fossils from Talitsa Formation there are Osteichthyes remains (bones and scale), rare teeth and vertebrae of Selachii, planktonic and benthic foraminifers, radiolarians, spores and pollen, marine microphytoplankton, and coalified plant detritus. At the formation base, there were encountered the redeposited foraminifers of Maastrichtian age, tests of which are corroded, covered by film of Fe-hydroxides.

Clayey sediments of the Talitsa Formation abruptly grade upward into opokas of the Serov Formation, which are light gray, characterized by conchoidal fracture and uniform structure. Lower opoka beds are intercalated with interlayers of clayey opoka and silty clay. All boreholes also penetrated brecciated opoka horizons.

Interesting data have been obtained in the Pershinskoe Quarry situated near the synonymous village on the Techa River right bank. Exposures in the quarry exhibit contacts between the Talitsa, Serov, and Irbit formations and yield fossil shark teeth. Exposed in the quarry walls are the following units (from the base upward; shark taxa are identified by Zhelezko):

Upper Strata of Talitsa Formation

(1) Black foliated clay with abundant silty admixture and with nests of brown sand; 0.6 m thick.

(2) Coarse-grained quartz sand with abundant gravel of quartz and various rocks; fossil shark teeth belong to *Palaeohypotodus rutoti* (Winkler), *Striatolamia striata* Winkler, *Glueckmanotodus heinzelini* Casier, *Cosmo-*

politodus ex gr. *nolfi* (Zhelezko), and *Squatina* sp.; 0.4 m thick.

(3) Dark gray silty clay; rock is dense, fine-laminated; 0.7 m thick.

Serov Formation

(4) Gray hard opoka with coarse fracture, up to 4 m thick.

(5) Small to coarse gravel with admixture of inequigranular sand; found shark tooth is that of *Glueckmanotodus heinzelini* Casier; 0.4 m thick.

(6) Gray to light gray opokas; rocks are splintery, vaguely laminated, locally ferruginate, up to 22 m thick.

Irbit Formation

(7) Pale, yellow, and white soft homogeneous diatomites up to 4 m thick.

In opinion of Zhelezko, the Selachii assemblage from the Talitsa Formation represents a shark community of an open sea and is identical to coeval assemblage from Paleocene deposits of the Anglo-Franco-Belgian basin.

In the northern area, the sequence of Gan'kino, Talitsa, and Serov formations, as well as character of their sediments, are close to those described above. Like everywhere in the trans-Urals, the basal beds of Talitsa Formation discordantly overlie here the Gan'kino Formation rocks, and the top of the former is overlain by sediments of the Serov Formation. Sections of northern boreholes, which penetrated most complete sections of the Talitsa Formation, are shown in Fig. 2.

In sections of boreholes 12 and 19, the Gan'kino Formation is composed of gray to light gray and greenish nonlaminated marl with interlayers of clayey and silty marls; these rocks bear unidentifiable fragments of bivalve shells. In boreholes 18 and 16, it is composed of light gray (with bluish tint) calcareous silty clay bearing coalified plant detritus. In Borehole LD-1, its interval corresponds to alternation of gray shale and calcareous clay beds.

The Talitsa Formation sequence penetrated by boreholes 19 and LD-1 is complete and can be divided into the lower and upper members. In Borehole 19, the lower member (depth interval of 163.0–185.0 m) shows a vague alternation of thin laminae of dark gray sandy clay and clayey sand. The medium- to fine-grained sand consists of angular and subangular grains of quartz, chert, feldspar, Paleozoic volcanics, glauconite, pyrite, and phosphorite. A bed of clayey-sandy opoka that is 4 m thick was penetrated at the member base. The upper member (depth interval of 142.0–163.0 m) is composed here of dark gray (nearly black) and brown wash clays, which are bioturbated and exhibit minor intercalations (nests and lenses) of medium- to fine-grained sandy material. Transition from these pelitic rocks to underlying deposits with a higher content of sandy fraction is gradual. In Borehole LD-1, the Talitsa Formation is of a similar composition in general and retains its two-member structure (depth intervals of 243.0–278.0 and 185–243.2 m, respectively), although sediments of its upper portion are lithified to the shale state and reveal fine-platy jointing. The two-member structure is indistinguishable however in the Turinsk reference Borehole K-1 and in sections of the southern area.

Boreholes 12 and LD-1 penetrated Shadrinsk Beds at the base of the Talitsa Formation. In Borehole 12, these beds of light bluish gray dense clay that is free of carbonate, but bears sandy admixture and shows conchoidal fracture (depth interval of 224.0–230.0 m), separate calcareous clays of the Gan'kino Formation from the typical Talitsa clay. In Borehole LD-1, their stratigraphic interval established between depth levels of 278.0 and 283.0 m is also composed of bluish clay vaguely interlaminated with dark gray clay of typical Talitsa habit.

The Serov Formation is commonly composed of opoka, clayey opoka, and siliceous clay beds.

The reference Borehole K-1 at the Turinsk site penetrated sequence of Mesozoic to Paleogene deposits more than 1000 m thick (Papulov and Sitnikova, 1964). Paleocene strata of the Talitsa Formation (depth interval of 196.0–313.0 m) rest here on clay of the Gan'kino Formation (depth interval of 313.0–364,7 m), being overlain by the Serov opokas (depth interval of 130.0–196.0 m). They represent a rather uniform sequence of shales with nests and thin interlayers of sandstone and siltstone, and with thin siderite laminae.

Sediments of Gan'kino, Talitsa, and Serov formations bear diverse organic remains: bivalves, cephalopods, Selachii, Osteichthyes, foraminifers, radiolarians, ostracodes, diatoms, silicoflagellates, dinocysts, spores and pollen of terrestrial plants, all displaying characteristic distribution patterns. For instance, foraminifers are most diverse in the Gan'kino Formation, being less representative in the Talitsa Formation and nearly missing from the Serov Formation. Dinocysts characteristic of two former formations are also very rare in the latter. Shark teeth commonly occurring in the Talitsa Formation may be occasionally found above this interval as well. Foraminifers and dinocysts described below are of prime significance for the Paleocene stratigraphy, while other fossil groups are of an auxiliary importance.

FORAMINIFERS AND RADIOLARIANS

As is established, Maastrichtian deposits of the Gan'kino Formation yield two foraminiferal assemblages named after index taxa *Gaudryina rugosa spinulosa* and *Spiroplectammina kasanzevi*. The lower *Gaudryina rugosa spinulosa* assemblage includes abundant and very diverse agglutinated and secretory benthic foraminifers, the preservation state of which is satisfactory to perfect. This assemblage of the early

Maastrichtian age is excluded from consideration in this work.

The upper *Spiroplectammina kasanzevi* assemblage is somewhat less diverse than the lower one and consists of less abundant, mostly of agglutinated and secretory taxa associated with some planktonic forms. In this case, the preservation state of tests is usually satisfactory, less frequently good. Principal taxa of the assemblage are *Rhabdammina* sp., *Bathysiphon* sp., *Glomospira* spp., *Ammodiscus* sp., *Spiroplectinella baudouiniana* (Orb.), *Spiroplectammina* sp., *S. kasanzevi* Dain, *S. variabilis* Neck., *S. brevis* Kiss., *Dorothia* sp., *D.* cf. *pupoides* (Orb.), *D. pupoides ovata* Podob., *Plectina convergens* (Kell.), *Orbignyna inflata* (Reuss), *Heterostomella foveolata* (Marss.), *Arenogaudryina granosa* Podob., *Martinottiella* sp., *Cyclogyra* sp., Nodosariidae spp., *Dentalina* spp., *Guttulina* sp., *G. acutata* Kusina, *G. trigonula* Reuss., *Angulogavelinella caucasica* (Subb.), *Valvulineria laevis* Brotz., *Gyroidinoides turgidus* (Hag.), *Eponides peracutus* Lipm., *E. proprius* Podob., *Gavelinella midwayensis* Plumm., *Cibicides globigeriniformis* Neck., *C. gankinoensis* Neck., *Praebulimina carseyae* (Plumm.), *Reussella minuta* (Marss.), *Bolivina plaita* Carsey, and *Bolivinoides senonicus* Dain. Associated planktonic species *Heterohelix* spp. occur as single specimens.

In the northern study area, the *Spiroplectammina kasanzevi* assemblage has been detected in boreholes 12, 16, 18, and LD-1. In the Maastrichtian deposits recovered by Borehole 19, this assemblage is missing, because its stratigraphic range corresponds here to a break in sedimentation. Another important fact is that northward of Borehole 12 it is lacking species *Brotzenella praeacuta* of stratigraphic importance. In the southern area, the assemblage is known from all borehole sections. It is characteristic of the upper Maastrichtian *Spiroplectammina kasanzevi* Zone of biostratigraphic foraminiferal scale accepted for the trans-Urals and West Siberia.

In the southern trans-Urals, there were distinguished the lower *Brotzenella praeacuta* and upper *Hanzawaia ekblomi* subzones of the *Spiroplectammina kasanzevi* Zone, which are dated back to the initial and terminal late Maastrichtian, respectively (Amon, 1990, 1997). These subzones are well correlated with the Cretaceous foraminiferal zones known in southeastern areas of the East European paleobiogeographic province (Naidin *et al.*, 1984). In central and southeastern areas of West Siberia, their equivalents are the lower *Bolivina plaita* and upper *Heterostomella foveolata* subzones (Kisel'man, 1974).

In boreholes 304, 306, and 308 drilled in the Shadrinsk field, there is distinguishable only the lower subzone of the *Spiroplectammina kasanzevi* Zone. This *Brotzenella praeacuta* Subzone yields here *Spiroplectammina kasanzevi* Dain, *S. rosula* (Ehr.), *Siphogaudryina stephensoni distincta* Podob., *Nodosaria* spp., *Nodosaria* cf. *bacillum* Defr., *Dentalina* spp., *Guttulina* spp., *Valvulineria imitata* (Olss.), *Bolivina incrassata gigantea* Wicher, *Bolivinoides senonicus* Dain, *Gavelinella midwayensis* (Plumm.), *G. danica* (Brotz.), *G. welleri* (Plumm.), *Cibicidoides bembix* (Marss.), *Brotzenella praeacuta* (Vass.), *Cibicides kurganicus* Neck., *C. globigeriniformis* Neck., *C. gankinoensis* Neck., *Bulimina omskensis* Kiss., *B. rosenkrantzi* (Brotz.), *B. ovata* Orb., and some other forms. As is shown above, the subzone under consideration is of the initial late Maastrichtian age, and consequently a part of the upper Maastrichtian interval can be missing from western sections of the Gan'kino Formation located close to the shoreline.

In the southern area, the overlying Shadrinsk Beds bears foraminifers, preservation state of which is poor to satisfactory. These are *Lenticulina roemeri* (Reuss), *L.* sp., *Nodosaria* cf. *bacillum* Defr., *Globulina* sp., *Cibicides* sp., *Bulimina ovata* Orb., *Globorotalia pseudobulloides* (Orb.), and *Guttulina trigonula (Reuss)* (boreholes 304 and 306). The concurrent assemblage from Borehole 3-K (depth level of 110 m), suburbs of the town of Shadrinsk (Papulov and Umova, 1956), is somewhat different in composition. It includes *Globigerina bulloides* Orb., *G. pseudobulloides* Plumm., *G. triloculinoides* Plumm., *G.* ex gr. *aspera* (Ehr.), *Globigerinella voluta* White, *Glomospira charoides* (Park. et Jones), *Lenticulina romeri* (Reuss), *Ammodiscus* sp., *Trochammina* sp., and *Haplophragmoides* sp. (identified by F.V. Kipriyanova). We attribute these taxa to the *Globorotalia pseudobulloides* assemblage whose stratigraphic range corresponds to that of *Globigerina taurica* assemblage from Turgai and to the lower Danian zones NP 1-2, (Beniamovskii *et al.*, 1989a; Amon, 1990).

Microfossils characterizing in southern sections the rocks of the Talitsa Formation proper are distributed in the following manner; lower beds of this subdivision yield scarce foraminifers and radiolarians, whereas the upper ones bear spores and pollen. In Borehole 304, foraminifers and radiolarians have been established within the depth range of 120.1–132.5 m, whereas spores and pollen are characteristic of the interval of 102.8–119.6 m. The assemblage of poorly to satisfactory preserved foraminifers includes the following taxa: *Lenticulina roemeri* (Reuss), *L.* sp., *Nodosaria* cf. *bacillum* Defr., *Bulimina ovata* Orb., *Globorotalia pseudobulloides* (Orb.), *Ceratobulimina cretacea* Cushm. et Harr., *Guttulina trigonula* (Reuss), *Globulina* sp., *Eponides* sp., *E. tenera* Orb., *Cibicides* sp., *Glomospirella* sp., *Rhizammina* sp., *Haplophragmoides* sp., *Bimonilina* sp., and *Ammodiscus* sp. They occur in association with redeposited late Senonian forms *Bulimina ovata* Orb., *Ceratobulimina cretacea* Cushm. et Harr., and *Nodosaria* cf. *bacillum* Defr., representing as a whole the *Globorotalia pseudobulloides* assemblage of the Shadrinsk Beds.

In the northern area, the lower *Globorotalia pseudobulloides* and upper *Glomospira gordialiformis*-

Cyclammina koksuvorovae assemblages are known from deposits of the Talitsa Horizon. The *Globorotalia pseudobulloides* assemblage established in the lower member of the Talitsa Formation near its base is most representative in Borehole 19 (depth interval of 178.0–185.0 m). Foraminifers rather rare in core samples are in a satisfactory preservation state and represent agglutinated and secreting benthic and planktonic forms. Their assemblage includes *Rhabdammina* sp., *R. irregularis* Carp., *R.* cf. *cylindrica* Glaesn., *Bathysiphon* sp., *B. rufescens* Cushm., *B.* aff. *nodosariaformis* Subb., *Proteonina* sp., *P. complanata* (Franke), *Probotellina distorta* Bulat., *Glomospira* sp., *G. charoides* (Park.), *Reophax difflugiformis* Brady, *Dentalina cylindrica* Lipm., *D. obliqua* Orb., *Reussella paleocenica* (Brotz.), *Globulina rotundata* (Born.), *Allomorphina hofkeri* Pozar., *Nonionella ovata* Brotz., *Globorotalia pseudobulloides* (Plumm.), *G. compressa* (Plumm.), *Globigerina triloculinoides* Plumm., *G.* cf. *kozlowskii* Brotz. et Pozar., *G. trivialis* Subb., and *G. varianta* Subb.

The concurrent assemblage from boreholes LD-1 and 12 is lacking planktonic forms, thus being less diverse, but it retains the same group of agglutinated benthic taxa. In these boreholes, its stratigraphic range spans the Shadrinsk Beds and basal clay beds of the Talitsa Formation. In boreholes 16 and 18, the assemblage has not been found.

The *Glomospira gordialiformis-Cyclammina koksuvorovae* assemblage from overlying beds is found to be most complete in Borehole 19 (depth interval of 161.0–173.0 m), where rare foraminifers are satisfactorily preserved and represented only agglutinated benthic forms. These are *Rhabdammina* sp., *R. irregularis* Carp., *R. discreta* Brady, *R. cylindrica* Glaesn., *Rhizammina algaeformis* Brady, *Proteonina* cf. *complata* (Franke), *Pelosinella didera* Loebl. et Tapp., *Technitella spiculitesta* Bulat., *Hippocrepinella acuta* Hoegl., *Hyperammina friabilis* Brady, *Probotellina distorta* Bulat., *Glomospira gordialiformis* Podob., *Reophax* sp., *R. difflugiformis* Brady, *R. ampullacea* Brady, *Ammoscalaria* sp., *A.* cf. *friabilis* (Ehrem.), *Haplophragmoides* sp., *H. granosum* Lipm., *H. perifero-excavata* Subb., *Trochammina* sp., *T. pentacamerata* Lipm., *T. complanata* Lipm., and *Cyclammina koksuvorovae* Uschak. This assemblage is known in addition from boreholes 16, 18, 12, and 11, but it has not been established in Borehole LD-1.

Deposits of the Serov Formation are practically lacking foraminifers. The only exception is Borehole 304, in which single tests of *Spiroplectammina spectabilis* (Grzyb.) were found at the depth level of 91.8 m. Opokas of the Serov Formation are barren of foraminifers. The species mentioned above is of a wide stratigraphic range (lower Eocene) and of a low significance for the Paleogene stratigraphy.

The *Gaudryina rugosa spinulosa* and *Spiroplectammina kasanzevi* assemblages from Cretaceous strata correspond in their ranges to synonymous foraminiferal zones distinguished in the trans-Urals and West Siberia (Podobina, 1989; Amon, 1997). They are, as is mentioned before, of the early and late Maastrichtian ages, respectively. Data on distribution of foraminifers imply that some upper beds of the Gan'kino Formation have been locally eroded in the study region (e.g., in Borehole 19 drilled in the northern area and in sections of the Shadrinsk hydrological field).

The *Globigerina pseudobulloides* assemblage spanning the interval of the Shadrinsk Beds and basal Talitsa strata can be represented either by association of planktonic and benthic taxa, or by agglutinated benthic forms only. Planktonic foraminifers, especially *Globigerina triloculinoides* Plumm., *G.* cf. *kozlowskii* Brotz. et Pozar., *G. trivialis* Subb., and *G. varianta* Subb., which are important for the Lower Paleogene stratigraphy, are useful for the precise interregional correlation. They imply that *Globigerina pseudobulloides* assemblage of the central trans-Urals can be correlated with concurrent assemblages from a series of remote regions. These are the Danian assemblage of the El'burgan Horizon and Goryachii Klyuch Formation of the Caucasus (Subbotina, 1950), foraminifers of the middle Danian *Globoconusa daubjergensis-Subbotina triloculinoides* Zone distinguished in Dagestan (Samyshkina, 1983), Danian foraminiferal assemblage of Poland (Pozaryska, 1965), the middle Danian assemblage of *Globigerina edita* Zone known in southern Europe (Lamolda *et al.*, 1983), the lower Danian *Eoglobigerina danica* assemblage of Denmark (Bang, 1979), and the *Globoconusa daubjergensis* assemblage of the zone P1 in the standard zonation of planktonic oceanic foraminifers (Berggren, 1972).

The foraminiferal assemblage under consideration can be correctly correlated with that of the *Cibicidoides incognitus* Zone of West Siberia (Kisel'man, 1978) based on several species in common, such as *G. varianta, G. triloculinoides, R. paleocenica*, and *N. ovata.* Less obvious is its correlation with assemblages characterizing zones in the Paleogene foraminiferal zonation elaborated for West Siberia by Podobina (1998). In this case, we can found an analogy comparing the *Globigerina pseudobulloides* assemblage with foraminifers of the *Ammoscalaria friabilis* Zone, especially with their taxa known from the latter zone interval in Borehole 1 drilled in a meridional-stream area of the Vasyugan River (Podobina, 1998).

In its variety consisting predominantly of agglutinated benthic forms, the *Globigerina pseudobulloides* assemblage can be correctly correlated with the *Rzehakina fissistomata* assemblage of agglutinated foraminifers known from upper strata of the Solan Formation and from the Beloveza Formation of the external flysch zone of Carpathian Mountains (Magura group of nappes in Czech Republic; Bubik *et al.*, 1999). In lithology, the upper Solan strata resemble very much the Talitsa Horizon (the same fine to less frequent alternation of dark clay and clayey sand laminae) and simi-

larly yield an assemblage dominated by agglutinated benthic foraminifers. It is important simultaneously that the lower boundary of *Rzehakina fissistomata* Zone is dated quite precisely, being situated in the mentioned flysch sequence immediately above the nannoplankton zone CC26 (terminal upper Maastrichtian), *Abathomphalus mayaroensis* Zone of planktonic foraminifers (terminal upper Maastrichtian), and radiolarian *Amphipyndax tylotus* Zone of the upper Maastrichtian. In the external flysch zone of Carpathian Mountains, exactly this level is accepted for the Cretaceous–Paleogene boundary.

As is mentioned above, the *Globorotalia pseudobulloides* Zone corresponds to the *Globigerina taurica* Zone of the North Turgai area and to the lower Danian nannoplankton zones NP1 and NP2 (Beniamovskii *et al.*, 1989a; Amon, 1990). Its range may be also corresponding to that of the *Globoconusa daubjergensis* Zone established in the Bel'sher and Atanbas members of the southwestern Turgai depression (Beniamovskii *et al.*, 1993). According to Beniamovskii and his colleagues, the last unit corresponds to zone NP3 of the nannoplankton scale, and the Danian Stage stratotype spans in that scale the interval of NP1-NP3 zones. With due regard for all the data, we conclude that the *Globorotalia pseudobulloides* Zone of the central trans-Urals corresponds in range to the entire Danian Stage

The *Glomospira gordialiformis-Cyclammina koksuvorovae* assemblage characterizing in the study region the lower member of the Talitsa Formation is represented by boreal foraminiferal taxa of Siberia. It is identical in composition to the synonymous assemblage distinguished and described by Podobina in central and southern areas of West Siberia. In accord with the new zonal scale elaborated for Paleogene foraminifers of West Siberia, Podobina (1998) regarded this zone as spanning conjoint parts of the *Ammoscalaria friabilis* (Selandian) and *Glomospira gordialiformis-Cibicidoides favorabilis* (Thanetian) zones. Consequently, the distribution range of *Glomospira gordialiformis–Cyclammina koksuvorovae* Zone of the trans-Urals may correspond to the Selandian and Thanetian (partially) stages that is consistent with presence of *C. speciosum* dinocyst assemblage at the same level in Borehole 18-A.

Radiolarian skeletons have been encountered in the same Cretaceous and Paleocene beds, which bear foraminifers. Two radiolarian assemblages are characteristic of the Gan'kino Formation and the other one of the Talitsa Formation. The *Sethocyrtis tintinabulum* radiolarian assemblage coexisting with foraminifers of the *Gaudryina rugosa spinulosa* assemblage in basal Gan'kino beds is excluded from consideration in this work. The *Diacanthocapsa foveata-D. ancus* assemblage from overlying stratigraphic interval occurs in association with foraminifers of the *Spiroplectammina kasanzevi* assemblage. Rare radiolarian skeletons from this interval are in a satisfactory to poor preservation state. Taxa identified among them are *Cenosphaera* sp., *C. minor* Lipm., *Cromyodruppa* sp., *C.* cf. *concentrica* Lipm., *Orbiculiforma* sp., *O. maxima* Pess., *O. renillaeformis* (Camp. et dark), *O. australis* Pess., *Patellula verteroensis* Pess., *Porodiscus* sp., *P. vulgaris* Lipm., *P. delicatulus* Lipm., *Tholodiscus* cf. *fresnoensis* (Forem.), *Crucella* sp., *Theocapsomma* sp., *T. comys* Forem., *Diacanthocapsa* sp., *D. ancus* (Forem.), *D. foveata* Kozl., *Amphipyndax* sp., *A. tylotus* Forem., *Stichocapsa asymbatos* (Forem.), and *Dictyomitra multicostata* Zittel. This assemblage is characteristic of boreholes 12 and 18. It is of the late Maastrichtian age in the trans-Urals (Kozlova, 1977; Amon, 1997). Several species, such as *A. tylotus*, *T. comys*, *S. asymbatos*, and *O. renillaeformis*, imply that the assemblage range is correlative with the *Amphipyndax tylotus* Zone that is dated, based on concurrent assemblages of nannoplankton and planktonic foraminifers, back to the late Maastrichtian in the Magura area of the external flysch zone of Carpathian Mountains (Bubik *et al.*, 1999).

Radiolarians from the Talitsa Formation are scarce and so poorly preserved that identification of their genera or species is possible by occasion. Being confined to basal strata of the formation (Borehole 19, depth interval of 178.0–184.0 m; Borehole 18, depth interval of 158.0–171.0 m; Borehole 16, depth interval of 117.0–151.0 m; Borehole 12, depth interval of 200.0–209.0 m; Borehole 11, depth level 204.5), they are distributed within ranges of the *Globorotalia pseudobulloides* and *Glomospira gordialiformis-Cyclammina koksuvorovae* zones. The identified radiolarian taxa are *Cenosphaera* sp., C. cf. *irregularia* Boriss., *C.* cf. *micra* Boriss., *C.* cf. *pila* Boriss., *Carposphaera* sp., *Cenellipsis* cf. *variabilis* Boriss., *Cenodiscus* cf. *mirus* Boriss., *C.* cf. *magnus* Boriss., *C.* cf. *longus* Boriss., *Trochodiscus* cf. *aculeatus* Boriss., *Porodiscus* sp., *P. libum* (Boriss.), *Spongodiscus* sp., *S.* cf. *trims* Boriss., *Stylotrochus* sp., *Cromyodruppa* sp., *C. singularia* Boriss., and *Cromyocarpus ovatus* Grig. The assemblage corresponds to the *Cromyocarpus ovatus* Zone of the early Paleocene age that has been distinguished in the trans-Urals by Grigor'eva (1975) and corresponds to the Danian-Selandian interval of the West European scale.

The overlying strata of the Talitsa Formation are nearly barren of radiolarians. Their single specimens (e.g., from Borehole 18, depth interval of 150.0–154.0 m) are in a very bad preservation state: primary organogenic opal of skeletons is recrystallized into chalcedony or quartz.

MICROPHYTOPLANKTON (DINOCYSTS)

Dinocysts are known from carbonate-free rock varieties of the Gan'kino Formation and from all borehole sections of the northern area, in which deposits of the Talitsa Formation have been sampled to analyze microphytoplankton. In addition, these microfossils characterize the Talitsa Formation rocks from the Pershinskoe

Quarry and from Borehole IG-32 drilled in the southern area.

Near the top of the Gan'kino Formation penetrated by Borehole LD-1, there is distinguished the *Thalassiphora pelagica-Spiniferites cornutus cornutus* assemblage of dinocysts that includes the Late Cretaceous species *Disphaerogena carposphaeropsis* O. Wetz., *Senoniasphaera protrusa* Clarke et Verd., *Scriniodinium campanulum* Gocht, *Spongodinium delitiense* Morg., and *Palaeotetradinium silicorum* Defl. Some other species, which appeared in the late Maastrichtian, become widespread at the higher stratigraphic level. These are *Thalassiphora pelagica* Eis., *Spiniferites cornutus cornutus* Gerl., *Senoniasphaera inornata (Drugg)* Stover et Evitt, and *Muratodinum fimbriatum* Drugg. As it has been shown in the type sections, all the species listed above are of a high importance for stratigraphy of the upper Maastrichtian and for recognition of the Cretaceous–Paleogene boundary (Hansen, 1977, Wilson, 1987; Firth, 1987).

The Talitsa Horizon is sampled for the dinocyst analysis in boreholes LD-1, 18-A, Elan-8, 91, and 11. More than 50 taxa representing the *Senoniasphaera inornata* assemblage have been identified in the lower Talitsa Subformation and Shadrinsk Beds. Among them, stratigraphically important taxa are *Carpatella cornuta* Grig., *Cribroperidinium wetzelii* (Lejeune-Carp.) Sarj., *Danea californica* Cooks, et Eis., *Fibradinium annetorpense* Morg., *Fibrocysta ovalis* (Hansen) Lent. et Will., *Spiniferites septatus* Cooks, et Eis., *Scuticulabolus lapidaris* (O. Wetz.) Loebl., *Palaeocystodinium benjamini* Drugg., *P. lidiae* (Gorka) Dav., *P. bulliformum* loann., *P. golzowenze* Alb., *Palaeoperdinium pyrophorum* (Ehr.) Sarj., *Phelodinium magnificum* (Stenley) Stov. et Evitt, *Senoniasphaera inornata* (Drugg) Stover et Evitt, *Spiniferites cornutus* (Gerl.) Sarj., *Spinidinium clavus* Harl., *Thalassiphora pelagica* (Eis.) Eis. et Gocht, *Th. delicata* Will. et Down., *Trithyrodinium evittii* Drugg, and *Xenocodinium* spp.

In the *Senoniasphaera inornata* assemblage, late Maastrichtian dinocysts coexist with characteristic Danian *C. cornuta, D. californica, F. ovalis*, and *Xenicodinium* species, which have been widely used in practice of interregional correlation (Hansen, 1977; Firth, 1987). Consequently, the *Senoniasphaera inornata* assemblage of the trans-Urals is undoubtedly of the Danian age, and species *Carpatella cornuta* present among others points to its appearance at the very beginning of the Danian Stage. According to summarizing work by Powell (1992), stratigraphic range of *C. cornuta* is restricted by the interval of nannoplankton zones NP1 and NP2 (a part). In the central segment of the trans-Urals, lower beds of the Talitsa Formation and Shadrinsk Beds yield species *Carpatella cornuta* implying that there is no significant hiatus at the Paleocene base in the region. Beyond this segment, we recognized the *Senoniasphaera inornata* assemblage in the northern and southern trans-Urals and in northern sections of the Turgai depression. Spores and pollen occur as single grains in the considered stratigraphic interval.

Higher in the sequence, in rocks of the upper Talitsa Subformation, there is established the *Alterbidinium circulum–Cerodinium speciosum* assemblage of dinocysts. Its characteristic taxa are *Alterbidinium circulum* (Heilm.-Claus.) Lent. et Will., *A. minus* (Alb.) Lent. et Will., *Cerodinium speciosum* (Alb.) Lent. et Will., *C. markovae* (Vozzh.) *Lent. et Will.*, (Alb.), *C. depressum* (Morg.) Lent. et Will., *C. striatum* (Drugg) Lent. et Will., *Deflandrea denticulata* Lent. et Will., *Fromea laevigata* Drugg, *Fibradinium annetorpense* Morg., *Isabelidinium acuminatum* (Cooks, et *Eis.*) Stov. et Evitt, *Palaeocystodinium australinum* (Cooks.) Lent. et Will., *P. lidiae* (Gorka) Dav., *P. golzowense* Alb., *Palaeocystodinium* sp. A, *Palaeoperidinium pyrophorum* (Ehr.) Sarj., *Palaeotetradinium minusculum* (Alb.) Stover et Evitt, *Phelodinium magnificum* Stanley, *Senegalinium ? dilwynense* (Cooks et Eis.) Stov. et Evitt, and *Spinidinium densispinatum* Stanley.

Assemblages of similar taxonomic composition are widespread in the trans-Urals, being confined to analogues of the Talitsa Formation (Vasil'eva, 1990). Dinocysts assemblages with *Cerodinium speciosum* are known not only from West Siberia and Turgai, but also from the Paleocene Verkhnii Stryi Formation of the Skiby zone in Ukraine, from the Inkerman Formation of Crimea, and from the Goryachii Klyuch Formation of northern Caucasus (Andreeva-Grigorovich, 1991; Kul'kova and Shatskii, 1990). The *Cerodinium speciosum* assemblage of a similar composition has been distinguished as well at the base of the Selandian type section (zones 1 and 2) in the central Jutland area of Denmark, where it is attributed to the Selandian and even Thanetian (Heilmann-Clausen, 1985, Powell, 1988). Despite the fact that many aforementioned species are abundant in Selandian deposits, the idea to restrict the assemblage range by Selandian and, especially, by Thanetian stages seems doubtful. The careful analysis of distribution ranges of separate dinocyst taxa leads to an alternative age interpretation.

The alternative solution can be based on the following important arguments. First, the characteristic species *Alterbidinium circulum* is known exclusively from the topmost limestone beds of the Danian Stage stratotype (Heilmann-Clausen, 1985), whereas Selandian deposits are practically lacking this and some other species (*S. densispinatum, S. clavus, S. dilwynense,* and *I. acuminatum*). Second, species *C. speciosum* found at the base of the "Kerteminde Marl" in the Selandian interval proper do not occur in association with *C. speciosum* and *A. circulum* (Heilmann-Clausen, 1985). In the trans-Urals, two last species appear in the Talitsa Formation sequence simultaneously and continue to occur in stable association higher in the sequence. It is most likely that *C. speciosum* appears below the Selan-

Table 1. Distribution ranges of dinocyst assemblages in the Pershinskoe Quarry (southern area) and borehole sections (northern area; intervals of stratigraphic hiatus are shadowed)

System	Series	Subseries	Stage	This work (zones and pertinent assemblages)		Borehole LD-1	Borehole 18-A	Borehole Elan-8	Borehole 91	Pershinskoe Quarry	Formations of the trans-Urals
Paleogene	Paleocene	upper	Thanetian	*A. homomorphum*		*A. homomorphum*	no zones	no data	no data	*A. homomorphum*	Serov
				C. speciosum	*A. margarita*	no zones			*C. speciosum*	*A. margarita*	Talitsa
			Selandian		*I. viborgense*					unexposed	
					A. circulum	*A. circulum*		*A. circulum*			
		lower	Danian	*S. inornata*		*S. inornata*	*S. inornata*	*S. inornata*	no data		
					C. cornuta	*C. cornuta*			*S. inornata/C. cornuta*		
Cretaceous	Upper		Maastrichtian	*Th. pelagica – S. cornutus cornutus*		*Th pelagica – S. cornutus cornutus*		no zones	no data		Gan'kino

dian base, within the interval corresponding to a hiatus in the stratotypes. An additional argument in favor of this conclusion is the dinocyst zonation elaborated by Andreeva-Grigorovich (1985) for the Crimea–Caucasus region, in which the base of *C. speciosum* Zone coincides with the base of nannoplankton zone NP4 bearing the *Ellipsolithus macellus* assemblage, thus being situated below the Selandian base.

Everywhere in the trans-Urals, macerates from samples of the Talitsa Formation rocks, which bear the *Alterbidinium circulum–Cerodinium speciosum* assemblage described above, reveal presence of spores and pollen sometimes prevailing in abundance over other palynomorphs. The *Trudopollis menneri–Anacolosidites insignis–Inaperturopollenites–Stereisporites* palynological assemblage identified practically in all sampling sites of the upper Talitsa Subformation in the study area has stratigraphic range concurrent to that of the dinocyst assemblage under consideration. Summary data on palynomorphs distinguished in borehole sections recovered in various segments of the trans-Urals reveal a peculiar feature in stratigraphic distribution of dinocysts and palynological remains: the former dominate over the latter in the lower Talitsa Subformation, whereas spores and pollen of terrestrial plants are more abundant that dinocysts in the upper subformation. This peculiarity does not contradict data on distribution of foraminifers and radiolarians. It may be regarded as indication of a short-term regression that affected the trans-Uralian sea basin in the terminal early Paleocene.

An upper interval of stratigraphic range of the *Cerodinium speciosum* assemblage, characteristic of which is species *Isabelidinium? viborgense* Heilm.-Claus., should be correlated most likely with the Selandian Stage proper. In the trans-Uralian sections, the *Isabelidinium viborgense–Cerodinium speciosum* assemblage is established in uppermost beds of the Talitsa Formation (Borehole IG-32 and others drilled southward of the study region). It is important that this assemblage of an inherited character is lacking such forms as *Alterbidinium circulum* and *Alisocysta margarita,* the last of which is zonal index species of the Thanetian Stage in the stratotype of the latter.

The *Alisocysta margarita* assemblage of dinocysts has been distinguished recently within the 2-m-thick interval composed of alternating dark clay and gravel beds of the Talitsa Formation and of lower opokas of the Serov Formation, which are exposed in the Pershinskoe Quarry, Dalmatovo district of the Kurgan oblast (Akhmet'ev *et al.*, 2001). In addition to index species *Alisocysta margarita,* the assemblage includes *Lentinia wetzelii* (Morg.) Bujak, *Deflandrea dissoluta* Vozzh., *Deflandrea denticulata* Alb., *Cerodinium leptodermum* (Vozzh.) Lent. et Will., *C. medcalfii* (Stov.) Lent. et Will., *C. speciosum* (Alb.) Lent. et Will., *Senegalinium obscurum* (Drugg) Stov. et Evitt, and some other forms of a lesser stratigraphic significance. The same assemblage is characteristic of sandy deposits of the Sokolovsky Member in the northern Turgai depression (Vasil'eva, 1994). In the Sokolovsky and Belinsky

Table 2. Correlation chart for microfossil assemblages from the central trans-Urals and coeval analogues (abbreviation GSS means General Stratigraphic Scale)

Cretaceous	Paleogene									System
Upper	Paleocene									Series
	Lower			Upper						Subseries
Maastrichtian upper	Danian			Selandian		Thanetian				Stage
	P1		P2	P3		P4			P5	Planktonic foraminifers, GSS zones
	NP1	NP2	NP3	NP4	NP5	NP6	NP7	NP8	NP9	Nannoplankton, GSS zones
	D1		D2	D3		D4			D5a	Dinocysts, standard zonation C-3 in Europe
P. grallator	*Danea mutabilis*			no zones						Dinocysts, zones and subzones after Hansen, 1977
Th. pelagica	*Ch. inornatum*		*H. cryptovesiculata*							
	D. californica			*C. speciosum*				*A. homomorphum*		Dinocyst zones after Andreeva-Grigorovich, 1991
	C. cornuta		*C. striatum*							
Th. pelagica–S. cornutus cornutus	*S. inornata*			*C. speciosum*					*A. homomorphum*	Dinocyst zones (assemblages), this work
	C. cornuta			*A. circulum*		*I. viborgrnse*		*A. margarita*		
Spiroplectammina kasanzevi–Bulimina rosenkrantzi	*Ammoscalaria friabilis*							*Glomospira gordialiformis–Cibicidoides favoribilis*		Foraminiferal zonal scale for West Siberia after Podobina 1989, 1998, modified
Spiroplectammina kasanzevi	*Globorotalia pseudobulloides*			*Glomospira gordialiformis–Cyclammina koksuvorovae*					no zones	Foraminiferal zones, this work
Gan'kino	Talitsa								Serov	Formations, members, and beds of the trans-Urals
Upper member	Shadrinsk Beds		Lower	Upper						

quarries, this member bears different groups of microfossils and is reliably dated back to the early Thanetian based on the *Heliolithus riedeli* assemblage of nannoplankton characteristic of zone NP8 (Beniamovskii *et al.*, 1989b). Accordingly, the trans-Uralian *Alisocysta margarita* assemblage of dinocysts characterizing sandy deposits near the top of the Talitsa Formation and close to the base of the Serov Formation is of the early Thanetian age. It is also remarkable that stratigraphic range of *Alisocysta margarita* corresponds to an upper portion of distribution interval of *Cerodinium speciosum*.

Thus, the analyzed composition of microphytoplankton assemblages distinguished in the Talitsa Formation of the trans-Urals leads to some necessary comments. First, the *Cerodinium speciosum* Zone included in many stratigraphic schemes is a composite undivided unit. Second, the *Alterbidinium circulum–Cerodinium speciosum* assemblage characteristic of its basal interval should be dated based on the first index taxon that appears at the top of the Danian Stage in the stratotype area. It is likely that the *A. circulum–C. speciosum* assemblage is of the Montian age. Third, the *Isabelidinium? viborgense* assemblage of Selandian age proper is distinguishable in the upper Talitsa Subformation of the trans-Urals. And finally, topmost beds of this subformation and overlying basal strata of the Serov Formation bear the early Thanetian *Alisocysta margarita* assemblage. It is important that all three assemblages span together the stratigraphic range of such zonal index species as *Cerodinium speciosum*. The *Alterbidinium circulum* assemblage is most persistently occurring in borehole sections (Tables 1 and 2). Distribution areas of others should be verified based on additional materials.

The overlying opoka beds of the Serov Formation recovered by boreholes in the central trans-Urals are frequently barren of dinocysts. The *Apectodinium homomorphum–Cerodinium speciosum glabrum* assemblage is known in the north from Borehole LD-1 and in the south from the Pershinskoe Quarry and Borehole IG-32 drilled at the Petropavlovskoe site of the Kurgan oblast. This assemblage is widespread however in the southern trans-Urals and northern Turgai, being characteristic of the clay-opoka member overlying the Sokolovka sandstone sequence (Beniamovskii *et al.*, 1989b; Vasil'eva, 1994). Leaving aside the problem of detailed correlation, we should mention that it is undoubtedly of the late Thanetian age. Correlation between the analyzed sections that is based on dinocyst and other biostratigraphic zones is shown in Tables 1 and 2.

CONCLUSION

Data considered above show that stratigraphy of the Upper Cretaceous to Paleocene deposits in the central trans-Urals is more complex than that commonly accepted in generalizing works. The correlation profiles plotted for a series of boreholes drilled along the eastern flank of the Urals, 30 to 120 km away from mountain chains, elucidates geological structure of the Cretaceous–Paleogene sequence, distribution patterns of studied microfossils, and succession of their guide taxa and biostratigraphic zones. Hypsometric data on the Talitsa Formation base and lithological characteristics of sediments constituting the Gan'kino Formation imply that near the town of Irbit (a bit away to the southwest) there is an arching of Paleozoic basement, a domelike structure extending in meridional direction that is crossed by the profile. Most likely, this is a southeastern flank of the Serov-Ivdel tectonic ledge that dissected waves of the Paleogene (maybe Cretaceous as well) transgression, which advanced from the northeast (Fig. 4).

In the central trans-Urals, the Maastrichtian and Paleocene stages can be incompletely represented in places. The complete ranges of the Gan'kino and Talitsa Formation are established in the southern trans-Urals and eastward, in West Siberia. In western sections (e.g., in those of the Shadrinsk field), the Gan'kino Formation is locally lacking the upper Maastrichtian strata. In boreholes drilled near the town of Irbit, the upper Talitsa Subformation is lacking its strata bearing the *Glomospira gordialiformis–Cyclammina koksuvorovae* assemblage of foraminifers. In contrast, deposits of the lower Talitsa Subformation are widespread everywhere. The Paleocene transgression was more active and intense than the Cretaceous one, as it is evident from presence of basal gravely-pebble horizon and general lithology of the lower Talitsa Subformation, sediments of which are more widespread in the study region than those of the Gan'kino Formation. That transgression was interconnected with the global eustatic sea-level rise in the Paleocene. Judging from certain facies of the Talitsa Formation and from compositions of microfauna and phytoplankton, the transgression weakened by the end of the early Paleocene and even gave way to a regression. The Selandian and early Thanetian transgressive waves have not been recorded everywhere, whereas transgression of the late Thanetian (Serov) time was most intense.

The early Paleocene transgression that commenced in the Danian time was very active during its initial phase: quick flooding eroded Paleozoic rocks in cliffs of the proximal coast and Maastrichtian sediments of the Gan'kino Formation, which floored the shallow zone of paleobasin. The reworked Gan'kino sediments are partially removed from the study region, and some material "diluted" by terrigenous influx from the west and southwest was redeposited *in situ* to form a thin Shadrinsk Beds of bluish carbonate-free clay beds (recall that these and basal clay beds of the Talitsa Formation bear corroded Maastrichtian foraminifers). As the reworking phase was short-term, the Shadrinsk Beds are of a very limited distribution. The erosion of upper Gan'kino strata seems to be a rather characteristic event in marginal areas of the West Siberian basin. A

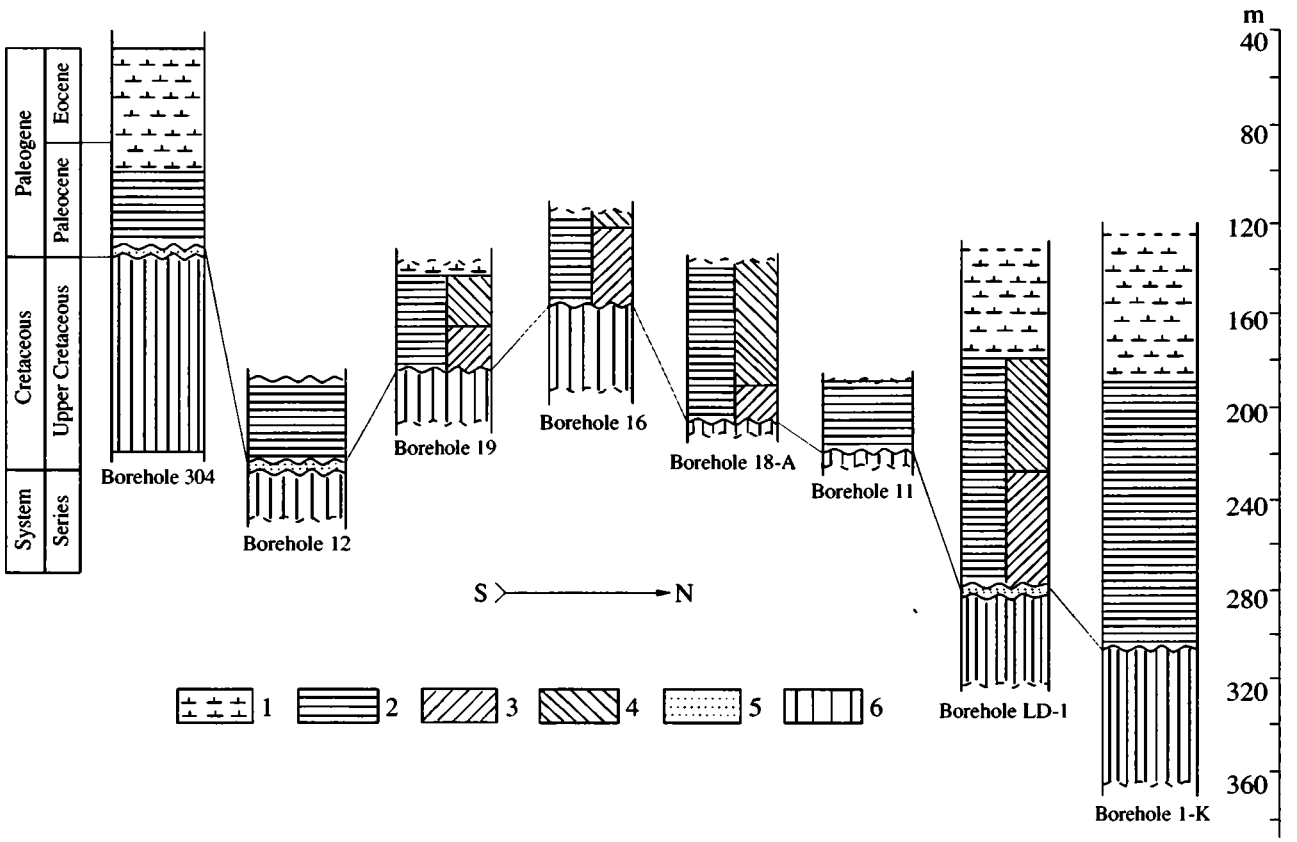

Fig. 4. Schematic correlation profile for the meridional (S-N) series of borehole sections (correlation line denotes the Talitsa Formation base; except for Borehole 304, all other are situated in the northern area): (1) Serov Formation; (2) Talitsa Formation with lower (3) and upper(4) subformations; (5) Shadrinsk Beds; (6) Gan'kino Formation.

similar though more intense erosion that locally eliminated about a half of the Maastrichtian sequence is also recorded in southeastern West Siberia (Podobina, 1998). The described geological situation fit well a global model of the Danian Stage and Cretaceous–Paleogene boundary, which was elaborated by Naidin (Naidin, 1985; Naidin and Beniamovskii, 1988) and confirmed by Akhmet'ev *et al.*, (2001).

Foraminifers and dinocysts are of prime significance for detailed stratigraphy of the Talitsa Horizon. Across the boundary between Gan'kino and Talitsa formations, especially when Shadrinsk Beds and Danian planktonic foraminifers are missing from this level, changes in compositions of foraminiferal assemblages are so impressive that one may assume a mass extinction of foraminiferal biota at the end of the Maastrichtian.

Foraminiferal assemblages characterizing Maastrichtian and Paleocene deposits of the study region are representative, diverse in taxonomic composition, and persistently occurring. The corresponding, easily recognizable foraminiferal zones are lacking diachronous or "overlapping" boundaries. They represent reliable stratigraphic markers, and many of them or their equivalents are known in many areas of and outside West Siberia. Radiolarian assemblages are of auxiliary significance. The *Cromyocarpus ovatus* radiolarian assemblage from the Talitsa Formation consists entirely of the Peri-Tethyan forms characteristic of the Russian platform. Being widespread in the region, it is usually represented by poorly preserved forms. Its stratigraphic range is not very clear: the lower boundary of *Cromyocarpus ovatus* Zone is obviously corresponding to the Danian Stage base, but its upper boundary may be either inside or at the top of the Selandian Stage.

Four microphytoplankton assemblages of a distinct stratigraphic importance are established in the Talitsa Horizon of the trans-Urals. The lower *Senoniasphaera inornata* assemblage includes species *Carpatella cornuta*, the index taxon of the Danian Stage base. Higher in the sequence, within the traditional *Cerodinium speciosum* Zone, we discriminated from each other the *Alterbidinium circulum* assemblage corresponding to the Montian level, the *Isabelidinium ?viborgense* assemblage of Selandian Stage, and the *Alisocysta margarita* assemblage of the early Thanetian age. The last one is characteristic of the uppermost Talitsa and basal Serov beds. The overlying strata of the Serov Formation bear the late Thanetian *Apectodinium homomorphum–Cerodinium speciosum glabrum* assemblage, the

range of which corresponds to the standard *Apectodinium hyperacanthum* Zone (Table 2).

Teeth of Selachii (sharks and skates) are infrequent in borehole sections, but this does not mean that these fishes were scarce in the near-shore zone of the West Siberian sea of the Paleocene time. There is an excellent example of abundant Selachii remains from the Pershinskoe Quarry. The "Selachii biozones" represent so far an exotic term for the Paleocene stratigraphy, but available data on distribution of corresponding paleontological remains in Paleogene sequences of Eurasia suggest that biostratigraphic subdivisions of this kind can be successfully used for interregional and subglobal correlations.

Reviewers G.N. Aleksandrova and M.A. Akhmet'ev

REFERENCES

Akhmet'ev, M.A., Aleksandrova, G.N., Amon, E.O., *et al.*, Biostratigraphy of the Marine Paleogene in the West Siberian Plate, *Stratigr. Geol. Korrelyatsiya*, 2001, vol. 9, no. 2, pp. 30–57.

Amon, E.O., On the Cretaceous–Paleogene Boundary in the Central and Southern Trans-Urals: data on Stratigraphic Ranges of Microfauna Assemblages, *Problemy stratigrafii Urala. Mezozoi i kainozoi* (Problems of Stratigraphy in the Urals: Mesozoic and Cenozoic), Sverdlovsk: Ural. Otd. Akad. Nauk SSSR, 1990, pp. 25–39.

Amon, E.O., Stratigraphic Scheme for Cretaceous Deposits of the Urals, *Ob"yasnitel'naya zapiska k stratigraficheskim skhemam Urala (mezozoi, kainozoi)* (Explanatory Notes to Stratigraphic Schemes of the Urals: Mesozoic and Cenozoic), Yekaterinburg: Ross. Akad. Nauk, 1997, pp. 27–60.

Andreeva-Grigorovich, A.S., Phytoplankton-Based Paleogene Zonation in the Southern USSR, *Doctoral (Geol.–Min.) Dissertation*, Kiev: Inst. of Geosciences, 1991, p. 47.

Bang, I., Foraminifera in the Lowermost Danian of Denmark, *Cretaceous-Tertiary Boundary Events*, Copenhagen, 1979, pp. 108–115.

Beniamovskii, V.N., Levina, A.P., Naidin, D.P., *et al.*, New Data on Paleogene Marine Deposits in the Turgai Depression, *Geol. Geofiz.*, 1989, no. 9, pp. 47–56.

Beniamovskii, V.N., Levina, A.P., Pronin, V.G., *et al.*, Paleocene Deposits in the Turgai Depression, *Izv. Vyssh. Uchebn. Zaved., Geol. Razved.*, 1989, no. 10, pp. 3–14.

Beniamovskii, V.N., Vasil'eva, O.N., Levina, A.P., and Pronin, V.G., Paleogene of the Southern Trans-Urals, Pt. 1: Paleogene of the Southern Turgai Depression, *Izv. Vyssh. Uchebn. Zaved., Geol. Razved.*, 1993, no. 6, pp. 22–56.

Berggren, W.A., Cenozoic Time Scale—Some Implications for Regional Geology and Paleobiogeography, *Lethaea*, 1972, vol. 5, no. 2, pp. 195–215.

Bubik, M., Bak, M., and Svabenicka, L., Biostratigraphy of the Maastrichtian to Paleocene Distal Flysch Sediments of the Raca Unit in the Uzgrun Section (Magura Group of Nappes, Czech Republic), *Geol. Carpathica*, 1999, vol. 50, no. 1, pp. 33–48.

Firth, J.V., Dinoflagellate Biostratigraphy of the Maastrichtian to Danian Interval in the US Geological Survey Albany Core, Georgia, USA, *Palynology*, 1987, no. 11, pp. 199–216.

Grigor'eva, A.I., Radiolarians from the Upper Cretaceous and Paleogene of the Eastern Urals and Trans-Uralian region verkhnego mela i paleogena vostochnogo sklona Urala i Zaural'ya, *Tr. Inst. Geol. Geokhim. UNTs AN SSSR* (Yekaterinburg), 1975, vol. 119, pp. 102–110.

Hansen, J.M., Dinoflagellate Stratigraphy and Echinoid Distribution in Upper Maastrichtian and Danian Deposits From Denmark, *Bull. Geol. Soc. Denmark*, 1977, vol. 26, pp. 1–26.

Heilmann-Clausen, C., *Dinoflagellate Stratigraphy of the Uppermost Danian to Ypresian in the Viborg 1 Borehole, Central Jutland, Denmark*, Copenhagen: Geol. Surv. Denmark, 1985.

Il'ina, V.I., Kul'kova, I.A., and Lebedeva, N.K., *Mikrofitofossilii i detal'naya stratigrafiya morskogo mezozoya i kainozoya Sibiri* (Microfossils and Detailed Stratigraphy of Marine Mesozoic and Cenozoic in Siberia), Novosibirsk: Nauka, 1991.

Kisel'man, E.N., Foraminiferal Assemblages from Paleogene Deposits of West Siberia, *Paleogen i neogen Sibiri (paleontologiya i stratigrafiya)* (Paleogene and Neogene of Siberia: Paleontology and Stratigraphy), Novosibirsk: Nauka, 1978, pp. 41–50.

Kisel'man, E.N., Upper Cretaceous Foraminiferal Assemblages of the *Spiroplectammina kasanzevi* Zone in Eastern Areas of the West Siberian Plain, *Tr. Sovm. Nauchno-Issled. Inst. Geol. Geofiz. Mineral. Syr'ya*, 1974, no. 192, pp. 122–127.

Kozlova, G.E., Peculiarities of Zonal Radiolarian Assemblages from Maastrichtian Deposits, *Tez. dokl. VIII Vsesoyuzn. mikropaleontol. soveshch.* (Abstracts, 8th All-Union Micropaleontol. Conference), Moscow: Geol. Inst. Akad. Nauk SSSR, 1977, pp. 84–85.

Kul'kova, I.A. and Shatskii, S.B., Dinocyst Zonal Subdivisions in Marine Paleogene of the West Siberian Plain, *Geol. Geofiz.*, 1990, no. 1, pp. 25–31.

Lamolda, M.A., Crue-Etxelarria, X., and Proto-Decima, F., The Cretaceous-Tertiary Boundary in Sopelana (Biscay, Basque Country), *Zitteliniana*, 1983, vol. 10, pp. 663–670.

Naidin, D.P., The Cretaceous–Paleogene Boundary: Stratigraphic Aspects, *Byull. Mosk. O–va Ispyt. Prir., Otd. Geol.*, 1985, vol. 60, no. 5, pp. 71–85.

Naidin, D.P. and Beniamovskii, V.N., About the Upper Limitation of the Danian Stage, Pt. 1: Stratotypes of Paleocene Stages, *Izv. Vyssh. Uchebn. Zaved., Geol. Razved.*, 1988, no. 10, pp. 3–15.

Naidin, D.P., Beniamovskii, V.N., and Kopaevich, L.F., A Scheme of Upper Cretaceous Biostratigraphic Subdivisions in the European Paleobiogeographic Province, *Vestn. Mosk. Univ., Ser. Geol.*, 1984, no. 5, pp. 3–15.

Papulov, G.N. and Sitnikova, Z.I., *Mezozoiskie i paleogenovye otlozheniya raiona Turinskoi opornoi skvazhiny v Srednem Zaural'e* (Mesozoic and Paleogene Deposits in the Area of Tura Reference Borehole, Central Trans-Urals), Sverdlovsk: Akad. Nauk SSSR, 1964.

Papulov, G.N. and Umova, L.A., Cretaceous and Paleogene Deposits on the Iset River Right Bank, Shadrinsk Area, *Sbornik po voprosam stratigrafii no. 3* (Collection of Works on Stratigraphic Problems no. 3), Moscow: USSR Academy of Sciences, 1956, pp. 178–186.

Podobina, V.M., *Foraminifery i zonal'naya stratigrafiya verkhnego mela Zapadnoi Sibiri* (Foraminifers and Upper Cretaceous Zonation in West Siberia), Tomsk: Tomsk. Gos. Univ., 1989.

Podobina, V.M., *Foraminifery i biostratigrafiya paleogena Zapadnoi Sibiri* (Foraminifers and Paleogene Biostratigraphy in West Siberia), Tomsk: Nauch.-Tekhn. Lit., 1998.

Powell, A.J., A Modified Dinoflagellate Cyst Biozonation for Latest Palaeocene and Earliest Eocene Sediments from the Central North Sea, *Rev. Palaeobot. Palynol.*, 1988, vol. 56, no. 3/4, pp. 327–344.

Powell, A.J., Dinoflagellate Cysts of the Tertiary, *A Stratigraphic Index of Dinoflagellate Cysts*, Powell, A.J., Ed., London: British Micropaleontol. Soc., 1992, pp. 155–251.

Pozaryska, K., Foraminifera and Biostratigraphy of the Danian and Montian in Poland, *Paleontol. Polonica*, 1965, no. 14, pp. 1–156.

Samyshkina, K.G., *Foraminifery i stratigrafiya melovykh otlozhenii Vostochnogo Kavkaza* (Foraminifers and Stratigraphy of Cretaceous Deposits in the Eastern Caucasus), Moscow: Nauka, 1983.

Subbotina, N.N., Microfauna and Stratigraphy of the El'burgan and Goryachii Klyuch Horizons, *Tr. Vses. Nauchno-Issled. Geol.-Razved. Inst.*, 1950, no. 51, pp. 5–112.

Vasil'eva, O.N., *Palinologiya i stratigrafiya morskikh otlozhenii paleogena Yuzhnogo Zaural'ya* (Palynology and Stratigraphy of Paleogene Deposits in the Southern Trans-Urals), Sverdlovsk: Ural. Otd. Ross. Akad. Nauk, 1990.

Vasil'eva, O.N., Late Paleocene Dinocysts from the Sokolovo Sequence of the Turgai Depression, *Palinologicheskie kriterii v biostratigrafii Zapadnoi Sibiri* (Palynological Criteria in Biostratigraphy of West Siberia), Tyumen: ZapSibNIGNI, 1994, pp. 109–113.

Vasil'eva, O.N., Amon, E.O., and Zhelezko, V.I., Dinocysts, Stratigraphy and Stratigraphy of the Talitsa Formation (Paleocene), Central Trans-Urals, *Ezhegodnik-2000 Inst. Geol. Geokhim.* (Ezheg.-2000 Inst. Geol. Geochim.), Yekaterinburg: Ural. Otd. Ross. Akad. Nauk, 2001, pp. 3–10.

Wilson, G.J., Dinoflagellate Biostratigraphy of the Cretaceous-Tertiary Boundary, Mid-Waipara River Section, North Canterbury, New Zealand, *N.Z. Geol. Surv. Rec.*, 1987, no. 20, pp. 8–15.

Stratigraphy and Geological Correlation, Vol. 11, No. 3, 2003, pp. 293–304. Translated from Stratigrafiya. Geologicheskaya Korrelyatsiya, Vol. 11, No. 3, 2003, pp. 91–103.
Original Russian Text Copyright © 2003 by Bubenshchikova.
English Translation Copyright © 2003 by MAIK "Nauka/Interperiodica" (Russia).

Pliocene–Lower Quaternary Planktonic Foraminiferal Biostratigraphy and Paleoceanology, ODP Hole 677A

N. V. Bubenshchikova

Shirshov Institute of Oceanology, Russian Academy of Sciences, Moscow

Received July 19, 2000; in final form, November 23, 2000

Abstract—Planktonic foraminifers from the Pliocene and Lower Quaternary sediments of ODP Hole 677A are thoroughly studied. Many encountered zonal taxa are demonstrated to be the reliable biostratigraphic markers. Planktonic foraminiferal zones PL1b to Pt1 of the Berggren's scale (Berggren *et al.*, 1995) are distinguished in the depth interval of 30–210 m in the hole. Changes in planktonic foraminiferal assemblages from the sediments of Site 677A were under influence of the climate-controlled dynamics of surface water masses in the eastern equatorial Pacific during the period from 4.6 to 0.65 Ma. A sharp decrease in abundance of equatorial-tropical species about 3.4 Ma is correlated with termination of the surface water exchange between the Pacific and Atlantic tropical zones owing to the emergence of the Central American land bridge. Surface water temperatures were reconstructed using the method of Barash (1970). The highest temperatures are estimated for the terminal early Pliocene (26.4°C) and the late Pliocene (26.6°C), and the lowest ones for the initial early Pliocene (18.4°C) and the mid-late Pliocene (19.6°C). Cold events are recorded in sediments 4.6–4.3, 2.8–2.5, and 1.7–1.2 Ma old, while periods of 4.3, 4.18–3.4, 2.5–2.3, and 1.0 Ma correspond to the warm ones. In general, the mid-early Pliocene, mid-late Pliocene, and the initial Pleistocene characterize the cold-water conditions, whereas the terminal early and late Pliocene correspond to warm-water environments.

Key words: planktonic foraminifers, Pliocene–Quaternary sediments, biostratigraphic range, datums, paleoclimatic events, paleotemperatures.

INTRODUCTION

The Late Neogene evolution of the eastern equatorial Pacific was repeatedly investigated by experts in paleoceanology (Saito, 1976; Keigwin, 1982a, b; Prell, 1985; Farrell and Prell, 1991; Ushakova *et al.*, 1995). The climatic impact of the Central American land bridge formation on change of the surface- and deep-water circulation in the region and the World Ocean was demonstrated (Keigwin, 1982b; Haug and Tiedemann, 1998). Variations of the hydrologic regime in the Panama Basin are discussed in this paper using the detailed zonal stratigraphy of planktonic foraminifers from the Pliocene–lower Pleistocene sediments of Site 677A and data of quantitative paleotemperature analysis.

The present-day surface water circulation in the Panama Basin is largely controlled (Fig. 1) by the Peru Current, a branch of the South Equatorial Current, or by the Equatorial Countercurrent (*Tikhii okean*, 1981). The southward California Current and the northward Peru Current transport cold waters to the region. Near the equator, their water mass rises to the surface thus forming the upwelling zone off the American coast. This zone coincides with the Equatorial Divergence Zone. The average annual temperature in the region is 24°C (*Tikhii okean*, 1981), but the seasonal changes of circulation result in temperature fluctuations from 17° to 27°C within the 50-m-thick surface water layer (Levitus, 1982). The dynamic oceanographic regime characteristic of the eastern equatorial Pacific as a whole gives rise to emergence of a latitudinal belt between 4° S to 2° N that is of a high biological productivity and hosts a planktonic foraminiferal assemblage peculiar for the equatorial region: tropical species coexist here with cold-water forms (Thunnel and Reynolds, 1984; Chen and Prell, 1998).

In the Panama Basin, the flourishing of *Neogloboquadrina (N.) dutertrei* and abundance peaks of *N. pachyderma* dex. and *Globorotalia (Gr.) menardii* are registered in February and March during the most intense upwelling associated with a shallow depth of the thermocline and low surface water temperatures (Table 1). Another foraminiferal group of *Globigerinita (Gt.) glutinata, Globigerinoides (Gs.) ruber*, and *Globigerina (G.) bulloides* is maximum abundant in summer, when the thermocline position is deeper and surface water temperatures are high (Thunnel and Reynolds, 1984). Species characteristic of the present-day Panama Basin (see Table 1) prevail in the Pliocene–Quaternary planktonic foraminiferal assemblages and may serve as indicators of hydrologic conditions comparable with the recent ones.

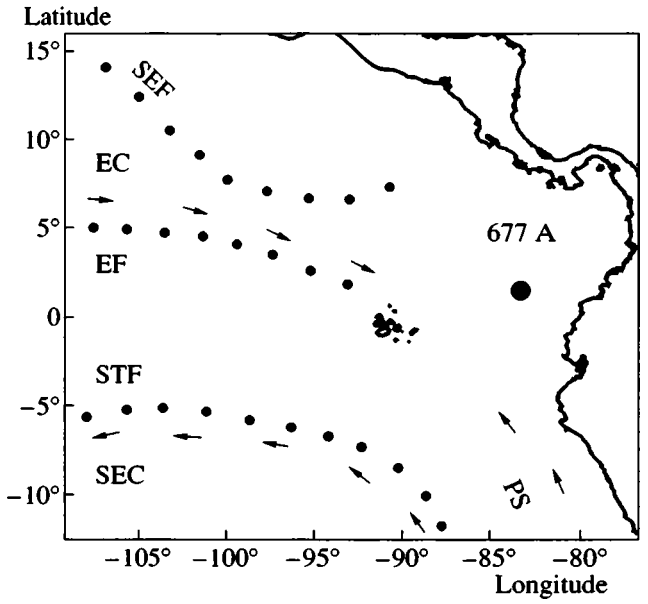

Fig. 1. Map of surface-water circulation in the eastern equatorial Pacific (*Tikhii okean*, 1981) and location of Hole 677A: (SEC) South Equatorial Currents; (EC) Equatorial Countercurrent; (PC) Peru Current; (STF) South Tropical Front; (EF) Equatorial Front; (SEF) Subequatorial Front; arrows mark the current direction and points the position of fronts.

MATERIALS AND METHODS

Site 677A (1°12.14′ N, 83°44.22′ W) of the ODP Leg 111 was drilled on the southern flank of the Costa Rica Rift at the bottom depth of 3461 m. The Pliocene–Lower Quaternary sediments recovered by the hole are mainly represented by siliceous and nanno-foraminiferal oozes. Recent deposits are accumulated in the Panama Basin within the depths range from 3200 to 4000 m of the foraminiferal lysocline (Chen and Prell, 1998). I studied 66 samples from the section of Hole 677A, which enable the mean time resolution of 60 thousand years. For quantitative foraminiferal analyses, I used the fraction coarser than 100 μm. About 300 planktonic foraminiferal tests were counted in each sample and percentages of species, except for *Gt. glutinata*, were calculated. *Gt. glutinata* is widespread in the Pliocene–Lower Quaternary sediments of the North Pacific and often constitutes 30–60% of foraminiferal assemblages, that is why one may suspect its cosmopolitan character (Bubenshchikova, 1996). Table 2 presents the results of the foraminiferal analysis. Additionally, ratios of planktonic to benthic foraminifers, the "foraminiferal number" (the number of shells per 1 g of sediment), and the total number of species were calculated. I used the taxonomy and contracted generic names suggested by Kennett and Srinivasan (1983) with some additions (Rögl and Bolli, 1973). The Late Neogene summary zonation (Berggren *et al.*, 1995) was taken as a basis for paleoceanologic reconstructions. The Neogene–Quaternary boundary is placed in it at the base of the Olduvai Subchron (1.81 Ma).

The annual surface water temperatures were calculated, using the Barash methods of paleotemperature analysis (Barash, 1970; Barash and Blyum, 1975), based on proportions between climatic groups of planktonic foraminifers and the resultant table for the pelagic zone of the World Ocean with the temperature range from 8 to 30°C (Ivanova, 1983).

The general similarity between the modern and Pliocene–Lower Quaternary thanatocoenoses was established previously in the quantitative study of planktonic foraminifers in 576 samples from the North Pacific and simultaneous generalization of the published materials (Bubenshchikova, 1996). For instance, percentage of now-living species in the studied thanatocoenoses of Hole 677A decreases with the age of sediments and corresponds to 94–100% in the Early Pleistocene, 70–100% in the late Pliocene, 52–85% in the terminal and 50–77% in the initial early Pliocene. Paleoecological data obtained earlier for Pliocene species from comparison of their distribution area during a given period (Bubenshchikova and Blyum, 1996) were used to discriminate certain climatic groups of the extinct species, which are ranked (Table 2) as subpolar (SP), temperate (TP), subtropical (ST), tropical (T), and equatorial-tropical (ET). Accordingly, it is possible to use in the Pliocene reconstructions the relation between the particular climatic groups of planktonic foraminifers known in the present-day ocean and the annual surface water temperatures (Barash and Blyum, 1975; Ivanova, 1983).

BIOSTRATIGRAPHY

The recognition of planktonic foraminiferal tropical zonations in the Late Neogene sediments of the eastern equatorial Pacific is usually difficult because of absence of stratigraphically important species. Analyzing the representative factual material from Site 677A, I detected however a number of such forms, the zonal

Table 1. Percentages of planktonic foraminifer species in the sediment traps set in the Panama Basin (Thunnel and Reynolds, 1984)

Species	Range of concentrations (%)	Mean concentrations (%)
N. dutertrei	7.0–59.5	27.23
Gt. glutinata	5.3–43.5	23.53
Gs. ruber	4.6–26.8	14.88
G. bulloides	0.6–19.0	13.32
Gr. menardii	1.1–9.0	4.65
N. pachyderma dex.	0.2–7.4	2.99
Gs. sacculifer	0.8–13.0	2.86
Others	0.0–29.1	10.54

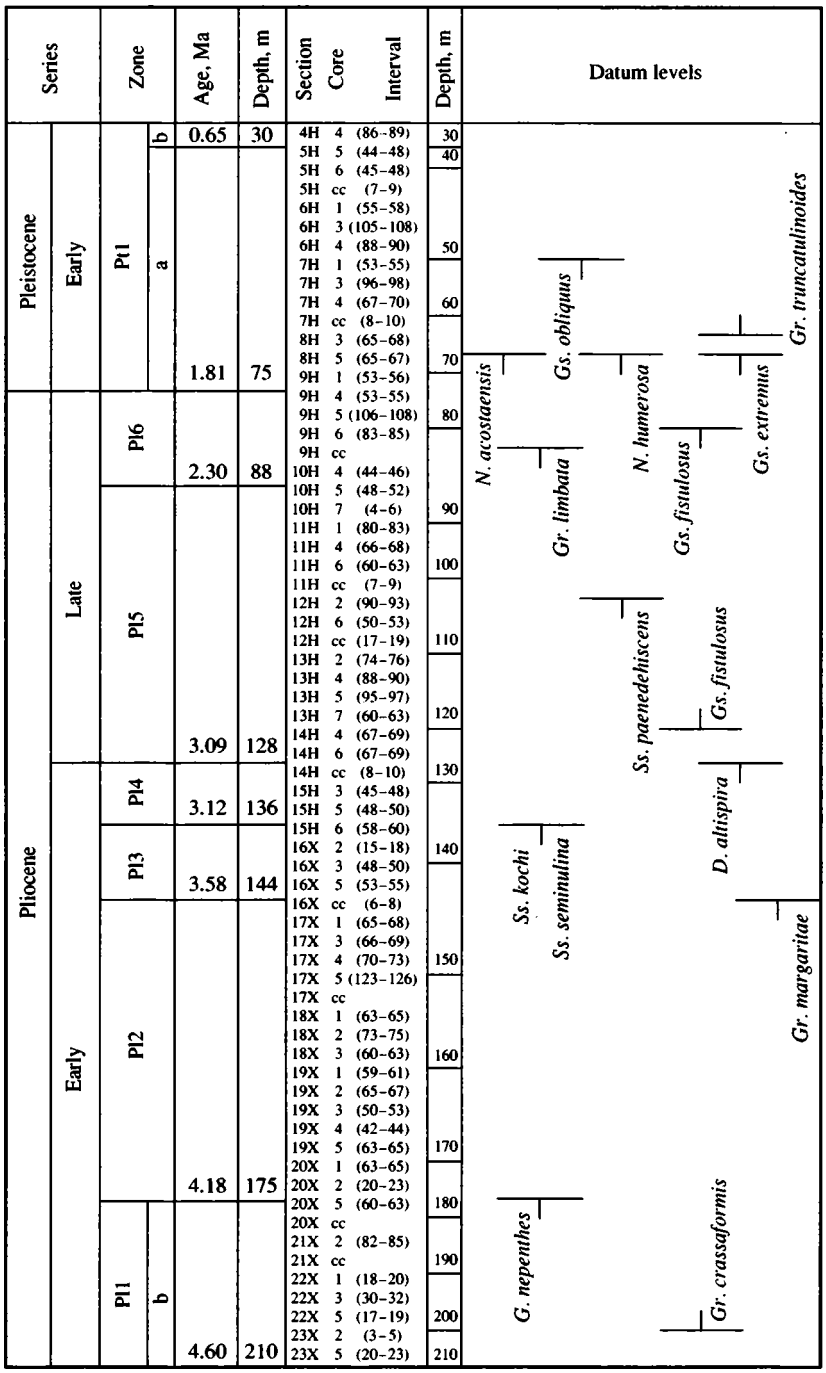

Fig. 2. Biostratigraphic subdivision of the Pliocene–Lower Quaternary sediments at the Site 677A according to zonation of Berggren *et al.* (1995); symbols as in Fig. 3.

index species included, (Fig. 2) which were missed by previous researchers (Jenkins and Houghton, 1989. These are *G. nepenthes, Gr. margaritae, Gr. truncatulinoides, Gr. limbata* (the synonym of *Gr. pseudomiocenica* according to the adopted taxonomy), *Sphaeroidinellopsis (Ss.) paenedehiscens, Ss. kochi, Globoquadrina (Gq.) pseudofoliata*, and some others (Table 2). In my opinion, stratigraphic ranges of *G. decoraperta, Gs. obliquus, Gs. extremus, N. humerosa, N. acostaensis, Ss. seminulina, Gr. crassaformis, Gr. flexuosa, Sa. dehiscens, Gq. venezuelana, Dentoglobigerina (D.) altispira, Pulleniatina (Pu.) primalis, Pu. obliquiloculata*, and *Gs. fistulosus* are somewhat different as well. The data obtained show that the Berggren's zonation (Berggren *et al.*, 1995), contrary to the previously applied ones (Jenkins and Orr, 1972; Keig-

Table 2. Distribution ranges of planktonic foraminifers in the Pliocene–Lower Quaternary sediments, Hole 677A, and climatic groups of taxa

Sample	Species	*Gq. venezuelana* ST	*G. nepenthes* T	*Gr. margaritae* ET	*Ss. kochi* ET	*Ss. seminulina* ET	*Ss. paenedehiscens* ET	*D. altispira* ET	*Gr. puncticulata* ST	*Gr. exilis* ET	*Gr. multicamerata* ET	*Gr. pertenuis* ET	*Gr. limbata* ET	*Gs. extremus* T	*Gs. obliquus* T	*Ge. praecalida* ST	*G. decoraperta* T	*Gr. flexuosa* T	*N. acostaensis* ST	*N. humerosa* ST	*Pu. primalis* ET	*B. praedigitata* ET	*Gq. pseudofoliata* ET	*Gr. menardii* ET	*Gr. sciula* ST	*Gr. pumilio* T	*Gs. ruber* T	*Gs. conglobatus* T	*Gs. quadrilobatus* ET
4H 4																								17.9	0.5		9	0.5	1.5
5H 5																								34	0.6		5		1.6
5H 6																						0.2		6.6	0.8		9.2	+	1.8
5H cc																								23.2	0.8		10.5	+	0.8
6H 1																								17	0.3		20.2	1.6	5
6H 3																	0.3							3.5			11.1		4.5
6H 4																						0.5		12.8			16.6	0.8	3
7H 1															+						0.3	0.3		16.3	1.1	2	22.9	1.1	3.1
7H 3															0.3						0.6			8.3	0.3		36.1	0.3	3
7H 4																					0.4			+	0.4		15.4		1.6
7H cc															+						1.5			12.3	1		26.6	+	0.8
8H 3														0.9					0.9	3.5	0.9			13		6	20.7		2.7
8H 5																			3.9	2.2				19.5		4.4	19.4	0.5	0.5
9H 1	Pt1a																		0.4	0.7	4	0.4		43	0.7	8	19.5		8
9H 4															+		0.4	0.4	0.4	2.4	0.4	0.4		+		3.2	38	0.4	4.2
9H 5																			0.7					23.2	1.5	4.3	32	0.7	3.7
9H 6													0.3					+	1.2	2.5	0.3			9.8		4	24.7	0.3	5.3
9H cc																			1.3	1.7				14.4	1.4	3	24.4		4
10H 4	PL6													0.5			0.5		2.8	2.4	4.3	0.5	0.5		0.5	2.8	38.4	1	5.5
10H 5										0.2	+		1.5						0.8	7.3	2.7			16.9	1.9	3.8	21.8	1.1	1.1
10H 7													0.4	0.8							3.5		0.4	14.6	2.8		29.8	0.4	2.8
11H 1													0.8				0.4		2	3.6	1.6		+	16.2	0.4	+	29.7		3.3
11H 4													8	+		+	0.8		3.7	10.4	3			28.3	0.8	1	15.2	+	+
11H 6													5.4			0.4			0.4		1.5			7.3	0.4		6.5	0.4	14
11H cc													0.6	0.6	0.3	0.4				2	2			9.2	0.6	0.6	9.3	0.8	5.3
12H 2							0.7						2.7	0.7					6.8	10.3				15.7			28.8		4.2
12H 6													+	0.6	2.2				1.9	0.6				2	0.9		13		9.5
12H cc													5.1	0.9	1.3				7.4	2.9	0.6	0.3		11.6			31.1		7.3
13H 2								0.2					3.8		0.8		1		5.2	4	0.8		+	8.4	1.5		19.4	0.2	8.2
13H 4													0.5	0.5	1.2		1.4		10.4	5.2	0.5			5.5	0.3		17.6	+	6.6
13H 5													2.4	3	5.1	0.3	5.4		8	7.5	1.6			4.6	0.6		13.6	+	4.3
13H 7													0.3	0.7	1.7		4.4		5	4.1	1.9		0.5	+	0.9		16.3	0.3	14.6
14H 4							0.3						0.5	2.4	11.2		0.3	+	5.3	3.5	4			+	0.8		32.8		8.2
14H 6	PL5							3.6					1.6		0.8	0.5	0.8	3.2	6	6.9	2			1.6	0.5		6		6.2
14H cc								0.7					1.1	1.1	3.8		2	+	6.2	2.8	2			9.8	0.7		9.2		7.8
15H 3								0.3	0.6				3.5	2.2	6.5	1			3.8	10.1	2.8	0.3	0.3	12.8	0.3		9.1		8
15H 5	PL4		+	0.6	0.6									0.7	9		0.3		3.5	2.3	3.2	+		4.6	1.3		3.5	1	13
15H 6				0.8	+		1.3							1	3		1	0.6	3.8	4.6	1			5.7	0.5		9.4	+	12.1
16X 2					1.5		1								8.4			0.5	2	1	4.3	+	0.5	7.7	1			0.5	
16X 3							13		0.5				2	0.7	3	0.2	1.7	+	3	1.2	13.5	0.7	0.5	9.6	1		15	0.5	4.2
16X 5	PL3	0.6						1.2				0.6	10.8	0.6	3.6				4.8	1.2	17.5		3	18.6	0.6		5.5	+	9.1
16X cc					2.2			7.7					1.6		3.2				2.2	3.2	3.8		0.6	13.2			11	0.6	24.8

Gs. sacculifer ET	G. *bulloides* TP	*G. falconensis* ST	*G. quinqueloba* TP	*Gl. uvula* TP	*N. pachyd.* sin. SP	*N. pachyd.* dex.TP	*N. pseudopima* TP	*O. suturalis* T	*O. universa* T	*C. nitida* ET	*Gd. hexagona* ET	*Ge. aequilateralis* ET	*St. tokelauae* ST	*T. humilis* ST	*Sa. dehiscens* ET	*Gr. tumida* T	*Gr. ungulata* ET	*N. duertrei blowi* T	*N. duertrei* T	*Gr. crassaformis* ST	*G. rubescens* T	*Pu. obliq.* dex.ET	*Pu. obliq.* sin. ET	*Gr. inflata* ST	*Gs. fistulosus* ET	*Gr. tosaensis* ST	*Gr. truncat.* dex. ST	*Ge. calida* ST	*Gl. glutinata*
		0.5	1		1		19.4				1				1	3.5	1	31.8	6	1.5	2.9		+						9
+	1	3.3	1	0.2		0.7	9.1		0.5			0.5	+		0.5	17.3		14.7	5		2		2.4					0.6	21
1.5	4.8	0.5	3.4	0.4	0.2	23.7	8.7	0.4	0.4	+		0.5				1.5	+	21	7.6		4.6		2					0.2	26
+	3		0.8	0.4	0.4	13.1	4.1					+				2.3	1.1	18.4	13.9	+	3.7	0.8	2.3					0.4	24
0.3	2.2	0.6	0.6			12.5	7.1	0.3	0.6		0.3	0.3			+	2	0.3	18.3	7		1.9		1.6						27
0.6	2.5	0.6	1			38	4.2		0.6		0.3	0.6			0.9	0.6		14.7	8.3		3		4.4				0.3	+	26
+	3.5		2.5			19.6	6.4		0.8		1.2	0.5			0.5	4.3		18.3	3.5		2.6	0.5	0.8	0.8				0.5	36
0.3	2	1.4	1.8			18.8	2		0.9		0.9	0.3			0.3	2.3	1.4	6.8	6.5		4	0.3	2.3	+				0.6	44
	3		0.6			16.4	4.2		0.9							4.5	0.3	12.8	4.8		1.8		1.8						19.5
	3.6	0.4	1.2		0.4	25.8	11.4	0.4	3.5			+						29.6	4.7		1.2		+						12
	2.7	0.8	1.5		0.8	18.8	6.4		+						0.4	3.5		15.3	1		3.8					0.8	2	+	21
	1.7						10.4		0.9							0.9	0.9	20	14	+	2.6							+	27
	3.9					1	4.9								0.5	0.5	1.6	27.4	9.3		0.5								23
	0.5					1	0.7								1.8	5.1		3.6	1		0.7		0.5					0.4	12
0.8	0.4	1.2	0.4			3.2	9		0.4		0.4				0.4	10.6		9	11	0.4	2.2							0.4	29
	3.6	1.4				0.7		0.7	0.7			0.7			1.4	0.7		20.4	2.2		1.4								26
0.6	4.6	1.5		0.3	0.3	2.1	5	0.3	2.8			0.6	+		0.6	8	1.2	10.5	9.3		3				0.3			0.6	32
0.3	1.6	1				2.7	8.1	0.3	1.7		0.7	0.7			0.3	5		19.4	5.7		1.3		0.3					0.7	25
0.5	2.3	0.5				0.5	5.6		0.5		0.5				1	3.8		15.6	4.7		3.8		0.5					0.5	20
	5.4	0.8		0.4	0.4	3	3.4		0.8	0.4	1.5				0.4	6.3	0.8	9.2	1.5	0.4	5.4	0.4	0.4						28
0.4	6.3					0.4	5.5	0.4	0.4		0.4	0.4			0.4	1.2	+	13.8	5.1	2.8	0.4	1.5		+					36
	2					0.8	1.7		0.4		0.4	0.4			0.4	4.4	+	15.4	10.5	4	1.2			0.4					9
	0.8	0.8				2.1	2.7				0.8	0.3			0.8	1		13.1	3.2	0.5	2.7								15
	8.8					3.5	5.8	0.4	0.4		0.4	0.4		1.1	+	1.2		21	19.2		1.5								22.5
	13.2	0.3			8.7	11	2.7	1.1	3.7		0.6				0.5	0.3		16.8	6.5	0.3	1.4	0.6		0.6	+				34
	2.7				0.7		7.5						+		0.7			12.2	0.7	+	5.6								8
	0.5				19.4	10.6	3.6	0.6	2.2		0.3			0.3	+	1.8		23	6.4	+	0.6								13
	4.2					1.6	5.1				0.3				0.9	1.3		15.7	0.6		1.8								18
+	2.7	0.2			10.3	1.7	5		0.8	+	0.4	0.2			0.2	0.8		18.4	3.1		2.7								17
	3.5					2.6	5.2		0.9		0.2	0.2			0.2			28	5.8	0.2	3.5								20
	0.9	1				3.7	11.1	0.3	1.6	+	+	0.6		0.6	0.3	0.6		15.6	4.3		3				+				31
	4.6		0.2			2.9	12.1	0.3	0.5		1	0.3			1.7		0.3	13.8			11.6			+	+				19
0.8	2.7					2.6	3.7	0.5	2.1		0.5	0.5			0.5	6.1		6.7			4								7
0.5	2.4	0.8	0.5			2.4	9.5		0.8		+				0.5	30	1.2	7.7	0.8		3.2								15
0.3	4.8	1	0.7		1.4	3	19.6		0.3		0.3	0.3			0.6	0.3		16.8	1.4		2								18
0.8	4.9	1.4				8.4	7.6		1		3.2	1	+			+		6.7		0.3	3.1								11
	9	1.3				6.7	16.4		+		0.6	0.3			1	1.6		12.2	0.3	0.3	6.7								21
0.3	3	0.5		0.3	0.5	7.2	17.6	+	0.3		0.8	+			1.3	2.6	+	17.2	0.6	0.3	2.7								17
1	4.9					3.8	13.1	0.5	+		1.5				0.5	28.4		11.4	0.5		6								45
0.9	2.9	0.8				1.7	9.6		+		1	1.5		0.2	+	1		5.7	0.7	1.5	2.2								39
0.6	2.4	0.6				0.6	5.5				0.6				0.6	4.8		6.6											15
	3.2						6.5				1.2	0.6	+		2.2	8.8		2.2	0.6	0.6									10

Table 2. (Contd.)

Sample	Species	*Gq. venezuelana* ST	*G. nepenthes* T	*Gr. margaritae* ET	*Ss. kochi* ET	*Ss. seminulina* ET	*Ss. paenedehiscens* ET	*D. altispira* ET	*Gr. puncticulata* ST	*Gr. exilis* ET	*Gr. multicamerata* ET	*Gr. pertenuis* ET	*Gr. limbata* ET	*Gs. extremus* T	*Gs. obliquus* T	*Ge. praecalida* ST	*G. decoraperta* T	*Gr. flexuosa* T	*N. acostaensis* ST	*N. humerosa* ST	*Pu. primalis* ET	*B. praedigitata* ET	*Gq. pseudofoliata* ET	*Gr. menardii* ET	*Gr. scitula* ST	*Gr. pumilio* T	*Gs. ruber* T	*Gs. conglobatus* T	*Gs. quadrilobatus* ET
17X	1						0.9	2.5					5.2		7.2		0.9	0.6	2.2	2	8.1			20.3	0.6		10.6	0.3	6
17X	3			0.3		0.3		1.6					1.1		1.9				10	5.7	0.6	0.3		36.6	0.8		10.5	0.8	4.3
17X	4					0.4	+	0.4	+			0.7	1	1.4	7.7				7.7	6.6	0.7	1.4		25	0.3		9.5	2.4	6.3
17X	5					0.5	+	1.4					1.7	0.3	6.3		0.9		1.9	0.7	15.7	+	0.3	14.7	0.9		3.9		22.8
17X	cc					0.8	1.1	3.8						0.4	6				0.8	0.8	8.3	0.4	0.4	34	0.8		3		14.4
18X	1					+		2.5					+	0.6	9		0.3	0.3	3.7	1.4	18			5.9	2		0.6		9.3
18X	2					1.2	0.5	10.5					1.7		13			0.5	1.5	0.9	12.5			11.5			1.5	0.3	13.2
18X	3					0.5	2.8	1					2.3		12.2			0.5	1.4	1.4	7.5	0.5	1	23.9	0.5		2.3		11.7
19X	1					1.9	0.9	5.6					3.3			0.9		+	1.4	0.5		+		11.2	1.9		0.5	0.5	14
19X	2					+	+	21.3					+	0.6	2.8	+	0.5	+	3.4	3.4	2.2	1.7	+	9.5	1.8		+	+	10.3
19X	3					+	1	3.4						0.5	10.3		0.5	2	2		0.5	1.5	1	5.9	0.5				24.7
19X	4				+	1.3	1.6	1.6					2.2		6		0.9	0.3	1.6	1.3	4.1			17.4	0.6		0.3	+	6.7
19X	5					0.4	1.6	3.2					2	+	4	0.8	2	0.4	4		2.8		+	10.8	0.4		13.7	0.4	11.2
20X	1	PL2				0.8	0.8	9.8			0.4		9	0.4	6.2		1.9	0.4	2.5	1.4	9.5			16	1				10
20X	2		+	1		0.6	1.2	8.4					11.1	0.6	12.2		3.7	1.2	2.2	3.7	1.2			16	0.3		0.3	0.6	8
20X	5		0.8	0.3		0.3	0.9	7.5					1.6	1	17		5	+	8.8	3.9	4.3			9.8	0.3				6.8
20X	cc		+	0.4		1.6	4	9.1					13	+	6.3		0.8	0.4		3.2	7.9			12.7	1.2				10.5
21X	2				+	1.6	1.2	9.2					5	0.7	7.9		1.8	0.2	4.2	2.8	1.8		0.2	6.7	0.2			1.8	13.4
21X	cc	PL1b			+	0.4	1.2	15.5					2.8	2.4	12.7		0.8		0.8	2.7	2.4		0.8	14.7	0.2			0.4	11.5
22X	1		0.3			2	0.5	0.8					2.6	0.6	7.7		1.5	0.3	1.5	1.3	2.3		1.3		1			0.3	10.9
22X	3	+	0.5		0.6	1.3	3.7	7.1					4.2	1.8	4.5	+	1.3		1.8	2.1			0.3	3.2	1.3		0.3	0.3	10.5
22X	5	+	0.8			0.4	1	4.2					4.8	0.4	7.5	0.4	0.6		4.2	1.3	1.3		0.2	11.9	1.4				7
23X	2	+			0.2	0.6	2.5	3.8					3.3	1	7.3		1.4		1.5	0.4	0.5		0.6	2	0.6			0.2	4
23X	5	+	2.9		1.4	2.2	5.8	6.8					4	1	11		2.5	0.9	7.2	0.8			0.8	2.5	0.6		0.4		3.6

Note: (SP) subpolar, (TP) temperate, (ST) subtropical, (T) tropical, and (ET) equatorial–tropical groups of species; symbol "+" denotes presence of species; (*O. bilobata* is present in Sample 14H4).

win, 1982a; Saito, 1985; Jenkins and Houghton, 1989, and others), can be used with a slight modification (Fig. 2) to subdivide the sediments of Hole 677A.

Levels of evolutionary and ecologic changes in planktonic foraminiferal assemblages are successfully used for the biostratigraphic subdivision of deep-sea sediments. At the same time, diachronism of datum levels marking events of species appearance or extinction in different climatic zones and separate realms has been established in specialized works. It is conceivable that in the regions with a dynamic oceanographic regime, e.g., in the Panama Basin, the first and last occurrence levels of species in the section may discordant with datums of their evolutionary appearance and extinction. The comparison of the sedimentation rate curves (Fig. 3), which have been plotted with due account for the appearance and extinction of nannoplankton (Houghton, 1989), radiolarian (Alexandrovich, 1989), and planktonic foraminifer species, suggests that most of the recorded events are isochronous, traceable in various regions of the Pacific (Berggren *et al.*, 1995). Most of the planktonic foraminiferal datums (Fig. 3) are reliable biostratigraphic markers for the subdivision of the Pliocene–Lower Quaternary sediments of the Panama Basin. In the case of a steady sedimentation, the earliest findings of stratigraphic markers *Sa. dehiscens* (about 4.35 Ma) and *Gs. fistulosus* (2.9 Ma) and the last occurrence of *Gr. limbata* (2.0 Ma) are recorded at Site 677A later, as compared to the corresponding datums reported by Berggren *et al.*, (1995), while the disappearance of *Gs. fistulosus* (1.9 Ma) took place here earlier (Fig. 3)

In the section of Hole 677A, I distinguished planktonic foraminiferal zones Pl1b to Pt1 (Fig. 2 and Table 2). The studied interval is above the Miocene-Pliocene boundary and incompletely represents the lower

Gs. sacculifer ET	*G. bulloides* TP	*G. falconensis* ST	*G. quinqueloba* TP	*Gt. uvula* TP	*N. pachyd.* sin. SP	*N. pachyd.* dex. TP	*N. pseudopima* TP	*O. suturalis* T	*O. universa* T	*C. nitida* ET	*Gd. hexagona* ET	*Ge. aequilateralis* ET	*St. tokelauae* ST	*T. humilis* ST	*Sa. dehiscens* ET	*Gr. tumida* T	*Gr. ungulata* ET	*N. dutertrei blowi* T	*N. dutertrei* T	*Gr. crassaformis* ST	*G. rubescens* T	*Pu. obliq.* dex. ET	*Pu. obliq.* sin. ET	*Gr. inflata* ST	*Gs. fistulosus* ET	*Gr. tosaensis* ST	*Gr. truncat.* dex. ST	*Ge. calida* ST	*Gt. glutinata*
0.3	2.5	1.3				2.5	8.7				1.2	0.6			0.3	3.7		8.4			3.1								19
	6.7					1.4	8.1		0.3		0.5				0.6	2.7		3.8	1.1										9
0.7	5.6					1.7	12.2		0.3		0.4		+		0.4	1.7		3.5			2								28
0.6	1.9	0.3		0.2		2.9	5.3	0.3	0.4		0.7	0.7	+					10.6	1.2		2.9								23
0.8	6.8					0.4	5.2				0.4				2	2.2		6.4	0.8	+	+								47
	7.9					9	13	0.6			2.5	0.6	+			0.6		9.2	2		1								19
	0.5	0.2				1	14.7				0.5	0.3			0.3			7.7	0.5	5	0.5								25
	1.4	0.5				0.9	3.2	0.5			1.4	1			0.5	8.9		6.1	0.5	4.7	0.9								21
0.5	2.3					4.7	23.8				1					4.2		17.3	2.3		1.3								53
0.6	3.9	1.1				3.4	4.5	+	+		1.7	1.7		0.5		11.2		12.9	+	+	1								4
0.5	2			0.4		2	10.8		+		0.5	1			+	0.5		25.1	3.4										42
0.3	8.9	0.3				4.1	10.6	0.3	0.3		1.6	0.9				10.1		13	0.6		3.1								31
1	1.2	4				6.4	17.3				0.4	0.4	+			1.6		8.8			1.2								12
	0.7	1			2.8	1.4	8.5	0.4	0.7		1.4	0.8	+			3.2		9											48
0.6	3.1	1.8			5.3	1.5	7.7	0.6	0.3		0.9	+				2.5		3.4											24
0.6	0.7	0.6			2.4	2.6	9.5		0.3		1.6	0.5	+			0.8		12.1											46
	0.4	3.2		0.4	4.3	9.1	2.7	+	1.2		+	+	+		1.2	1.6		4.8											29
	2.2	0.7	0.5		16.6	6.5	2.8	0.2				0.5	+		0.7	3		6.2	1.4										31
0.4		0.8				3.6	11.2		+		1.2	0.8			+	+		12.7											45
	1.3				24	0.7	13.6		0.3		1.3	0.5				8		10.8	2.6		2								32.5
	1				15.7	2.7	9	0.3			0.3	1				13.2		8.3	1.6	0.3	2.1								18.5
	0.8				5.6	3.5	18		0.2		4.4		+			9.8		8.3	0.6	0.4	1								39
0.2	2	0.6			32	8	8.6				1					6.9		5.4			5.4								32
	0.4	2		1	1	12	8	1	0.4		1.8	0.8				10		5	0.4		1.8								43

Pliocene sediments. Foraminifers characterizing sediments of the early Pliocene Zone Pl1b are *Gr. margaritae, D. altispira, Ss. paenedehiscens, Ss. kochi*, and *Ss. seminulina*, which are inherited from the Miocene. Latest specimens of *Gq. venezuelana* and *G. nepenthes* and the earliest ones of *Gr. crassaformis* and *Sphaeroidinella (Sa.) dehiscens* are also recorded in this zone. The overlying early Pliocene zones Pl2, Pl3, and Pl4 are defined in accord with datum levels of *Gr. margaritae, Ss. seminulina*, and *D. altispira*. In addition, sediments of zones Pl2 and Pl3 yield few specimens of *Gr. pertenuis* and *Gr. multicamerata*, whereas *Ss. kochi* disappears near the base of the Zone Pl3.

Composition of planktonic foraminiferal assemblage of the late Pliocene Zone Pl5 is substantially different. *Ss. paenedehiscens, Ge. praecalida, Gq. pseudofoliata*, and *Gr. limbata* disappeared successively within it and *Gs. fistulosus, Gr. pumilio, Pu. obliquiloculata, Ge. calida*, and *Gr. ungulata* appeared there. Few specimens of the Pliocene forms *Gr. exilis, Gr. multicamerata, Gr. conomiozea, Gr. puncticulata*, and of modern *Gr. inflata* are also present in this assemblage. In the late Pliocene Zone Pl6, *Gs. extremus, N. acostaensis, N. humerosa, Gr. flexuosa*, and *G. decoraperta* become extinct. The planktonic foraminiferal assemblage of the Zone Pt1a is most similar to the present one. The top of the zone is marked by extinction of *Gs. obliquus, Gr. fistulosus*, and *Pu. primalis; Gr. pumilio* disappears in its middle part. Few specimens of *Gr. tosaensis* and *Gr. truncatulinoides* occur within the zone.

Thus, the stratigraphic distribution of 60 planktonic foraminiferal species and morphological varieties has been established, and 34 among them are the modern forms (Table 2). Twenty five species became extinct and nine forms appeared during the studied time span. As for the species of foraminiferal climatic groups mentioned above (Table 2), their general diversity decreased owing to the disappearance of tropical and

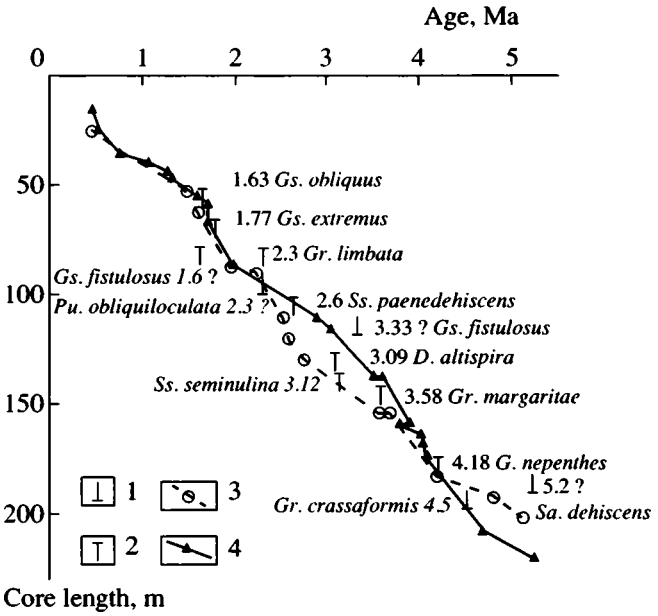

Fig. 3. Secular variations of sedimentation rate at the Site 677A: (1) first and (2) last occurrence levels of planktonic foraminifers (this work), ages in Ma after Berggren *et al.* (1995); (3) nannofossils (Houghton, 1989); (4) radiolarians (Alexandrovich, 1989).

equatorial-tropical forms, whereas the subtropical taxa were predominantly developing. The species diversity as a whole decreased from 48 forms in the early Pliocene to 34 in the Early Pleistocene.

According to the curve of accumulation rate based on nine planktonic foraminiferal datum levels, the early–late Pliocene (3.08 Ma) and Pliocene–Quaternary (1.81 Ma) boundaries are defined at the depth levels of 128 and about 75 m below the sea floor (Fig. 3). Sedimentation rate calculated from the planktonic foraminiferal data, decreased from 54 m/m.y. in the early Pliocene to 44 m/m.y. in the late Pliocene, and down to 41 m/m.y. in the Early Pleistocene.

PALEOCEANOLOGIC RECONSTRUCTIONS

High sedimentation rate and lithologic features of the section indicate that the Pliocene–Quaternary sediments recovered by Hole 677A accumulated under conditions of a high biological productivity characteristic of the present-day Panama Basin. To reconstruct the conditions of accumulation of planktonic foraminiferal assemblages and variations of the carbonate compensation depth (CCD) in Hole 677A, I used the following

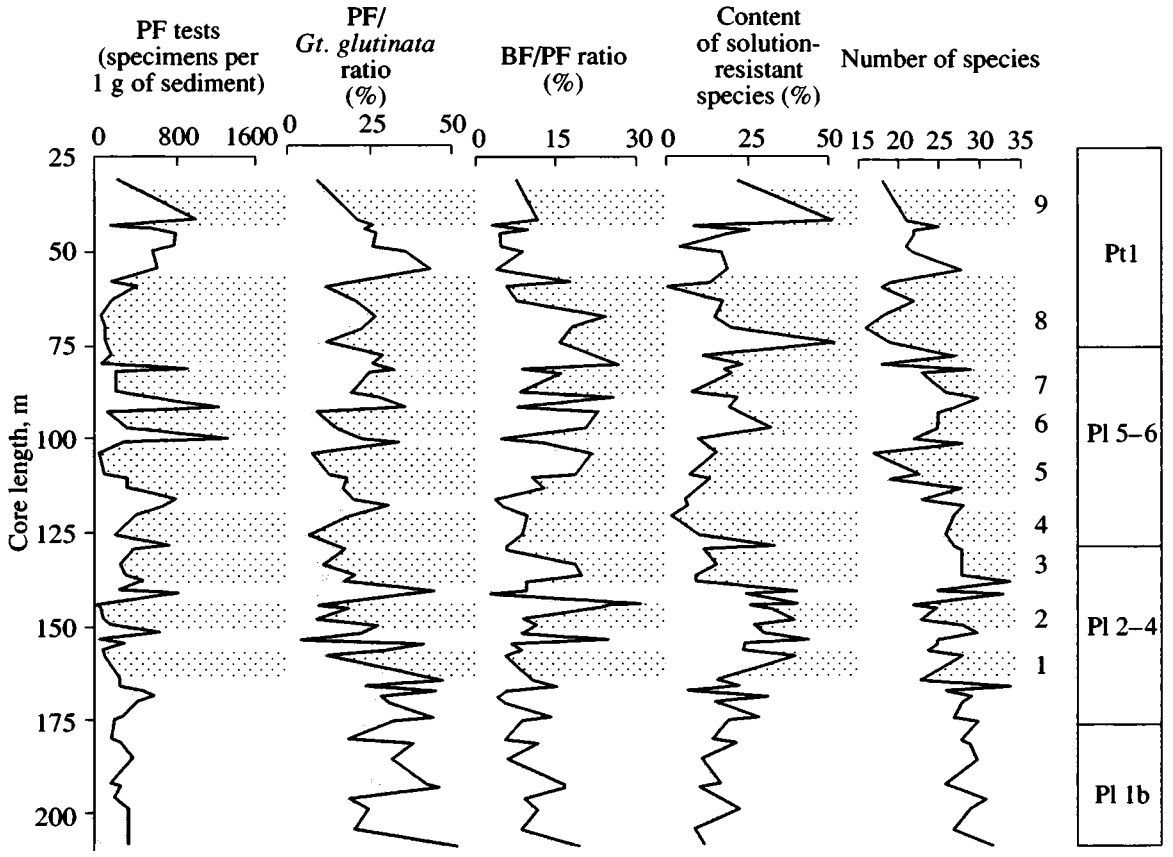

Fig. 4. Pliocene–Lower Quaternary horizons (1–9) of Hole 677A, Panama Basin, accumulated in periods of the CCD rise; abbreviations PF and BF denote planktonic and benthic foraminiferal tests; solution-resistant species are *Gr. tumida, Gr. menardii,* and *Pu. primalis.*

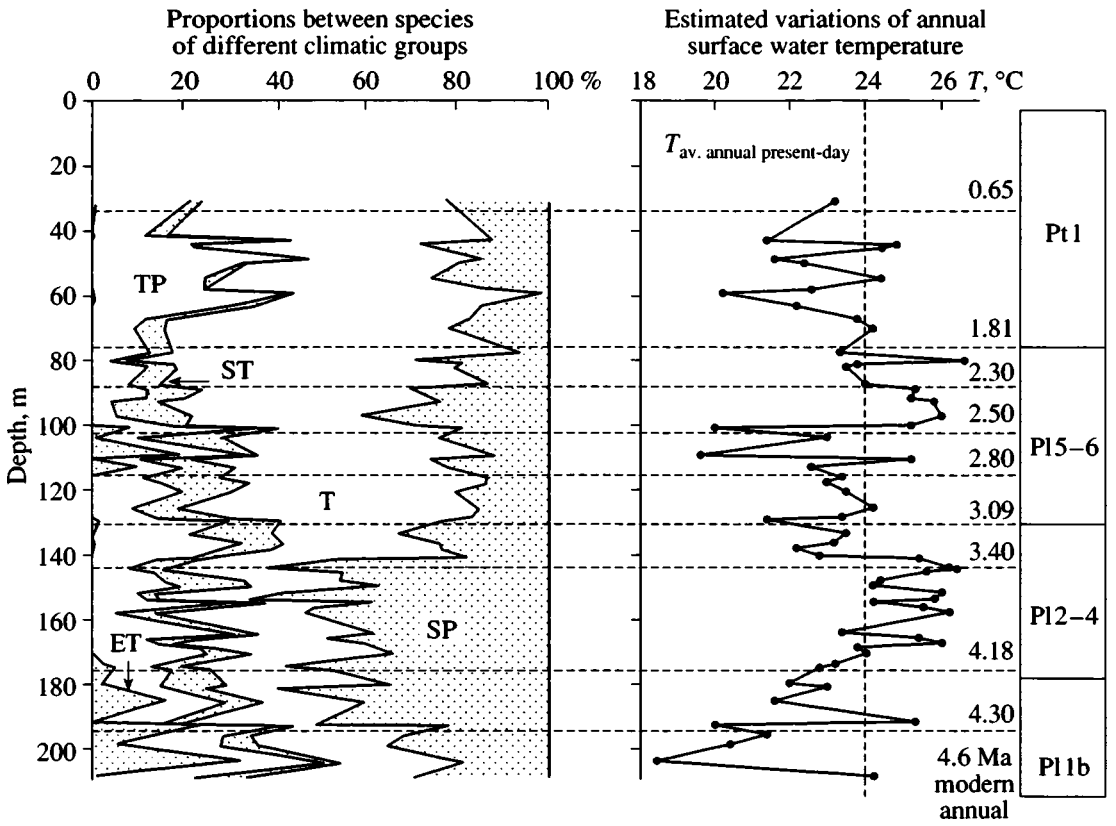

Fig. 5. Secular variations of surface water temperature and proportions between planktonic foraminiferal species of different climatic groups in Pliocene–Lower Quaternary thanatocoenoses at the Site 677A: (SP) subpolar, (TP) temperate, (ST) subtropical, (T) tropical, and (ET) equatorial-tropical species.

parameters: the foraminiferal number; ratio of benthic to planktonic foraminifers calculated as (BF/BF+PF) × 100%; percentages of *Gt. glutinata* in the foraminiferal assemblages; number of foraminiferal species; and overall concentrations of forms most resistant to dissolution, such as *Gr. tumida, Gr. menardii*, and *Pu. primalis* (Fig. 4).

The use of *Gt. glutinata* concentrations among other analyzed parameters is dictated by its peculiar distribution in the Pliocene–Lower Quaternary deposits of the North Pacific. Earlier (Bubenshchikova, 1996), I showed a cosmopolitan character of this species whose concentrations may be as high as 30–60% of the foraminifer assemblage as a whole, though its predominance in subtropical and tropical realms and its relation to highly productive oceanic zones was also noted. It was also recognized that considerable variations of that species content from 0.5 to 60% resulted not only from ecologic reasons, but also from dissolution.

Despite a complicated character of curves shown in Fig. 4, the following regularities can be marked. In the early Pliocene, i.e., from 4.6 to 3.8 Ma (210–155-m interval in the section), conditions of sedimentation (productivity of planktonic foraminifers, the CCD level, and characteristics of water mass) were relatively stable. The preservation of planktonic foraminifers was comparatively good, as it is evident from the high concentrations of *Gt. glutinata*, relatively low content of solution-resistant species, and low benthic-to-planktonic form ratios (Fig. 4). In the subsequent period from 3.8 to 0.65 Ma (155–30 m below sea floor), there were recorded nine extended intervals of the decreased abundance and species diversity of planktonic foraminifers, within which concentrations of *Gt. glutinata* are reduced, while the content of solution-resistant species and benthic-to-planktonic form ratios grow. These data indicate a decline of planktonic foraminiferal productivity and/or the CCD rise and more intense dissolution of foraminiferal tests in the intervals 1 to 9 (Fig. 4). However, the content of solution-resistant species is below 25%, suggesting a relatively well preservation of foraminiferal assemblages at that time except for those in samples 5H5 and 9H1, which were excluded from the paleotemperature analysis. The deep-sea drilling records indicate the betterment and deterioration of carbonate preservation in the Atlantic and Pacific oceans, respectively, beginning from 4.6 Ma that was associated with the gradual closure of the Panama Strait and with changes in the bottom- and surface-water circulation (Haug and Tiedemann, 1998). The results obtained for Hole 677A well agree with this conclusion.

Let us consider now the data on species climatic groups of foraminifers and inferable temperatures of surface water (Fig. 5). The Lower Pliocene sediments (4.6–3.09 Ma) yield contrasting thanatocoenoses characterized by the predominance of foraminifers of non-contiguous SP-M and ET climatic groups (Fig. 5, *I*). The content of T and ST species is significantly lower than in the low-latitude assemblages of the open ocean (Ivanova, 1983). Assemblages with predominance of species of non-contiguous climatic groups, i.e., the contrasting thanatocoenoses, are characteristic of the frontal zones and upwelling areas (Os'kina and Blyum, 1984). Thus, a more significant seasonal contrast of surface water temperatures than in the present Panama Basin was characteristic of the early Pliocene. The surface-water circulation was more intense in general than nowadays. The temperature minimums evidently reflect the influence of the Equatorial Divergence, Peru Current, and the associated upwelling. The temperature maximums were likely related to periods of a weakened water uplift and strengthened equatorial countercurrent, and also to open connections between the Atlantic and Pacific tropical regions at that time.

Variations in abundance of members of the *N. dutertrei* lineage (*N. pachyderma* sin.–*N. pachyderma* dex.–*N. pseudopima–N. dutertrei blowi*), which are the upwelling indicators in the Panama Basin (Tables 1 and 2), enable the following conclusions on the circulation intensity. From 4.6 to 4.3 Ma, the upwelling of cold water was most intense in the period from 4.3 to 4.18 Ma and gradually weakened afterward; its influence was minimal during the time span of 4.18–3.4 Ma and increased again from 3.4 to 3.09 Ma though not up to the level characteristic of the mid-early Pliocene.

The oxygen isotope investigations showed positive excursions of $\delta^{18}O$ in planktonic foraminiferal tests from the equatorial Pacific in the periods of 4.2–4.0 Ma (Whitman and Berger, 1992), 4.45–4.325 Ma (Prentice *et al.*, 1993), 4.6–4.3 Ma (Jansen *et al.*, 1993), and 4.0 Ma (Shackleton *et al.*, 1995), which support our conclusion that these were periods of a relatively cold climate (Fig. 5). Micropaleontological and isotope data for the equatorial Pacific indicate a relatively warm period from 5.0 to 3.3–3.0 Ma (Keigwin, 1982a,b; Prell, 1985; Whitman and Berger, 1992; Prentice *et al.*, 1993; Jansen *et al.*, 1993).

A considerable abundance of ET species (*Gs. quadrilobatus, D. altispira, Gr. menardii*, and *Gr. limbata*) in the early Pliocene (Fig. 5 and Table 2) shows that the surface water temperatures during the weakened upwelling in the Panama Basin were higher than nowadays and reached the maximum values at 4.18–3.4 Ma. A sharp decrease in concentrations of these species and lower contrast of thanatocoenoses in general at about 3.4 Ma (Fig. 5) indicate changes in hydrologic conditions, evidently owing to the uplift of the Central American threshold and to the terminated communication between surface water masses of the Pacific and Atlantic tropical areas. According to our data (Fig. 5), this event and related changes in planktonic foraminiferal assemblages happened rapidly. However, biogeographic evidences from other groups of microfauna suggest that the event lasted longer, from 3.8 to 3.0 Ma (Jenkins and Orr, 1972; Saito, 1976; Keigwin, 1982b; and others). The uplift of the Central American Isthmus created outlines of the Atlantic and Pacific basins similar to the recent ones and gave rise to circulation and properties of the bottom-water resembling those of the Quaternary (Haug and Tiedemann, 1998). According to our data, this event is recorded in carbonate sediments at Site 677 at the level of 3.8 Ma (Fig. 4).

The late Pliocene sediments (3.09–1.81 Ma) are more rich in foraminifers of T and ST groups and depleted in taxa of ET and M groups, i.e., their thanatocoenoses are less contrasting (Fig. 5). *Gs. ruber* and *N. dutertrei blowi* dominate among T species, *N. acostaensis* and *N. humerosa*, among ST forms, and *N. pseudopima* among M taxa (Table 2). In the period of 2.8–2.5 Ma, the contrast between thanatocoenoses sharply increased and they became close in composition to those of the mid-early Pliocene (4.6–4.3 Ma), despite the lower abundance of foraminifers from SP and ET groups. In the terminal late Pliocene (2.5–1.81) Ma, thanatocoenoses were most similar in composition to the low-latitude tropical assemblages of the open ocean (Ivanova, 1983). They were dominated by *Gr. menardii, Gs. ruber, N. dutertrei blowi*, and *N. dutertrei* characteristic of the present-day Panama Basin.

According to general structure of planktonic foraminiferal assemblage, their species composition, and variations in abundance of species of the *N. dutertrei* lineage, the seasonal contrast of surface water temperatures during the late Pliocene was likely lower than in the early Pliocene. In the period of 3.09 to 2.8 Ma, the upwelling was less intense than in the terminal early Pliocene and strengthened again in the period of 2.8 to 2.5 Ma. It was similar to the recent tropical upwelling in the Panama Basin during the time span of 2.5–1.8 Ma.

Nowadays there is a lot of data implying that the major glaciation epoch began in the Northern Hemisphere 2.8–2.4 Ma ago (e.g., Keigwin, 1982b; Prell, 1985). Oxygen isotope records in planktonic and benthic foraminiferal tests indicate that, according to different estimates, the glaciation peaks occurred 2.4 Ma (Keigwin, 1982b), 2.54 Ma (Jansen *et al.*, 1993), and 2.8–2.85 Ma ago (Whitman and Berger, 1992). The mid-late Pliocene thanatocoenoses close in composition to those of the early Pliocene, formed 2.8 to 2.5 Ma ago according to results of this study (Fig. 5), i.e., most likely during the strengthened circulation of surface water, when its temperature decreased in response to glaciation in the Northern Hemisphere. The comparison of temperature values estimated for the

Early and mid-late Pliocene (Fig. 5) also suggests that glaciation in the northern polar region produced a lesser impact on hydrologic conditions in the Panama Basin than climatic changes in the Southern Hemisphere, which were responsible for the cold event of the early Pliocene.

In sediments recovered by Hole 677A, the Pliocene–Pleistocene boundary marks the beginning of a relatively cold event recorded at about 1.7 Ma, and comparatively cold-water conditions in the region were characteristic of the subsequent period. The species composition of corresponding thanatocoenoses is similar to that of the modern foraminiferal assemblages (Tables 1, 2), though representatives of the M group, among which *N. pachyderma* dex. and *N. pseudopima* dominated, were more abundant in this time than now. These thanatocoenoses most likely reflect changes in the surface-water circulation, which controlled development of microfauna in colder conditions than those of the present-day Panama Basin; the environments were likely close to those of the terminal Early and initial late Pliocene.

Thus, this study shows that the changes in planktonic foraminiferal assemblages from Hole 677A were under strong influence of the climate-controlled dynamics of surface water masses in the eastern equatorial Pacific during the period of 4.6 to 0.65 Ma.

The paleotemperature plot for Hole 677A (Fig. 5) demonstrates the mean secular variations against the background of substantial fluctuations of surface water temperatures during the formation period of studied thanatocoenoses of planktonic foraminifers. The maximum temperatures are estimated for the terminal early (26.4°C) and late Pliocene (26.6°C), and the minimal ones for the initial early Pliocene (18.4°C), mid-late Pliocene (19.6°C), and for the beginning of the Early Pleistocene (20.2°C). The general amplitude of temperature fluctuations is 8°C. The resolution ability of the paleotemperature plot is insufficient for correlation of estimated thermal peaks with the Pliocene oxygen isotope stages (Shackleton *et al.*, 1995), about a hundred of which has been distinguished within the last 3 Ma at Hole 677A (Shackleton and Hall, 1989). It should be noted that the global paleoreconstructions for the mid-Pliocene (or Pliocene optimum) did not reveal a significant rise of surface water temperatures in low latitudes of the World Ocean above their present-day level (Dowsett *et al.*, 1996).

The comparison between paleotemperature (Fig. 5) and sedimentation rate (Fig. 3) plots resulted in recognition of several thermal events. Cold events are recorded within the time intervals of 4.6–4.3, 2.8–2.5, and 1.7–1.2 Ma, and warm events correspond to periods of 4.3, 4.18–3.4, 2.5–2.3, and 1 Ma. The mid-early Pliocene, mid-late Pliocene, and the initial Pleistocene characterize in general the cold-water conditions, while the terminal early and late Pliocene, warm-water ones.

CONCLUSIONS

The general biostratigraphic zonation after Berggren *et al.* (1995) is used for the first time to subdivide sedimentary sequence of Hole 677A, and planktonic foraminiferal zones PL1b to Pt1 are distinguished in this sequence within the subbottom depth interval of 30–210 m. The early-late Pliocene (3.09 Ma) and Pliocene-Quaternary (1.81 Ma) boundaries are situated in the studied section at the levels of about 128 and 75 m below bottom, respectively.

Many planktonic foraminiferal datums are found to be the reliable biostratigraphic markers in the Panama Basin sediments. The following events are established to be diachronous in comparison with those dated by Berggren *et al.* (1995): the appearance of *Sa. dehiscens* at 4.35 Ma and *Gs. fistulosus* at 2.9 Ma, and the last occurrence of *Gr. limbata* at 2.0 Ma and *Gs. fistulosus* at 1.9 Ma.

The distinguished intervals of the decreased planktonic productivity and/or changes of the Pacific bottom waters beginning from 3.8 Ma are marked by decline in abundance of planktonic foraminifers and by lower diversity of their species and lesser concentration of *Gt. glutinata.* In contrast, abundance of solution-resistant species and benthic-to-planktonic species ratios increase within these intervals.

Changes in composition of planktonic foraminiferal assemblages from sediments at Site 677 reflect impacts of the climate-controlled dynamics of surface water masses in the eastern equatorial Pacific during the period of 4.6–0.65 Ma.

A sharp decrease in abundance of equatorial-tropical species about 3.4 Ma ago indicates a transformation of hydrologic regime. This event is correlated with the termination of the surface water exchange between the Pacific and Atlantic tropical zones owing to the emergence of the Central American threshold.

ACKNOWLEDGMENTS

I am grateful to the DSDP and ODP authorities for core samples shipped for investigation. This work was supported by the Russian Academy of Sciences, project no. 350/1999 for young scientists.

REFERENCES

Alexandrovich, J.M., Radiolarian Biostratigraphy of ODP Leg 111, Site 677A, Eastern Equatorial Pacific, Late Miocene through Pleistocene, *Proc. ODP Sci. Res.*, 1989, vol. 111, pp. 245–263.

Anderson, C., Pliocene Calcium Carbonate Sedimentation Patterns of the Ontong Java Plateau, *Marine Geol.*, 1998, vol. 150, nos. 1–4, pp. 51–71.

Barash, M.S. and Blyum, N., C. Recent Thanatocoenoses of Planktonic Foraminifers in the Northern and Equatorial Atlantics, *Okeanologiya* (Moscow), 1975, vol. 15, no. 1, pp. 108–115.

Barash, M.S., *Planktonnye foraminifery v osadkakh Severnoi Atlantiki* (Planktonic Foraminifers from the North Atlantic Sediments), Moscow: Nauka, 1970.

Berggren, W.A., Hilgen, F.J., Langereis, C.G., *et al.*, Late Neogene Chronology: New Perspectives in High-Resolution Stratigraphy, *Bull. Geol. Soc. Am.*, 1995, vol. 107, no. 11, pp. 1272–1287.

Bubenshchikova, N.V. and Blyum, N.S., Pliocene–Quaternary Biostratigraphy and Planktonic Foraminifera Evolution in the North Pacific, *Stratigr. Geol. Korrelyatsiya*, 1996, vol. 4, no. 3, pp. 71–80.

Bubenshchikova, N.V., Paleoceanology of the North Pacific during the Pliocene–Early Quaternary Time, Implications of Planktonic Foraminifers, *Cand. Sci. (Geol.–Min.) Dissertation*, Moscow: Institute of Oceanology, 1996, p. 31.

Chen, M.T. and Prell, W.L., Faunal Distribution Patterns of Planktonic Foraminifers in Surface Sediments of the Low Latitude Pacific, *Palaeogeogr. Palaeoclimatol. Palaeoecol*, 1998, vol. 137, pp. 55–77.

Dowsett, H., Barron, J., and Poore, R., Middle Pliocene Sea Surface Temperatures: a Global Reconstruction, *Marine Micropaleontol.*, 1996, vol. 27 (1-4), pp. 13–25.

Farrell, J.W. and Prell, W.L., Pacific $CaCO_3$ Preservation and ^{18}O Since 4 Ma: Paleoceanic and Paleoclimatic Implication, *Paleoceanography*, 1991, vol. 6, no. 4, pp. 485–498.

Haug, G.H. and Tiedemann, R., Effect of the Formation of the Isthmus of Panama on Atlantic Ocean Thermohaline Circulation, *Nature* (London), 1998, vol. 393, pp. 673–676.

Hougton, S.D., Late Neogene Calcareous Nannofossil Biostratigraphy and Paleoceanography of ODP Hole 677A, Panama Basin, *Proc. ODP Sci. Res.*, 1989, vol. 111, pp. 277–285.

Ivanova, E.V., Analysis of Paleotemperatures Based on Planktonic Foraminifers, *Okeanologiya* (Moscow), 1983, vol. 23, no. 3, pp. 456–463.

Jansen, E., Mayer, L.A., Backman, J., *et al.*, Evolution of Pliocene Climate Cyclicity at Hole 806B (5–2 Ma): Oxygen isotope record, *Proc. ODP Sci. Res.*, 1993, vol. 130, pp. 349–360.

Jenkins, D.G. and Houghton, S.D., Late Miocene to Pleistocene Planktonic Foraminifers From ODP Site 677, Panama Basin, *Proc. ODP Sci. Res.*, 1989, vol. 111, pp. 289–294.

Jenkins, D.G. and Orr, W.N., Planktonic Biostratigraphy of the Eastern Equatorial Pacific DSDP Leg 9, *Initial Rep. Deep Sea Drill. Project*, Washington: US Gov. Print. Off., 1972, vol. 9, pp. 1059–1193.

Keigwin, L.D., Neogene Planktonic Foraminifera from Deep Sea Drilling Project Sites 502 and 503, *Initial Rep. Deep Sea Drill. Project*, Washington: US Gov. Print. Off., 1982a, vol. 68, pp. 296–289.

Keigwin, L.D., Isotopic Paleoceanography of the Caribbean and East Pacific: Role of Panama Uplift in Late Neogene Time, *Science*, 1982b, vol. 217, pp. 350–353.

Kennett, J.P. and Srinivasan, M.S., *Neogene Planktonic Foraminifera: A Phylogenetic Atlas*, Strasburg: Hutchinson, 1983.

Levitus, S., Climatological Atlas of the World Ocean, *Dept. Commerce NOAA Prof. Pap.*, 1982, no. 13, pp. 1–173.

Os'kina, N.S. and Blyum, N.S., Structure of Planktonic Foraminifer Thanatocoenosis as an Indication of Oceanic Circulation and Fronts, *Okeanologiya* (Moscow), 1984, vol. 24, no. 6, pp. 942–947.

Prell, W.L., Pliocene Stable Isotope and Carbonate Stratigraphy (Holes 572C and 573A): Paleoceanographic Data Bearing of the Question of Pliocene Glaciation, *Initial Rep. Deep Sea Drill. Project*, Washington: US Gov. Print. Off., 1985, vol. 85, pp. 723–734.

Prentice, M.L., Fries, J.K., Simonds, G.G., *et al.*, Neogene Trends in Planktonic Foraminifer ^{18}O From Site 807: Implication for Global Ice Volume and Western Equatorial Pacific Sea-Surface Temperatures, *Proc. ODP Sci. Res.*, 1993, vol. 130, pp. 281–306.

Rogl, F. and Bolli, H.M., Holocene to Pleistocene Planktonic Foraminifera of Leg 15, Site 147 (Cariaco Basin Trench, Caribbean Sea) and Their Climatic Interpretation, *Initial Rep. Deep Sea Drill. Project*, Washington: US Gov. Print. Off., 1973, vol. 15, pp. 553–615.

Saito, T., Geological Significance of Coiling Direction in the Planktonic Foraminifera *Pulleniatina*, *Geology*, 1976, vol. 4, pp. 305–309.

Saito, T., Planktonic Foraminiferal Biostratigraphy of Equatorial Pacific Sediments, *Initial Rep. Deep Sea Drill. Project*, Washington: US Gov. Print. Off., 1985, vol. 85, pp. 621–654.

Shackleton, N.J. and Hall, M.A., Stable Isotope History of the Pleistocene at ODP Site 677, *Proc. ODP Sci. Res.*, 1989, vol. 111, pp. 295–316.

Shackleton, N.J., Hall, M.A., and Plate, D., Pliocene Stable Isotope Stratigraphy of Site 846, *Proc. ODP Sci. Res.*, 1995, vol. 138, pp. 337–357.

Thunell, R.C. and Reynolds, L.A., Sedimentation of Planktonic Foraminifera: Seasonal Changes in Species Flux in the Panama Basin, *Micropaleontol.*, 1984, vol. 30, pp. 241–260.

Tikhii okean (The Pacific Ocean), Leningrad: Nauka, 1981.

Ushakova, M.G., Blyum, N.S., and Bubenshchikova, N.V., Trends of Climatic Changes in the Equatorial East Pacific during the Neogene–Quaternary Time, *Sovremennyi i iskopaemyi mikroplankton Mirovogo okeana* (Contemporary and Fossil Microplankton of the World Ocean), Moscow: Nauka, 1995, pp. 119–131.

Whitman, J.M. and Berger, W.H., Pliocene–Pleistocene Oxygen Isotope Record, Site 586, Ontong Java Plateau, *Marine Micropaleontol.*, 1992, vol. 18, pp. 171–198.

Stratigraphy and Geological Correlation, Vol. 11, No. 3, 2003, pp. 305–312. Translated from Stratigrafiya. Geologicheskaya Korrelyatsiya, Vol. 11, No. 3, 2003, pp. 104–112.
Original Russian Text Copyright © 2003 by Kosov.
English Translation Copyright © 2003 by MAIK "Nauka/Interperiodica" (Russia).

To the Problem of Milankovitch Paleoclimatic Cycles

A. A. Kosov

Institute of Systems Dynamics and Control Theory, Siberian Branch, Russian Academy of Sciences, ul. Lermontova 134, Irkutsk, 664033 Russia

Received May 15, 2000; in final form, December 12, 2001

Abstract—The suggested hypothesis is in sympathy with the new concept of astronomical theory of paleoclimate (Bol'shakov and Bol'shakov, 1999) that implies a greater climatic impact of eccentricity fluctuations than it follows from the Milankovitch theory. The solar tide-producing force considerably increases (by 17%) in periods of maximum eccentricity parameter that may result in activation of volcanic activity causing greenhouse effect in the atmosphere. According to Milankovitch theory, the integral insolation of the Earth increases by 0.1% in the same periods. These two factors are favorable for synchronous climatic warming in both hemispheres of our planet.

Key words: paleoclimate, glaciations, Milankovitch theory, eccentricity, obliquity of the ecliptic, climatic precession, tide-producing forces, paleovolcanism, greenhouse effect.

INTRODUCTION

When traces of recurrent glaciations, which covered in the past much greater areas of the Earth than now, were recognized in 19th century, they gave rise to hypotheses and scientific theories seeking for factors of climatic oscillations responsible for development of glacial sheets and interglacial epochs. Among these climate-controlling factors, there were tested possible effects of several phenomena, such as the solar constant variations, the transit of solar system, by rotation around the Galaxy center, through the cosmic dust clouds and relevant decrease of solar energy arriving at the earth's surface, changes in concentration of carbon dioxide and other gases, which may cause the greenhouse effect, etc. (Berg, 1938; Monin, 1972; Velichko, 1973; Budyko *et al.*, 1985; Kotlyakov, 1994). The astronomical theory of climate by Milankovitch (1930) was rightfully acknowledged by scientific community. It implies that glaciation epochs in the Northern Hemisphere coincided in time with periods of extremely low insolation in high latitudes of this hemisphere during the summer calorific half years. Despite all the distinctions in basic climate-controlling phenomena, three other theories mentioned above cardinally differ from the Milankovitch theory, as they assume synchronism of climatic changes in both hemispheres of the Earth, while the latter argues instead for their antiphase character.

The spectral analysis of paleoclimatic records in oceanic bottom sediments (Shackleton *et al.*, 1990), in ice core sections recovered in Greenland (GRIP and GRIP-2) and Antarctica (Kotlyakov, 1994), and in bottom sediments of the Lake Baikal (Kachukov *et al.*, 1998) revealed their obvious cyclicity with periods of 100, 41, 23, and 19 k.y., which respectively coincide with periods of changes in three orbital parameters—eccentricity of the Earth's orbit e, angle between the equatorial and ecliptic planes ε, and angular distance between the vernal equinox point and perihelion longitude (precession) ω. This coincidence cannot be accidental, and the idea that periodical changes in orbital parameters modulate the climatic fluctuations on the Earth is out of doubts now. Since insolation was expressed by Milankovitch as the explicit function of indicated orbital parameters, synchronism of terrestrial climatic and astronomical parametric fluctuations seems as if it proves the adequacy of his theory. The comprehensive analysis of the issue (Bol'shakov and Bol'shakov, 1999) showed, however, the following aspects of discrepancy between the insolation diagrams plotted by Milankovitch and real paleoclimatic records:

(1) Not all the glaciations detectable and dated using the oxygen isotope scale characterizing the oceanic bottom sediments correspond to the calculated insolation minimums in high latitudes of the Northern Hemisphere during the summer calorific half years, and clear criteria applicable for discrimination of glacial epochs in the insolation diagrams are unknown.

(2) Some glaciations took place in the periods of low values of the eccentricity parameter that finds no explanation in the Milankovitch theory.

(3) Periods with duration of 100 k.y., which correspond to the eccentricity variation frequency that is theoretically calculated by means of approximate integration of equations describing secular perturbations of celestial mechanics, are most clearly expressed in natu-

ral paleoclimatic signals. In the Milankovitch theory, they should be, in contrast, less significant than the periods controlled by the variation frequency of ecliptic obliquity and precession, because he evaluated the eccentricity contribution indirectly, using the so-called "climatic precession" $e\sin\omega$.

In addition, I should mention that the above conclusions obtained from oceanic oxygen isotope records find support, at least for the last 5 m.y., in recent results of the project "Baikal–Drilling" aimed to investigate bottom sediments of that lake (Kachukov *et al.*, 1998). Moreover, data on ice core sections drilled in Greenland and Antarctica (Kotlyakov, 1994) allow him to formulate one more conclusion:

(4) Temperature in polar regions of both hemispheres changed simultaneously (at least, during one complete climatic cycle 100 k.y. long) and parallel with concentrations of carbon dioxide and methane in the atmosphere, the high content of which leads to the greenhouse effect.

It is difficult to find explanation to these facts in terms of the Milankovitch theory, because in equation expressing the insolation variations during summer semiannual periods the term of "climatic precession" is taken with different signs for opposite hemispheres, and in absolute value its significance in high latitudes is comparable with that of ecliptic obliquity. It is also noteworthy that in the 1930s, when there was no isotopic data on oceanic deposits and glacial sheets, Berg (1938), judging from biogeographic data on the bipolar distribution of marine animals, argued that warming and cooling events should be synchronous in both hemispheres and regarded as "improbable the astronomic factors of glaciations, which predict the alternate mode of glacial epochs in two hemispheres" (ibid., p. 420). Analyzing data of continental geology and paleogeography in comparison with curves of secular insolation variations, Velichko (1973, 1991) arrived at the conclusion that the Milankovitch theory "is incompatible with the concrete paleogeographic data" (Velichko, 1991, p. 11).

Bol'shakov and Bol'shakov (1999) suggested the new concept modifying the insolation theory by Milankovitch. They paid greater attention to variations of eccentricity that, when getting greater, increases, according to formulae used by Milankovitch, the integral annual insolation of the Earth as $(1 - e^2)^{-1/2}$. At the same time, they assumed that atmospheric and oceanic currents are able to smooth thermal gradients over the globe and to decrease thereby the impact of ecliptic obliquity and precession variations on the climate, although their general meaning is as suggested by Milankovitch.

Thus, according to the new concept climatic oscillations depend, like in the Milankovitch theory, on changes in insolation, which are controlled by variations of orbital parameters (variations of solar constant are also allowed). In terms of the concept, the irradiation-climatic (IC) curve is plotted as a linear combination of three parameters, which are variable with time and have constant weighting coefficients chosen based on considered qualitative indicators. In my opinion, the IC curve plotted by Bol'shakov and Bol'shakov (1999) is better corresponding to real paleoclimatic signals, and their qualitative evaluation of climatic effects related to orbital parameters seems to be well grounded.

I also agree with their conclusion that the quantitative analysis of these effects may be realistic only in a model, which takes into consideration, in addition to insolation, all other necessary factors, i.e., the configuration of continents and oceans, land and sea-bottom topography, composition of atmosphere and hydrosphere in their dynamics with due account for provenances and balance of key components, atmospheric and oceanic currents, energy reflection and radiation, albedo, etc. At the same time, I feel it necessary to develop farther qualitative aspects of the new concept, including the elucidation of possible factors alternative to insolation, which are interconnected with variations of orbital parameters and may influence the climate. This is necessary to soundly substantiate and to define more precisely the construct of quantitative model of paleoclimate.

The main objective of this work is to attract attention of specialists to such a factor alternative to insolation as the eccentricity-modulated variations of solar tide-producing force, which hypothetically may activate the volcanic activity in periods of high eccentricity parameter thus causing global warming because of growing concentration of carbon dioxide in the atmosphere and related greenhouse effect. This additional factor is able to amplify the relative contribution of eccentricity variations, accented in the work by Bol'shakov and Bol'shakov (1999), to climatic effects. Like in their work, I plotted a paleoclimatic (PC) curve (the term irradiation is omitted, because not only insolation is taken therewith into account) using the other weighting coefficients. As is shown below, this curve is well correlative with the oxygen isotope curve, if the lag in time of 8 k.y. is allowed.

CLIMATIC INFLUENCE OF VOLCANIC ACTIVITY

Volcanoes erupting colossal volumes of ash, dust, gases, and aerosols change the atmosphere composition, thus being responsible for the short-term (less than 10 years) or longer periods of climatic changes. Catastrophic eruptions of ash and aerosols decrease clarity of the atmosphere causing the short-term cooling (Budyko *et al.*, 1986). On the other hand, the volcanic activity opening a principal channel for mantle degassing secures a considerable influx of carbon dioxide and keeps its balance in the atmosphere. As is confidently established based on geochemical data (Budyko *et al.*, 1985, Figs. 24 and 25), concentration of carbon

dioxide in the atmosphere was in covariance with eruption rate of volcanic rocks during the last 500 Ma. The revealed general decrease of volcanic activity with time is explained therewith by declining abundance of radioactive elements, decay of which is responsible for heating of the Earth's deep layers, whereas cyclicity of the process with periods of about 100 m.y. long is regarded as a consequence of thermal convection in the mantle (Budyko *et al.*, 1985, p. 128). It is assumed as well (Budyko *et al.*, 1985, p. 129) that shorter rhythms can be also expected. The latter can be controlled by various factors including those, which are independent of the processes in the crust and mantle of the Earth.

Cyclicity of volcanism in southeastern Asia with periods of 400 and 100 k.y. long has been established by Rasskazov (1998) who analyzed the available Ar–Ar dating results. As he suggested, "the episodic endogenic activity of the Earth responsible for the recurrent periods of volcanism can be interconnected with orbital cycles of the planet." It is unclear, however, what kind of possible factors was responsible for the established cyclicity of volcanic events, and to what extents it was manifested worldwide. Nevertheless, the "Milankovitch frequencies" of 400 and 100 k.y. calculated for the Earth's orbit eccentricity variations and for periods of volcanic activity may suggest interconnection of both phenomena. In my opinion, the latter could be modulated by perturbation action of tide-producing forces, the solar component of which depends on the distance between our planet and the sun.

In terms of stability theory (Abdulin *et al.*, 1987), an active volcano before eruption can be regarded as a system in equilibrium, in which the pressure forces of magma and volcanic fluids work against the gravity and tensile strength of volcanic plug (in the case of submarine volcanoes, one should take into consideration the water pressure as well). That system is of a "low stability," and the closer the eruption moment, the less stable the system. In this critical state, any external impact, even if it is negligible as compared to counterbalancing forces, destroys the equilibrium causing the system transition to the other state of equilibrium, i.e., to the process of eruption. The greater the external impact during the given geochronological period, the higher the probability that equilibrium in such a critical system, as an active volcano, will be destroyed and followed by eruption. In these periods, other things being equal, the volcanic activity of the planet may increase considerably, though the catastrophic eruptions may be less frequent (the external influence "blows off steam" earlier and easier).

The external impact of this kind can be triggered by the tide-producing forces, the solar component of which is variable, depending on the Earth's orbit eccentricity.

SOLAR TIDE-PRODUCING FORCES AS DEPENDING ON THE EARTH'S ORBIT ECCENTRICITY

As is known (Monin, 1972; Beletskii, 1977), the tide-producing force is in direct proportion to the attracting mass and inversely as the cube of distance to that mass:

$$F = k\frac{M}{r^3}. \qquad (1)$$

The tide-producing forces resulting from the gravitational attraction of the Moon and Sun are most important for the Earth. Taking the corresponding mass and distance values, we can easily calculate from (1) that the solar tide-producing force corresponds now to 0.46 of the lunar one. In other words, the gravitational attraction of the Sun is approximately twice weaker than that of the Moon (Monin, 1972, p. 15).

In the last several million years, orbital parameters of the Moon remained almost unchanged (Monin, 1972; Avsyuk, 1996), and the lunar tide-producing force during this period can be regarded as a constant. The Earth's orbit around the Sun is another case. Given its eccentricity increase from $e = 0$ (circular orbit) to $e = 0.05$ (according to Berger *et al.*, 1991, this took place during the last million years) and the constant greater semi-axis a in accord with the Laplace theorem, the shortest distance from the Earth to the Sun (perihelion) r_π calculated using the expression) $r_\pi = a(1 - e)$ (Beletskii *et al.*, 1977) should be equal to 0.95 of the circular orbit radius. As it follows from equation (1), the solar tide-producing force increases at this moment by factor of $1/0.95^3 = 1.166$, i.e., by nearly 17%, and the net variation can be by 5.4% greater. The last value is much higher than the integral insolation increase (0.1%) calculated by Milankovitch.[1]

When the Earth is at the perihelion during the epoch of higher eccentricity parameter, we obtain not only increment of the solar tide-producing force, but also the greater integral work it did throughout the annual cycle. In fact, if $t \in [0.1]$ is a time moment of a given annual cycle, $r(t)$ is the Earth distance from the Sun, and $\nu(t)$ is true anomaly at the moment t, then these parameters enter, according to the first and second Kepler's laws, into the following equations (Beletskii *et al.*, 1977, p. 17):

$$r = \frac{a(1-e^2)}{1+e\cos\nu}, \quad r^2\frac{d\nu}{dt} = \sqrt{\mu a(1-e^2)}, \qquad (2)$$

where μ is a coefficient proportional to the Newtonian attraction constant.

[1] Editorial note. Author takes into consideration only the Keplerian term of solar attraction.

According to equations (1) and (2), the net annual work of solar tide-producing forces is proportional to the integral

$$\int_0^1 \frac{dt}{r^3(t)} = \int_0^{2\pi} \frac{d\nu}{r(\nu)\sqrt{\mu a(1-e^2)}}$$

$$= \frac{1}{a^{3/2}\sqrt{\mu}(1-e^2)^{3/2}} \int_0^{2\pi} (1+e\cos\nu)d\nu$$

$$= \frac{2\pi}{a^{3/2}\sqrt{\mu}(1-e^2)^{3/2}}.$$

Therefore, when the eccentricity parameter increases from zero to 0.05, this work increases by 0.37% that is again much greater than the integral insolation increment.

Thus, when eccentricity of the Earth's orbit grows, the integral insolation increment, climatic effect of which is accented in the Milankovitch theory, is considerably lower than the increment of solar contribution to the tide-producing forces at the perihelion moment and throughout the annual cycle. Of course, it is unnecessary to expect the linear interconnection between the volcanic activity and the modulating signal of this kind, and the problem can be discussed in a probabilistic aspect only. Nevertheless, I think that the modulating signal of a relatively high magnitude transmitted through the channel "eccentricity—tide-producing forces—volcanic activity—greenhouse effect—climatic warming" should be not less effective than in the channel "eccentricity—integral insolation—climate." Both channels produce one-way effect and emphasize, like in the new concept under discussion (Bol'shakov and Bol'shakov, 1999), the prime significance of eccentricity variations for climatic changes on out planet. In addition, they should operate synchronously in both hemispheres in distinction from consequences of the Milankovitch theory, in which the insolation formulae for northern and southern latitudes include the antiphase terms of "climatic precession."

The climatic impact of tide-producing forces interrelated with eccentricity variations, which are relatively more important than variations of other orbital parameters, can be also realized through other channels having no interconnection with the volcanic activity. As is shown (Shilo and Vashchilov, 1989), the tide-producing forces can be regarded as a peculiar "tectonic pump" able to deliver, via active tectono-magmatic zones, endogenic vapor and gases from depth to the surface. In periods of high eccentricity parameters, when the increased annual work of solar tide-producing forces is proportionate to $(1 - e^2)^{-3/2}$, the higher pump power accelerates the emanation rate of gases responsible for the atmospheric greenhouse effect.

The tide-related activation of present-day tectonic processes on the Earth has been established by experimental measurements in the moments of new and full moon, when tide-producing forces are maximal. As is shown by measurements in such an active tectonic region as the Pamirs (Volodichev *et al.*, 1997), these moments are marked by peak intensities of neutron radiation, which are believed to be interrelated with the peak emanation of radiogenic radon from deep-seated faults and associated fractures. It is shown as well (Volodichev *et al.*, 2001) that many important series of earthquakes coincide in time with the new and full moon phases, because the intense tide-related events are thought to be able to trigger the tectonic processes, maturation of which was controlled before by the inherent tectonic factors. The analogous correlation between tidal and tectonic processes on the Moon, where it is manifested more clearly because of a higher gravitational attraction of the Earth, has been established and described by Avsyuk (1996).

Thus, the long-period variations of tide-producing forces, which are interconnected with the eccentricity variations of the Earth's orbit, seem to be able to change the efficiency of the triggering tidal mechanism with respect to volcanic activity and "tectonic pump," both enabling emanation of greenhouse gases from the Earth's mantle and deep crust. The results obtained by Shilo *et al.*, (1989) allow me to mention one more channel, through which the eccentricity variations and tide-producing forces may influence the terrestrial climate. In distinction from triggering effect of aforementioned mechanisms, this one is directly controlled by variations of tide-producing energy in various geochronological periods. As is estimated (Shilo *et al.*, 1989), the summary energy of solar and lunar gravitational attraction, which must be eventually transformed, according to physical laws, into the heat within the Earth's crust, is one order of magnitude greater than the total insolation energy reaching at present the planet surface. In terms of eccentricity variation model, the solar contribution equal to nearly 32% of this "tidal heat" is proportionate to $(1 - e^2)^{-3/2}$, thus being able to change the annual terrestrial heat balance to a greater extent than the concurrent increment of integral insolation, which is proportionate to $(1 - e^2)^{-1/2}$ according to formulae used by Milankovitch.

It is important that all the potential channels, which could be able to transform the eccentricity variations into climatic and other effects, operate in-phase and synchronously in both hemispheres of the planet. Thus, among variations of the Earth's orbital parameters, those of eccentricity are distinctly noteworthy for their climatic effect, as it was accented not long ago (Bol'shakov and Bol'shakov, 1999). The real contribution of each channel to climatic oscillations is unclear yet, and this problem can be solved only after creation

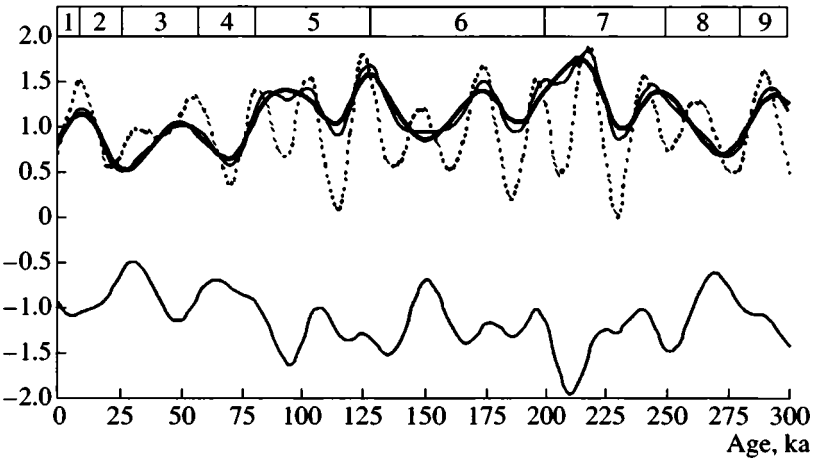

Fig. 1. Width-variable space between plotted functions (thin-line curves) $K_N(\tau)$ (Northern Hemisphere) and $K_S(\tau)$ (Southern Hemisphere) that is interpreted as "paleoclimatic band" visualizing climatic changes during the last 300 k.y.; firm heavy line is paleoclimatic curve $K_1(\tau)$ synthesizing variable parameters for both hemispheres. The dotted line depicting variations of the monthly average insolation at the latitude of 65° N is normalized to the magnitude interval [–1, +1] and displaced for the unity upward. The upper scale shows the numbered oxygen isotope stages recorded in oceanic sediments.

of a model adequately fitting the multidisciplinary database.

PLOTTED PALEOCLIMATIC CURVES

Let us denote the time variable (age in k.y.) as $\tau > 0$ and the orbit eccentricity, ecliptic obliquity, and perihelion longitude at the given time as $e(\tau)$, $\varepsilon(\tau)$, and $\omega(\tau)$, respectively. Then, according to the recently suggested approach (Bol'shakov and Bol'shakov, 1999) and theory of celestial mechanics describing evolution of the orbital parameters indicated above, the problem of plotting the paleoclimatic curve $K(\tau)$ posed by Milankovitch can be reduced to the functional relation $K(\tau) = f(\tau, e(\tau), \varepsilon(\tau), \omega(\tau)$, i.e., to the definition of function $f(\tau, x, y, z)$. As it has been correctly noted (Bol'shakov and Bol'shakov, 1999), the adequate theoretical solution of the problem is hardly possible. It is natural therefore to use instead the desired function a linear combination in the stationary variant, by which the coefficients implicitly depend on time.

The used mathematical procedure is described below. In distinction from the previous approach (Bol'shakov and Bol'shakov, 1999), the variation curves are plotted for two hemispheres of the Earth.

Let us consider the time span $T = = [\tau_1, \tau_2]$, assuming that $e_{max} = \max_{\tau \in T} e(\tau)$, $e_{min} = \min_{\tau \in T} e(\tau)$, and $e_0 = (e_{max} + e_{min})/2$, $\Delta e(\tau) = 2(e(\tau) - e_0)/(e_{max} - e_{min})$. The relative variability $\Delta\varepsilon(\tau)$ of the ecliptic obliquity $\Delta\omega(\tau)$, or $\Delta\omega(\tau)$ of the "climatic precession" $e(\tau)\sin\omega(\tau)$, can be defined in the same way. Within the given time span T, all three curves will be oscillating between (–1) and (+1) reaching the extreme limitations and having the identical amplitudes of negative and positive deviations. With due account for influence of each orbital parameter and for zero-time reference of precession, the paleoclimatic curve $K_N(\tau)$ for the Northern Hemisphere can be plotted for geometric visualization using the formula

$$K_N(\tau) = a_e\Delta e(\tau) + a_\varepsilon\Delta\varepsilon(\tau) - a_\omega\Delta\omega(\tau) + 1, \quad (3)$$

where nonnegative coefficients a_e, a_ε, and a_ω mean specific contributions of each orbital parameter, and their sum is equal to unity. The $K_N(\tau)$ values may vary thereby between 0 and 2 not necessarily reaching the extreme limitations.

Similarly, the paleoclimatic curve for the Southern Hemisphere obtains geometric visualization by formula

$$K_S(\tau) = -[a_e\Delta e(\tau) + a_\varepsilon\Delta\varepsilon(\tau) + a_\omega\Delta\omega(\tau)] - 1, \quad (4)$$

and $K_S(\tau)$ values may vary between –2 and 0 not necessarily reaching again the extreme limitations.

Being plotted in the same diagram, curves (3) and (4) never intersect each other and delineate a band of variable width from 0 to 4. This "paleoclimatic band" is interesting by implication: its bottlenecks must correspond to cooling periods (and to glaciations), while the wide portions must mark warming phases (interglacial epochs).

Two hemispheres of the Earth differ from each other in configuration of land and oceanic areas, and their climatic reaction should be different, even if the insolation intensity is identical in both. It is reasonable, therefore, to use different weighting coefficients when plotting the paleoclimatic curves for the Earth as a whole according to equations:

$$K_1(\tau) = a_N K_N(\tau) - (1 - a_N)K_S(\tau),$$
$$K_0(\tau) = K_1(\tau) - 1, \quad (5)$$

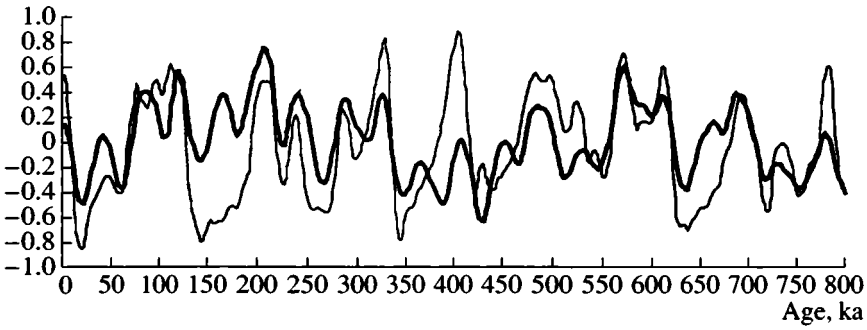

Fig. 2. Correlation diagram of paleoclimatic curve $K_0(\tau)$ (firm heavy line), which is plotted for the paleomagnetic Brunhes Chron (the last 800 k.y.) and displaced toward the future for 8 k.y., and of concurrent oxygen isotope curve (ODP Site 677) smoothed for intervals of 5 adjacent points and normalized to the magnitude interval [−1, +1] (thin line).

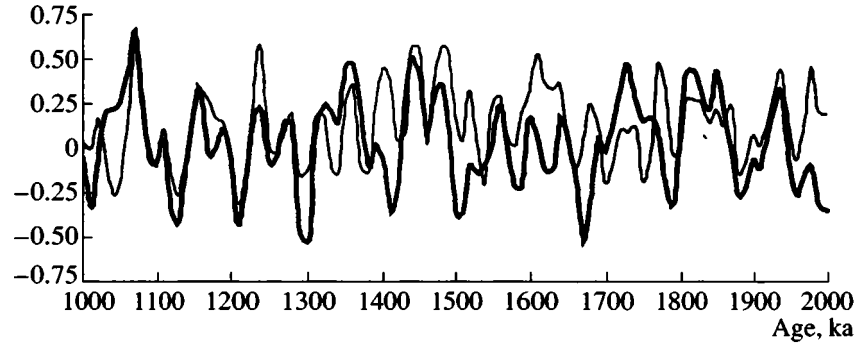

Fig. 3. Correlation diagram of paleoclimatic curve $K_0(\tau)$ (firm heavy line), which is plotted for the time span of 1000–2000 ka and displaced toward the future for 8 k.y., and of concurrent oxygen isotope curve (ODP Site 677) smoothed for intervals of 5 adjacent points and normalized to the magnitude interval [−1, +1] (thin line).

where $a_N \in [0.1]$ is the weighting coefficient characterizing the Northern Hemisphere. This hemisphere is usually thought to be of leading importance in climatic changes and controls synchronism of temperature fluctuations in two hemispheres that has not been predicted by the Milankovitch insolation theory.[2] When $a_N = 0.5$, i.e., by a symmetrical approach to both hemispheres, two curves (5) become independent of "climatic precession" variations. Given that coefficient attains the other values, the curves (5) will be synthesizing variations of all three orbital parameters with due regard to specific contribution of each hemisphere. The curve $K_0(\tau)$ is limited in modulus by 1, and the curve $K_1(\tau)$ will be approaching the curve $K_N(\tau)$, if coefficient a_N tends to 1.

The reconciliation of weighting coefficients a_e, a_ε, a_ω, and a_N is very important for the procedure of plotting the paleoclimatic (PC) curves. The curves shown in presented diagrams are plotted using the following values: $a_e = 0.44$, $a_\varepsilon = 0.33$, $a_\omega = 0.23$, and $a_N = 0.65$, all selected to obtain the best correlation between curves. The PC curves, characterizing variations of $K_N(\tau)$ in the Northern Hemisphere and shown in Figs. 2 and 3, are plotted according to proportion 1 : 0.75 : 0.16 between the coefficients, which is close (except for the precession-related value) to that used by Bol'shakov and Bol'shakov (1999) in their work. The curves illustrating secular variations in oxygen isotope (OI) and orbital parameters are plotted using data published by Shackleton *et al.*, (1990) and Berger *et al.*, (1991), respectively.

As one can see from Fig. 1, the narrower and wider segments of the "paleoclimatic band" correspond respectively to the even cooling and odd warming stages of the OI record. The PC curve $K_1(\tau)$ is smoothing the precession-induced distinctions between two hemispheres. Correlation between the summer insolation peaks and OI stages is far from being perfect: the deepest insolation minimums are situated against the warming OI stages 5 and 7, whereas a local insolation maximum corresponds to one of the coolest event that took place 150 k.a. ago. Discordances of this kind remain to be valid for older periods than that limited by the age mark of 300 ka chosen to simplify Fig. 1.

Figure 2 illustrates the indicative similitude relationship between the PC and OI curves: nearly all peaks in variations of orbital parameters are correlative with real climatic events recorded in the last curve, though to a different extent in separate periods and with a time gap of 8 k.y. The formal correlation coefficient for two

[2] Neglect with respect to inertness of accumulation and thawing of ice sheets is unavoidable in this case.

Fig. 4. The paleoclimatic curve $K_0(\tau)$ smoothed for each moment within the averaging intervals of 300 k.y. (firm heavy line and right-side ordinate) and correlated with changes in abundance of diatoms (vol %) in sediments deposited in the Lake Baikal during the first glaciation period (thin broken line and left-side ordinate reproduced from Fig. 7 of Kachukov *et al.*, 1998).

curves is not very high (0.55), but their visual similitude is obvious. The most obvious distinction between two curves under comparison is seen, like in the curves plotted earlier (Bol'shakov and Bol'shakov, 1999), opposite the age mark of about 170 ka, as the OI record at ODP Site 677 does not show here a proper response to the local peak of the PC curve. Such a response can be found, however, in the well-known SPECMAP curve (reproduced by Kachukov *et al.*, 1998).

The indicative similarity between the $K_0(\tau)$ variations and OI records at ODP Site 667 is traceable as far in the past as 1–2 Ma. As one can see in Fig. 3, all maximums and minimums of the curves under comparison practically coincide (a chance that the time lag accepted as equal to 8 k.y. could vary with time and possible calibration errors of OI scale may well be responsible for local discrepancy). Even if the reflection of climatic signals was nonlinear in OI records and varied with time, the similitude of curves shown in Fig. 3 is not less obvious than that characterizing the Brunhes Chron (Fig. 2).

The PC curves plotted in accordance with equations (5) are in covariance with real paleoclimatic signals of older epochs too, the OI records of which are known not only in oceans, but in continental areas as well, e.g., in the Lake Baikal, where sedimentation was directly controlled by the continental climate of Asia (Kachukov *et al.*, 1998). The necessity of checking the theoretical constructs from this viewpoint was first accented few years ago (Bol'shakov and Bol'shakov, 1999).

The continuous paleoclimatic record in sediments of that lake has been investigated by scientists involved in the project "Baikal–Drilling" who established that during the last 5 m.y. there were two cold periods about as long as 300 k.y.: one between 2.82 and 2.48 Ma and the other one between 1.75 and 1.45 Ma (Kachukov *et al.*, 1998). These were periods, when mountain glaciers, which first appeared around the lake, resulted in deposition of deep-water pelitomorphic clay (sedimentation product of glacial milk) almost lacking the diatom frustules characteristic of sediments deposited in other cooling epochs of the Pleistocene.

The first period of glaciation around the Lake Baikal corresponds in time to the relative minimum of the $K_0(\tau)$ curve opposite the age mark of 2.819 Ma, which is one of the deepest (–0.619)[3] within the period of last 5 m.y. It is necessary to note here that the concurrent insolation in July at the latitude of 65° N (430)[4] is comparable with that in the period of 2.82–2.75 Ma (not less than 422) and at present (426), being considerably higher than its minimum value (387) within the whole period of 5 m.y. Accordingly, the Milankovitch theory is unable to predict the necessary cooling event at the corresponding time. In addition, a relatively low value of the monthly average insolation at the same latitude in July (401) is calculated for the time of 2.937 Ma, but the corresponding cooling event (Kachukov *et al.*, 1998, Fig. 7) was less intense and insufficient for development of glaciation.

Glaciation that took place 1.67 m.y. ago in the second cold period is correlative with the deep (–0.526) relative minimum of the PC curve $K_0(\tau)$ opposite the age mark of 1.679 Ma. At the latitude of 65° N, the monthly average insolation in July at that time (433) is again comparable with the present-day value and with that characterizing the period of 1.7–1.65 Ma (not less than 422). Thus, I agree with the previous conclusion (Bol'shakov and Bol'shakov, 1999) that the insolation diagrams are inappropriate for recognition of the past glacial epochs. The OI variations in continental deposits of the Lake Baikal support this conclusion that has been originally derived from comparison of theoretical constructs with oceanic OI records.

The aforementioned cold periods approximately as long as 300 k.y., which have been established by working group of the project "Baikal–Drilling," find no explanation in terms of the insolation hypothesis: we

[3] The only lower value of –0.625 corresponds to the age mark of 1.302 Ma.

[4] Here and below, the monthly average insolation values calculated from published data (Berger et al., 1991) are given in W/m^2.

have none of the desired deep minimums of the monthly average insolation in July at the latitude of 65° N within the period of 3.0–2.7 Ma, and the mean insolation during that period is practically indistinguishable form mean values, which can be calculated for any other period of the same duration. Simultaneously, Fig. 4 clearly demonstrates that the first event of intense cooling that resulted in glaciation around the Lake Baikal is well correlative with one of deepest (below –0.1) relative minimums opposite the age mark of 2.65 Ma in the PC curve $K_0(\tau)$ averaging data for the intervals of 300 k.y.

CONCLUSION

Data and argumentation presented above lead to the following conclusions:

(1) In the new concept of astronomic theory of paleoclimate (Bol'shakov and Bol'shakov, 1999), the climatic impact of eccentricity variations is shown to be noticeably more significant in comparison with that of other variable parameters of the Earth's orbit, such as the ecliptic obliquity and perihelion longitude (precession). This concept corresponds to real oxygen isotope records of climatic signals in oceanic sediments and continental diatomaceous deposits of the Lake Baikal better than the Milankovitch theory relating past glaciations to the summer semiannual insolation minimums.

(2) The variable insolation is not the only possible mechanism transforming variations of orbital parameters into climatic changes on the Earth. An alternative way is the assumed modulation of volcanic activity and related changeable influx of greenhouse gases into the atmosphere under influence of tide-producing forces, the energy of which depends on the distance between our planet and the Sun. Other channels of extraterrestrial influence appear to be possible as well.

(3) Confident and convincing quantitative dynamics of climatic changes subject to variations of orbital parameters and other factors can be understood only after creation of a more advanced model based on the classical Milankovitch theory still retaining its scientific meaning and on the Bol'shakov new concepts discussed in this work, which better correspond to present-day data on paleoclimatic events.

ACKNOWLEDGMENTS

I am grateful to Yu.N. Avsyuk and A.A. Velichko for their valuable comments used to improve an original version of the manuscript. The work was partially supported by the Russian Foundation for Basic Research in cooperation with the Irkutsk administration, project no. 01-01-97201-p2001Baikal and by the program Integration of Siberian Division, Russian Academy of Sciences.

Reviewers Yu.N. Avsyuk and A.A. Velichko

REFERENCES

Abdullin, R.Z., Anapol'skii, L.Yu., Kozlov, R.I., *et al.*, *Metod vektornykh funktsii Lyapunova v teorii ustoichivosti* (Lyapunov Method of Vector Functions in Stability Theory), Voronov, A.A. and Matrosov, V.M., Eds., Moscow: Nauka, 1987.

Avsyuk, Yu.N., *Prilivnye sily i prirodnye protsessy* (Tide-Producing Forces and Natural Processes), Moscow: OIFZ RAN, 1996.

Beletskii, V.V., *Ocherki o dvizhenii kosmicheskikh tel* (Essays on Motion of Space Bodies), Moscow: Nauka, 1977.

Berg, L.S., *Osnovy klimatologii* (Fundamentals of Climatology), Leningrad: Uchpedgiz, 1938.

Berger, A. and Loutre, M.F., Insolation Values for the Climate of the Last 10 Million Years, *Quaternary Sci. Rev*, 1991, vol. 10, pp. 297–317.

Bol'shakov, V.A. and Bol'shakov, P.V., Astronomical Theory of Paleoclimate: A New Concept, *Stratigr. Geol. Korrelyatsiya*, 1999, vol. 7, no. 6, pp. 3–13.

Budyko, M.I., Golitsin, G.S., and Izrael', Yu.A., *Global'nye klimaticheskie katastrofy* (Global Climatic Catastrophes), Moscow: Gidrometeoizdat, 1986.

Budyko, M.I., Ronov, A.B., and Yanshin, A.L., *Istoriya atmosfery* (History of the Atmosphere), Leningrad: Gidrometeoizdat, 1985.

Kachukov, V., Lykov, D., Pevzner, L., *et al.*, Sediments of the Lake Baikal as a Continuous Record of Climatic Changes during the Last 5 Million Years, *Geol. Geofiz.*, 1998, vol. 39, no. 2, pp. 139–156.

Kotlyakov, V.M., *Mir snega i l'da* (The World of Snow and Ice), Moscow: Nauka, 1994.

Milankovitch, M., "Mathematische Klimalehre und astronomische Theorie der Klimaschwankungen." Berlin: Borntreger, 1930. Translated under the title *Matematicheskaya klimatologiya i astronomicheskaya teoriya kolebanii klimata*, Moscow: Nauchn.-Tekh. Lit., 1939.

Monin, A.S., *Vrashchenie Zemli i klimat* (Rotation of the Earth and Climate), Leningrad: Gidrometeoizdat, 1972.

Rasskazov, S.V., Volcanic Periods 5 m.y. Long in the Late Cenozoic Geodynamic Hierarchy of Southeastern Asia, *Metallogeny, Fuel Resources, and Geodynamics of the North Asian Craton and Framing Orogenic Belts*, Irkutsk: Institute of Geochemistry, 1998, pp. 69–70.

Shackleton, N.J., Berger, A., and Peltier, W., An Alternative Astronomical Calibration of the Lower Pleistocene Time Scale Based on ODP Site 677, *Trans. Roy. Soc. Edinb.*, 1990, vol. 81, pp. 251–261.

Shilo, N.A. and Vashchilov, Yu.Y., Terrestrial Tides as a Tectonic Pump and Vibrator, *Dokl. Akad. Nauk SSSR*, 1989, vol. 307, no. 4, pp. 833–836.

Velichko, A.A., *Prirodnyi protsess v pleistotsene* (A Natural Process in the Pleistocene), Moscow: Nauka, 1973.

Velichko, A.A., Global Climatic Changes and Reaction of Landscape Geosphere, *Izv. Akad. Nauk SSSR, Ser. Geogr.*, 1991, no. 5, pp. 5–22.

Volodichev, N.N., Kuzhevskii, B.M., Nechaev, O.Yu., *et al.*, A Phenomenon of Neutron Intensity Peaks at the New- and Full-Moon Phases, *Kosmich. Issled.*, 1997, vol. 35, no. 2, pp. 144–154.

Volodichev, N.N., Podorol'skii, A.N., Levin, B.V., *et al.*, Series of High-Magnitude Earthquakes as Correlated with New- and Full-Moon Phases, *Vulkanol. Seismol.*, no. 1, pp. 60–67.

Subscribe to the journals from the Russian Academy of Sciences

Translated and Published by MAIK "Nauka / Interperiodica"
(International Academic Publishing Company "Nauka / Interperiodica")
Distributed Worldwide by INTERPERIODICA

Copy this form to mail or fax your order today

	TITLE	Volume	ISSN	ISSUES	RATE IN US DOLLARS US/CAN	RATE IN US DOLLARS INTERNATIONAL	YOUR ORDER
❑	Biophysics	48	0006-3509	6 + 1 Suppl.	$3,341	$3,483	$ _____
❑	Computational Mathematics and Mathematical Physics	43	0965-5425	12	$3,216	$3,913	$ _____
❑	Doklady Earth Sciences	388-393A	1028-334X	9	$3,766	$4,327	$ _____
❑	Doklady Mathematics	67-68	1064-5624	6	$1,842	$2,115	$ _____
❑	Entomological Review	83	0013-8738	9 + 2 Suppl.	$3,412	$3,880	$ _____
❑	Eurasian Soil Science	36	1064-2293	12 + 1 Suppl.	$2,839	$3,270	$ _____
❑	Geochemistry International	41	0016-7029	12 + 2 Suppl.	$3,234	$3,707	$ _____
❑	Geology of Ore Deposits	45	1075-7015	6	$1,270	$1,455	$ _____
❑	Geomagnetism and Aeronomy	43	0016-7932	6	$987	$1,134	$ _____
❑	Geotectonics	37	0016-8521	6	$770	$835	$ _____
❑	Herald of the Russian Academy of Sciences	73	1019-3316	6	$2,145	$2,726	$ _____
❑	Izvestiya, Atmospheric and Oceanic Physics	39	0001-4338	6 + 1 Suppl.	$1,247	$1,339	$ _____
❑	Izvestiya, Physics of the Solid Earth	39	1069-3513	12	$1,123	$1,242	$ _____
❑	Journal of Communications Technology and Electronics	48	1064-2269	12	$3,723	$4,281	$ _____
❑	Journal of Computer and Systems Sciences International	42	1064-2307	6	$2,700	$3,105	$ _____
❑	Journal of Ichthyology	43	0032-9452	9 + 2 Suppl.	$2,932	$3,374	$ _____
❑	Laser Physics	13	1054-660X	12	$2,263	$2,732	$ _____
❑	Oceanology	43	0001-4370	6 + 1 Suppl.	$1,127	$1,208	$ _____
❑	Paleontological Journal	37	0031-0301	6 + 6 Suppl.	$3,580	$4,126	$ _____
❑	Pattern Recognition & Image Analysis	13	1054-6618	4	$905	$1,036	$ _____
❑	Petroleum Chemistry	43	0965-5441	6	$3,679	$3,820	$ _____
❑	Petrology	11	0869-5911	6	$1,270	$1,455	$ _____
❑	The Physics of Metals and Metallography	95-96	0031-918X	12 + 2 Suppl.	$3,586	$4,131	$ _____
❑	Physics of Particles and Nuclei	34	1063-7796	6 + 1 Suppl.	$2,965	$3,150	$ _____
❑	Polymer Science. Series A	45	0965-545X	12	—	—	$ _____
❑	Polymer Science. Series B	45	1560-0904	6	—	—	$ _____
❑	Polymer Science. Series C	45	Pending	1	—	—	$ _____
	Polymer Science. Ser. A+B+C	45	—	19	$4,121	$4,764	$ _____
❑	Proceedings of the Steklov Institute of Mathematics	240-243	0081-5438	4 + 2 Suppl.	$1,853	$2,136	$ _____
❑	Russian Journal of Inorganic Chemistry	48	0036-0236	12 + 1 Suppl.	$4,045	$4,651	$ _____
❑	Russian Journal of Mathematical Physics	10	1061-9208	4	$796	$905	$ _____
❑	Russian Journal of Physical Chemistry	77	0036-0244	12 + 1 Suppl.	$4,007	$4,612	$ _____
❑	Russian Metallurgy (Metally)	—	0036-0295	6	$1,958	$2,134	$ _____
❑	Stratigraphy and Geological Correlation	11	0869-5938	6	$1,270	$1,455	$ _____
❑	Studies on Russian Economic Development	14	1075-7007	6	$918	$1,053	$ _____
❑	Thermal Engineering	50	0040-6015	12	$1,966	$2,257	$ _____
❑	Thermophysics and Aeromechanics (only distribution)	10	0869-8643	4	$842	$1,010	$ _____
						TOTAL	_____

❶ Name _____
Institution _____
Address _____
_____ State _____
City _____ Country _____
Zip/Postal Code _____
Telephone (_____)

Delivery is not made until payment is received
To order by phone call **1 800 633-4931**
or (205) 995-1567 outside the US and Canada

❷ ❑ My payment for $_____ is enclosed.
OR
❑ Bill me. My library's purchase order number is _____

❸ Send this order and payment to:
INTERPERIODICA
P.O. Box 1831
Birmingham, AL 35201-1831
Or fax this order form to (205) 995-1588

Order now for immediate delivery. All journals will be published in 2003!

MAIK "Nauka/Interperiodica" Publishing

is pleased to present to the international scientific community simultaneous Russian- and English-language publication of the journals of the Russian Academy of Sciences

MAIK "Nauka/Interperiodica" 2003 volumes include the following titles:

- *Biophysics*
- *Computational Mathematics and Mathematical Physics*
- *Doklady Earth Sciences*
- *Doklady Mathematics*
- *Entomological Review*
- *Eurasian Soil Science*
- *Geochemistry International*
- *Geology of Ore Deposits*
- *Geomagnetism and Aeronomy*
- *Geotectonics*
- *Herald of the Russian Academy of Sciences*
- *Izvestiya, Atmospheric and Oceanic Physics*
- *Izvestiya, Physics of the Solid Earth*
- *Journal of Communications Technology and Electronics*
- *Journal of Computer and Systems Sciences International*
- *Journal of Ichthyology*
- *Laser Physics*
- *Oceanology*
- *Paleontological Journal*
- *Pattern Recognition and Image Analysis*
- *Petroleum Chemistry*
- *Petrology*
- *Physics of Particles and Nuclei*
- *Polymer Science, Series A*
- *Polymer Science, Series B*
- *Polymer Science, Series C*
- *Proceedings of the Steklov Institute of Mathematics*
- *Russian Journal of Inorganic Chemistry*
- *Russian Journal of Mathematical Physics*
- *Russian Journal of Physical Chemistry*
- *Russian Metallurgy (Metally)*
- *Stratigraphy and Geological Correlation*
- *Studies on Russian Economic Development*
- *The Physics of Metals and Metallography*
- *Thermal Engineering*
- *Thermophysics and Aeromechanics**

* *Thermophysics and Aeromechanics* is only distributed by MAIK "Nauka/Interperiodica" Publishing

Please direct all inquiries about the above journals to: INTERPERIODICA, P.O. Box 1831, Birmingham, AL 35201-1831. For faster service call toll-free (800) 633-4931 or (205) 995-1567 (outside US and Canada). Fax: (205) 995-1588, E-mail: interperiodica@ebsco.com

- *Applied Biochemistry and Microbiology*
- *Automation and Remote Control*
- *Biochemistry (Moscow)*
- *Biology Bulletin*
- *Colloid Journal*
- *Combustion, Explosion, and Shock Waves**
- *Cosmic Research*
- *Differential Equations*
- *Doklady Biochemistry and Biophysics*
- *Doklady Biological Sciences*
- *Doklady Chemistry*
- *Doklady Physical Chemistry*
- *Fluid Dynamics**
- *Functional Analysis and Its Applications**
- *Glass Physics and Chemistry*
- *High Energy Chemistry*
- *High Temperature*
- *Human Physiology*
- *Inorganic Materials*
- *Instruments and Experimental Techniques*
- *Journal of Analytical Chemistry*
- *Journal of Applied Mechanics and Technical Physics**
- *Journal of Evolutionary Biochemistry and Physiology*
- *Journal of Mining Science**
- *Journal of Structural Chemistry**
- *Kinetics and Catalysis*
- *Lithology and Mineral Resources*
- *Mathematical Notes**
- *Microbiology*
- *Molecular Biology*
- *Problems of Information Transmission*
- *Programming and Computer Software*
- *Protection of Metals*
- *Radiochemistry*
- *Russian Chemical Bulletin**
- *Russian Journal of Applied Chemistry*
- *Russian Journal of Bioorganic Chemistry*
- *Russian Journal of Coordination Chemistry*
- *Russian Journal of Developmental Biology*
- *Russian Journal of Ecology*
- *Russian Journal of Electrochemistry*
- *Russian Journal of General Chemistry*
- *Russian Journal of Genetics*
- *Russian Journal of Marine Biology*
- *Russian Journal of Nondestructive Testing*
- *Russian Journal of Organic Chemistry*
- *Russian Journal of Plant Physiology*
- *Russian Microelectronics*
- *Siberian Mathematical Journal**
- *Solar System Research*
- *Theoretical and Mathematical Physics**
- *Theoretical Foundations of Chemical Engineering*
- *Water Resources*

* *The journal* is produced under contracts between Plenum Publishing and the Russian Academy of Sciences and/or its divisions, the institutes, and the editorial boards, and under contract and subcontract between Kluwer Academic/Plenum Publishers and MAIK "Nauka/Interperiodica"

Please direct all inquiries about the above journals to: Kluwer Academic/Plenum Publishers, P.O. Box 322, 3300 AH Dordrecht, The Netherlands. Phone: (31 78) 657-6392. Fax: (31 78) 657-6474, E-mail: orderdept@wkap.nl

- *Acoustical Physics*
- *Astronomy Letters*
- *Astronomy Reports*
- *Crystallography Reports*
- *Doklady Physics*
- *JETP Letters*
- *Journal of Experimental and Theoretical Physics*
- *Optics and Spectroscopy**
- *Physics of Atomic Nuclei*
- *Physics of the Solid State*
- *Plasma Physics Reports*
- *Semiconductors*
- *Technical Physics*
- *Technical Physics Letters*

* *Optics and Spectroscopy*: Optical Society of America, 2010 Massachusetts Ave., NW, Washington, DC 20036-1023, Attn.: Publications Department. Tel. (202) 223-8130, (800) 582-0416. Fax: (202) 416-6140.

Please direct all inquiries about the above journals to: American Institute of Physics, Circulation and Fulfillment Services, Suite 1NO1, 2 Huntington Quadrangle, Melville, NY 11747-4502 USA. Tel. (516) 576-2270, 1-800-344-6902. Fax: (516) 349-9704, E-mail: subs@aip.org

International Academic Publishing Company "Nauka/Interperiodica" (MAIK "Nauka/Interperiodica")
Profsoyuznaya ul., 90, Moscow, 117997, Russia. Phone: 7 (095) 336-1600. Fax: 7 (095) 336-0666.
E-mail: compmg@maik.ru. http://www.maik.ru

MAIK "Nauka/Interperiodica" Publishing

is pleased to present to the international scientific community simultaneous Russian- and English-language publication of the journals of the Russian Academy of Sciences

MAIK "Nauka/Interperiodica" 2003 volumes include the following titles:

- *Biophysics*
- *Computational Mathematics and Mathematical Physics*
- *Doklady Earth Sciences*
- *Doklady Mathematics*
- *Entomological Review*
- *Eurasian Soil Science*
- *Geochemistry International*
- *Geology of Ore Deposits*
- *Geomagnetism and Aeronomy*
- *Geotectonics*
- *Herald of the Russian Academy of Sciences*
- *Izvestiya, Atmospheric and Oceanic Physics*
- *Izvestiya, Physics of the Solid Earth*
- *Journal of Communications Technology and Electronics*
- *Journal of Computer and Systems Sciences International*
- *Journal of Ichthyology*
- *Laser Physics*
- *Oceanology*
- *Paleontological Journal*
- *Pattern Recognition and Image Analysis*
- *Petroleum Chemistry*
- *Petrology*
- *Physics of Particles and Nuclei*
- *Polymer Science, Series A*
- *Polymer Science, Series B*
- *Polymer Science, Series C*
- *Proceedings of the Steklov Institute of Mathematics*
- *Russian Journal of Inorganic Chemistry*
- *Russian Journal of Mathematical Physics*
- *Russian Journal of Physical Chemistry*
- *Russian Metallurgy (Metally)*
- *Stratigraphy and Geological Correlation*
- *Studies on Russian Economic Development*
- *The Physics of Metals and Metallography*
- *Thermal Engineering*
- *Thermophysics and Aeromechanics**

* *Thermophysics and Aeromechanics* is only distributed by MAIK "Nauka/Interperiodica" Publishing

Please direct all inquiries about the above journals to: **INTERPERIODICA**, P.O. Box 1831, Birmingham, AL 35201-1831.
For faster service call toll-free (800) 633-4931 or (205) 995-1567 (outside US and Canada). Fax: (205) 995-1588, E-mail: interperiodica@ebsco.com

- *Applied Biochemistry and Microbiology*
- *Automation and Remote Control*
- *Biochemistry (Moscow)*
- *Biology Bulletin*
- *Colloid Journal*
- *Combustion, Explosion, and Shock Waves**
- *Cosmic Research*
- *Differential Equations*
- *Doklady Biochemistry and Biophysics*
- *Doklady Biological Sciences*
- *Doklady Chemistry*
- *Doklady Physical Chemistry*
- *Fluid Dynamics**
- *Functional Analysis and Its Applications**
- *Glass Physics and Chemistry*
- *High Energy Chemistry*
- *High Temperature*
- *Human Physiology*
- *Inorganic Materials*
- *Instruments and Experimental Techniques*
- *Journal of Analytical Chemistry*
- *Journal of Applied Mechanics and Technical Physics**
- *Journal of Evolutionary Biochemistry and Physiology*
- *Journal of Mining Science**
- *Journal of Structural Chemistry**
- *Kinetics and Catalysis*
- *Lithology and Mineral Resources*
- *Mathematical Notes**
- *Microbiology*
- *Molecular Biology*
- *Problems of Information Transmission*
- *Programming and Computer Software*
- *Protection of Metals*
- *Radiochemistry*
- *Russian Chemical Bulletin**
- *Russian Journal of Applied Chemistry*
- *Russian Journal of Bioorganic Chemistry*
- *Russian Journal of Coordination Chemistry*
- *Russian Journal of Developmental Biology*
- *Russian Journal of Ecology*
- *Russian Journal of Electrochemistry*
- *Russian Journal of General Chemistry*
- *Russian Journal of Genetics*
- *Russian Journal of Marine Biology*
- *Russian Journal of Nondestructive Testing*
- *Russian Journal of Organic Chemistry*
- *Russian Journal of Plant Physiology*
- *Russian Microelectronics*
- *Siberian Mathematical Journal**
- *Solar System Research*
- *Theoretical and Mathematical Physics**
- *Theoretical Foundations of Chemical Engineering*
- *Water Resources*

* *The journal* is produced under contracts between Plenum Publishing and the Russian Academy of Sciences and/or its divisions,the institutes, and the editorial boards, and under contract and subcontract between Kluwer Academic/Plenum Publishers and MAIK "Nauka/Interperiodica"

Please direct all inquiries about the above journals to: **Kluwer Academic/Plenum Publishers**, P.O. Box 322, 3300 AH Dordrecht, The Netherlands. Phone: (31 78) 657-6392. Fax: (31 78) 657-6474, E-mail: orderdept@wkap.nl

- *Acoustical Physics*
- *Astronomy Letters*
- *Astronomy Reports*
- *Crystallography Reports*
- *Doklady Physics*
- *JETP Letters*
- *Journal of Experimental and Theoretical Physics*
- *Optics and Spectroscopy**
- *Physics of Atomic Nuclei*
- *Physics of the Solid State*
- *Plasma Physics Reports*
- *Semiconductors*
- *Technical Physics*
- *Technical Physics Letters*

* *Optics and Spectroscopy*: Optical Society of America, 2010 Massachusetts Ave., NW, Washington, DC 20036-1023, Attn.: Publications Department. Tel. (202) 223-8130, (800) 582-0416. Fax: (202) 416-6140.

Please direct all inquiries about the above journals to: **American Institute of Physics**, Circulation and Fulfillment Services, Suite 1NO1, 2 Huntington Quadrangle, Melville, NY 11747-4502 USA. Tel. (516) 576-2270, 1-800-344-6902. Fax: (516) 349-9704, E-mail: subs@aip.org

International Academic Publishing Company "Nauka/Interperiodica" (MAIK "Nauka/Interperiodica")
Profsoyuznaya ul., 90, Moscow, 117997, Russia, Phone: 7 (095) 336-1600; Fax: 7 (095) 336-0666,
E-mail: compmg@maik.ru, http://www.maik.ru